Synthese von Fettsäure-Mimetika und deren Charakterisierung als PPARalpha/gamma-Agonisten und duale mPGES-1/5-LO-Inhibitoren

Dissertation zur Erlangung des Doktorgrades der Naturwissenschaften

Vorgelegt beim Fachbereich
Biochemie, Chemie und Pharmazie der
Goethe-Universität Frankfurt am Main

Heiko Zettl
aus Schönheide

Frankfurt, 2009
(D30)

vom Fachbereich 14 Biochemie, Chemie und Pharmazie der

Goethe-Universität Frankfurt als Dissertation angenommen

Dekan: Prof. Dr. Dieter Steinhilber

Gutachter: Prof. Dr. Manfred Schubert-Zsilavecz

Prof. Dr. Gisbert Schneider

Datum der Disputation: 13.11.2009

Inhaltsverzeichnis

1. Zielsetzung **1**

2. Einleitung **2**

2.1. PPAR 2

2.1.1. Molekularbiologie und physiologische Funktionen 2

2.1.2. Medizinische Chemie 12

2.1.3. Klinische Einsatzgebiete von PPAR-Aktivatoren 26

2.2. mPGES-1 und 5-LO 30

2.2.1. Molekularbiologie und physiologische Funktionen 30

2.2.2. Medizinische Chemie 36

2.2.3. Klinische Perspektive von dualen mPGES-1/5-LO-Inhibitoren 39

3. Ergebnisse & Diskussion **41**

3.1. Struktur-Wirkungs-Beziehungen 41

3.1.1. PPAR 41

3.1.2. mPGES-1 und 5-LO 50

3.2. Chemische Synthesen 53

3.2.1. Pirinixinsäurederivate 53

3.2.2. 2-(Phenylthio)-hexansäurederivate und Analoga 55

4. Zusammenfassung **58**

5. Bibliographie **64**

6. Publikationsübersicht **74**

6.1. Publikationen in Peer-Reviewed Journals 74

6.2. Reviews in Peer-Reviewed Journals 76

6.3. Andere Beiträge 77

7. Lebenslauf **78**

8. Eidesstattliche Versicherung **82**

9. Danksagung **83**

10. Anhang **85**

10.1. Abkürzungen 85

10.2. Nachdrucke der Publikationen 87

1. Zielsetzung

Im menschlichen Körper haben Fettsäuren eine Vielzahl von regulatorischen Funktionen inne. Diese sind einerseits sensorischer Natur resultierend aus der exogenen Zufuhr von Fettsäuren mit der Nahrung und deren Rolle als eine der Hauptenergiequellen des Organismus. Andererseits werden Fettsäuren auch endogen synthetisiert und fungieren als autokrine und parakrine Mediatoren. Folglich gibt es eine Vielzahl von Enzymen und Rezeptoren, die am Stoffwechsel von exogenen wie auch endogenen Fettsäuren beteiligt sind. Aufgrund ihrer Beteiligung an einer Reihe von pathophysiologischen Prozessen stellen sie wichtige Targets für die Entwicklung von neuen Arzneistoffen dar. Da für entsprechende Affinität meist eine gewisse Ähnlichkeit mit den natürlichen Liganden erforderlich ist, wird der Begriff "Fettsäure-Mimetika" für in diesem Sinne wirksame synthetische Substanzen verwendet.

Die folgende Arbeit verfolgt einen medizinisch-chemischen Ansatz ausgehend von der Pirinixinsäure (WY14,643) als geeignete Leitstruktur für Aktivatoren von Peroxisomen Proliferator-aktivierten Rezeptoren (PPARs) sowie für Inhibitoren von zwei Schlüsselenzymen der Arachidonsäurekaskade: der 5-Lipoxygenase (5-LO) und der mikrosomalen Prostaglandin E_2-Synthase-1 (mPGES-1). Mittels Struktur-Wirkungs-Beziehungen wurde die Pirinixinsäure im Hinblick auf diese Targets strukturell optimiert (gezeigt am Beispiel HZ52) und zusätzlich basierend auf diesen Erkenntnissen eine neue Leitstruktur in Form der 2-(Phenylthio)-hexansäurederivate (gezeigt am Beispiel HZ64) etabliert.

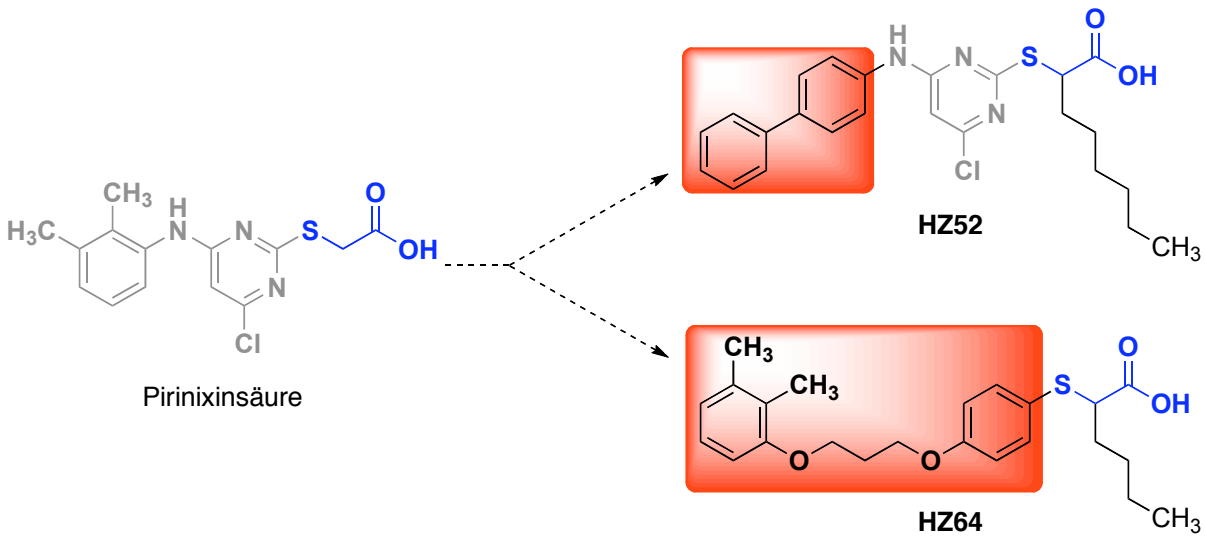

2. Einleitung

2.1. PPAR

2.1.1. Molekularbiologie und physiologische Funktionen

2.1.1.1. Struktureller Aufbau und Subtypen

Die Peroxisomen Proliferator-aktivierten Rezeptoren (PPARs) bilden eine Unterfamilie der nukleären Rezeptoren. Sie sind Liganden-aktivierte Transkriptionsfaktoren und kontrollieren die Expression einer Vielzahl an Genen, die hauptsächlich zur Aufrechterhaltung der Lipid-Homöostase dienen[1]. Es sind drei Subtypen der PPARs identifiziert (PPARα, PPARβ Synonym PPARδ, PPARγ), die sich in ihrer physiologischen Funktion, Gewebeverteilung und Ligandenspezifität unterscheiden. Im Fall von PPARγ sind des Weiteren zwei Isoformen bekannt (PPARγ1 und γ2), wobei PPARγ2 um 30 Aminosäuren am N-Terminus verlängert ist und beide Isoformen eine unterschiedliche Gewebeverteilung aufweisen. Nach der *nuclear receptor* (NR)-Nomenklatur werden die drei Subtypen mit NR1C1 (PPARα), NR1C2 (PPARβ/δ) sowie NR1C3 (PPARγ) bezeichnet[2].

Alle nukleären Rezeptoren gleichen sich im prinzipiellen Aufbau. In der jeweiligen Sequenz finden sich stets drei verschiedene Domänen wieder: eine am N-Terminus angesiedelte, Liganden-unabhängige Transaktivierungs-Domäne (bezeichnet als AF-1; *activation function-1*), die zentrale DNA-Bindungs-Domäne (DBD) mit zwei charakteristischen Zink-Finger Motiven und am C-Terminus die Liganden-Bindungs-Domäne (LBD) mit einer für alle nukleären Rezeptoren hoch konservierten Tertiärstruktur[3]. Die regulatorische Kontrolle der Aktivierung von PPARs durch Phosphorylierung findet an der AF-1 statt. Die LBD beinhaltet eine die zweite, Liganden-abhängige Aktivierungs-Domäne (AF-2; *activation function-2*), an der die Regulation durch die Rekrutierung von Cofaktoren wie *steroid receptor coactivator-1* (SRC-1) und *cAMP response element binding protein (CREB) binding protein* (CBP) möglich ist[4,5,6]. Der Sequenzvergleich zwischen den drei Subtypen in Abb. 1 veranschaulicht die gemeinsamen Strukturmerkmale, die Prozentzahlen geben die identischen Aminosäuren in Bezug auf PPARα an.

Abb. 1: Schematischer Überblick und funktionelle Gliederung der Sequenz von PPARs.

Einteilung in die funktionellen Domänen A-F. Die Zahlen geben die jeweilige Postition der Aminosäure an, die Prozentzahlen die Identität der Sequenz im Vergleich mit PPARα. Domäne C wird auch als DNA-Bindungs-Domäne (DBD) bezeichnet, Domäne D als „hinge region" (engl. Scharnier) und die Domänen E/F als Liganden-Bindungs-Domäne (LBD). AF-1=*activation function-1*, AF-2=*activation function-2*.

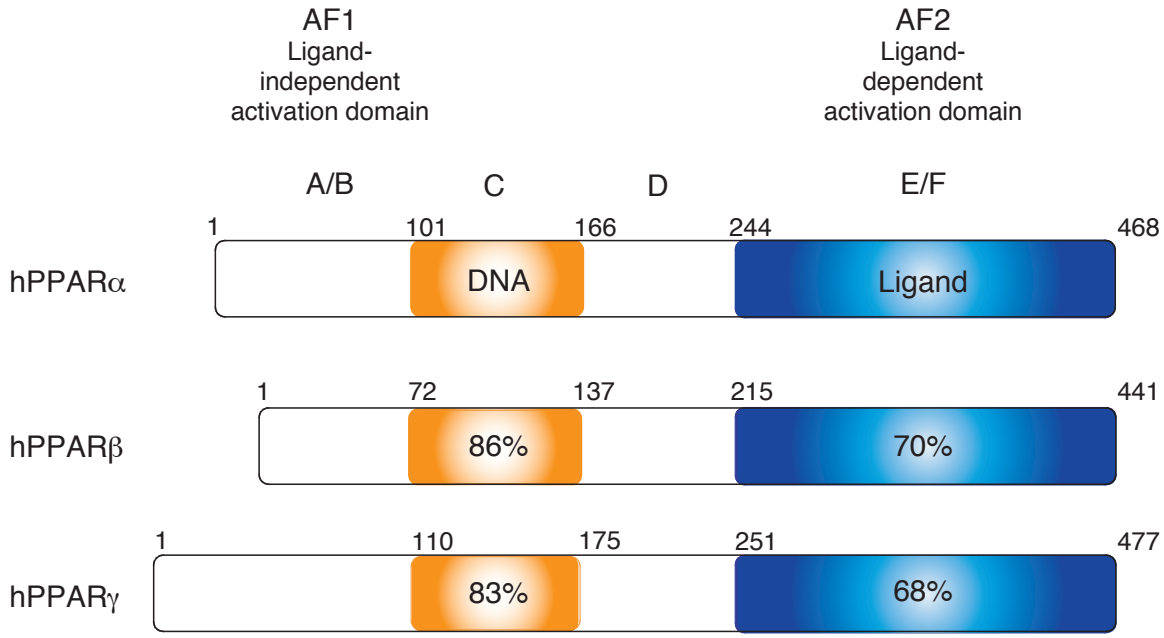

Der detaillierte Aufbau der PPAR-LBD konnte durch kristallografische Studien der jeweiligen Subtypen aufgeklärt werden: Insgesamt 13 α-Helices und ein viergliedriges β-Faltblatt formen die Bindetasche mit einem Volumen von ca. 1300 Å[3] [7,8]. Abb. 2 zeigt beispielhaft die Holo-Kristallstruktur der PPARα-LBD (erstellt mit dem Agonisten GW590735, Struktur siehe Tab. 3) und veranschaulicht die räumliche Anordung der einzelnen Helices[9]. Es existiert mittlerweile eine Vielzahl an publizierten Kristallstrukturen für alle Subtypen, die erste wurde im Jahr 1998 von *Nolte et al.* (Holo-PPARγ mit dem Agonisten Rosiglitazon) publiziert[7,10]. Es folgten Apo-PPARβ im Jahr 2000 und schließlich 2001 Holo-PPARα mit dem Agonisten GW409544[8,11]. Alle Subtypen zeigen eine Y-artige Ausformung im Inneren der LBD, die Bindetasche von PPARβ ist etwas kleiner als die vergleichbar großen von PPARα und PPARγ[2]. Der gesamte Bereich im Inneren besitzt hydrophoben Charakter. Eine besondere Rolle bei der Ligandenbindung spielt die Helix-12, die die AF-2 Domäne beinhaltet. Diese zeichnet sich durch ein dynamisches Verhalten aus und wird durch ein Wasserstoffbrücken-Netzwerk mit dem Liganden in ihrer aktiven

Konformation stabilisiert[12]. Das Netzwerk ist charakteristisch für alle PPAR-Subtypen und wird von vier polaren Aminosäuren ausgebildet, die neben Helix-12 zu den Helices H3, H5 und H11 gehören (siehe Tab. 1). Von Seiten des Liganden wird zur Ausbildung der Wasserstoff-Brücken stets eine acide Kopfgruppe benötigt.

Abb. 2: Kristallstruktur der Holo-PPARα-LBD, erstellt mit dem Agonisten GW590735 (nicht gezeigt). Zuordnung der einzelnen Helices nach *Sierra et al.*[9].

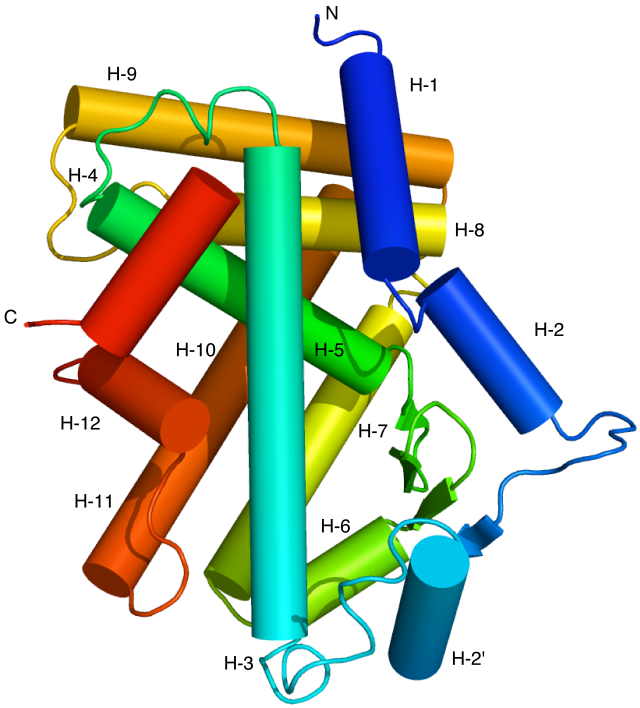

Tab. 1: Übersicht über die an der Ausbildung des Wasserstoffbrücken-Netzwerkes beteiligten Aminosäuren von PPAR[7].

Helix	PPARα	PPARβ	PPARγ
H3	Ser280	Thr289	Ser289
H5	Tyr314	His323	His323
H11	His440	His449	His449
H12	Tyr464	Tyr473	Tyr473

Den Eingang zur Bindetasche bilden die Helix 3 und das viergliedrige β-Faltblatt, im Fall von PPARα begrenzt durch eine Wasserstoffbrücke zwischen Tyr334 und

Glu282. Diese erfordert insbesondere von raumgreifenden Liganden eine hohe Flexibilität und ist einmalig für PPARα, da Tyr334 bei PPARβ und γ mutiert ist[13]. Die Unterschiede zwischen den einzelnen Subtypen und deren Selektivität hinsichtlich ihrer jeweiligen Liganden sind bedingt durch den Austausch einzelner Aminosäuren im Inneren der Bindetasche und werden näher in Kapitel 2.1.2.2. anhand von Ligandenbindungs-Modellen diskutiert.

2.1.1.2. Funktion auf zellulärer Ebene

Die Regulation der Genexpression durch PPAR ist ein komplexer Prozess und bezieht eine Reihe anderer zellulärer Faktoren (siehe Abb. 3) mit ein. PPAR bildet Heterodimere mit einem anderen nukleären Rezeptor, dem Retinoid-X-Rezeptor (RXR), wodurch eine Bindung an die DNA erst möglich wird. Zusammengehalten wird der PPAR/RXR-Komplex durch drei verschiedene Verknüpfungspunkte, an denen die Oberflächen beider Rezeptoren miteinander interagieren[14]. Die Aktivierung des PPAR/RXR-Heterodimers kann neben der Ligandenbindung an PPAR zusätzlich auch über dessen Phosphorylierung an der AF-1 oder über Agonisten des RXRs erfolgen, was am Beispiel von 9-*cis*-Retinsäure gezeigt wurde[15,16]. Des Weiteren wird die PPAR-Aktivität durch die Bindung diverser Coaktivatoren und Corepressoren reguliert.

Im inaktiven Zustand ist PPAR mit den Histon-deacetylierenden Corepressoren *nuclear receptor co-repressor* (NCoR) und *silencing mediator for retinoid and thyroid receptor* (SMRT) assoziiert[17,18]. Durch Histon im deacetylierten Status wird die Transkription inhibiert[19]. Coaktivatoren hingegen, wie SRC-1 und *PPAR binding protein* (PBP), sind in der Lage, Histon zu acetylieren und induzieren darüber nach erfolgter Ligandenbindung die Transkription[20,21]. Die Bindung von Coaktivatoren über die AF-2 Domäne erfolgt durch ein für alle nukleären Rezeptoren typisches bindendes Motiv mit der Aminosäurensequenz LXXLL[22]. Auch die Erkennung und Bindung an die DNA wird durch ein spezifisches Motiv vermittelt, das *peroxisome proliferator response element* (PPRE), bestehend aus der direkten Wiederholung von zwei Hexanucleotiden mit der Basenfolge AGGTCA — X — AGGTCA, wobei X zumeist ein einzelnes beliebiges Nucleotid als Zwischenstück ist (in einigen Ausnahmen ist X=2)[23]. Aufgrund seiner direkten Wiederholung wird es auch als *direct repeat-1* (DR-1) bezeichnet. Die Bindung an PPRE erfolgt mittels der beiden Zink-Finger-Motive der PPAR-DBD, während RXR mit der DNA *downstream*

interagiert[24]. Die Stabilität des PPAR/RXR-DNA-Komplexes wird entscheidend von der Konformation der PPAR-LBD beeinflusst, was für einen großen Einfluss der Art des PPAR-Liganden auf die nachfolgende Genregulation spricht[14]. Verantwortlich für die Unfähigkeit der PPARs, als Monomere an die DNA zu binden, ist die intrinsisch hoch flexible A/B-Domäne: Durch deren Abtrennung konnte eine DNA-Bindung von Monomeren erreicht werden[25]. Hinsichtlich der Stärke der Bindung an die DNA können PPREs in drei funktionelle Gruppen (stark, mittel, schwach) unterteilt werden, entscheidend für die PPAR-Subtypselektivität wie auch für die Stärke der Bindung sind hierbei die in 5'-Richtung flankierenden Nucleotide. Generell bindet PPARγ stärker als die anderen beiden Subtypen[26]. Nachdem dieser Prozess durchlaufen wurde, kommt es zur Aktivierung der RNA-Polymerase und daraus resultierend zur Subtyp-abhängigen Genexpression, deren physiologische Auswirkungen im folgenden Kapitel diskutiert werden.

Abb. 3: Schematische Darstellung der Transkriptionsaktivierung durch den PPAR/RXR-Heterodimer-Komplex. Das PPRE ist anhand der entsprechenden Nucleotide (AGGTCA — X — AGGTCA) dargestellt.

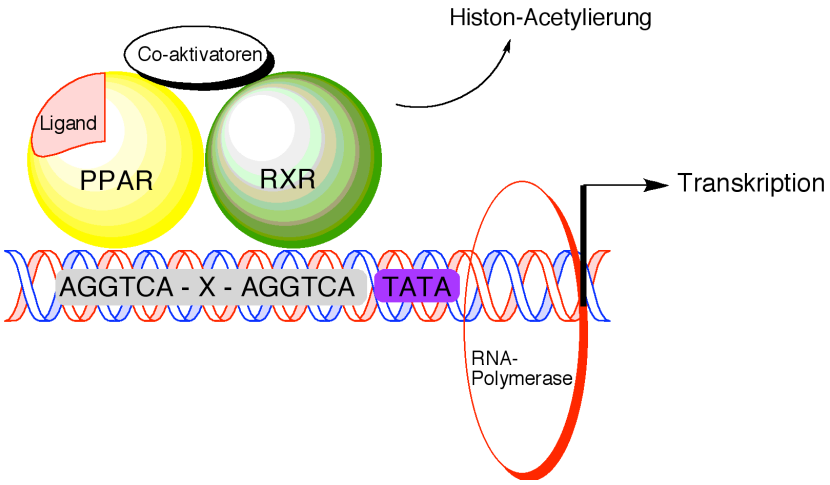

2.1.1.3. Funktion im Organismus

Das Verständnis der physiologischen Rolle von PPAR geht in den Anfang der 1990er Jahre zurück, als zunächst die Kontrolle der β-Oxidation von Fettsäuren in den Peroxisomen von Leberzellen durch PPARα und der Einfluss von PPARγ auf die Adipogenese nachgewiesen werden konnte[27,28]. Aufgrund der unterschiedlichen Gewebeverteilungen und physiologischen Funktionen bietet sich an dieser Stelle eine differenzierte Betrachtung der einzelnen Subtypen an, welche in Abb. 4

zusammengefasst wird.

Abb. 4: Physiologische Effekte der PPAR-Aktivierung, differenziert nach den einzelnen Subtypen[29].

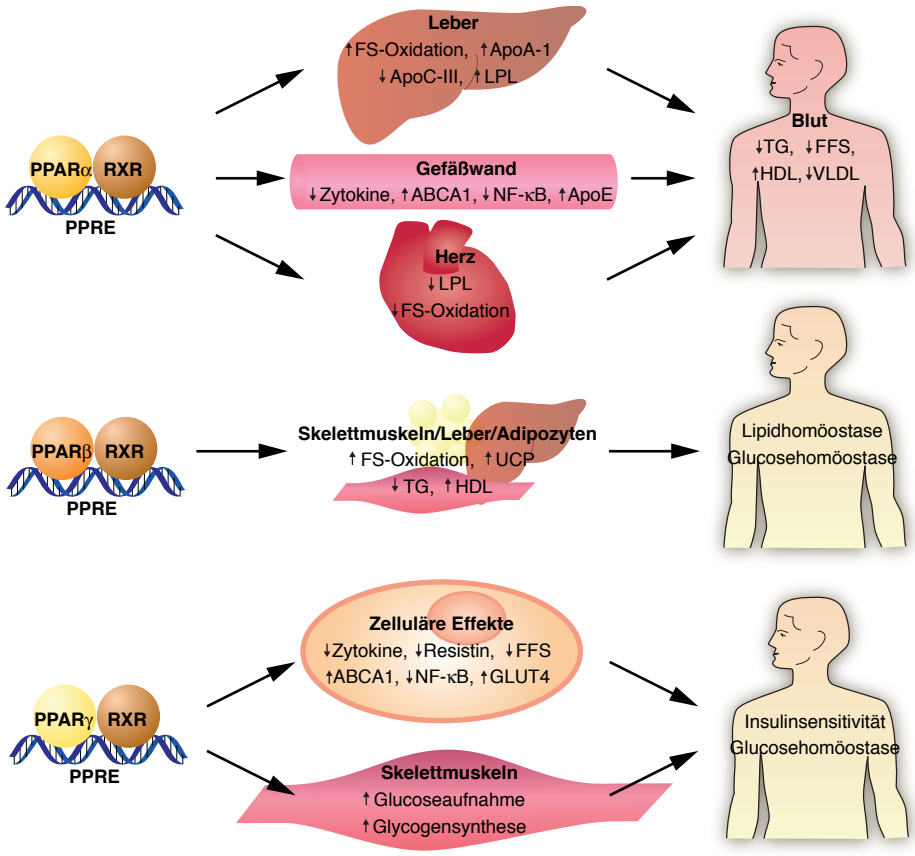

(a) PPARα

Das Expressionsmuster von PPARα ist sehr vielfältig. Der Rezeptor findet sich sowohl in vielen Organen und Geweben wie Leber, Niere, Herz, Skelettmuskel und braunem Fettgewebe als auch in diversen Gefäßzellen wie Endothelzellen und glatten Gefäßmuskelzellen und in Monozyten/Makrophagen[30]. Hinsichtlich der kontrollierten biologischen Prozesse steht der Lipidstoffwechsel im Mittelpunkt: PPARα spielt eine entscheidende Rolle in der Energie-Homöostase sowie im Metabolismus von Fettsäuren. Die zentralen Mechanismen sind hier die Regulation der mitochondrialen und peroxisomalen β-Oxidation und der Fettsäureaufnahme in die Zelle. Eine weitere wichtige Eigenschaft von PPARα ist die Fähigkeit, die

Expression von proinflammatorischen Genen zu unterdrücken und damit Einfluss auf das Entzündungsgeschehen zu nehmen. Assoziiert mit veränderten Lipidparametern spielt dieses bei der Pathologie der Atherosklerose eine große Rolle. Die katabole Wirkung auf den Fettsäurestoffwechsel kombiniert mit antiinflammatorischen Wirkungen an der Gefäßwand bilden denn auch die pharmakologische Grundlage für den therapeutischen Einsatz von PPARα-Agonisten bei Dyslipidämien[31].

PPARα ist wesentlich an der Regulation des Metabolismus wichtiger Lipoproteine wie *very low density lipoprotein* (VLDL) und *high density lipoprotein* (HDL) sowie des Blutspiegels von freien Fettsäuren (FFS) und Triglyceriden (TG) beteiligt (siehe Abb. 4). In der Leber fördert PPARα die Genexpression von mehreren Proteinen, die die Aufnahme und anschließende β-Oxidation von mittel- und langkettigen FFS vermitteln. Dies führt zu einem *shift* weg von der TG-Synthese hin zu katabolen Prozessen. Um den Transport durch VLDL-Partikel zu ermöglichen, werden FFS in der Leber in TG überführt. VLDL wird stetig in der Leber mit dem Ziel der (Energie-)Versorgung von peripheren Geweben mit FFS produziert. Die Steuerung der VLDL-Synthese erfolgt u.a. über den Spiegel an FFS und TG im Blut, die Aufnahme in periphere Gewebe wird durch die Lipoprotein-Lipase (LPL) vermittelt. PPARα stimuliert die Genexpression der LPL, was neben der Suppression des hepatischen Apolipoproteins C3 (ein natürlicher Inhibitor der LPL) als Hauptursache für den klinisch signifikanten TG-senkenden Effekt von PPARα-Agonisten diskutiert wird (siehe Abb.5)[32,33]. Die mRNA-Expression von Apolipoprotein A1 und A2, Hauptbestandteile der antiatherogenen HDL-Partikel, wird durch PPARα aktiviert[34]. Evidenz für die antiatherosklerotische Aktivität von PPARα liefern ebenfalls die anti-inflammatorischen Effekte in Zellen der Gefäßwand, wo die Adhäsion und Migration von Monocyten/Makrophagen verhindert wird[35]. Dies geschieht einerseits durch die Suppression der Produktion von proinflammatorischen Cytokinen wie Interleukin-6 und von Zytokin-induzierter *vascular cellular adhesion molecule-1* (VCAM-1) Expression (siehe Abb. 5)[36]. Andererseits erhöht PPARα die Expression von *inhibitors of κB* (I-κBs), welche im Cytoplasma mit dem proinflammatorischen nukleären Transkriptionsfaktor *nuclear factor-κB* (NF-κB) assoziiert sind und deren Erhöhung die Translokation von NF-κB zum Nukleus und somit die Aktivierung der inflammatorischen NF-κB-Signaltransduktionskaskade vermindern[37,38]. Zusätzlich wird in Makrophagen der Transporter *ATP-binding cassette A1* (ABCA-1) hochreguliert, der den Efflux zellulären Cholesterols vermittelt und somit für den ersten Schritt des reversen Cholesterol-Transportes verantwortlich ist[39].

Abb. 5: Von PPARα regulierte, bei Dyslipidämien und Atherosklerose relevante Gene der Leber und Gefäßwand.

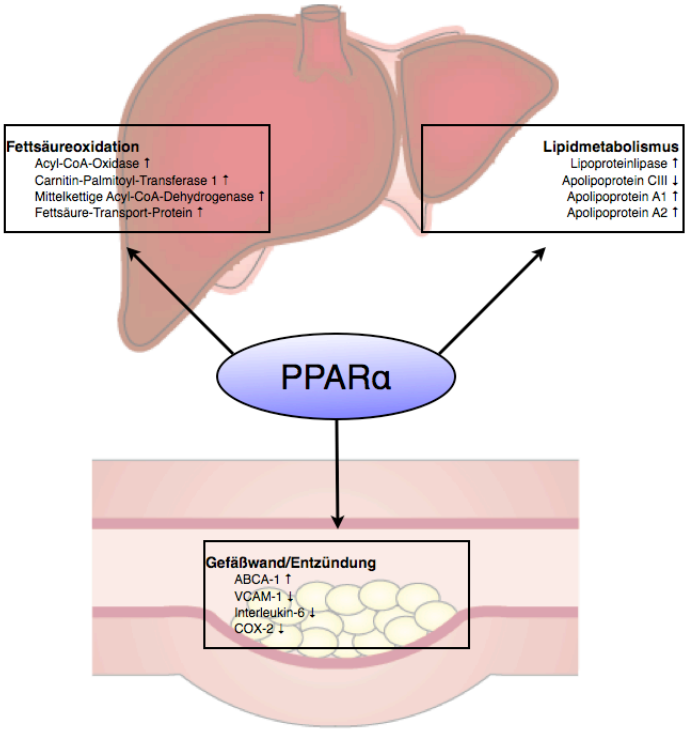

(b) PPARβ/δ

Im Vergleich zu den beiden anderen Subtypen gilt PPARβ aufgrund seiner ubiquitären Expression und dem lange Zeit vorherrschenden Mangel an synthetischen Agonisten als am wenigsten erforscht. Mit der Verfügbarkeit von selektiven synthetischen Aktivatoren und genetisch modifizierten Mäusen (PPARβ *knock out* und Überexpression) konnte in dieser Dekade vieles über die physiologische Rolle dieses Rezeptors aufgeklärt werden[40]. Erste funktionelle Untersuchungen konnten einen Einfluss auf Embryonalentwicklung, epidermale Differenzierung und Wundheilung belegen[41]. Von therapeutischem Interesse sind jedoch wiederum die metabolischen Effekte: Beeinflusst werden wie auch bei PPARα Gene des oxidativen Fettsäuremetabolismus, bei PPARβ allerdings eher im Skelettmuskel als in der Leber. Die Aktivierung von PPARβ führt bei der Energiegewinnung im Muskel zu einer Verschiebung von der schnellen Glycolyse hin zum langsameren oxidativen Fettsäureabbau. Es konnte bei fettleibigen Mäusen eine antiadipogene Wirkung sowie eine generelle Verbesserung von Parametern des metabolischen Syndromes (verbesserte Glucosesensitivität der β-Zellen und

Insulinsensitivität der Peripherie) beobachtet werden[42]. Antiatherogen wirkt PPARβ-Aktivierung durch Aktivierung des reversen Cholesteroltransportes, was zu erhöhtem HDL-Cholesterol im Plasma führt. Mechanistisch konnte eine vermehrte Expression von ABCA-1 nachgewiesen werden[43]. Neben dieser Vielzahl an positiven Effekten im Hinblick auf das metabolische Syndrom gibt es jedoch eine anhaltende Debatte über die Rolle von PPARβ bei der Entstehung von intestinalen Tumoren, nachdem eine Überexpression bei humanen und murinen colorectalen Tumorzellen gezeigt wurde[44]. Problematisch ist weiterhin, dass aufgrund der Unterschiede in der metabolischen Regulation bei Nagern und Primaten im Vergleich zum Menschen die Extrapolation tierexperimenteller Ergebnisse auf die Reaktionen des menschlichen Körpers äußerst schwierig ist[45]. Es bleibt daher die Auswertung von laufenden Phase II-Studien mit selektiven PPARβ-Agonisten abzuwarten, die ein präziseres Urteil über die physiologische Rolle beim Menschen und über die Eignung als pharmakologisches Target erlauben wird.

(c) PPARγ

Die Verteilung von PPARγ im Organismus ist die definierteste unter den PPARs: Der Rezeptor ist stark exprimiert im Fettgewebe, deutlich weniger dagegen in Zellen des Immunsystems, Skelettmuskels, Herzens, Dünndarms und der Leber[46]. Hinsichtlich seiner beiden Isoformen PPARγ1 und PPARγ2 kommt PPARγ2 spezifischer im Fettgewebe vor.

Funktionell gilt PPARγ als der Hauptregulator der Adipogenese. Der Rezeptor wird während der Differenzierung von Präadipocyten zu Adipocyten induziert und sowohl im weißen als auch im braunen Fettgewebe hoch exprimiert. Die existenzielle Rolle konnte mittels PPARγ-null Zellen in chimären Mäusen, in denen keine Ausdifferenzierung der Präadipocyten stattfand, nachgewiesen werden[47]. Von größerer therapeutischer Relevanz ist jedoch der Einfluss von PPARγ auf die Lipid- und Glucosehomöostase (siehe Abb. 4 und 6). Durch PPARγ wird die Aufnahme und Speicherung von zirkulierenden FFS ins Fettgewebe gefördert, was einerseits deren Blutspiegel senkt und andererseits zu einer Umverteilung von Lipiden u.a. aus der Leber und den Skelettmuskeln hin zum Fettgewebe führt[48]. Dies ist insofern von besonderem Interesse, da eine Akkumulation von Lipiden in Leber und Skelettmuskel mit Insulinresistenz und folglich ausbleibender Glucoseaufnahme aus dem Blut einhergeht[49]. Zu den aktivierten Genen des Lipidstoffwechsels gehören jene die verantwortlich sind für die Expression von LPL, Fettsäure-Transport-Protein,

Glycerol-Transporter Aquaporin 7, *adipocyte Protein-2* (aP2), *phosphoenolpyruvate carboxykinase* (PEPCK) und *scavanger receptor CD36*[48]. Eine verbesserte Insulinsensivität bewirkt die Aktivierung von PPARγ zudem durch eine *de novo* Differenzierung von großen Adipocyten zu kleineren, in der Summe sensitiveren Adipocyten[50]. Die endokrinen Funktionen des Fettgewebes werden durch PPARγ ebenfalls beeinflusst: So wird die Expression des Peptidhormones Adiponectin gefördert, dessen Blutspiegel direkt mit der Insulinsensitivität und indirekt mit der Gesamtmasse an Fettgewebe korreliert[51,52]. Die Pathogenese der Insulinresistenz ist verbunden mit der Infiltration des Fettgewebes durch Makrophagen und deren Produktion von Entzündungsmediatoren wie Tumor-Nekrose-Faktor α (TNFα) und den Interleukinen (IL) IL-1β und IL-6[53]. Während der Differenzierung von Monocyten zu Makrophagen und in aktivierten Makrophagen wird PPARγ verstärkt exprimiert[54]. Diese Differenzierung kann einerseits klassisch zu inflammatorischen M1-Makrophagen führen, andererseits jedoch auch zu alternativ-aktivierten antiinflammatorischen M2-Makrophagen, wobei letzterer Prozess von PPARγ vermittelt wird[55]. Die beeinflussten Gene in myeloiden Zellen (v.a. Makrophagen und dendritische Zellen) gleichen weitgehend denen in Adipocyten[56]. In atherosklerotischen Läsionen wurde eine direkte Korrelation von M2-Makrophagen und der PPARγ-Expression nachgewiesen[57]. Zudem unterdrückt PPARγ in glatten Gefäßmuskelzellen die Expression von TNFα[58]. Folgerichtig konnte basierend auf diesen molekular-pharmakologischen Ergebnissen eine antiatherosklerotische Wirksamkeit von PPARγ-Aktivatoren im Tiermodell beobachtet werden[59]. Bei der Bewertung ist allerdings zu beachten, dass die Kontrolle von inflammatorischen Genen von vielen nukleären Rezeptoren vermittelt wird und die beeinflussten Signaltransduktionswege möglicherweise redundant aktiviert werden können, was insbesondere für die Erklärung und Adressierung therapeutischer Phänomene wichtig ist[60].

Aufgrund seiner Aktivität bei der Ausdifferenzierung von Adipocyten lag es nahe, den Einfluss von PPARγ auf die Tumorgenese zu untersuchen. Für eine Reihe von Tumorzellen verschiedener Genese wurden wachstumshemmende und/oder differenzierungsfördernde Wirkungen durch PPARγ-Aktivatoren nachgewiesen. Da allerdings möglicherweise auch *off-target* Effekte mit erfasst wurden, gibt es bis heute keinen klaren Konsensus über die Relation von Tumorwachstum und PPARγ[48,61].

Abb. 6: Auswirkungen der PPARγ-Aktivierung auf endokrine Mediatoren des Fettgewebes („Adipokine“) und daraus resultierend auf andere Organe.

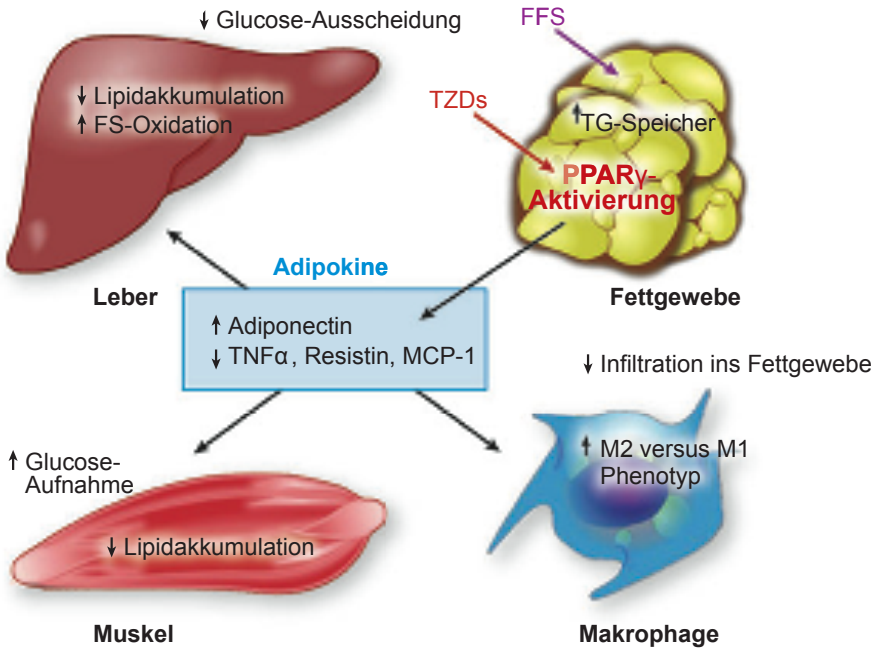

2.1.2. Medizinische Chemie

2.1.2.1. Natürliche Liganden und allgemeine Struktur synthetischer Liganden

Als endogene Liganden von PPAR sind eine strukturell relativ heterogene Gruppe von Fettsäuren und deren Derivaten bekannt, wenngleich die *in vivo*-Funktionen zellulär auftretender PPAR-Aktivatoren noch weitgehend unerforscht sind. Da die physiologische Funktion in der Lipidhomöostase zuerst aufgeklärt wurde, war das Konzept von PPARs als Fettsäure-Rezeptor naheliegend. Die ersten Erkenntnisse wurden mit Hilfe fraktionierten menschlichen Serums an PPARα gewonnen; es konnten Palmitinsäure, Ölsäure, Linolsäure und Arachidonsäure als Aktivatoren identifiziert werden[62]. Aufgrund der hohen Aktivierungskonzentrationen und schlechten biophysikalischen Eigenschaften sind Fettsäuren jedoch für ein auf Ligandenbindung basiertes Assaysystem wenig geeignet. Ein breites Screening von Fettsäuren gelang schließlich *Xu et al.* mit Hilfe eines Verdrängungsassays unter Verwendung synthetischer Radioliganden[11]. Eine Vielzahl von Fettsäuren zeigte

Affinität, dennoch wird in der Literatur die Rolle von PPAR viel mehr als Lipidsensor denn als Fettsäure-Rezeptor diskutiert[63]. Die wichtigsten Gründe für immer noch vorherrschende Kontroversität sind die *in vivo*-Übertragbarkeit von Ergebnissen aus funktionellen Assays mit überexprimierten Rezeptoren, die intrazelluläre Lokalisation von PPAR (mit der daraus folgenden Schwierigkeit der intrazellulären Konzentrationsbestimmung eventueller Liganden) und nachgewiesene Lipid-mediatoren die PPAR zwar aktivieren, aber nicht direkt binden bzw. eine Reihe mit PPAR verschalteter Targets parallel aktivieren[63].

Die drei PPAR-Subtypen unterscheiden sich im Hinblick auf ihr Profil an bindenden Fettsäuren: Die Selektivität nimmt in der Reihe PPARα-PPARβ-PPARγ zu. Während PPARα mit gesättigten und ungesättigten Fettsäuren interagiert, bindet PPARγ nur einige ungesättigte Fettsäuren (siehe Abb. 7).

Abb. 7: Fettsäuren als endogene Liganden von PPAR.

Die Bindung an PPARγ nimmt mit dem Grad der Unsättigung zu. Die Zahlenwerte geben den IC50 [µM] für den jeweiligen PPAR-Subtyp an, bestimmt im Verdrängungsassay mit synthetischen Radioliganden[11].

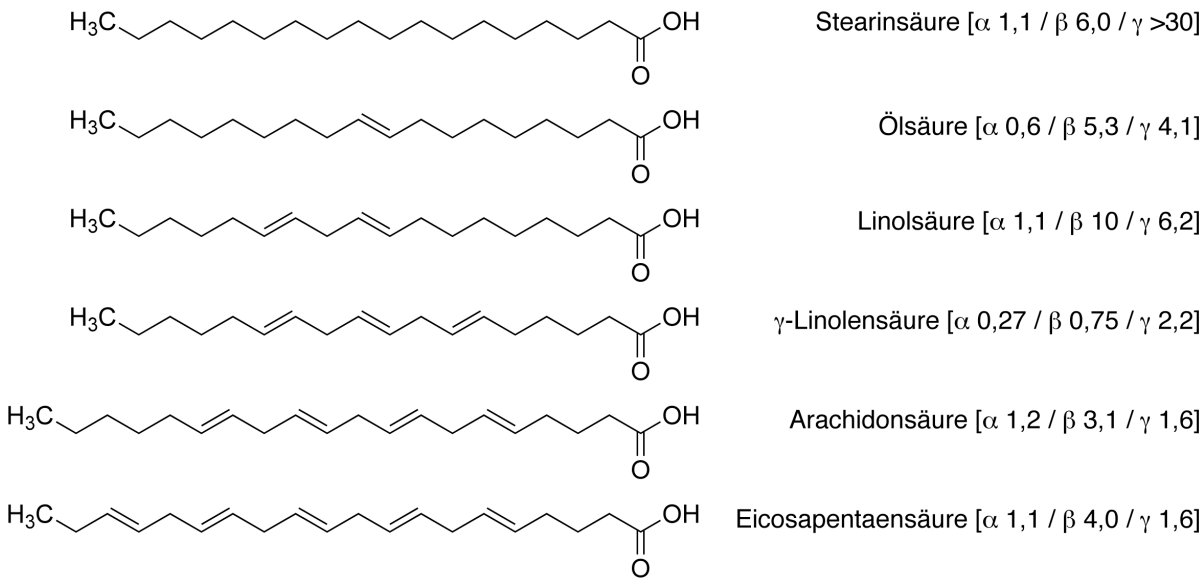

Erwähnenswert ist weiterhin, dass diverse Stoffwechselprodukte der Arachidonsäure, gebildet durch den 5-Lipoxygenase (5-LO)- und Cyclooxygenase (COX)-Biosyntheseweg, als Aktivatoren von PPARα und PPARγ nachgewiesen wurden. Dies sind beispielsweise die Prostaglandine (PG) 15d-PGJ_2 und PGD_1/

PGD_2 aus dem COX-*pathway* (als PPARγ-Aktivatoren) und die Leukotriene (LT) 8(*S*)-HETE (PPARα), 9-HODE, 13-HODE und 15-HETE (jeweils PPARα/γ) als 5-LO-Produkte[64,65]. Bei der Interpretation dieser Ergebnisse ist allerdings zu berücksichtigen, dass die G-Protein-gekoppelten Rezeptoren der PG und LT weitaus niedrigere Konzentrationen für ihre Aktivierung benötigen als für eine Aktivierung von PPAR erforderlich ist. Hinzu kommt, dass diese Eicosanoide proinflammatorisch wirken wohingegen für PPAR-Aktivierung ein antiinflammatorischer Effekt belegt ist[63].

2.1.2.2. Ligandenbindung

Verglichen mit den endogenen Liganden ist die Situation bei synthetischen PPAR-Agonisten weitaus klarer und deren Strukur-Wirkungs-Beziehungen (*structure-activity relationships*, SAR) und physiologische Effekte sind gut erforscht. Basierend auf den Fettsäuren als endogene Liganden haben alle synthetischen PPAR-Agonisten einen vergleichbaren Aufbau als Fettsäure-Mimetika, bestehend aus einer aciden Kopfgruppe und einem variierenden lipophilen Rest. Einen Vorschlag für eine generelle Grundstruktur von PPAR-Agonisten lieferten u.a. *Kuhn et al.* (siehe Abb. 8). Dieser wurde um die Hauptdeterminanten des Selektivitätsprofiles erweitert und ist der weiteren Diskussion zugrunde gelegt[66].

Abb. 8: Generelle Struktur synthetischer PPAR-Agonisten abgewandelt nach *Kuhn et al.*[66].

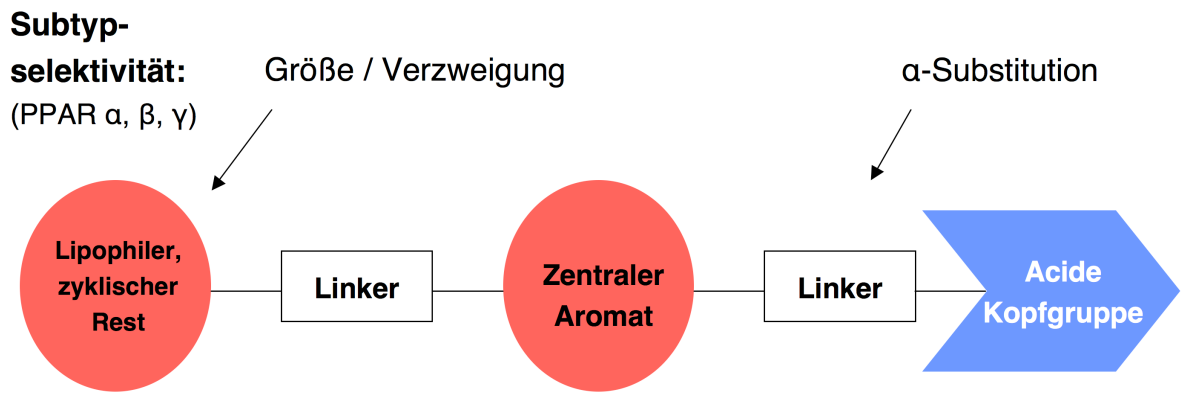

Die Bindemodi von endogenen wie auch synthetischen PPAR-Agonisten wurden durch eine Reihe von publizierten Kristallstrukturen aufgeklärt. Basierend darauf können detaillierte SAR erfasst und mit Hilfe von Docking-Methoden auch Bindemodi

mit hoher Wahrscheinlichkeit vorhergesagt werden. Wie bereits in Kapitel 2.1.1.1. erwähnt, existiert ein über alle Subtypen konserviertes Netzwerk von vier polaren Aminosäuren (vgl. Tab. 1), über die die Bindung der essenziellen aciden Kopfgruppe des Liganden und die folgende Aktivierung des Rezeptors durch Stabilisierung der aktiven Konformation der AF2-Helix erfolgt (vgl. Abb. 9 und 10). Dieser Bereich ist die einzige hydrophile Region im Inneren der PPAR-LBD und bildet somit die Grundlage dafür, dass die Liganden mit Ausnahme der aciden Kopfgruppe einen lipophilen Charakter besitzen (vgl. Abb. 8 und 10).

Für die Unterteilung der hydrophoben Regionen der Bindetasche existieren in der Literatur mehrere Vorschläge, im Folgenden wird derjenige von *Pirard* diskutiert und für die Interpretation von SAR zugrunde gelegt[67]. Dieser schlägt eine Unterteilung in eine linke und rechte distale Bindetasche ergänzt durch eine linke proximale Seitentasche (relevant vor allem bei PPARα und PPARγ) vor (vgl. Abb. 9). Deren Charakter beachtend werden hydrophobe und sterische Interaktionen als Hauptdeterminanten für die Subtypselektivität genannt.

Die erste wichtige Möglichkeit, die Affinität zu den einzelnen Subtypen zu beeinflussen, besteht in der Einführung von lipophilen Substituenten (z.B. Alkylketten, Aromaten) in räumlicher Nähe (meist in α-Position) zur aciden Kopfgruppe (meist eine Carbonsäure). Möglich sind außerdem unterschiedlich raumgreifende Bioisostere der aciden Kopfgruppe. Zugrundeliegend sind Subtyp-abhängig die einzelnen Aminosäuren der linken proximalen Seitentasche und der polaren Region. Im Fall von PPARβ werden durch das vergleichsweise große Met453 (Val444 bei PPARα bzw. Leu453 bei PPARγ) keine größeren α-Substituenten als Dimethyl toleriert und somit wird die linke proximale Seitentasche nicht besetzt[68]. Die größten Substituenten erlaubt PPARγ. Dies ist durch den Ersatz von Gly284 durch das größere Cys275 bei PPARα sowie die Möglichkeit von π-π-Interaktionen mit Phe363 (Ile354 bei PPARα) im Inneren der Tasche erklärbar[69,70]. In der polaren Region bei PPARγ ist durch den kleineren Histidinrest 323 (vgl. PPARα Tyr314) deren Besetzung mit raumgreifenden aciden Kopfgruppen (z.B. Thiazolidindion) möglich, woraus eine Selektivität für diesen Subtyp resultiert[8].

Durch Einführung von Substituenten in α-Position zur aciden Kopfgruppe erzeugen diese zumeist ein Chiralitätszentrum. In der Folge kommt es zu unterschiedlichen Bindemodi der einzelnen Enantiomere. Dies ist bedingt durch einen differierenden Grad der Stabilisierung der für die Aktivierung essenziellen Helix-12, auf Grund

dessen sich die einzelnen Enantiomere abhängig von der Größe des α-Substituenten in ihrer Potenz und in ihrem maximalen Aktivierungsgrad unterscheiden[71].

Die meisten PPAR-Agonisten binden mit ihrem raumgreifenden lipophilen Molekülteil in der linken distalen Tasche. In dessen Variation besteht neben der Einführung von α-Substituenten eine zweite wichtige Möglichkeit, die Subtypselektivität zu beeinflussen. Als wichtige begrenzende und differenzierende Aminosäuren schlägt *Pirard* hier für PPARα Ile272 und Met330 (entsprechend Ile281 und Val 339 bei PPARγ) vor, im Fall von dem nicht direkt vergleichbaren PPARβ werden Leu262 und Arg284 genannt[67]. Neue Einblicke in mögliche Ligand-Rezeptor-Interaktionen im Inneren der PPAR-LBD gewährte die 2007 von *Sierra et al.* publizierte Kristallstruktur von PPARα mit dem Agonisten GW590735 (Struktur siehe Tab. 3): Dieser besitzt als Linker im linken Teil des Moleküles (vgl. Abb. 8) eine Carbonsäureamid-Funktion, deren Carbonyl-Sauerstoff unter Zuhilfenahme zweier Wassermoleküle mit Ser280 und Thr283 Wasserstoffbrücken ausbildet und deren NH-Gruppe durch die umgebenden schwefelhaltigen Aminosäuren Cys276, Met355 und Met330 stabilisiert wird. Eine Subtyp-spezifische Substituenteninteraktion in diesem Bereich wird durch Met330 (Leucin bei PPARβ, Valin bei PPARγ) möglich. Zusammenfassend geben diese Interaktionen einen plausiblen Erklärungsansatz für die über 500-fache Selektivität von GW590735 für PPARα[9].

Nichtsdestotrotz sind zielgerichtete Interaktionen in den distalen Bindetaschen noch nicht in ihrer Gesamtheit erforscht und bieten ein großes Potenzial beim Design neuer PPAR-Agonisten mit determiniertem Selektivitätsprofil.

Abb. 9: Bindung des Agonisten Tesaglitazar (Struktur vgl. Kap. 2.1.2.3. (d)) an PPARα.

Einteilung der PPARα-LBD in drei hydrophobe Bindetaschen (links proximal und distal, rechts distal) nach *Pirard* und Ausbildung des charakteristischen Wasserstoffbrückennetzwerkes der aciden Kopfgruppe mit den Aminosäuren der polaren Region (erstellt von Dr. Ewgenij Proschak) [13, 67].

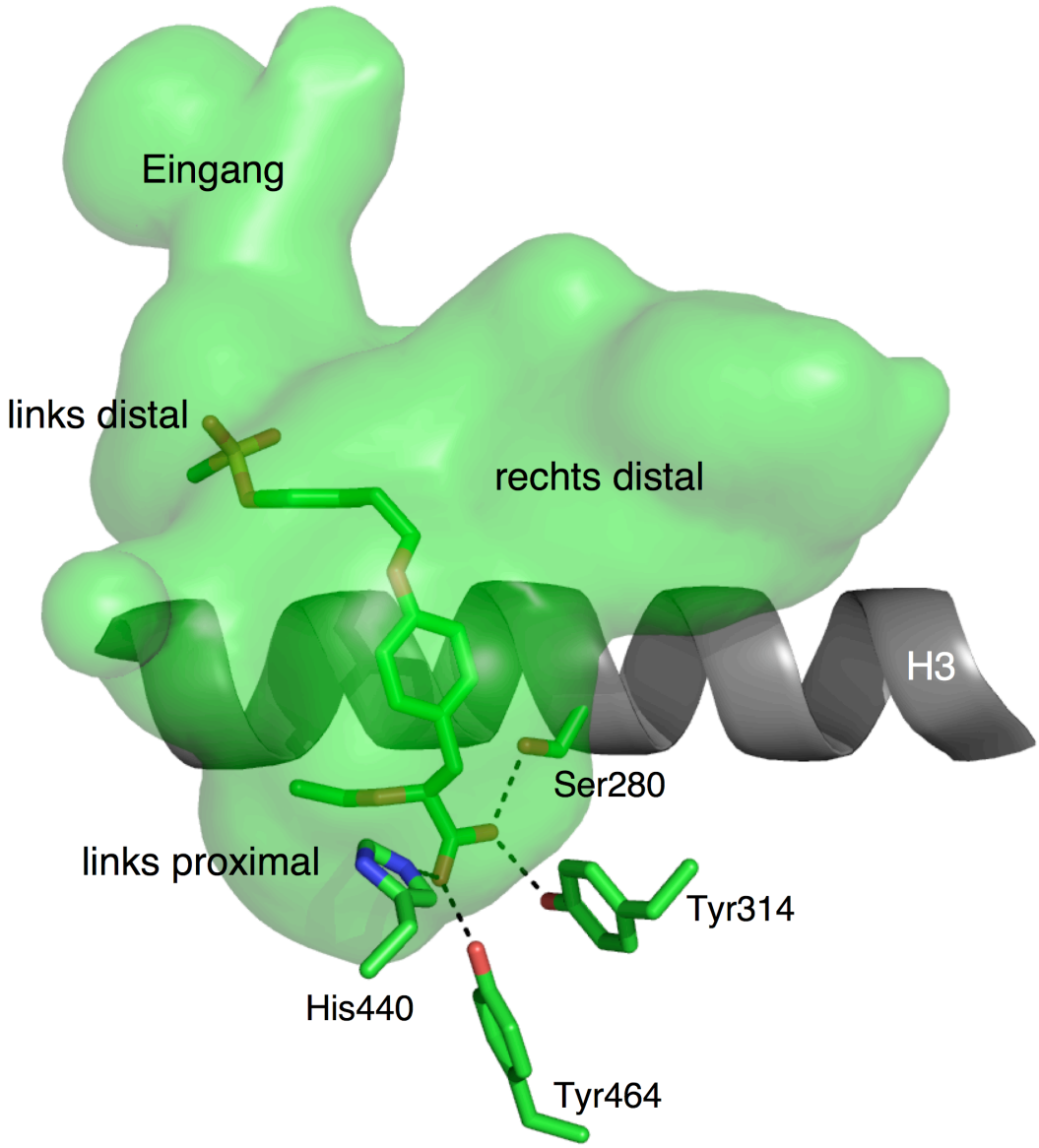

Abb. 10: Vergleichende Darstellung der Ligandenbindung an PPARα und PPARγ.

Bindung eines Fibrates (Strukturen vgl. Kap. 2.1.2.3. (a)) an PPARα und von Rosiglitazon (Struktur vgl. Kap. 2.1.2.3. (c)) an PPARγ und mit Ausbildung des charakteristischen Wasserstoff–brückennetzwerkes (erstellt von Prof. Dr. Dieter Steinhilber).

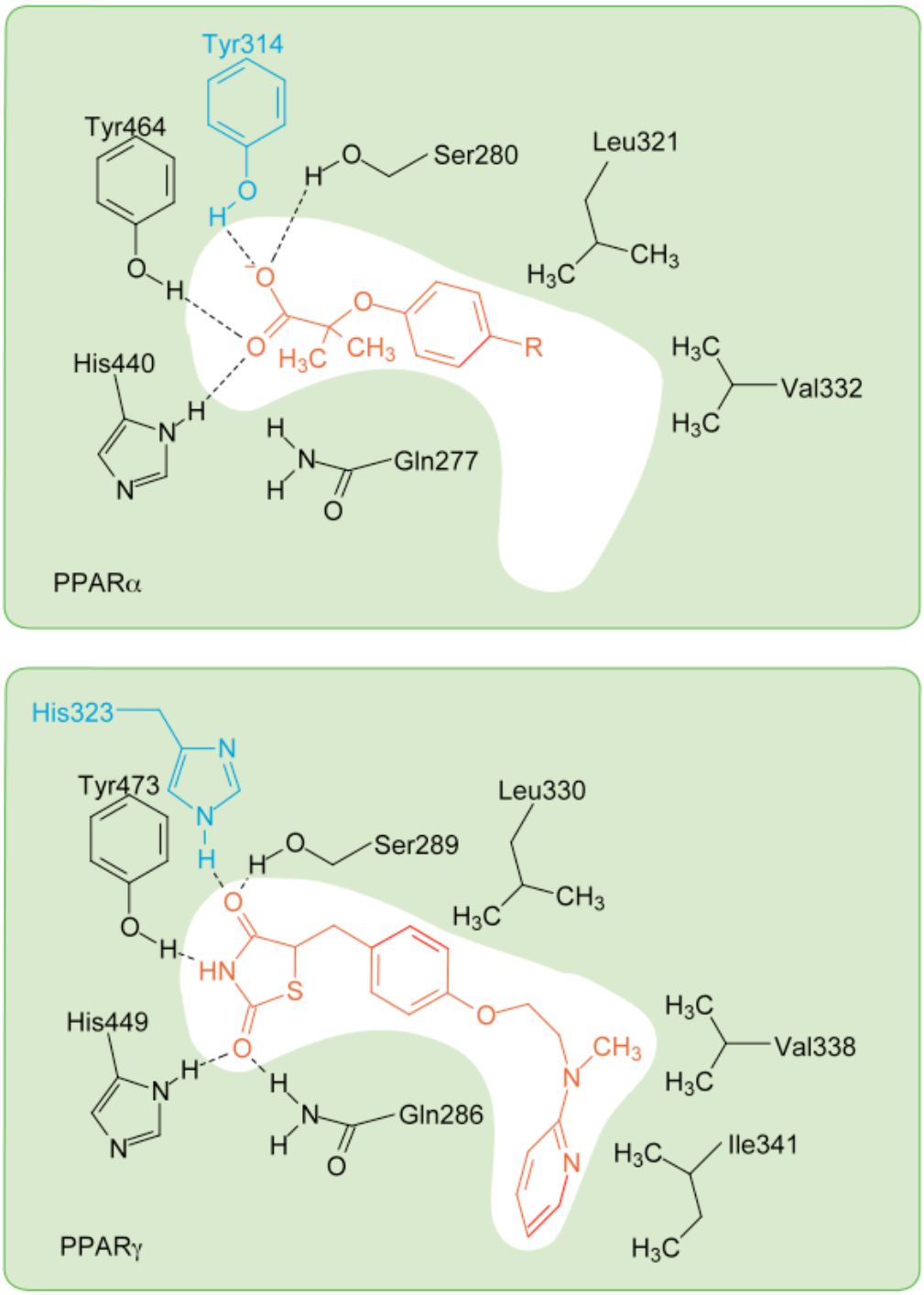

2.1.2.3. Struktur-Wirkungs-Beziehungen bekannter PPAR-Aktivatoren

(a) PPARα-Agonisten: Fibrate und Weiterentwicklungen

Die ersten PPAR-Agonisten, die seit Ende der 1960er Jahre lange vor der Entdeckung ihres Wirkmechanismus therapeutisch zur Behandlung von Dyslipidämien eingesetzt wurden, sind die als Fibrate bezeichneten PPARα-Agonisten. Charakteristisch für die Fibrate ist die Partialstruktur der 2-Hydroxy-2-methyl-propionsäure als acide Kopfgruppe, die mit lipophilen aromatischen Substituenten verethert ist. Bei der Betrachtung der im zellulären Assay am humanen PPAR erhaltenen EC_{50}-Werte fällt auf, dass diese Verbindungen nur im mittleren mikromolaren Bereich aktiv sind und somit lediglich als schwach wirksam eingestuft werden können. Clofibrat und Fenofibrat besitzen eine rund 10-fache Selektivität für PPARα versus PPARγ, wohingegen Bezafibrat vielmehr als *pan*-Agonist denn als PPARα-Agonist zu bezeichnen ist, da er alle Subtypen in vergleichbaren Konzentrationen aktiviert (siehe Tab. 2). Ein weiteres therapeutisch eingesetztes Fibrat ist das 2,2-Dimethylpentansäurederivat Gemfibrozil, dessen EC_{50}-Werte im Bereich von Fenofibrat liegen[72].

Tab. 2: Übersicht über die Fibrate und deren EC_{50}-Werte bestimmt in einem zellulären PPAR-GAL4 Transaktivations-Assay[73]. (ia: inaktiv)

Substanz	Struktur	PPAR EC_{50} [µM]		
		α	β	γ
Clofibrat	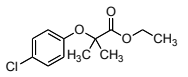	**55**	**ia**	**~500**
Fenofibrat	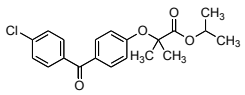	**30**	**ia**	**300**
Bezafibrat	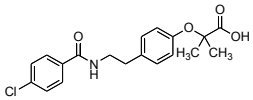	**50**	**20**	**60**

Als Referenzsubstanz für PPARα-Agonisten wird in zellulären Assaysystemen vielfach Pirinixinsäure (Synonym WY14,643) eingesetzt, die als Leitstruktur auch Grundlage für die in dieser Arbeit vorgestellten Verbindungen ist. Pirinixinsäure ist ein 2-Thioessigsäurederivat mit einem Pyrimidin als zentralem Aromat und daran

substituiert einem charakteristischen 2,3-Dimethylanilin-Strukturelement (vgl. nachfolgende Struktur, EC_{50}-Werte nach *Rau et al.*[74]). Die Synthese wie auch die lipidsenkenden Eigenschaften wurden erstmals 1984 von *d`Atri et al.* beschrieben[75].

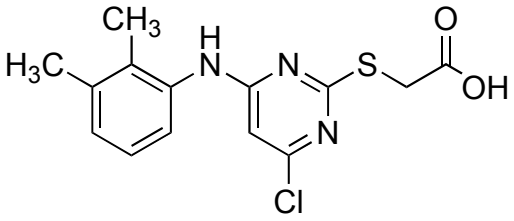

Pirinixinsäure

PPARα	36 μM
PPARβ	ia
PPARγ	54 μM

Mit der Erforschung der biologischen Funktion von PPARα und insbesondere nach Publikation der Kristallstruktur sind in den letzten Jahren verbesserte, hochaktive und selektive PPARα-Agonisten publiziert worden[8]. Eine repräsentative Auswahl dieser Verbindungen ist in Tab. 3 vorgestellt, wobei bisher nur GW590735 und LY518674 die klinische Entwicklung erreichten[76]. Bei der Betrachtung dieser beiden Verbindungen fällt auf, dass die Fibrat-Grundstruktur in Form der aciden Kopfgruppe beibehalten wurde. Die Affinität für PPARα ist im Vergleich zu den klassischen Fibraten um ca. Faktor 1000 gestiegen, gleichzeitig können sie als selektiv aufgefasst werden. Es wurde jeweils eine Carbonsäureamid-Partialstruktur (im Fall von LY518674 als Teil des Heterozyklus) eingeführt, die jedoch invers zu der in Bezafibrat angeordnet ist (vgl. dazu in Kap. 2.1.2.2.) die Diskussion der Kristallstruktur von PPARα mit GW590735). Zusätzlich wurde die Struktur im linken Teil um einen *para*-substituierten Aromaten verlängert[9,77]. Von der Vielzahl an publizierten und *in vitro*-charakterisierten PPARα-Agonisten ist hier einer der bislang potentesten von *Desai et al.* dargestellt sowie derjenige von *Faucher et al.* mit einer neuartigen Sulfonsäureamid-Partialstruktur als acide Kopfgruppe (siehe Tab. 3)[78,79]. *Desai et al.* zeigen in ihrer Arbeit auch den Einfluss des Chiralitätszentrums ihrer Leitstruktur in α-Position zur Carbonsäure auf die PPAR-Aktivität und somit eine Optimierung der Fibrate durch Modifikation des α-Substituenten und des lipophilen linken Molekülteiles. *Faucher et al.* variierten die acide Kopfgruppe und fanden schließlich ein Trifluormethyl-substituiertes Sulfonsäureamid als ebenfalls nanomolar aktive Verbindung[79].

Tab. 3: Struktur neuartiger, hoch selektiver und potenter PPARα-Agonisten.

Die Entwicklung von GW590735 und LY518674 ist bis in die klinische Prüfung fortgeschritten[9,77]. Eine Weiterentwicklung der von Faucher et al. (2008) und Desai et al. (2003) publizierten Substanzen ist bis dato nicht berichtet[78,79]. (nb: nicht bestimmt, ia: inaktiv)

Substanz	Struktur	PPAR EC_{50} [µM]		
		α	β	γ
GW590735	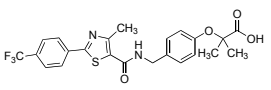	**0,004**	**2,83**	**>10**
LY518674	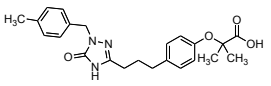	**0,046**	**>10**	**>10**
Faucher et al.	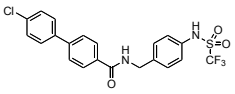	**0,005**	**>10**	**1,1**
Desai et al.	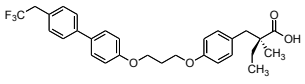	**>0,001**	**nb**	**ia**

(b) PPARβ-Agonisten

Mit der Erkenntnis, dass PPARβ an einer Vielzahl metabolischer Prozesse beteiligt ist, wuchs zunehmend auch das Interesse am Design selektiver PPARβ-Agonisten. Allerdings ist dieses Konzept durch mangelnde klinische Daten im Vergleich zu den anderen beiden Subtypen noch nicht ausgereift[40]. Strukturelles Kennzeichen der PPARβ-Agonisten ist eine „schlanke“ acide Kopfgruppe. Diese ist in der Regel realisiert durch eine α-unsubstituierte Carbonsäure. Beispielhaft gezeigt sei hier die klinisch am weitesten fortgeschrittene Substanz GW501516, beschrieben als selektiver PPARβ-Agonist mit einem EC_{50} von 1nM[43,76].

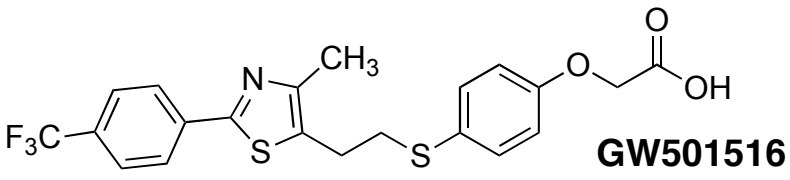

GW501516

(c) PPARγ-Agonisten: Thiazolidindione und selektive PPARγ-Modulatoren

Die neben den Fibraten zweite klinisch relevante Klasse von PPAR-Agonisten sind die PPARγ-aktivierenden Thiazolidindione (TZD; syn. Glitazone), die zur Behandlung des Typ 2 Diabetes mellitus (T2DM) eingesetzt werden. Die namensgebende acide Thiazolidindion-Kopfgruppe bewirkt durch ihren sterischen Anspruch in Kombination mit dem *para*-Substitutionsmuster des zentralen Aromaten die Subtypselektivität für PPARγ[80]. Die TZD Rosiglitazon und Pioglitazon sind in Deutschland zugelassen zur Therapie des T2DM als Monotherapie falls eine Gabe von Metformin nicht angezeigt ist sowie als Kombinationstherapie mit Metformin und Sulfonylharnstoffen bei unzureichender Blutzuckereinstellung. Troglitazon erreichte die Zulassung aufgrund seiner Lebertoxizität nie. Entstanden sind die TZD ursprünglich aus den Fibraten, wobei die α-Dimethyl-Carbonsäure durch bioisosteren Ersatz gegen den Thiazolidinon-Heterozyklus ausgetauscht wurde. Im rechten Teil sind die Moleküle strukturell identisch. Bei der Betrachtung des linken Teiles fällt der gemeinsame Pyridinring bei Rosiglitazon und Pioglitazon als möglicher Wasserstoffbrückenakzeptor auf. Alle in Tab. 4 gezeigten Verbindungen sind im nanomolaren Bereich aktiv und selektiv gegenüber PPARα und PPARβ.

Tab. 4: Thiazolidindione und deren *in vitro*-Aktivität[73].

Substanz	Struktur	PPAR EC_{50} [µM]		
		α	β	γ
Rosiglitazon	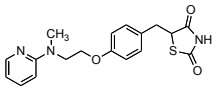	**ia**	**ia**	**0,043**
Pioglitazon	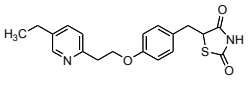	**ia**	**ia**	**0,58**
Troglitazon	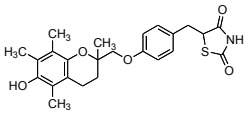	**ia**	**ia**	**0,55**

Da die als Volllagonisten wirkenden TZD mit Nebenwirkungen wie Ödembildung und Gewichtszunahme assoziiert sind, wird bei neuartigen Verbindungen zumeist das Konzept der selektiven PPARγ-Modulatoren (sPPARγM) angewendet (siehe Tab. 5).

Die Rationale bei dieser Klasse besteht darin, dass durch einen Partialagonismus, d.h. einer lediglich teilweisen und damit selektiveren Beeinflussung der nachgeschalteten Genregulation, das Nebenwirkungsprofil gegenüber den TZD verbessert werden soll. Adaptiert wurde dieses Konzept von Modulatoren der ebenfalls nukleären Estrogen-Rezeptoren (Tamoxifen und Raloxifen), die klare therapeutische Vorteile gegenüber Vollagonisten zeigen. Der erste sPPARγM war die 1999 publizierte Substanz GW0072, deren Partialagonismus mit lediglich 20% der maximalen Aktivierung eines Vollagonisten die Autoren anhand einer Kristallstruktur auf molekularer Ebene erklären konnten: GW0072 bindet an PPARγ in einer Weise, bei der die Helix-12 nicht stabilisiert wird und in der Folge keine Coaktivatoren rekrutiert werden können[81]. Ein vergleichbarer Bindemodus wurde auch für PA-082 vorgeschlagen, das aufgrund des Fehlens einer Säurefunktion kaum noch Ähnlichkeit mit der Grundstrukur bekannter PPAR-Aktivatoren besitzt[82]. Nähere Untersuchungen dieses Mechanismus ergaben, dass eine Wasserstoffbrücke zur Aminosäure Tyr473 für die Aktivierung der AF-2 Helix essenziell ist und diese bei sPPARγM nicht ausgebildet wird[83].

Der momentan in der klinischen Entwicklung am weitesten fortgeschrittene sPPARγM ist Metaglidasen (z.Zt. in Phase III), das (*S*)-Enantiomer der bereits in den 1970er Jahren klinisch untersuchten Substanz Halofenat. Metaglidasen ist ein schwacher PPARγ-Agonist (EC_{50}=10µM bei nur 15% max. Aktivierung) und kann durch seine hydrolyseempfindliche Carbonsäureesterstruktur als Prodrug angesehen werden. Nach erfolgter Bindung werden im Vergleich zu Rosiglitazon keine Coaktivatoren rekrutiert. Die Aktivierung von PPARγ erreicht Metaglidasen durch die Fähigkeit, Corepressoren aus dem PPAR/RXR-Komplex zu verdrängen[84].

Tab. 5: Selektive PPARγ-Modulatoren (sPPARγM) und deren *in vitro*-Aktivität an PPARγ.

Die prozentuale Aktivität bezieht sich auf die Aktivierung durch die Vollagonisten Rosiglitazon oder Pioglitazon[85].

Substanz	Struktur	EC_{50} [µM] % max. Aktivierung PPARγ
GW0072	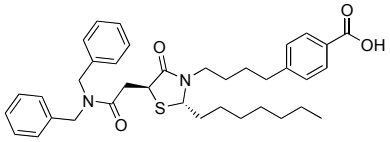	**0,2** max. = 20%
PA-082	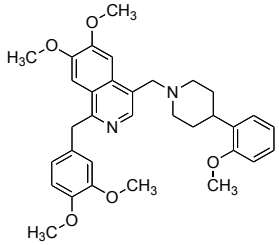	**0,25** max. = 40%
Metaglidasen	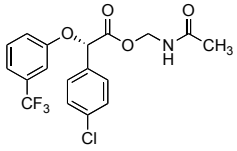	**10** max. = 15%

(d) Duale PPARα/γ-Agonisten: Glitazare

Basierend auf der häufigen Assoziation von Störungen des Lipid- und Glucosestoffwechsels im metabolischen Syndrom entstand der lukrative Ansatz, die therapeutischen Effekte der Fibrate mit denen der TZD durch dualen Agonismus an PPARα und PPARγ zu kombinieren. Da bis dato alle in diese Richtung entwickelten Substanzen aufgrund ihres Nebenwirkungsprofils in der Klinik gescheitert sind, bedarf dieses Konzept einer Weiterentwicklung, um zu sicheren dualen PPARα/γ-Agonisten zu gelangen.

Der medizinisch-chemische Ansatz war zunächst, durch die Vergrößerung des α-Substituenten die Fibrate an das Pharmakophor der TZD anzunähern und somit die Aktivität an PPARγ zu steigern[86]. So findet sich denn auch bei den meisten der als Glitazare bezeichneten dualen PPARα/γ-Agonisten eine α-substitierte Carbonsäure als acide Kopfgruppe (siehe Tab. 6). Neben Erhöhung der PPARγ-Aktivität

verhindert der α-Substituent gleichzeitig eine Bindung an PPARβ. Beachtenswert ist weiterhin das Strukturelement 5-Methyl-2-phenyloxazol des Muraglitazars, das sich bei vielen publizierten PPAR-Agonisten wiederfindet, und die Substanz MK0767. Sie zeigt, dass durch strukturelle Modifikationen auch Thiazolidindione PPARα-agonistisch wirken können. Im linken Molekülteil findet sich eine Carbonsäureamid-Partialstruktur, deren möglicher Beitrag zur PPARα-Aktivität von *Sierra et al.* dargelegt wurde und in Kapitel 2.1.2.2. diskutiert ist[9]. Im Hinblick auf das Selektivitätsprofil der bisher entwickelten Glitazare fällt auf, dass diese stets präferenziell PPARγ oder aber beide Subtypen balanciert aktivieren. Einen möglichen neuen Ansatz stellen PPARα-präferenzielle duale PPARα/γ-Agonisten dar, deren Nutzen-Risiko-Bewertung noch aussteht.

Tab. 6: Ausgewählte duale PPARα/γ-Agonisten (Glitazare) und deren *in vitro*-pharmakologische Charakterisierung[76].

Substanz	Struktur	PPAR EC_{50} [µM]	
		α	γ
Tesaglitazar	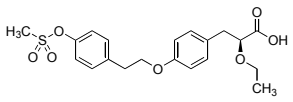	**1,2**	**1,3**
Muraglitazar	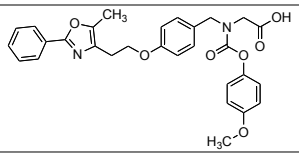	**0,32**	**0,11**
Ragaglitazar	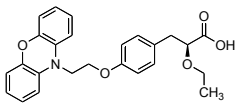	**0,98**	**0,09**
MK0767	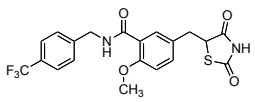	**0,15**	**0,08**

(e) *pan*-PPAR-Agonisten

Ein weiterer Kombinationsansatz ist die Aktivierung aller drei PPAR-Subtypen durch sogenannte *pan*-PPAR-Agonisten. Viel versprechende tierexperimentelle Daten liefert hier das 3-Indolylpropionsäurederivat Indeglitazar, dass außerdem das Konzept der selektiven PPAR-Modulation für PPARβ und PPARγ verwirklicht (EC_{50}-Werte siehe Abb.). Im Tiermodell zeigte Indeglitazar aufgrund seiner lediglich 45-

prozentigen Aktivierung von PPARγ nicht die Glitazon-typische Ödembildung mit assoziierter Gewichtszunahme bei gleichzeitiger effektiver Senkung von Blutglucose und wichtigen Lipidparametern. Aktuell befindet sich Indeglitazar in Phase II klinischer Entwicklung zur Therapie von Patienten mit T2DM[87].

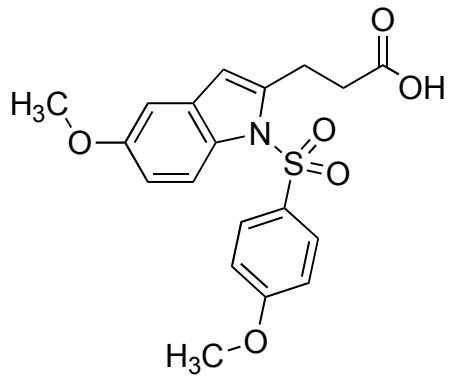

Indeglitazar

PPARα	0,99 μM
PPARβ	1,3 μM (67% max. Aktivierung)
PPARγ	0,85 μM (45% max. Aktivierung)

Es existieren ebenfalls Verbindungen mit den Kombinationsansätzen PPARα/β und PPARβ/γ, klinische Studien zu deren Wirksamkeit und Unbedenklichkeit stehen allerdings noch aus.

2.1.3. Klinische Einsatzgebiete von PPAR-Aktivatoren

2.1.3.1. Status quo - Fibrate und Glitazone

Die Fibrate (Clofibrat, Fenofibrat, Bezafibrat und Gemfibrozil) sind in Deutschland zur Behandlung von bestimmten Dyslipidämien (Hypertriglyceridämie und gemischte Hyperlipidämie, falls eine Gegenanzeige für ein Statin vorliegt) zugelassen. Dyslipidämien gelten als primäre Risikofaktoren für die Entwicklung einer Atherosklerose mit schwerwiegenden kardiovaskulären Komplikationen als Folge. Nachdem die Fähigkeit der Fibrate, diverse proatherosklerotische Surrogatparameter (in erster Linie TG-Senkung, moderate HDL-Erhöhung) im Blut zu verbessern, bereits in den 1970er Jahren nachgewiesen wurde, folgten seit den 1990er Jahren große Endpunktstudien um die antiatherosklerotische Wirksamkeit zu beurteilen[88,89]. Eindeutig positive Ergebnisse lieferte die VA-HIT-Studie (Veteran`s Administration HDL Intervention Trial), bei der 2531 Patienten über 6 Jahre mit Gemfibrozil vs. Placebo behandelt wurden. Es konnte in der Verumgruppe eine statistisch signifikante Reduktion des relativen Risikos für nicht-tödlichen Herzinfarkt

bzw. Tod kardiovaskulärer Ursache um 22% gezeigt werden. Zur Interpretation ist anzumerken, dass die profitierenden Patienten zumeist eine bestehende kardiovaskuläre Erkrankung in Kombination mit Insulinresistenz hatten und keine Statin-Therapie erhielten. Als Hauptursache für die Wirksamkeit der Gemfibrozil-Therapie wurde die moderate Erhöhung (+6%) der abnormal erniedrigten HDL-Spiegel ausgemacht[90]. Die größte Fibrat-Studie (Fenofibrate Intervention and Event Lowering in Diabetes; FIELD) mit fast 10000 Patienten konnte hingegen keine statistisch signifikante Reduktion des kardiovaskulären Risikos zeigen[91]. Allerdings kam es in der FIELD-Studie zu einer Verfälschung der Ergebnisse, da Patienten der Placebogruppe während der Studie teilweise Statine erhielten[92]. Zusammenfassend kann man festhalten, dass die Fibrate proatherosklerotische Surrogatparameter erfolgreich senken, wogegen hinsichtlich der kardiovaskulären Endpunkte möglicherweise nur bestimmte noch detaillierter zu charakterisierende Subgruppen (Patienten mit assoziiertem metabolischen Syndrom bzw. Insulinresistenz) profitieren.

Die Glitazone Rosiglitazon und Pioglitazon werden auch als Insulin-Sensitizer bezeichnet. In Deutschland sind sie zur Behandlung des T2DM zugelassen (als Monotherapie bei einer Gegenanzeige für Metformin, als Zweifach- bzw. Dreifach-Kombinationstherapie mit Metformin bzw. Metformin und einem Sulfonylharnstoff). Die Wirksamkeit im Hinblick auf anerkannte Surrogatparameter des T2DM konnte für beide Vertreter in diversen Studien nachgewiesen werden. So reduzierte Pioglitazon bei Patienten mit T2DM im Vergleich zu Placebo Hämoglobin A1c (HbA_{1c}) um –1,4% und den postprandialen Glucosespiegel um –57,5mg/dl. Gleichzeitig konnte auch ein positiver Effekt auf Lipidparameter (Triglyceride –16,6%; HDL +12,6%) beobachtet werden[93]. In diesen ersten Studien kristallisierten sich jedoch auch die für die Substanzklasse charakteristischen Nebenwirkungen Ödembildung und Gewichtszunahme heraus[94]. Insbesondere die beobachtete Ödembildung hat eine bis heute anhaltende Diskussion und in der Folge große klinische Studien angestoßen, ob eine Therapie mit Glitazonen mit einem erhöhten kardiovaskulären Risiko einhergeht und welche Konsequenzen dies hat. Bei der näheren Untersuchung zeigt sich überraschenderweise, dass Rosiglitazon und Pioglitazon diesbezüglich unterschiedlich bewertet werden müssen. Eine Metaanalyse aus 2007 von *Nissen* und *Wolski* ergab eine Assoziation von Rosiglitazon mit einem signifikant erhöhten Risiko für Herzinfarkte und einem erhöhten Risiko für Tod kardiovaskulärer Ursache mit Borderline-Signifikanz[95]. Eine weitere Metaanalyse bestätigt zwar ein

erhöhtes Risiko für kardiovaskuläre Ereignisse, jedoch ohne Auswirkung auf vorzeitigen Tod[96]. Anders die Situation bei Pioglitazon: Hier ergab eine Metaanalyse ein signifikant vermindertes Risiko für Herzinfarkt, Schlaganfall und Tod. Einzig das Risiko für schweres Herzversagen wird durch Pioglitazon erhöht, wenngleich dies ohne Auswirkungen auf die Gesamtmortalität bleibt[97]. Mechanistisch konnte gezeigt werden, dass die Ödembildung auf eine durch PPARγ-Aktivierung induzierte erhöhte renale Na^+-Rückresorption im Sammelrohr zurückzuführen ist[98].

Ein interessanter Aspekt der Glitazone ist deren Fähigkeit, die Manifestation des T2DM zu verzögern[99]. Solch ein präventiver Effekt ist insbesondere für die Zulassungsbehörden eine Herausforderung, die Indikationen für eine Therapie mit Glitazonen so zu formulieren, dass Personen mit hohem Risiko für T2DM davon profitieren könnten[100].

2.1.3.2. Neue Strategien und Perspektive

Die logische Weiterentwicklung der etablierten PPAR-Agonisten sollte deren Kombination sein: Der duale Agonismus von PPARα und PPARγ verspricht positive Effekte zur Behandlung von Dyslipidämien und Insulinresistenz, die im Metabolischen Syndrom bei vielen Patienten assoziiert sind. Nach der International Diabetes Foundation (IDF) wird das Metabolische Syndrom als Zusammentreffen von Adipositas mit zwei weiteren Risikofaktoren wie T2DM, Dyslipidämie und Hypertonie definiert. In den USA wird das Metabolische Syndrom mittlerweile als Epidemie angesehen. Bei der Therapie ergibt sich aufgrund der Vielzahl an behandlungsbedürftigen einzelnen Risikofaktoren das Problem der Polypharmazie. Folglich sind neue Wirkstoffe mit der Fähigkeit, das Metabolische Syndrom in seiner pathologischen Gesamtheit zu verbessern, sehr vonnöten.
In der Tat sind die als Glitazare bezeichneten dualen PPARα/γ-Agonisten in der Lage, eine Vielzahl der kritischen Surrogatparameter des Metabolischen Syndromes zu verbessern. Beispielsweise konnte Muraglitazar in einer Studie versus Pioglitazon bei durch Metformin nicht optimal eingestellten Diabetikern HbA_{1c} (–1,14%) wie auch den Triglyceridspiegel (–28%) signifikant senken und gleichzeitg HDL-Cholesterol um 19% erhöhen. Allerdings traten die bekannten Nebenwirkungen der Glitazone (Ödembildung und Gewichtszunahme) bei diesen Substanzen verstärkt auf[101]. In einer folgenden Studie wurde das kardiovaskuläre Risiko von Muraglitazar schließlich eindeutig negativ bewertet, was zur Einstellung der klinischen

Entwicklung in Phase III führte. Das relative Risiko für Herzinfarkt, Schlaganfall oder Tod mit kardiovasklulärer Ursache betrug hier 2,23[102]. Ähnlich viel versprechende Ergebnisse lieferte anfangs Tesaglitazar, dessen Entwicklung jedoch schließlich aufgrund verminderter Creatinin-Clearance und glomerulärer Filtrationsrate eingestellt wurde[103,104]. Bei Ragaglitazar wurden verstärkt Tumore der Harnblase bei Ratten beobachtet, folglich scheiterte auch dessen klinische Entwicklung[105]. Es bleibt zunächst die Frage zu beantworten, welche der zum Abbruch der Studien führenden Nebenwirkungen der Substanzklasse und somit mechanistisch dem dualen PPARα/γ-Agonismus zuzuschreiben sind. Hier scheinen kardiovaskuläre Komplikationen das Hauptproblem zu sein, die vereinzelt beobachteten cancerogenen Effekte sind höchstwahrscheinlich substanzspezifisch[106]. Evidenz hierfür liefert auch die bei den Glitazonen aufgekommene Diskussion um die kardiovaskuläre Sicherheit, möglicherweise kommt es zu negativen supra-additiven Effekten durch die duale PPARα/γ-Aktivierung. Ein Schlüssel zu diesem Problem könnte im Selektivitätsprofil der bisher klinisch evaluierten Glitazare liegen (vgl. Kap. 2.1.2.3. (d)): Diese zeigen alle eine stärkere Aktivierung von PPARγ gegenüber PPARα (bei Tesaglitazar PPARα≈PPARγ). Klinisch wurden denn auch stets verstärkt die kardiovaskulär problematischen Nebenwirkungen beobachtet, die bereits von den Glitazonen bekannt und mit der PPARγ-Aktivierung assoziiert sind. Auswege könnten nun ein Selektivitätsprofil zugunsten von PPARα sowie die Anwendung des sPPARγM-Konzeptes auf duale PPARα/γ-Agonisten sein. Neuartige Substanzen, die sich insbesondere im Grenzbereich von PPARα-Selektivität und dualem PPARα-präferenziellem PPARα/γ-Agonismus bewegen, werden in dieser Arbeit vorgestellt.

Erwähnt seien des Weiteren die ebenfalls in klinischer Evaluation befindlichen Konzepte der sPPARγM und des *pan*-PPAR-Agonismus. Mit GW677954 (Struktur nicht bekannt) befindet sich ein *pan*-Agonist in laufender Phase II der klinischen Prüfung. Metaglidasen, ein sPPARγM in Phase II/III (vgl. 2.1.2.3. (c)), wird bei der Behandlung des T2DM als vergleichbar effektiv wie Rosiglitazon und Pioglitazon angegeben, jedoch mit vermindertem Risiko für Ödembildung und Gewichtszunahme[107].

Umfassend diskutiert sind die Neuentwicklungen im Bereich der PPAR-Agonisten außerdem im Review von *Rau und Zettl et al.*, der als Anhang I in dieser Arbeit abgedruckt ist[76].

2.2. mPGES-1 und 5-LO

2.2.1. Molekularbiologie und physiologische Funktionen

2.2.1.1. Struktureller Aufbau der mPGES-1 und der 5-LO

(a) mPGES-1

Nach ihrer Entdeckung im Jahr 1999 durch *Jakobsson et al.* erfolgte 2008 ein großer Durchbruch bei der Strukturaufklärung der mikrosomalen Prostaglandin E_2-Synthase-1: *Jegerschöld et al.* gelang die Herstellung von 2D-Kristallen der mPGES-1 als Komplex mit dem essentiellen Cofaktor Glutathion[108,109]. Deren Analyse mittels Elektronen-Kristallographie ergab detaillierte Einblicke in die Struktur des Enzymes. Als Mitglied der MAPEG (*Membrane Associated Proteins in Eicosanoid and Glutathione metabolism*)-Protein Familie bildet die mPGES-1 wie alle anderen strukturell charakterisierten Vertreter dieser Gruppe Homotrimere. Die Monomere sind aus 152 Aminosäuren aufgebaut, die sich zu vier transmembranären Helices (TM) von jeweils rund 30 Aminosäuren organsieren. Hinsichtlich ihrer Lokation in der Mikrosomenmembran sind TM-1 und TM-3 zum Lumen ausgerichtet, TM-2 und TM-4 hingegen zur cytosolischen Seite. TM-2 ist für die Trimerisierung verantwortlich, es bildet sich eine trichterartige Struktur die zur lumenalen Seite hin verschlossen ist. Durch zielgerichtete Mutagenese der mPGES-1 konnten die Aminosäuren Arg67, Glu77, Arg110 und Tyr117 hinsichtlich der Funktionalität als

essentiell nachgewiesen werden. In Analogie zur 2007 kristallisierten Leukotrien C4-Synthase (LTC4S) postulieren *Jegerschöld et al.* eine offene und eine geschlossene Konformation der mPGES-1. Dies wird durch die Flexibilität der TM-1 ermöglicht, die sich zur cytoplasmatischen Seite hin öffnet und gleichzeitig auch das aktive Zentrum beinhaltet [109,110].

Abb. 11: Trimere Struktur der mPGES-1.

Homologiemodell basierend auf der Struktur der Glutathionsynthase (erstellt von Dr.E.Proschak).

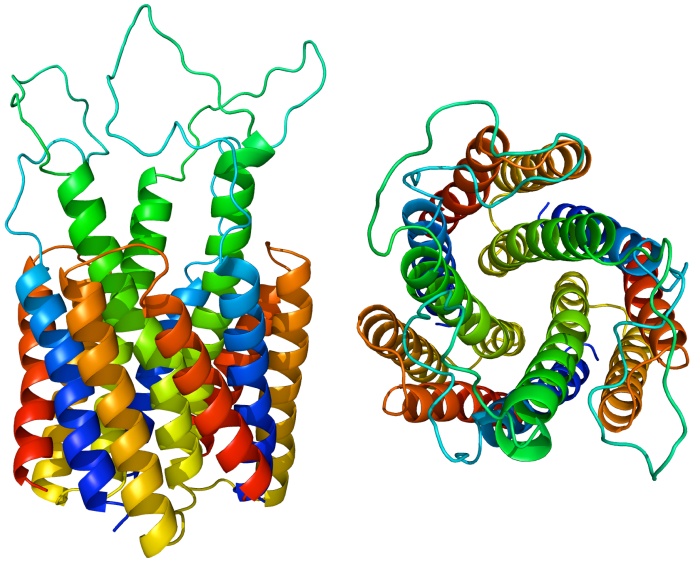

(b) 5-LO

Die humane 5-Lipoxygenase (5-LO) ist ein aus 672 oder 673 Aminosäuren bestehendes Enzym. Es existiert bis dato keine Kristallstruktur, allerdings wurde auf der Grundlage der kristallisierten 15-Lipoxygenase aus Kaninchen-Retikulozyten ein Homologiemodell erstellt (siehe Abb. 12) [111]. Danach ist die 5-LO ein monomeres Enzym mit einer größeren helikalen C-terminalen Domäne (Aminosäuren 121-673) und einer kleineren β-Faltblatt-artigen N-terminalen Domäne (Aminosäuren 1-114). Die C-terminale Domäne beinhaltet das katalytische Zentrum des Enzymes mit einem Eisen(II)-Ion, welches durch die Carboxylgruppe von Ile673, die Histidine His372, His367 und His550, das Asparagin Asn554 und ein Wassermolekül chelatartig verankert ist. Die N-terminale Domäne ist funktionell und strukturell mit C2-Domänen anderer Enzyme (z.B. cytosolische Phospholipase A_2, $cPLA_2$) vergleichbar und verantwortlich für die Bindung von Calcium und Lipiden an der

Zellmembran[112,113]. Die strukturelle Gemeinsamkeit der regulatorischen Domäne mit der *upstream* agierenden cPLA$_2$ ist auch die Voraussetzung für eine häufig beobachtete parallele Aktivierung beider Enzyme durch Stimuli der Leukotrien-Biosynthese.

Abb. 12: Homologiemodell der 5-LO basierend auf der Kristallstruktur der 15-LO[114].

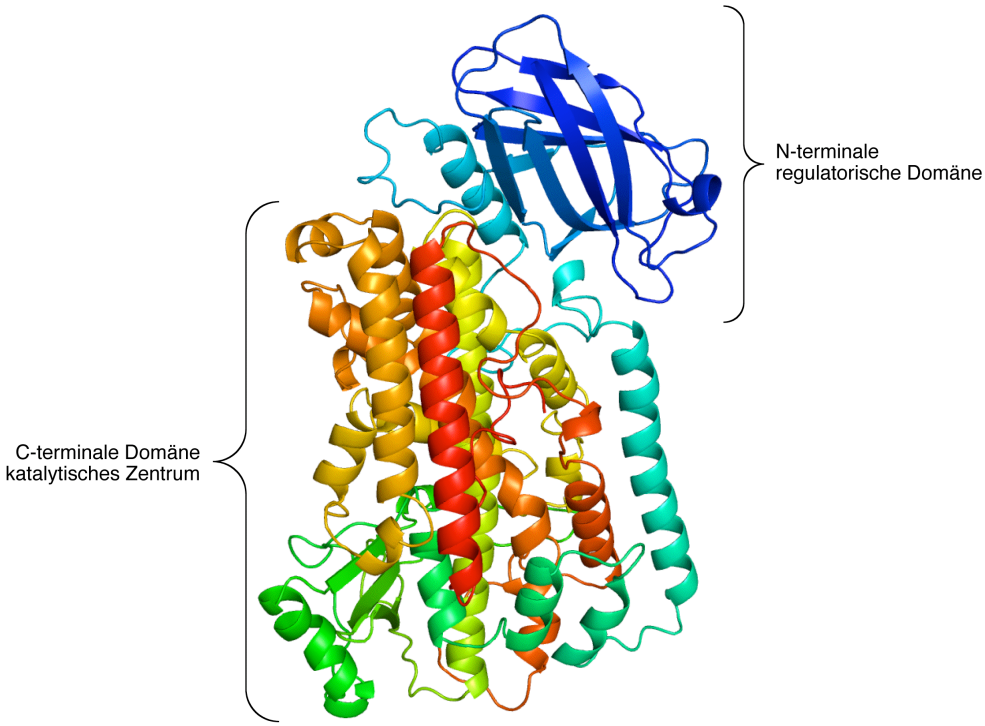

2.2.1.2. Funktion innerhalb der Arachidonsäurekaskade

Arachidonsäure (20:4ω6) (AA) ist der primäre und wichtigste Vorläufer von Eicosanoiden in Säugerzellen. Nach Stimulation der Zelle durch mechanische Traumata, spezifische Cytokine oder Wachstumsfaktoren wird AA aus zellulären Membranen durch Phospholipasen der A$_2$-Familie (PLA$_2$) freigesetzt. Danach erfolgt die Trennung in zwei unterschiedliche Signaltransduktionswege, aus denen mit den Prostaglandinen (PGs) und Leukotrienen (LTs) die beiden wichtigsten Klassen der Eicosanoide hervorgehen (siehe Abb. 13)[115].

Abb. 13: Schematische Übersicht der Arachidonsäurekaskade.

Die mPGES-1 und die 5-LO sind rot hervorgehoben sowie deren Substrate bzw. Produkte als Strukturformel dargestellt.

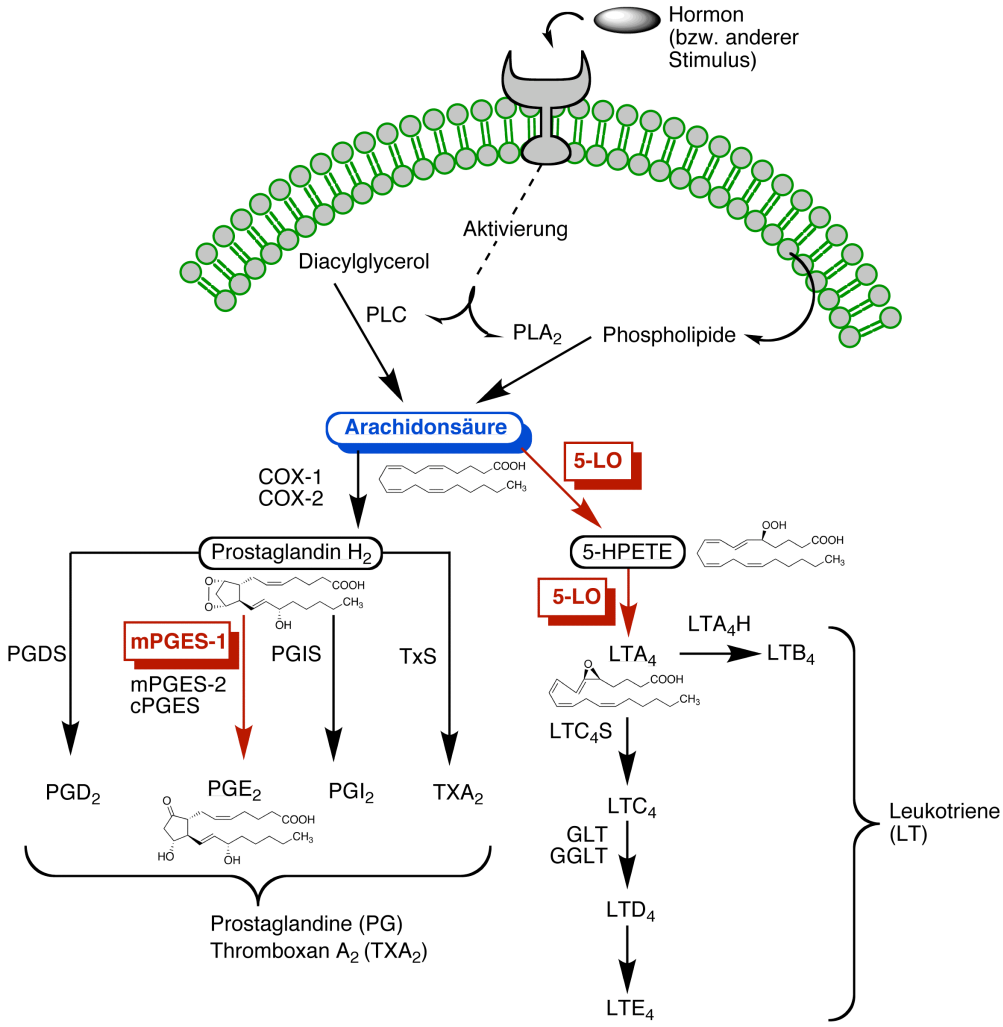

(a) mPGES-1

Prostaglandine werden in nahezu allen Zelltypen des menschlichen Körpers gebildet und fungieren als autokrine sowie parakrine Lipidmediatoren. Der erste Schritt der Prostaglandinbiosynthese wird von einem aus pharmakologischer Sicht äußert wichtigen Enzym katalysiert: der Cyclooxygenase. Diese existiert in zwei Isoformen (COX-1 und COX-2) und wird durch die Arzneistoffklassen der *non-steroidal antiinflammatory drugs* (NSAIDs) und der Coxibe (selektiv COX-2) inhibiert. COX bildet das intermediäre Endoperoxid Prostaglandin H_2 (PGH_2) ($t_{1/2}$=90-100s), dessen metabolisches Schicksal nun je nach Zelltyp intrinsisch entschieden wird[116]. So wird

beispielsweise in Thrombozyten und Makrophagen verstärkt proaggregatorisches Thromboxan A_2 gebildet. Für die Fragestellung dieser Arbeit ist jedoch die Biosynthese von proinflammatorischem Prostaglandin E_2 (PGE_2) und die daran beteiligten Enzyme von besonderem Interesse. PGE_2 wirkt durch die Bindung an spezifische G-Protein gekoppelte Rezeptoren, von denen vier Subtypen bekannt sind (EP_{1-4}). Hinsichtlich der PGE-Synthasen wurden insgesamt drei Isoformen identifiziert, von denen die cytosolische (cPGES) sowie die ebenfalls mikrosomale mPGES-2 konstitutiv exprimiert werden, wohingegen mPGES-1 hauptsächlich induzierbar ist. mPGES-1 katalysiert denn auch die Umsetzung jenem PGH_2, das durch die ebenfalls induzierbare, teilweise co-lokalisierte COX-2 bereitgestellt wird. Eine Hochregulation der mPGES-1 konnte in verschiedenen Entzündungs- und Tumormodellen beobachtet werden, folglich kommt es zu einer Induktion als Reaktion auf inflammatorische bzw. mitogene Stimuli[117,118]. So bewirkt eine Stimulation durch die Cytokine IL-1β oder TNFα eine erhöhte mPGES-1-Expression, die durch Glucocorticoide wie Dexamethason unterdrückt werden kann[119]. Mechanistisch kommt es zur Induktion durch die Aktivierung von *mitogen-activated protein* (MAP)-Kinasen, es konnte insbesondere die Beteiligung von Enzymen der *extracellular signal-regulated kinases* (Erk)-Subfamilie nachgewiesen werden [120]. Interessanterweise kann die PPARγ-Aktivierung die Induktion der mPGES-1 unterdrücken[121]. Dies geschieht über den die mPGES-1-Expression induzierenden Wachstumsfaktor *early growth response-1* (Egr-1), der durch PPARγ supprimiert und andererseits durch den proinflammatorischen Transkriptionsfaktor NF-κB induziert wird[122].

PGE_2 gilt als einer der wichtigsten Mediatoren von Fieber, Entzündung und Schmerz und spielt eine große Rolle bei der Pathogenese von rheumatoider Athritis und Osteoarthritis[123,124]. Bei Patienten mit aktiver rheumatoider Arthritis konnten in Synovialzellen besonders große Mengen an mPGES-1 nachgewiesen werden. Im Tiermodell geschah dies ebenfalls im ZNS nach proinflammatorischer Stimulation[125].

Zusammengenommen untermauern diese Ergebnisse die Attraktivität der mPGES-1 als pharmakologisches Target zur Intervention bei entzündlichen Erkrankungen (insbesondere aus dem rheumatoid-arthritischen Formenkreis). Der Bedarf an solchen neuen Therapiekonzepten wird besonders in dem Kontext deutlich, dass die Langzeittherapie mit *upstream* in der Arachidonsäurekaskade angreifenden NSAIDs und Coxibe mit einem erheblichen gastrointestinalem wie auch kardiovaskulärem

Risiko behaftet sind.

(b) 5-LO

Im Gegensatz zu den ubiquitären Prostaglandinen werden Leukotriene in erster Linie in inflammatorischen Zellen wie polymorphkernigen Leukocyten (PMNL), Makrophagen und Mastzellen gebildet. Die 5-LO ist eine nicht-Häm eisenhaltige Dioxygenase, die abhängig vom Zelltyp im Nukleus oder im Cytosol lokalisiert ist. In einem zweistufigen Mechanismus via intermediär gebildeter 5-HPETE katalysiert die 5-LO die Bildung von LTA_4, einem konjugierten Trien mit einer Epoxid-Partialstruktur (vgl. Abb. 12). Dieses wird sogleich zu LTB_4 oder LTC_4 metabolisiert, kann jedoch, wenn beispielsweise von Neutrophilen ins Plasma sezerniert, durch Albumin stabilisiert werden[126]. LTC_4 bildet zusmmen mit den *downstream* gebildeten LTD_4 und LTE_4 die Familie der Cysteinyl-Leukotriene (cysLT). Die Aktivierung der 5-LO wird hauptsächlich durch einen Anstieg der Calciumkonzentration und/oder Phosphorylierung, die durch MAP-Kinasen katalysiert wird, ausgelöst[127]. Für eine maximale Aktivität benötigt die 5-LO des Weiteren ATP (welches aber nicht hydrolisiert wird), stimuliert wird sie durch Phosphatidylcholin und Hydroperoxide von Fettsäuren[128]. Die Reaktion von endogen bereitgestellter AA zu LTA_4 findet an der Kernmembran statt und erfordert daher eine Migration der im Cytosol befindlichen 5-LO wie auch der $cPLA_2$ zum Nukleus. Den Transfer der AA von der $cPLA_2$ zur 5-LO übernimmt das *five lipoxygenase activating protein* (FLAP), durch dessen Inhibition die weitere Konversion durch die 5-LO komplett unterdrückt werden kann[129]. Möglich ist allerdings auch, dass exogene AA als Substrat dient. In diesem Fall findet die Reaktion im Cytosol statt[130].

Die von der 5-LO gebildeten LTs gelten als Entzündungsmediatoren und vermitteln unter anderem die Einwanderung von Phagozyten (LTB_4) sowie eine Erhöhung der Gefäßpermeabilität (LTC_4). Dies geschieht wie bei den PGs durch G-Protein gekoppelte Rezeptoren, von denen es je zwei für LTB_4 (BLT_1, BLT_2) und cysLT ($cysLT_1$, $cysLT_2$) gibt. Der hochaffine BLT_1 vermittelt insbesondere pro-inflammatorische Signale und Chemotaxis. $cysLT_1$ findet sich vor allem in der Lunge, wo eine Aktivierung zu Ödembildung, Bronchokonstruktion und Mucussekretion führt. Diese Eigenschaften machen den Rezeptor als Target für die Behandlung des Asthma bronchiale interessant, wofür $cysLT_1$-Antagonisten (z.B. Montelukast) auch therapeutisch verfügbar sind. Inhibition der *upstream* gelegenen 5-LO bewirkt somit eine Unterdrückung der Effekte von LTB_4 wie auch von LTC_4 und verspricht

ebenfalls einen (bereits durch Zileuton genutzten) therapeutischen Benefit bei Asthma bronchiale. Zusätzlich gibt es aber auch Evidenz für einen möglichen Einsatz bei kardiovaskulären Erkrankungen (Atherosklerose) und Tumorerkrankungen [131].

2.2.2. Medizinische Chemie

2.2.2.1. Strukur-Wirkungs-Beziehungen von mPGES-1-Inhibitoren

Die ersten identifizierten mPGES-1-Inhibitoren waren einige ungesättigte Fettsäuren (z.B. AA, Eicosapentaensäure) sowie bereits bekannte COX-Inhibitoren. Erwähnenswert sind hier Sulindac-Sulfid (IC_{50}=80µM) und NS-398 (siehe Tab. 7) [132]. Trotz schwacher Inhibition beider Substanzen lässt sich bereits ableiten, dass eine acide Funktion im Molekül erforderlich ist, wie sie sich auch beim natürlichen Substrat PGH_2 findet. Dies spricht zunächst auch für einen Angriff des Inhibitors an gleicher Stelle des Enzyms.

Der FLAP-Inhibitor MK-886 inhibiert mPGES-1 in niedrigen mikromolaren Konzentrationen und wurde als Leitstruktur von *Riendeau et al.* zur ersten nanomolar aktiven Klasse von selektiven mPGES-1-Inhibitoren optimiert (siehe Tab. 7) [133]. Die Rationale, einen FLAP-Inhibitor als Leitstruktur zu nutzen, bestand in der Tatsache, dass FLAP und mPGES-1 zu den Enzymen der MAPEG-Familie gehören, deren Mitglieder in ihrer Bindungsregion eine hoch konservierte Aminosäuresequenz aufweisen. Die MK-886-Derivate besitzen eine Fibrat-artige acide Kopfgruppe und einen zentralen Indol-Heterozyklus mit einem *p*-Chlorbenzyl-Substituenten am Stickstoff. Die Aktivitätssteigerung wurde letztendlich durch die Einführung von Biphenyl-Substituenten in 5-Position des Indol erreicht. Generell betrachtet besitzen diese Substanzen eine verzweigte, fettsäureartige Grundstruktur mit acider Kopfgruppe und großem lipophilen Rest. In zellulären Assays waren die MK-886-Derivate durch ihre hohe Plasmaproteinbindung jedoch weitaus schwächer aktiv als am rekombinanten Reinenzym. Daher konnte ihre *in vitro* beobachtete Selektivität *in vivo* nicht bestätigt werden und die Weiterentwicklung wurde in der Folge eingestellt [132].

Eine neuartige Gruppe von mPGES-1-Inhibitoren konnte durch ein *high throughput screening* von Merck Frosst indentifiziert werden: die Phenantrenimidazole [134]. Deren Struktur besitzt keinerlei Ähnlichkeit mit Fettsäuren legt eine andere Bindungsstelle

als die des natürlichen Substrates nahe. Der selektive, nanomolare mPGES-1 Inhibitor MF63 befindet sich derzeit in präklinischer Evaluation in diversen Schmerz- und Entzündungsmodellen ohne dabei die Nachteile der MK 886-Abkömmlinge zu zeigen [135].

Tab. 7: Auswahl bisher publizierter mPGES-1-Inhibitoren und deren *in vitro*-Aktivität (rekombinantes Reinenzym) [132].

Substanz	Struktur	IC_{50} [µM]
		mPGES-1
NS-398	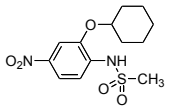	**20**
MK-886	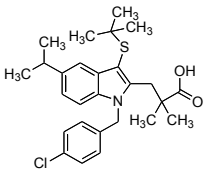	**1,6**
Riendeau et al.	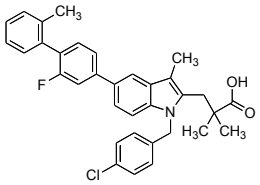	**0,003**
MF63	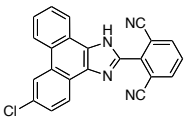	**0,001**

Der in klinischer Entwicklung am weitesten fortgeschrittene mPGES-1-Inhibitor ist Licofelone (IC_{50}-Werte siehe Abb.), obgleich diese Substanz ursprünglich als dualer COX/5-LO-Inhibitor konzipiert wurde. Neuere Untersuchungen ergaben, dass Licofelone selektiv COX-1 hemmt und die Suppression der PGE_2-Bildung anstelle der ursprünglich postulierten COX-2-Inhibition durch Blockade der mPGES-1 bewirkt wird [136]. Hinsichtlich der Inhibition der LT-Biosynthese erwies sich die ursprüngliche Charakterisierung als 5-LO-Inhibitor ebenfalls als inkorrekt, vielmehr konnte für Licofelone FLAP-Inhibition als hauptsächlicher Mechanismus nachgewiesen werden. Damit ist die Substanz wie das bereits diskutierte MK-886 ein dualer FLAP/

mPGES-1 Inhibitor[137].

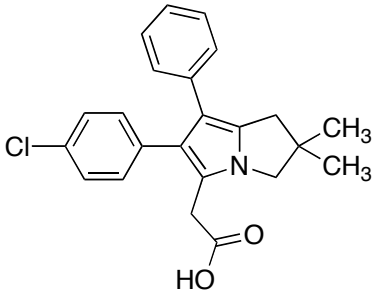

Licofelone

COX-1 0,6 μM
COX-2 >30 μM
mPGES-1 6μM
LT synth. 1,7μM

2.2.2.2. Struktur-Wirkungs-Beziehungen von 5-LO-Inhibitoren

5-LO-Inhibitoren können in drei Klassen eingeteilt werden: redoxaktive-, Eisenligand- und nicht-redoxaktive Inhibitoren. Als erstes wurden redoxaktive Substanzen wie Nordihydroguajaretsäure und Coumarinderivate identifiziert, die in den katalytischen Zyklus der 5-LO eingreifen und das zur Aktivierung essenzielle Eisen(III) reduzieren. Insbesondere aufgrund ihrer Unselektivität und den daraus resultierenden schweren Nebenwirkungen wie Methämoglobinbildung ist deren Entwicklung jedoch nicht weiter verfolgt worden.

Der einzige klinisch angewendete 5-LO-Inhibitor Zileuton, zugelassen in den USA zur Behandlung des Asthma bronchiale, gehört zur Klasse der Eisenligand-Inhibitoren (siehe Tab. 8). Diese wirken als Chelatbildner am zentralen Eisen-Ion und unterbrechen damit den katalytischen Zyklus. Chelatbildende funktionelle Gruppe ist hier eine *N*-Hydroxyharnstoff-Partialstruktur, ein bioisosterer Ersatz der metabolisch instabilen Hydroxamsäure. Limitierender Faktor ist für diese Substanzen wiederum das Nebenwirkungsprofil, was schließlich zur Entwicklung der nicht-redoxaktiven Inhibitoren führte. Repräsentanten dieser Klasse wie ZM 230487 und L-739,010 haben eine vergleichbare Struktur und sind in zellulären Testsystemen nanomolar aktiv (siehe Tab. 8). Charakteristisch für diese Verbindungen ist eine Tetrahydropyran-Partialstruktur, die in 4-Postition einen raumgreifenden aromatischen Substituenten trägt[138].

Tab. 8: Wichtige Eisenligand- und nicht-redoxaktive 5-LO-Inhibitoren und deren *in vitro*-Aktivität in zellulären Testsystemen (Zileuton: PMNL, andere: Granulozyten) [139, 140].

Substanz	Struktur	IC_{50} [µM]
		5-LO
Zileuton	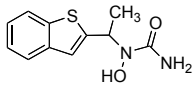	**0,4**
ZM 230487	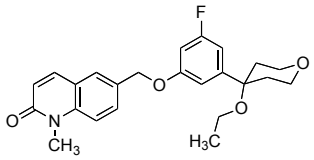	**0,05**
L-739,010	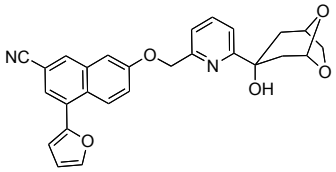	**0,02**

2.2.3. Klinische Perspektive von dualen mPGES-1/5-LO-Inhibitoren

Bei der bisherigen antiinflammatorischen Standardtherapie werden in erster Linie NSAIDs eingesetzt, die in die Arachidonsäurekaskade durch Inhibition der COX eingreifen. Während klassische NSAIDs sowohl die konstitutive COX-1 als auch die mehrheitlich induzierte COX-2 hemmen, sind deren Weiterentwicklung, die Coxibe, COX-2 selektiv. Aufgrund der durch die COX-1-Hemmung verminderten gastrointestinalen PG-Synthese können NSAIDs insbesondere bei Langzeittherapie schwerwiegende gastrointestinale Nebenwirkungen verursachen, die ein großes medizinisches wie auch sozio-ökonomisches Problem darstellen. Die ursprünglich zur Lösung dieses Problems entwickelten Coxibe besitzen zwar ein geringes ulcerogenes Potenzial, lenkten jedoch den Fokus auf eine weitere mögliche schwere Nebenwirkung durch COX-Inhibitoren: kardiovaskuläre Komplikationen. Dieses Risiko führte schließlich zur Marktrücknahme mehrerer Coxibe (lediglich Celecoxib und Etoricoxib sind verblieben) und wird auf eine Verschiebung des Prostacyclin/Thromboxan A_2-Gleichgewichtes zugunsten des proaggregatorischen Thromboxan A_2 zurückgeführt [141]. Nachfolgend begann auch eine Kontroverse über das

kardiovaskuläre Risiko der klassischen NSAIDs. Metaanalysen ergaben ebenfalls für Ibuprofen und Diclofenac eine Tendenz zu erhöhtem Herzinfarktrisiko, was auf die leicht blutdrucksteigernde Wirkung der NSAIDs zurückgeführt wird[142]. Vor diesem Hintergrund wird der Bedarf an neuen, sichereren antiinflammatorischen Therapieansätzen deutlich[143].

Als *downstream* von der COX agierendes Enzym katalysiert die induzierbare mPGES-1 lediglich die Bildung von proinflammatorischem PGE_2. Folglich bleibt die konstitutive PG-Synthese unbeeinflusst. Dies verspricht die Vermeidung der mit COX-Inhibitoren assoziierten Nebenwirkungen, wenngleich der klinische Beweis der Sicherheit sowie der antiinflammatorischen Wirksamkeit aufgrund der bis dato noch nicht ausreichend entwickelten selektiven mPGES-1-Inhibitoren noch aussteht. Die in Kap. 2.2.1.2. diskutierten Effekte in verschiedenen präklinischen Tiermodellen sind jedoch viel versprechend und mit der klinischen Entwicklung von selektiven mPGES-1-Inhibitoren ist in naher Zukunft zu rechnen[132].

Aufgrund der proinflammatorischen und ulcerogenen Eigenschaften der bei COX-Inhibition verstärkt produzierten Leukotriene wurde der Ansatz einer dualen COX/5-LO-Inhibtion entwickelt[144]. Solche Verbindungen konnten ihre antiinflammatorische Wirksamkeit in verschiedenen Tiermodellen nachweisen, doch wegen ihrer Unselektivität bzw. ihres Nebenwirkungsprofils gibt es gegenwärtig noch keinen zugelassenen Vertreter. Die duale mPGES-1/5-LO-Inhibition kann als Weiterentwicklung dieses Konzeptes angesehen werden, da sie selektiver in den PG-Stoffwechsel eingreift und ein verbessertes Nebenwirkungsspektrum verspricht. Erste entscheidende Aufschlüsse über eine duale Inhibition des PG- und LT-Stoffwechsels unter Einbeziehung der mPGES-1 wird hier das Schicksal von Licofelone geben, das sich momentan in Phase III klinischer Prüfung befindet (vgl. Kap. 2.2.2.1.)[145].

3. Ergebnisse & Diskussion

3.1. Struktur-Wirkungs-Beziehungen

3.1.1. PPAR

3.1.1.1. Pirinixinsäurederivate

Die vorgestellten Pirinixinsäurederivate sind Weiterentwicklungen basierend auf der Publikation von *Rau et al.*, wobei eine darin präsentierte Verbindung (**1**) zugleich Bestandteil dieser Arbeit ist[74]. Diese Publikation beinhaltet die systematische Untersuchung des Einflusses von *n*-alkyl-Substituenten in α-Position der Carboxygruppe von Pirinixinsäure auf die PPAR-Aktivität. Das Ergebnis ist eine Steigerung der Potenz an PPARα und PPARγ mit einem Optimum bei einer Kettenlänge von 4-6 Kohlenstoffatomen. Repräsentiert wird dies durch das α-*n*-Hexyl-substituierte **YS121** mit EC_{50}-Werten von 1,0µM für PPARα und 3,6µM für PPARγ (vgl. Tab. 9).

Darauf aufbauend war es das Ziel, die duale Aktivität an PPARα und PPARγ weiter zu erhöhen sowie Struktur-Wirkungs-Beziehungen im linken Molekülteil der Pirinixinsäure-Leitstruktur zu erheben. Zusätzlich wurde die hieraus erhaltene potenteste Verbindung in ihre Enantiomere getrennt, wodurch der Einfluss des Stereozentrums in α-Position zur Carbonsäure auf die PPAR-Aktivität spezifiziert werden konnte. Die Ergebnisse dieser Arbeit sind in Tab. 9 zusammengefasst (Originalarbeit siehe Anhang II,[146]). Ausnahmen bilden die in Tab. 9 ebenfalls aufgeführten Substanzen **10** und **11**, deren PPAR-Charakterisierung nicht publiziert ist (Synthese in Anhang IV,[147]).

Tab. 9: *In vitro*-pharmakologische Charakterisierung der Pirinixinsäurederivate an PPAR.

Substanz	Struktur	PPAR EC_{50} [µM]		
		α	β	γ
Pirinixin-säure	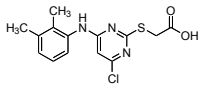	**39,8** ± 0,7 (100%)	**ia** [a)]	**53,7** ± 0,8 (79 ± 10%)
YS121	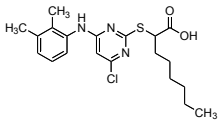	**1,0** ± 0,2 (146 ± 7%)	**ia** [a)]	**3,6** ± 0,2 (139 ± 35%)
1 (HZ47)	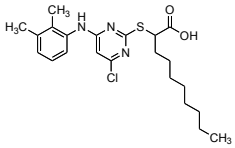	**2,0** ± 0,2 (114 ± 19%)	**nb**	**13,5** ± 1,3 (322 ± 50%)
2 (HZ09)	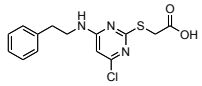	**ia**	**ia**	**ia**
3 (HZ20)	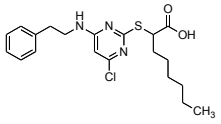	**12,9** ± 0,5 (279 ± 208%)	**ia** [a)]	**12,4** ± 1,3 (315 ± 237%)
4 (HZ10)	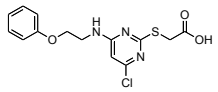	**ia**	**ia**	(17 ± 6%)
5 (HZ28)	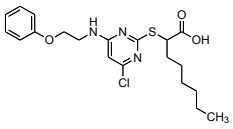	**6,7** ± 1,5 (125 ± 107%)	**ia** [b)]	**6,1** ± 0,2 (93 ± 12%)
6 (HZ42)	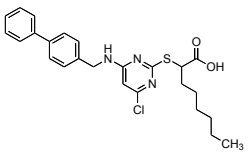	**6,0** ± 17,2 (71 ± 8%)	(82 ± 33%) [a)]	**12,2** ± 3,2 (225 ± 128%)
7 (HZ52)	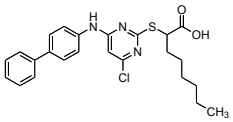	**0,32** ± 0,01 (141 ± 24%)	**ia** [b)]	**2,4** ± 0,1 (130 ± 42%)
8 (HZ65)	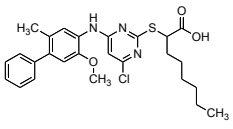	**0,63** ± 0,2 (138 ± 20%)	**ia** [b)]	**3,1** ± 0,5 (176 ± 3%)

Tab. 9 (Fortsetzung): *In vitro*-pharmakologische Charakterisierung der Pirinixinsäurederivate an PPAR.

Substanz	Struktur	PPAR EC_{50} [µM]		
		α	β	γ
9 (HZ56)	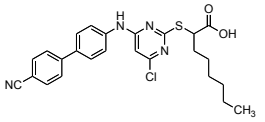	**0,19** ± 0,04 (155 ± 24%)	**ia** [b]	**1,5** ± 0,1 (134 ± 2%)
(***R***)**-9 (HZ56*R*)** ee=98,8%	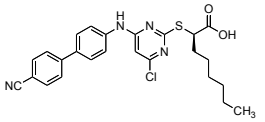	**0,03** ± 0,005 (113 ± 4%)	**ia** [b]	**1,1** ± 0,07 (123 ± 2%)
(***S***)**-9 (HZ56*S*)** ee=96,8%	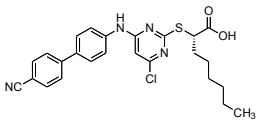	**2,2** ± 0,4 (147 ± 13%)	**ia** [b]	**3,4** ± 0,02 (143 ± 3%)
10 (HZ27)	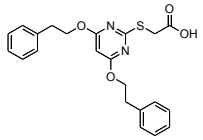	**ia** [b]	**ia** [a]	**3,7** ± 1,00 (111 ± 22%)
11 (HZ34)	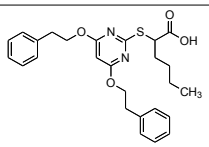	**ia** [b]	**ia** [a]	**8,3** ± 0,11 (61 ± 1%)

Die EC_{50}-Werte und Standardabweichungen sind basiert auf den Mittelwerten aus mindestens 3 Bestimmungen. Die Prozentwerte in Klammern geben die relative Aktivierung im Vergleich zur Positivkontrolle an. Im Fall von Substanzen ohne EC_{50}-Werte geben diese die prozentuale Aktivierung bei 100µM bzw. der angegebenen Konzentration an. Positivkontrollen sind 100µM Pirinixinsäure für PPARα, 1µM L165041 für PPARβ und 1µM Pioglitazon für PPARγ. ia: inaktiv bei 100µM oder bei angegebener Konzentration: a) bei 30µM, b) bei 10µM.

Nachdem die Einführung von Phenethyl- bzw. Phenoxyethyl-Substituenten (**2-5**) zu einer Wirkungsabschwächung gegenüber **YS121** führte, wurde eine Steigerung der Aktivität durch Substitution des 2,3-Dimethylphenyl-Strukturelementes mit Biphenyl-Substituenten unter Beibehaltung der α-*n*-Hexyl-Kette erreicht. So ist das unsubstituierte Biphenyl (**7**) an PPARα im nanomolaren Bereich aktiv (EC_{50} 0,32µM). Erstaunlicherweise führt die Einführung einer zusätzlichen Methylenbrücke zwischen der sekundären Aminogruppe und dem Biphenyl (**6**) zu einer deutlichen Abschwächung der PPARα/γ-Aktivität. Das *p*-Cyano-substituierte Derivat **9** ist schließlich mit EC_{50}-Werten von 0,19µM an PPARα und 1,5µM an PPARγ die potenteste Verbindung der Biphenyl-Serie und wurde daher für die genauere Untersuchung des Einflusses des Stereozentrums in der α-Position zur Carbonsäure auf die PPAR-Aktivität ausgewählt. Hierfür wurde die racemische Substanz mittels präparativer enantioselektiver HPLC in ihre beiden Enantiomere getrennt[148]. Die

theoretische Grundlage für diese Untersuchung ergibt sich aus der Adressierung der linken proximalen Bindetasche durch den α-*n*-Hexyl-Substituenten und die sich aus der Chiralität der präsentierten Verbindungen ergebenden unterschiedlichen Bindemodi für die einzelnen Enantiomere (vgl. Kap. 2.1.2.2.). Gezeigt ist dies in Abb. 14 (Docking von **(*R*)-9** an die PPARα-LBD).

Abb. 14: Docking von **(*R*)-9** an die PPARα-LBD.

In beiden Bildern ist die Orientierung der α-*n*-Hexyl-Kette in die linke proximale Bindetasche zu erkennen, die im Fall des (*S*)-Enantiomers nicht möglich ist.

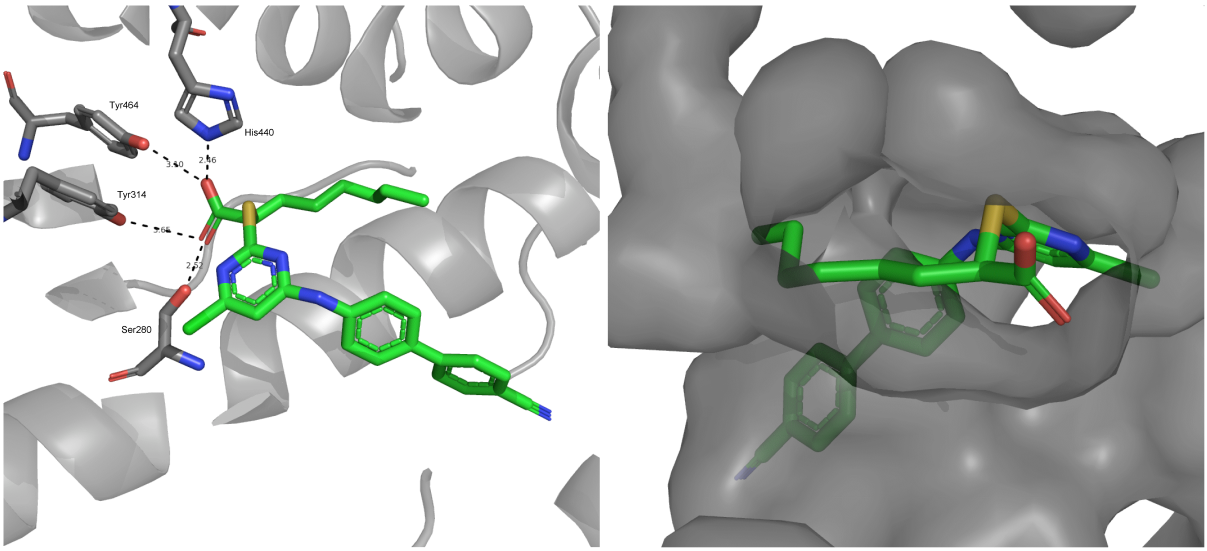

Die anhand der Dockingstudien ermittelte bevorzugte Bindung des (*R*)-Enantiomers konnte durch dessen biologische Aktivität bestätigt werden. So ist **(*R*)-9** mit einem EC_{50} von 0,03µM an PPARα das potenteste bis dato bekannte Pirinixinsäurederivat und ca. um den Faktor 70 aktiver als das entsprechende (*S*)-Enantiomer. An PPARγ zeigt sich lediglich ein geringer Aktivitätsunterschied zugunsten des (*R*)-Enantiomers, allerdings sind hier die Bindungsverhältnisse durch die deutlich größere linke proximale Bindetasche anders zu beurteilen.

Die beiden trisubstituierten Thiobarbitursäurederivate **10** und **11** aktivieren moderat PPARγ während sie sich an PPARα als inaktiv erwiesen. Interessanterweise führte die Einführung des *n*-Butyl-Restes in α-Position zur Carbonsäure bei **11** zu einer leichten Abschwächung der PPARγ-Aktivität.

Hinsichtlich ihrer potenziellen Eignung als neue Arzneistoffe zeigen die Biphenyl-

substituierten Pirinixinsäurederivate **7-9** mit einer rund 7-fachen Präferenz für PPARα gegenüber PPARγ ein Selektivitätsprofil, das zwischen dem der Fibrate (rund 10-fach PPARα-präferenziell und geringere Aktivität) und dem der Glitazare (PPARγ-präferenziell oder äquipotent) anzusiedeln ist. Nach dem bisherigen Scheitern der Glitazare (vgl. Kap. 2.1.3.2.) liegt in dieser Veränderung des Selektivitätsprofiles noch eine verbleibende Chance, Arzneistoffe mit dualem PPARα/γ-Agonismus klinisch zu etablieren.

3.1.1.2. 2-(Phenylthio)-hexansäurederivate und Analoga

Die 2-(Phenylthio)-hexansäurederivate bilden eine strukturell einheitliche Substanzklasse und wurden mit dem Ziel entwickelt, eine gegenüber den Pirinixinsäurederivaten andersartige, potentere Leitstruktur für PPAR-Agonisten zu etablieren (vgl. generelle Struktur in Abb. 8). Diese sollte zum einen ein *para*-Substitutionsmuster am zentralen Aromaten ermöglichen, was durch die Wahl der 4-Mercaptophenol-Partialstruktur erreicht wurde. Zum anderen sollte ein gegenüber den Pirinixinsäurederivaten längerer Spacer zwischen zentralem Aromaten und endständigem Zyklus eingeführt werden, was durch eine in 1- und 3-Position veretherte Propyleneinheit verwirklicht wurde. Als acide Kopfgruppe wurde die bereits bei den Pirinixinsäurederivaten positiv evaluierte 2-Mercaptohexansäure-Substruktur ausgewählt[74]. Folglich sind die Substanzen auf einer 2-(4-(3-Hydroxypropoxy)-phenylthio)-hexansäure-Grundstruktur aufgebaut, die mit unterschiedlichen lipophil substituierten Phenolen verethert ist (siehe Abb. 15). Hierbei wurden insbesondere die SAR von *ortho*- und *meta*-substituierten Phenylresten beleuchtet. Zusätzlich wurden von einer ausgewählten Verbindung (**16**, syn. **HZ64**) Analoga mit Variationen im Bereich der 2-Mercaptohexansäure-Substruktur hergestellt. Die Ergebnisse sind in den Tabellen 10 und 11 zusammengefasst (Originalarbeit siehe Anhang III, [149]).

Abb. 15: SAR der 2-(Phenylthio)-hexansäurederivate.

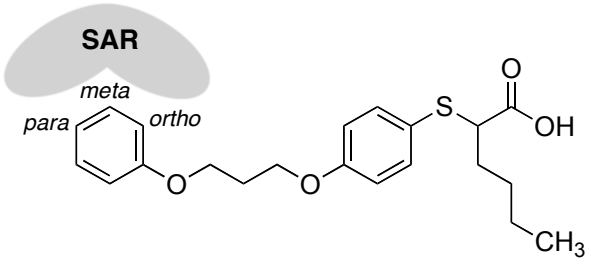

Tab. 10: *In vitro*-pharmakologische Charakterisierung der 2-(Phenylthio)-hexansäurederivate an PPAR.

Substanz	Struktur	PPAR EC_{50} [µM]		
		α	β	γ
12 (HZ96)	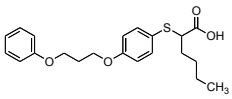	**0,29** ± 0,04 (76 ± 4%)	**ia**	**2,6** ± 0,35 (83 ± 6%)
13 (HZ93)	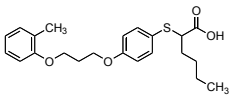	**0,25** ± 0,05 (64 ± 4%)	**ia**	**2,3** ± 0,50 (114 ± 12%)
14 (HZ94)	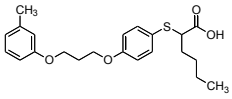	**0,09** ± 0,02 (80 ± 3%)	**ia**	**3,0** ± 0,41 (96 ± 7%)
15 (HZ103)	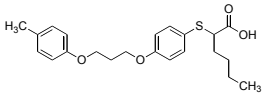	**0,085** ± 0,03 (91 ± 7%)	**ia**	**0,93** ± 0,12 (87 ± 33%)
16 (HZ64)	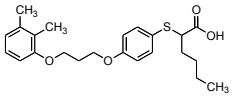	**0,056** ± 0,019 (113 ± 9%)	**ia**	**3,0** ± 0,22 (82 ± 3%)
(*R*)-16 (HZ64*R*) ee=86,0%	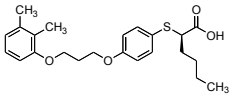	**0,011** ± 0,004 (115 ± 7%)	**ia**	**3,9** ± 0,83 (125 ± 10%)
(*S*)-16 (HZ64*S*) ee=98,6%	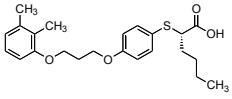	**1,7** ± 0,18 (94 ± 3%)	**ia**	**9,9** ± 1,44 (77 ± 7%)
17 (HZ126)	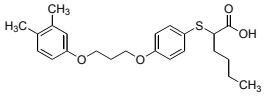	**0,021** ± 0,01 (72 ± 4%)	**ia**	**3,5** ± 0,10 (61 ± 1%)
18 (HZ83)	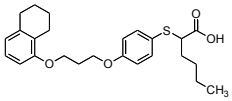	**0,19** ± 0,04 (101 ± 3%)	**ia**	**8,1** ± 0,50 (107 ± 5%)
19 (HZ117)	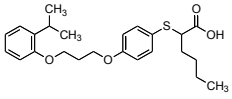	**2,0** ± 0,43 (89 ± 5%)	**ia**	**4,1** ± 0,32 (92 ± 5%)
20 (HZ115)	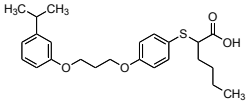	**0,15** ± 0,02 (98 ± 4%)	**ia**	**5,3** ± 0,30 (91 ± 4%)
21 (HZ114)	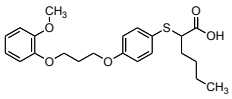	**0,55** ± 0,03 (92 ± 2%)	**ia**	**1,6** ± 0,41 (85 ± 6%)

Tab. 10 (Fortsetzung): *In vitro*-pharmakologische Charakterisierung der 2-(Phenylthio)-hexansäurederivate an PPAR.

Substanz	Struktur	PPAR EC_{50} [µM]		
		α	β	γ
22 (HZ112)	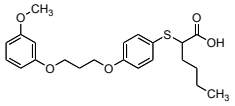	**0,049** ± 0,02 (85 ± 8%)	**ia**	**1,2** ± 0,16 (85 ± 4%)
23 (HZ113)	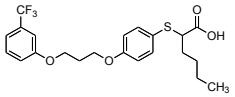	**0,025** ± 0,02 (75 ± 9%)	**ia**	**4,6** ± 0,19 (68 ± 2%)
24 (HZ87)	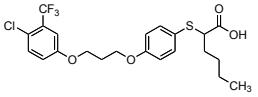	**0,39** ± 0,02 (65 ± 1%)	**ia**	**7,8** ± 0,40 (96 ± 4%)
25 (HZ75)	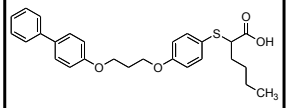	**0,11** ± 0,01 (125 ± 4%)	**ia**	**0,54** ± 0,06 (108 ± 4%)
26 (HZ55)	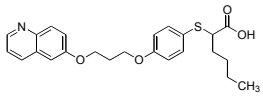	**0,22** ± 0,04 (95 ± 5%)	**ia**	**1,3** ± 0,90 (49 ± 3%)

Die EC_{50}-Werte und Standardabweichungen sind basiert auf den Mittelwerten aus mindestens 3 Bestimmungen. Die Prozentwerte in Klammern geben die relative Aktivierung im Vergleich zur Positivkontrolle an. Im Fall von Substanzen ohne EC_{50}-Werte geben diese die prozentuale Aktivierung bei 100µM bzw. der angegebenen Konzentration an. Positivkontrollen sind 1µM GW7647 für PPARα, 1µM L165041 für PPARβ und 1µM Pioglitazon für PPARγ. ia: inaktiv bei 10µM.

Den strukturellen Ausgangspunkt stellte die am Phenylrest unsubstituierte Verbindung **12** dar, die bereits ein nanomolar aktiver PPARα-Agonist und rund neunfach selektiv gegenüber PPARγ ist. Davon ausgehend wurde zunächst der Einfluss einer *mono*-Methylsubstitution am Phenyl untersucht. Bei der Analyse zeigt sich, dass die Einführung einer Methylgruppe in *ortho*-Stellung (**13**) keine Verbesserung bringt, wohingegen die *para*-Substitution (**15**) sowohl die PPARα als auch die PPARγ-Aktivität erhöht und die Methylgruppe in *meta*-Postition (**14**) zu einer selektiven Verbesserung der PPARα-Aktivität führt. Aufbauend auf diesen Ergebnissen wurden das 2,3-Dimethyl(**16**)- sowie das 3,4-Dimethyl(**17**)-Analogon synthetisiert. Die 2,3-Dimethylphenyl-Substruktur, ein bereits aus der Pirinixinsäure bekanntes Strukturelement, bewirkt eine weitere Verbesserung der PPARα-Aktivität gegenüber dem *meta*-Methyl-Derivat **14**. Daher wurde diese Verbindung (**16**) für eine Enantiomerentrennung mittels präparativer enantioselektiver HPLC ausgewählt, um den Einfluss des Stereozentrums in α-Position zur Carbonsäure zu untersuchen[148]. Die erhaltenen EC_{50}-Werte untermauern das bereits bei den

Pirinixinsäuren erhaltene Resultat, dass das (*R*)-Enantiomer als Eutomer fungiert und sich insbesondere bei der PPARα-Aktivierung ein erheblicher Unterschied zwischen (*R*)- und (*S*)-Konfiguration zeigt (vgl. Kapitel 3.1.1.1.). Die 3,4-Dimethyl-substituierte Verbindung **17** ist schließlich der potenteste racemische PPARα-Agonist aus der Serie der 2-(Phenylthio)-hexansäuren mit einem EC_{50} von 0,021µM.

Da bei den *mono*-Methyl-Analoga **13-15** die *meta*-Substitution in der Lage ist, die PPARα-Aktivierung selektiv zu verbessern, wurden in der Folge größere Substituenten (Methoxy und Isopropyl) jeweils in *ortho*- und in *meta*-Position eingeführt (**19-22**). Während der Isopropylrest in beiden Positionen verglichen mit der Methylsubstitution zu einer Wirkungsabschwächung führt, verbessert die *meta*-Methoxy-Substitution (**22**) die Aktivität an PPARα wie auch an PPARγ. Eine weitere PPARα-selektive Verbesserung bringt dem gegenüber die *meta*-Trifluormethyl-Substiution (**23**) mit einem EC_{50}-Wert von 0,025µM an PPARα und rund 180-facher Selektivität gegenüber PPARγ. Interessanterweise führt die Einführung eines dem Trifluormethyl benachbarten zusätzlichen Chloratoms in *para*-Stellung zu einer Wirkungsabschwächung (**24**).

Größere strukturelle Abweichung zeigen die Verbindungen **25** (Biphenyl-substituiert) und **26** (Chinolin-substituiert). Die Biphenyl-Substitution erhöht insbesondere die Potenz an PPARγ (EC_{50}=0,54µM) und führt somit zu einem dualen PPARα/γ-Agonismus mit einer rund fünffachen Präferenz für PPARα. Verbindung **26** ist ebenfalls ein PPARα-präferenzieller dualer PPARα/γ-Agonist mit einem therapeutisch viel versprechenden PPARγ-Modulator-Profil (49% maximale Aktivierung gegenüber Pioglitazon, vgl. Kapitel 2.1.2.3.(c)).

Zur detaillierten Untersuchung der SAR der 2-Mercaptohexansäure-Substruktur wurden basierend auf der 2,3-Dimethylphenyl-substituierten Verbindung **16** (syn. **HZ64**) das α-unsubsitutierte Analogon synthetisiert sowie das Schwefelatom durch eine Methylengruppe ersetzt. Die Ergebnisse sind in Tab. 11 zusammengefasst.

Tab. 11: *In vitro*-pharmakologische Charakterisierung der **16(HZ64)**-Analoga an PPAR.

Substanz	Struktur	PPAR EC_{50} [µM]		
		α	β	γ
16 (HZ64)	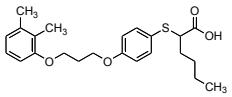	**0,056** ± 0,019 (113 ± 9%)	**ia**	**3,0** ± 0,22 (82 ± 3%)
27 (HZ99)	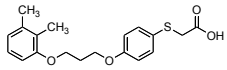	**0,60** ± 0,12 (81 ± 5%)	**1,4** ± 0,38 (52 ± 3%)	**3,8** ± 0,34 (77 ± 2%)
28 (HZ118)	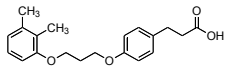	**13,8** ± 3,40 (63 ± 10%)	**11,2** ± 0,45 (72 ± 2%)	**15,7** ± 0,77 (54 ± 1%)
29 (HZ123)	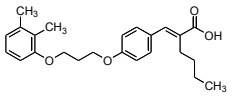	**ia**	**ia**	**ia**
30 (HZ122)	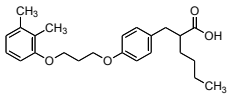	**1,5** ± 0,25 (73 ± 2%)	**ia**	**4,2** ± 0,53 (120 ± 9%)

Die EC_{50}-Werte und Standardabweichungen sind basiert auf den Mittelwerten aus mindestens 3 Bestimmungen. Die Prozentwerte in Klammern geben die relative Aktivierung im Vergleich zur Positivkontrolle an. Im Fall von Substanzen ohne EC_{50}-Werte geben diese die prozentuale Aktivierung bei 100µM bzw. der angegebenen Konzentration an. Positivkontrollen sind 1µM GW7647 für PPARα, 1µM L165041 für PPARβ und 1µM Pioglitazon für PPARγ. ia: inaktiv bei 10µM.

Die Entfernung des *n*-Butylrestes in α-Position zur Carbonsäure (**27**) führt zu einer Verbindung mit dem Profil eines *pan*-PPAR-Agonisten (vgl. Kapitel 2.1.2.3. (e)). Es kommt zu einer Wirkungsabschwächung an PPARα, wohingegen die PPARγ-Aktivität nahezu unbeeinflusst bleibt und die PPARβ-Aktivität neu hinzugewonnen wird. Der Ersatz des Schwefelatoms dieser α-unsubstituierten Verbindung durch eine Methylengruppe (**28**) führt zu einer deutlichen Wirkungsabschwächung an allen drei Subtypen. Das Methylenanalogon mit *n*-Butylrest (**30**) zeigt verglichen mit **16** einen sehr deutlichen Aktivitätsverlust an PPARα, wohingegen die PPARγ-Aktivität nahezu unbeeinflusst bleibt. Resultierend aus den SAR der Methylenanaloga lässt sich auf einen entscheidenden Einfluss des Schwefelatoms der 2-Mercapto-hexansäure-Substruktur auf die Potenz insbesondere an PPARα schließen.

Zusammenfassend ist es mit den 2-(Phenylthio)-hexansäuren gelungen, eine neue Substanzklasse zu etablieren, die je nach Substitutionsmuster als hochaktiv und selektiv PPARα-agonistisch oder aber als PPARα-präferenziell dual PPARα/γ-agonistisch charakterisiert werden kann. Dabei erwies sich die Leitstruktur als sehr robust und gut geeignet, nanomolar aktive Verbindungen zu konzipieren.

3.1.2. mPGES-1 und 5-LO

3.1.2.1. Pirinixinsäurederivate

Während die Pirinixinsäure sowohl an der mPGES-1 als auch an der 5-LO keine hemmende Wirkung zeigt, inhibiert das durch Einführung eines α-*n*-Hexyl-Restes erhaltene **YS121** beide Enzyme im niedrig mikromolaren Bereich. Diese Verbindung diente als Leitstruktur zur näheren Evaluation der SAR von α-*n*-Hexyl-substituierten Pirinixinsäurederivaten. Die Optimierung hinsichtlich der balancierten Inhibition beider Enzyme wurde letztlich wie auch bei PPAR durch die Biphenyl-Substitution erreicht. Die potentesten Verbindungen zeigen IC_{50}-Werte um 1µM an der mPGES-1 wie auch an der 5-LO und repräsentieren mit diesem Inhibitionsprofil eine bis dato in der Literatur noch nicht beschriebene Klasse von dualen mPGES-1/5-LO-Inhibitoren. Im Kontext einer pharmakologischen Beeinflussung der Arachidonsäurekaskade ist es erwähnenswert, dass keine der Substanzen signifikante COX-hemmende Eigenschaften zeigt. Die *in vitro*-pharmakologische Charakterisierung ist in Tab. 12 zusammengefasst (Originalarbeit in Anhang IV, [147]).

Tab. 12: *In vitro*-pharmakologische Charakterisierung der Pirinixinsäurederivate an mPGES-1, 5-LO und COX.

Substanz	Struktur	IC_{50} [µM]	5-LO IC_{50} [µM]		COX (prozentuale Aktivität bei 10µM)	
		mPGES-1	PMNL	pur. 5-LO	COX-1	COX-2
Pirinixin-säure	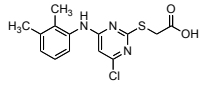	(99 ± 8%)	**ia**	**nb**	nb	nb
YS121	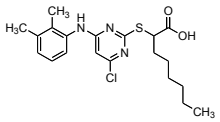	**3,9**	**4,1**	**6,5**	75,2	62,0
1 (HZ47)	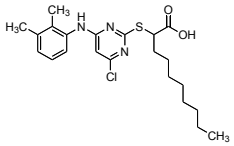	(38 ± 6%)	**0,95**	**nb**	nb	nb
3 (HZ20)	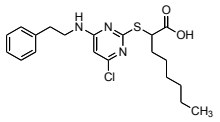	(73 ± 8%)	**3,0**	**nb**	nb	nb
5 (HZ28)	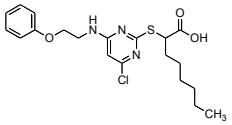	(82 ± 6%)	**4,2**	**nb**	nb	nb
6 (HZ42)	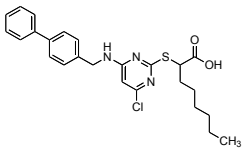	**1,3**	**1,0**	**2,0**	67,3	61,3
7 (HZ52)	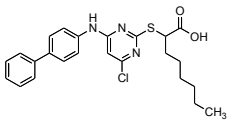	**1,6**	**0,7**	**1,5**	52,3	57,1
8 (HZ65)	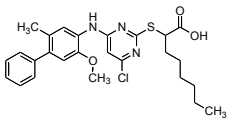	**2,1**	**0,5**	**2,0**	71,2	53,7

Tab. 12 (Fortsetzung): *In vitro*-pharmakologische Charakterisierung der Pirinixinsäurederivate an mPGES-1, 5-LO und COX.

Substanz	Struktur	IC_{50} [µM]	5-LO IC_{50} [µM]		COX (prozentuale Aktivität bei 10µM)	
		mPGES-1	PMNL	pur. 5-LO	COX-1	COX-2
9 (HZ56)	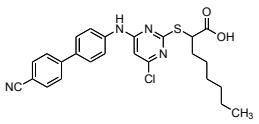	**1,7**	**0,4**	**1,5**	66,0	61,2
(***R***)-9 (**HZ56*R***) ee=98,8%	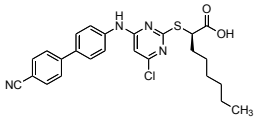	(37 ± 5%)	(3 ± 2%)	**nb**	nb	nb
(***S***)-9 (**HZ56*S***) ee=96,8%	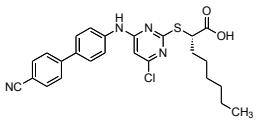	(23 ± 6%)	(3 ± 2%)	**nb**	nb	nb
10 (HZ27)	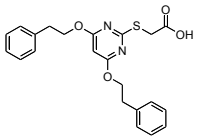	(70 ± 2%)	**7,6**	**nb**	nb	nb
11 (HZ34)	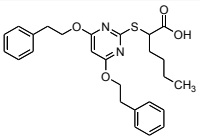	(49 ± 5%)	**1,2**	**nb**	nb	nb

Die IC_{50}-Werte sind basiert auf den Mittelwerten aus 3-4 Bestimmungen. Die Prozentwerte in Klammern geben die verbleibende Restaktivität bei 10µM an. nb: nicht bestimmt; ia: inaktiv bei 10µM.

Die Analyse der in Tab. 12 vorgestellten Verbindungen ergibt, dass alle Derivate als 5-LO-Inhibitoren im niedrig mikromolaren bzw. hoch nanomolaren Bereich aktiv sind. Die Leitstruktur erweist sich im Hinblick auf die 5-LO-Inhibition bei der Variation des linken lipophilen Molekülteiles als sehr robust. Interessanterweise inhibieren die strukturell stärker verschiedenen *bis*-Etherderivate **10** und **11** die 5-LO ebenfalls einstellig mikromolar, die α-alkyl-Substitution (**11**) wirkt sich auch bei dieser Strukturklasse aktivitätssteigernd aus.

Eine signifikante Hemmung der mPGES-1 hingegen zeigen lediglich die Biphenyl-substituierten Derivate **6**-**9**, die als duale mPGES-1/5-LO-Inhibitoren bezeichnet werden können. Essenzielle Strukturelemente für die mPGES-1-Inhibition sind weiterhin die Carbonsäurefunktion sowie die α-*n*-Hexyl-Substitution. Die dafür zugrunde liegenden SAR sind in der Publikation *Koeberle und Zettl et al.* detailliert beschrieben[147]. Als Leitstruktur für die mPGES-1-Inhibition diente wiederum

zunächst die α-*n*-Hexyl-substituierte Pirinixinsäure **YS121** mit einem IC_{50} von 3,9µM (siehe Tab. 12). Der Ersatz des 2,3-Dimethylphenylrestes durch Biphenylsubstituenten resultiert bei den Derivaten **6-9** an der mPGES-1 in IC_{50}-Werten zwischen 1,3 und 2,1µM, folglich gibt es keine steilen SAR im Substitutionsmuster des Biphenyls. Die potenteste 5-LO-Hemmung zeigt das *p*-Cyano-substituierte **9** mit einem IC_{50}-Wert von 0,4µM (gemessen in PMNL). Ein Effekt des Stereozentrums wie bei PPAR konnte beim Vergleich der inhibierenden Eigenschaften von **(*R*)-9** und **(*S*)-9** nicht nachgewiesen werden.

Die Schlüsselverbindung der dualen mPGES-1/5-LO-Inhibitoren ist schließlich das Biphenylmethylen-substituierte **6**. Mit IC_{50}-Werten von 1,3µM an der mPGES-1 und 1,0µM an der 5-LO (gemessen in PMNL) ist diese Verbindung ein balancierter dualer mPGES-1/5-LO-Inhibitor, der außerdem im Vergleich zu den anderen Biphenyl-substituierten Derivaten an PPAR vergleichsweise schwach aktiv ist (vgl. Tab. 9). Die Einführung der zusätzlichen Methylengruppe scheint daher ein mögliches Steuerelement zu sein, um an Selektivität zugunsten dualer mPGES-1/5-LO-Inhibiton gegenüber der PPAR-Aktivierung zu gewinnen. Basierend auf diesen Erkenntnissen wurde die Verbindung **6** für erste *in vivo*-Testungen in anti-inflammatorischen Tiermodellen ausgewählt.

3.1.2.2. 2-(Phenylthio)-hexansäurederivate und Analoga

Die erhaltenen Ergebnisse an mPGES-1 und 5-LO sind Bestandteile eines Patentes, dessen Einreichung zum Zeitpunkt der Abgabe der vorliegenden Dissertation noch nicht abgeschlossen ist (siehe Inanspruchnahme der Diensterfindung, Anhang V).

3.2. Chemische Synthesen

3.2.1. Pirinixinsäurederivate

Die Synthese der präsentierten Pirinixinsäurederivate folgt dem in Abb. 16 dargestellten Schema modifiziert nach der von *d`Atri et al.* publizierten Synthese der Pirinixinsäure aus dem Jahr 1984[75]. Ausgehend von Thiobarbitursäure wird diese zunächst durch Umsetzung mit dem entsprechenden α-Bromalkansäureethylester am Schwefelatom verethert. Darauf folgend werden in einer Reaktion mit Phosphorylchlorid beide Hydroxygruppen des Pyrimidinringes durch Chloratome

substituiert. Durch nukleophile Substitution eines dieser Chloratome mit einem kommerziell erhältlichen primären Amin (sowohl aromatisch als auch aliphatisch) gelingt schließlich die Einführung eines weiteren lipophilen Restes im linken Teil des Moleküles. Schließlich wird der resultierende Ester mittels Lithiumhydroxid zur gewünschten Carbonsäure verseift. Ein Seitenweg ausgehend von der am Schwefel veretherten Thiobarbitursäure (aus Schritt a)) führt über eine *Williamson*-artige Ethersynthese zur Darstellung von symmetrischen *bis*-Etherderivaten, welche dann analog zu den Aminderivaten verseift werden.

Von allen vorgestellten Verbindungen existiert neben der Carbonsäure stets auch der entsprechende Ethylester in elementaranalysenreiner Form. Alle relevanten Experimentaldaten zu den einzelnen Verbindungen befinden sich in den Supplementen der Publikationen *Zettl et al.* in *QSAR & Combinatorial Science* (Anhang II,[146]) sowie *Koeberle und Zettl et al.* in *Journal of Medicinal Chemistry* (Anhang IV,[147]).

Abb. 16: Synthese der Pirinixinsäurederivate.

Reagenzien und Bedingungen: a) (Z=H): 2-Bromessigsäureethylester (1,17eq), NaOH (1,08eq), H_2O/ EtOH (1:1), 60°C, 2h; (Z=*n*-Bu), (Z=*n*-Hex): 2-Bromhexansäureethylester (Z=*n*-Bu) / 2-Bromoctansäureethylester (Z=*n*-Hex) (1,5eq), Triethylamin (3,0eq), DMF, 80°C, 1,5-3h b) $POCl_3$ (18eq), *N,N*-Diethylanilin (1eq), RF, 2-3,5 h c) R-NH_2 (1,2eq), Triethylamin (3eq), EtOH, RF, 3,5-96h d) LiOH (3eq), EtOH, RT, 24h e) 2-Bromethylbenzen (2eq), K_2CO_3 (3eq), DMF, 80°C, 5-9h.

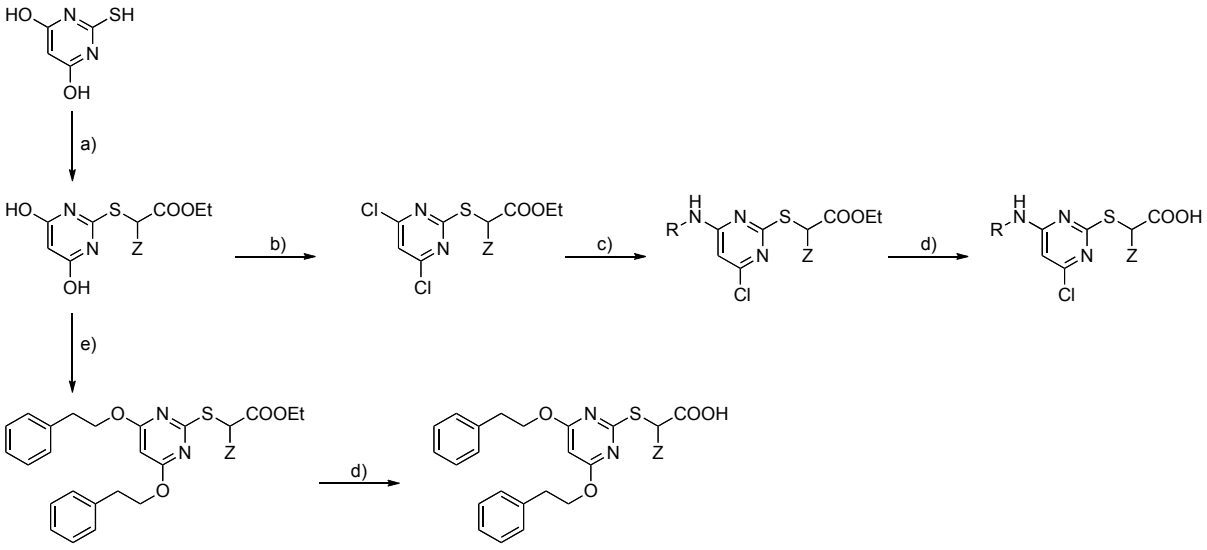

3.2.2. 2-(Phenylthio)-hexansäurederivate und Analoga

Die initiale Reaktion zur Darstellung der zweiten hier vorgestellten Substanzklasse stellt zunächst eine analog zu den Pirinixinsäurederivaten erfolgende Synthese eines Thioethers dar (siehe Abb. 17). Als Reaktionspartner dienen hier jedoch 4-Mercaptophenol und 2-Bromhexansäureethylester, wobei letzterer zur Einführung eines *n*-Butylrestes in α-Position zur Carbonsäure führt (für α-unsubstituierte Analoga entsprechend mit 2-Bromessigsäureethylester)[150]. Die phenolische Hydroxygruppe kann nun durch zwei mögliche gleichwertige Reaktionswege verethert werden: Einerseits kann zuerst der Propylenspacer durch Umsetzung des 4-Mercaptophenolderivates aus Schritt f) mit 3-Brompropan-1-ol eingeführt und als nächstes durch eine *Mitsunobu*-Reaktion mit dem entsprechenden kommerziell erhältlichen Phenolderivat der Aufbau des linken Molekülteiles abgeschlossen werden. Andererseits ist auch die Darstellung eines alkoholischen Zwischenproduktes aus dem jeweiligen Phenolderivat und 3-Brompropan-1-ol möglich, das wiederum in der Folge durch eine *Mitsunobu*-Reaktion mit dem 4-Mercaptophenolderivat aus Schritt f) gekoppelt werden kann[151,152]. Die Verseifung zur entsprechenden Carbonsäure erfolgt letztlich mit Lithiumhydroxid.

Wie bei den Pirinixinsäurederivaten wurden stets auch die Ester elementaranalysenrein dargestellt. Alle relevanten Experimentaldaten zu den einzelnen Verbindungen befinden sich im Supplement der Publikation *Zettl et al.* in *Bioorganic & Medicinal Chemistry Letters* (Anhang III, [149]).

Abb. 17: Syntheseweg der 2-(Phenylthio)-hexansäurederivate.

Reagenzien und Bedingungen: f) (Z=H): 2-Bromessigsäureethylester (1,1eq), Triethylamin (3eq), $CHCl_3$, RF, 1h; (Z=*n*-Bu): 2-Bromhexansäureethylester (1,0eq), Triethylamin (1,5eq), DMF, RF, 3h g) 3-Brompropan-1-ol (1,5eq), K_2CO_3 (2eq), RF, 48h h) Ar-OH, Alk-OH (1,1eq), TPP (1,5eq), DEAD (1,5eq) oder ADDP (1,5eq), THF, RT, 48-72h i) LiOH (10eq), MeOH/H_2O (4:1), 40°C, 4h.

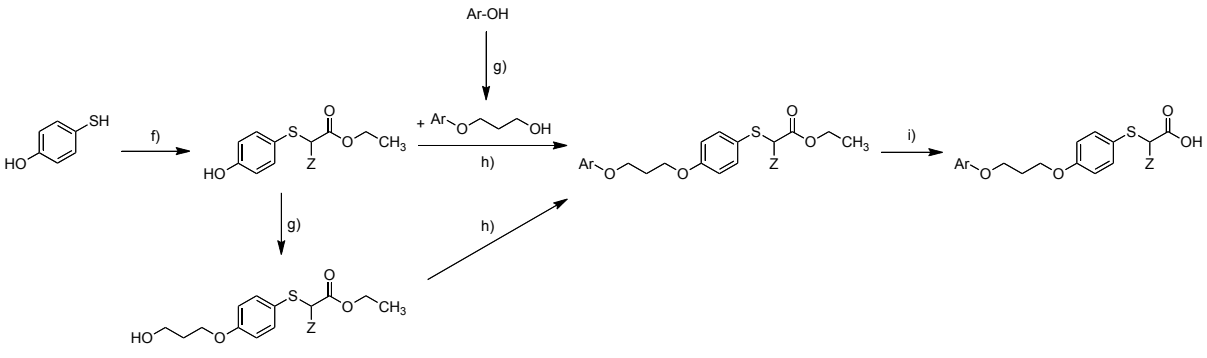

Als Weiterentwicklung der 2-(Phenylthio)-hexansäurederivate wurde für eine ausgewählte, an PPARα besonders aktive Verbindung (**16,** syn. **HZ64**) eine Synthesestrategie entwickelt, die es erlaubt, den Schwefel im Molekül durch eine Methylengruppe zu ersetzen (siehe Abb. 18). Der zentrale Schritt ist eine *Wittig-Horner*-Reaktion, die zu einem α-*n*-Butyl-substituierten Coumarsäurederivat führt[153]. Als CH-acide Verbindung dient hierbei ein Phosphonsäureester, der durch Umsetzung des α-Bromhexansäureesters mit Triethylphosphit gewonnen wird[154]. Die Aldehydkomponente ist ein 4-Hydroxybenzaldehydderivat, dessen linker Molekülteil bereits durch die bei den 2-(Phenylthio)-hexansäurederivaten vorgestellten Methoden aufgebaut wurde. Das resultierende Coumarinsäurederivat kann nun einerseits direkt und andererseits nach Hydrierung der exozyklischen Doppelbindung verseift werden. Das nach vorangegangener Hydrierung erhaltene Produkt stellt schließlich das eigentliche Kohlenstoff-Analogon **30** zu dem entsprechenden 2-(Phenylthio)-hexansäurederivat **16** dar.

Abb. 18: Synthesestrategie der Schwefelsubstitution.

Reagenzien und Bedingungen: j) Triethylphosphit (2eq), RF, 12h k) 3-Brompropan-1-ol (1,5eq), K_2CO_3 (2eq), RF, 48h l) Ar-OH, Alk-OH (1,1eq), TPP (1,5eq), DEAD (1,5eq), THF, RT, 96h m) R-CHO, 2-(Diethoxyphosphoryl)-hexansäureethylester (1,3eq), NaH (1,2eq), THF n) H_2, 10% Pd/C, EtOH o) LiOH (10eq), MeOH/H_2O (4:1), 40°C, 8-20h.

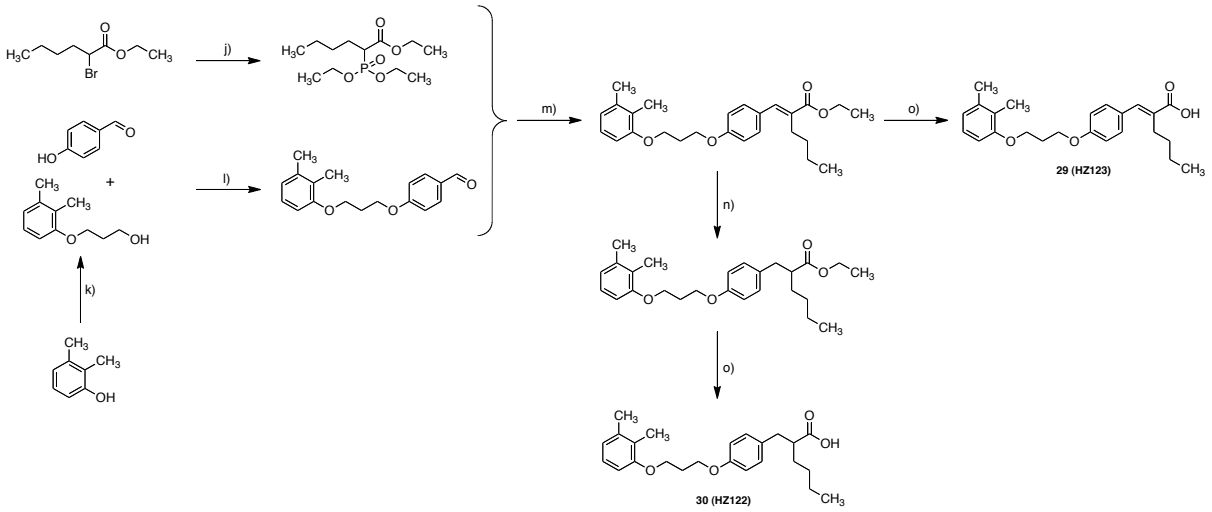

Zur Darstellung eines α-unsubstituierten Kohlenstoff-Analogons **28** wurde von kommerziell erhältlichem 3-(4-Hydroxyphenyl)-propansäureethylester ausgegangen, der mit dem entsprechenden Prekursor mittels einer *Mitsunobu*-Reaktion gekoppelt und anschließend verseift wird (siehe Abb. 19).

Abb. 19: Synthese des 3-Phenylpropansäurederivates.

Reagenzien und Bedingungen: p) 3-Brompropan-1-ol (1,5eq), K_2CO_3 (2eq), RF, 48h q) Ar-OH, Alk-OH (1,1eq), TPP (1,5eq), ADDP (1,5eq), THF, RT, 8h r) LiOH (10eq), MeOH/H_2O (4:1), 40°C, 3h.

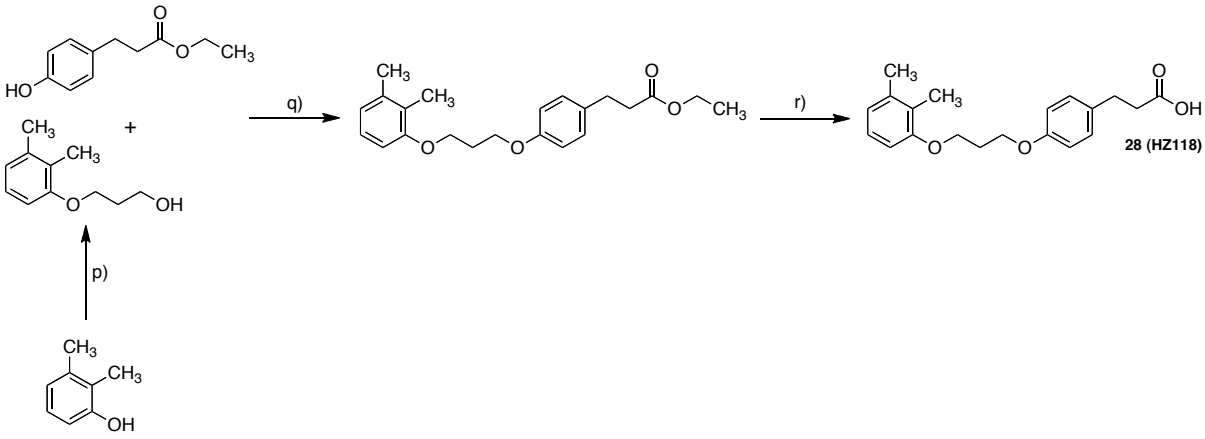

4. Zusammenfassung

Im menschlichen Körper haben Fettsäuren eine Vielzahl von regulatorischen Funktionen inne. Diese sind einerseits sensorischer Natur resultierend aus der exogenen Zufuhr von Fettsäuren mit der Nahrung und deren Rolle als eine der Hauptenergiequellen des Organismus. Andererseits werden Fettsäuren auch endogen synthetisiert und fungieren als autokrine und parakrine Mediatoren. Folglich gibt es eine Vielzahl von Enzymen und Rezeptoren, die am Stoffwechsel von exogenen wie auch endogenen Fettsäuren beteiligt sind. Aufgrund ihrer Beteiligung an einer Reihe von pathophysiologischen Prozessen stellen sie wichtige Targets für die Entwicklung von neuen Arzneistoffen dar.

Die vorliegende Arbeit verfolgt einen medizinisch-chemischen Ansatz ausgehend von Pirinixinsäure (WY14,643) als Leitstruktur für Aktivatoren von Peroxisomen Proliferator-aktivierten Rezeptoren (PPARs) sowie für Inhibitoren von zwei Schlüsselenzymen der Arachidonsäurekaskade: der 5-Lipoxygenase (5-LO) und der mikrosomalen Prostaglandin E_2-Synthase-1 (mPGES-1). Pirinixinsäure wurde durch Anwendung medizinisch-chemischer Prinzipien wie das der Bioisosterie strukturell hinsichtlich Selektivität und Potenz optimiert (Gruppe der α-*n*-Hexyl-Pirinixinsäurederivate) und zu einer neuen Leitstruktur weiterentwickelt (Gruppe der 2-(Phenylthio)-hexansäurederivate).

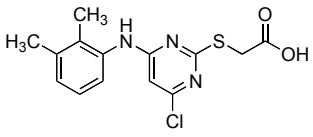

Pirinixinsäure

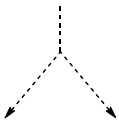

α-*n*-Hexyl-Pirinixinsäurederivate

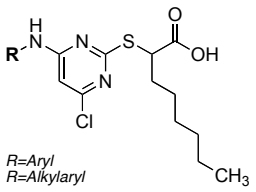

R=Aryl
R=Alkylaryl

Zettl et al., *QSAR & Combinatorial Science*, 2009.
Koeberle und Zettl et al., *Journal of Medicinal Chemistry*, 2008.

2-(Phenylthio)-hexansäurederivate

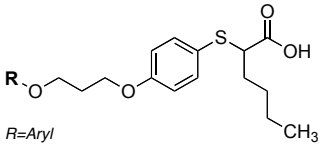

R=Aryl

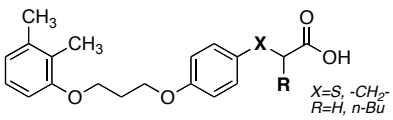

X=S, -CH_2-
R=H, n-Bu

Zettl et al., *Bioorganic & Medicinal Chemistry Letters*, 2009.

Für die α-*n*-Hexyl-Pirinixinsäurederivate sind deren Synthese sowie die *in vitro*-pharmakologische Charakterisierung an PPAR (*Zettl H, Dittrich M, Steri R, Proschak E, Rau O, Steinhilber D, Schneider G, Lämmerhofer M, Schubert-Zsilavecz M. Novel Pirinixic Acids as PPARalpha Preferential Dual PPARalpha/gamma Agonists. QSAR & Combinatorial Science 2009; 28, 576-586)* und an Schlüsselenzymen der Arachidonsäurekaskade (*Koeberle A, Zettl H, Greiner C, Wurglics M, Schubert-Zsilavecz M, Werz O. Pirinixic acid derivatives as novel dual inhibitors of microsomal prostaglandin E_2 synthase-1 and 5-lipoxygenase. Journal of Medicinal Chemistry 2008; 51, 8068-8076)* publiziert.

Im Fall der 2-(Phenylthio)-hexansäurederivate sind die Synthese sowie die *in vitro*-pharmakologische Charakterisierung an PPAR (*Zettl H*, *Steri R, Lämmerhofer M, Schubert-Zsilavecz M. Bioorganic & Medicinal Chemistry Letters 2009;* In press, Accepted manuskript, *e-published 18.05.2009*) veröffentlicht, wohingegen die Charakterisierung als duale mPGES-1/5-LO-Inhibitoren Teil eines laufenden Patentverfahrens ist und daher noch nicht präsentiert werden konnte.

Der Peroxisomen Proliferator-aktivierte Rezeptor (PPAR) mit seinen drei Subtypen α, β (syn. δ) und γ ist eines der am detailliertesten erforschten Targets zur Behandlung metabolischer Erkrankungen wie Dyslipidämien und Typ 2 Diabetes mellitus. PPARs fungieren als körpereigene Lipid- und Glucosesensoren, deren Blutspiegel sie durch die Induktion der β-Oxidation von Fettsäuren (PPARα) und die Erhöhung der Glucoseaufnahme in peripheren Geweben (PPARγ) regulieren. Therapeutisch genutzt wird dies durch die PPARα-agonistisch wirkenden Fibrate bei bestimmten Dyslipidämien und die PPARγ-agonistisch wirkenden Glitazone bei Typ 2 Diabetes mellitus. Trotz des erfolgreichen Einsatzes dieser beiden Arzneistoffklassen verbleibt ein großes Optimierungspotenzial beim Design neuer PPAR-Agonisten: Einerseits ist der therapeutische Einsatz von Fibraten (Wirksamkeit) wie auch von Glitazonen (Nebenwirkungsspektrum) limitiert, andererseits gibt es neben der Optimierung der einzelnen Wirkstoffklassen den viel versprechenden Ansatz, durch dualen PPARα/γ-Agonismus Störungen im Lipid- und Glucosehaushalt mit einem Wirkstoff zu behandeln. Allerdings sind alle bisherigen Versuche, duale PPARα/γ-Agonisten (sog. Glitazare) klinisch zu etablieren, an deren Nebenwirkungsprofil gescheitert. Bei der Suche nach den molekularpharmakologischen Ursachen für dieses Scheitern erwies sich insbesondere der PPARγ-Agonismus der Glitazare, der als mögliche Ursache kardiovaskulärer und renaler Komplikationen diskutiert wird, als problematisch. So wirken alle Glitazare als

Vollagonisten an PPARγ und sind hinsichtlich ihres Selektivitätsprofils PPARγ-präferenziell bzw. gleichwertig aktiv an PPARα. Hieraus ergeben sich alternative Konzepte beim Design neuer Wirkstoffe wie die der PPARγ-Modulation und des PPARα-präfenziellen dualen PPARα/γ-Agonismus. Letzteres wird sowohl durch die α-*n*-Hexyl-Pirinixinsäurederivate als auch durch bestimmte 2-(Phenylthio)-hexansäurederivate aufgegriffen. Die Hauptvertreter der 2-(Phenylthio)-hexansäurederivate sind wie die Fibrate PPARα-selektiv, beinhalten jedoch mit einer bis zu 1000-fach höheren *in vitro*-Aktivität erheblich größeres therapeutisches Potenzial.

Die Publikation zur Synthese und der *in vitro*-pharmakologischen Charakterisierung der α-*n*-Hexyl-Pirinixinsäurederivate an PPAR enthält einerseits die strukturelle Optimierung durch Variation der Aryl-Substitution des zentralen Pyrimidinringes der Leitstruktur und andererseits die durch Docking-Verfahren gestützte Untersuchung des Einflusses der Stereochemie auf die PPAR-Aktivierung. Letztlich konnte durch die Einführung von Biphenyl-Substituenten eine Verbesserung insbesondere der PPARα-Aktivität gegenüber der als strukturellen Referenz dienenden α-*n*-Hexyl-Pirinixinsäure (*Rau O, Syha Y, Zettl H, Kock M, Bock A, Schubert-Zsilavecz M. Alpha-alkyl substituted pirinixic acid derivatives as potent dual agonists of the peroxisome proliferator activated receptor alpha and gamma. Archiv der Pharmazie (Weinheim) 2008; 341, 191-195)* erreicht werden. Repräsentiert wird dies durch die *p*-Cyanobiphenyl-substituierte Verbindung HZ56, einen nanomolar aktiven PPARα-präferenziellen dualer PPARα/γ-Agonisten.

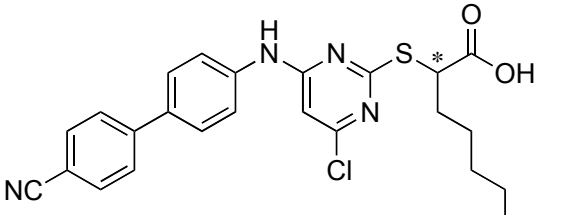

HZ56
PPARα EC_{50} = 0,19μM
PPARγ EC_{50} = 1,5μM

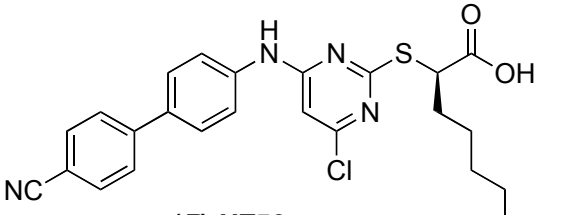

(*R*)-HZ56
PPARα EC_{50} = 0,03μM
PPARγ EC_{50} = 1,1μM

Zettl et al., *QSAR & Combinatorial Science*, 2009.

Mit Hilfe von präparativer enantioselektiver HPLC wurde HZ56 in seine Enantiomere getrennt. Deren *in vitro*-pharmakologische Charakterisierung ergab, dass das (*R*)-Enantiomer insbesondere bei PPARα als Eutomer fungiert. Dieses Ergebnis konnte mit Hilfe von Docking-Studien weiter untermauert werden. Hierbei wurde deutlich, dass die Besetzung der linken proximalen Bindetasche der PPARα-Liganden-Bindungs-Domäne durch den α-*n*-Hexyl-Rest lediglich im Fall einer (*R*)-Konfiguration

optimal erfolgen kann. Da die linke proximale Bindetasche von PPARγ größer ist als die von PPARα, wird der stereochemische Einfluss auf die biologische Aktivität hier weniger deutlich sichtbar als bei PPARα.

Die Arbeit zur Synthese und *in vitro*-pharmakologischen Charakterisierung der Substanzklasse der 2-(Phenylthio)-hexansäurederivate beinhaltet deren Konzeption und strukturelle Evolution zu potenten und selektiven PPARα-Agonisten.

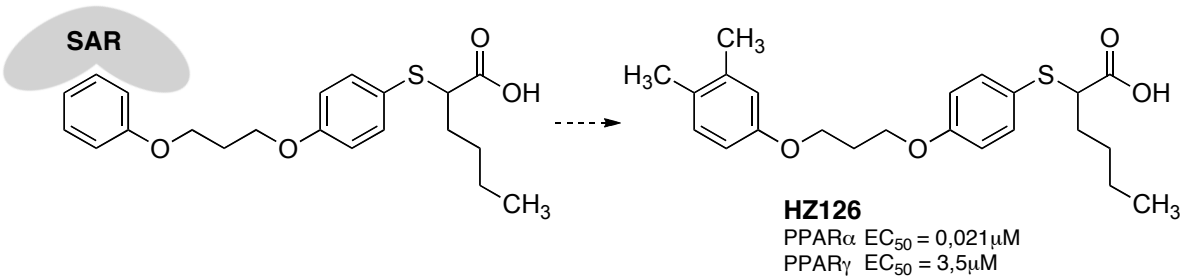

Zettl et al., *Bioorganic & Medicinal Chemistry Letters*, 2009.

Bei der Analyse der Struktur-Wirkungs-Beziehungen erwies sich die Leitstruktur als hochaktiv und sehr robust. Je nach Substitutionsmuster des lipophilen Molekülteils wurden hochaktive selektive PPARα-Agonisten wie auch PPARα-präferenzielle duale PPARα/γ-Agonisten dargestellt. Repräsentativ gezeigt ist die 3,4-Dimethylphenyl-substituierte Verbindung HZ126, ein niedrig nanomolar aktiver und selektiver PPARα-Agonist. Durch die Synthese von Kohlenstoff-Analoga und α-unsubstituierten Verbindungen wurde des Weiteren der Einfluss des Schwefelatoms und des *n*-Butylrestes in α-Position zur Carbonsäure auf die PPAR-Aktivität untersucht. Hierbei konnte gezeigt werden, dass beide Strukturelemente einen großen Beitrag zur hohen PPARα-Aktivität der Leitstruktur leisten. Wie auch bei den α-*n*-Hexyl-Pirinixinsäurederivaten wurde eine ausgewählte Verbindung in ihre Enantiomere getrennt und der Einfluss des Stereozentrums in α-Position zur Carbonsäure untersucht. Das Ergebnis untermauerte die Resultate der vorangegangenen Studie: Das (*R*)-Enantiomer wirkte als Eutomer, wobei der stereochemische Einfluss bei PPARα besonders deutlich war.

Die besondere Herausforderung bei der Suche nach neuen antiinflammatorischen Wirkstoffen liegt in deren kardiovaskulären und gastrointestinalen Sicherheit. Ein Ansatz, um diese von COX-Inhibitoren (NSAIDs) bekannten Nebenwirkungen zu umgehen, besteht in der Adressierung alternativer Enzyme innerhalb der Arachidonsäurekaskade. Als besonders aussichtsreiches Konzept gilt die Inhibition

der mikrosomalen Prostaglandin E_2-Synthase-1 (mPGES-1), einem *downstream* der COX agierenden Enzym, das induzierbar die Bildung von proinflammatorischem Prostaglandin E_2 katalysiert. Der Vorteil gegenüber einer COX-Inhibition liegt darin begründet, dass die Biosynthese von jenen Prostaglandinen, die wichtige physiologische Grundfunktionen im Gleichgewicht halten, unbeeinflusst bleibt. Gleichsam gilt auch die Inhibition der 5-Lipoxygenase (5-LO), die die als proinflammatorisch und ulcerogen geltenden Leukotriene produziert, als viel versprechend. Allerdings waren die therapeutischen Erfolge von 5-LO-Inhibitoren bisher eher ernüchternd. Darauf basierend könnte der kombinierte Ansatz einer dualen mPGES-1/5-LO-Inhibition zu antiinflammatorisch wirksamen Arzneistoffen ohne kardiovaskulärerem und gastrointestinalem Risiko führen. Bestimmte α-*n*-Hexyl-Pirinixinsäurederivate erfüllen dieses pharmakologische Profil und sind daher die ersten Vertreter einer neuen Wirkstoffklasse von dualen mPGES-1/5-LO-Inhibitoren.

Publiziert sind ausgewählte Synthesen und die *in vitro*-pharmakologische Charakterisierung von Pirinixinsäurederivaten an mPGES-1, 5-LO und COX. Die Arbeit beinhaltet eine umfassende Reihe an Pirinixinsäurederivaten mit Strukturvariationen in α-Position zur Carbonsäure und im Aryl-Substitutionsmuster des Pyrimidinringes. Hinsichtlich der α-Substitution zeigte sich, dass für Alkylreste eine Kettenlänge von mindestens 6 Kohlenstoffatomen für einen dualen Wirkmechanismus erforderlich ist. Als Leitstruktur für duale mPGES-1/5-LO-Inhibitoren ergab sich somit α-*n*-Hexyl-substituierte Pirinixinsäure, deren Aryl-Substitutionsmuster am zentralen Pyrimidin weiter optimiert wurde.

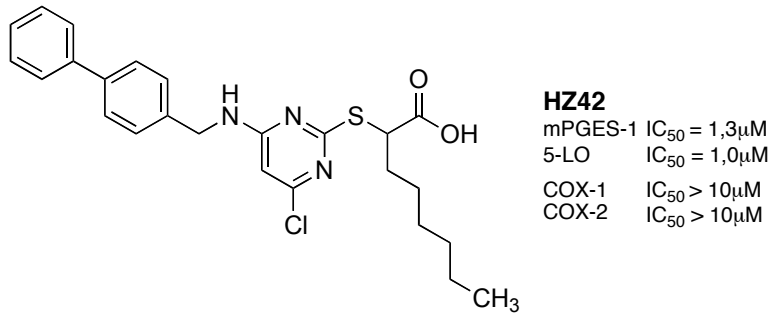

Koeberle und Zettl et al., *Journal of Medicinal Chemistry*, 2008.

Als vorteilhaft erwies sich die Substitution mit Biphenylresten, wodurch die Darstellung von niedrig mikromolar aktiven dualen mPGES-1/5-LO-Inhibitoren gelang. Beispielhaft gezeigt ist HZ42 mit einer zusätzlichen Methylengruppe zwischen dem Biphenylrest und der aromatischen Aminogruppe. Diese Verbindung

ist an beiden Enzymen nahezu gleich aktiv und hat außerdem ein ausgezeichnetes Selektivitätsprofil gegenüber beiden COX-Isoformen. Bei der Analyse der Strukur-Wirkungs-Beziehungen von unterschiedlichen Biphenylresten zeigte sich eine hohe strukturelle Toleranz hinsichtlich der dualen inhibitorischen Aktivität an der mPGES-1 und der 5-LO. Somit stellen die α-*n*-Hexyl-Pirinixinsäurederivate die ersten publizierten dualen mPGES-1/5-LO-Inhibitoren dar.

5. Bibliographie

1. Kliewer SA, Xu HE, Lambert MH, Willson TM. Peroxisome proliferator-activated receptors: from genes to physiology. Recent Prog Horm Res 2001; 56, 239-263.
2. Michalik L, Auwerx J, Berger JP et al. International Union of Pharmacology. LXI. Peroxisome proliferator-activated receptors. Pharmacol Rev 2006; 58, 726-741.
3. Gronemeyer H, Gustafsson JA, Laudet V. Principles for modulation of the nuclear receptor superfamily. Nat Rev Drug Discov 2004; 3, 950-964.
4. Werman A, Hollenberg A, Solanes G, Bjorbaek C, Vidal-Puig AJ, Flier JS. Ligand-independent activation domain in the N terminus of peroxisome proliferator-activated receptor gamma (PPARgamma). Differential activity of PPARgamma1 and -2 isoforms and influence of insulin. J Biol Chem 1997; 272, 20230-20235.
5. Onate SA, Tsai SY, Tsai MJ, O'Malley BW. Sequence and characterization of a coactivator for the steroid hormone receptor superfamily. Science 1995; 270, 1354-1357.
6. Chakravarti D, LaMorte VJ, Nelson MC et al. Role of CBP/P300 in nuclear receptor signalling. Nature 1996; 383, 99-103.
7. Zoete V, Grosdidier A, Michielin O. Peroxisome proliferator-activated receptor structures: ligand specificity, molecular switch and interactions with regulators. Biochim Biophys Acta 2007; 1771, 915-925.
8. Xu HE, Lambert MH, Montana VG et al. Structural determinants of ligand binding selectivity between the peroxisome proliferator-activated receptors. Proc Natl Acad Sci U S A 2001; 98, 13919-13924.
9. Sierra ML, Beneton V, Boullay AB et al. Substituted 2-[(4-aminomethyl)phenoxy]-2-methylpropionic acid PPARalpha agonists. 1. Discovery of a novel series of potent HDLc raising agents. J Med Chem 2007; 50, 685-695.
10. Nolte RT, Wisely GB, Westin S et al. Ligand binding and co-activator assembly of the peroxisome proliferator-activated receptor-gamma. Nature 1998; 395, 137-143.
11. Xu HE, Lambert MH, Montana VG et al. Molecular recognition of fatty acids by peroxisome proliferator-activated receptors. Mol Cell 1999; 3, 397-403.
12. Nagy L, Schwabe JW. Mechanism of the nuclear receptor molecular switch. Trends Biochem Sci 2004; 29, 317-324.
13. Cronet P, Petersen JF, Folmer R et al. Structure of the PPARalpha and -gamma ligand binding domain in complex with AZ 242; ligand selectivity and agonist activation in the PPAR family. Structure 2001; 9, 699-706.
14. Chandra V, Huang P, Hamuro Y et al. Structure of the intact PPAR-gamma-RXR-alpha nuclear receptor complex on DNA. Nature 2008;
15. Desvergne B, Wahli W. Peroxisome proliferator-activated receptors: nuclear control of metabolism. Endocr Rev 1999; 20, 649-688.
16. Kliewer SA, Umesono K, Noonan DJ, Heyman RA, Evans RM. Convergence of 9-cis retinoic acid and peroxisome proliferator signalling pathways through heterodimer formation of their receptors. Nature 1992; 358, 771-774.

17. Horlein AJ, Naar AM, Heinzel T et al. Ligand-independent repression by the thyroid hormone receptor mediated by a nuclear receptor co-repressor. Nature 1995; 377, 397-404.
18. Chen JD, Evans RM. A transcriptional co-repressor that interacts with nuclear hormone receptors. Nature 1995; 377, 454-457.
19. Xu L, Glass CK, Rosenfeld MG. Coactivator and corepressor complexes in nuclear receptor function. Curr Opin Genet Dev 1999; 9, 140-147.
20. Zhu Y, Qi C, Calandra C, Rao MS, Reddy JK. Cloning and identification of mouse steroid receptor coactivator-1 (mSRC-1), as a coactivator of peroxisome proliferator-activated receptor gamma. Gene Expr 1996; 6, 185-195.
21. Zhu Y, Qi C, Jain S, Rao MS, Reddy JK. Isolation and characterization of PBP, a protein that interacts with peroxisome proliferator-activated receptor. J Biol Chem 1997; 272, 25500-25506.
22. Hu X, Lazar MA. The CoRNR motif controls the recruitment of corepressors by nuclear hormone receptors. Nature 1999; 402, 93-96.
23. Lemberger T, Desvergne B, Wahli W. Peroxisome proliferator-activated receptors: a nuclear receptor signaling pathway in lipid physiology. Annu Rev Cell Dev Biol 1996; 12, 335-363.
24. DiRenzo J, Soderstrom M, Kurokawa R et al. Peroxisome proliferator-activated receptors and retinoic acid receptors differentially control the interactions of retinoid X receptor heterodimers with ligands, coactivators, and corepressors. Mol Cell Biol 1997; 17, 2166-2176.
25. Hsu MH, Palmer CN, Song W, Griffin KJ, Johnson EF. A carboxyl-terminal extension of the zinc finger domain contributes to the specificity and polarity of peroxisome proliferator-activated receptor DNA binding. J Biol Chem 1998; 273, 27988-27997.
26. Juge-Aubry C, Pernin A, Favez T et al. DNA binding properties of peroxisome proliferator-activated receptor subtypes on various natural peroxisome proliferator response elements. Importance of the 5'-flanking region. J Biol Chem 1997; 272, 25252-25259.
27. Dreyer C, Krey G, Keller H, Givel F, Helftenbein G, Wahli W. Control of the peroxisomal beta-oxidation pathway by a novel family of nuclear hormone receptors. Cell 1992; 68, 879-887.
28. Tontonoz P, Hu E, Graves RA, Budavari AI, Spiegelman BM. mPPAR gamma 2: tissue-specific regulator of an adipocyte enhancer. Genes Dev 1994; 8, 1224-1234.
29. Rau O, Zettl H, Popescu L, Steinhilber D, Schubert-Zsilavecz M. [New targets and drugs for treatment of lipid metabolism disorders]. Pharm Unserer Zeit 2007; 36, 142-148.
30. Kota BP, Huang TH, Roufogalis BD. An overview on biological mechanisms of PPARs. Pharmacol Res 2005; 51, 85-94.
31. Duval C, Muller M, Kersten S. PPARalpha and dyslipidemia. Biochim Biophys Acta 2007; 1771, 961-971.
32. Schoonjans K, Watanabe M, Suzuki H et al. Induction of the acyl-coenzyme A synthetase gene by fibrates and fatty acids is mediated by a peroxisome proliferator response element in the C promoter. J Biol Chem 1995; 270, 19269-19276.
33. Staels B, Vu-Dac N, Kosykh VA et al. Fibrates downregulate apolipoprotein C-III expression independent of induction of peroxisomal acyl coenzyme A oxidase. A potential mechanism for the hypolipidemic action of fibrates. J Clin Invest 1995; 95, 705-712.
34. Bard JM, Parra HJ, Camare R et al. A multicenter comparison of the effects of simvastatin and fenofibrate therapy in severe primary hypercholesterolemia, with particular emphasis on lipoproteins defined by their apolipoprotein composition. Metabolism 1992; 41, 498-503.

35. Marx N, Sukhova GK, Collins T, Libby P, Plutzky J. PPARalpha activators inhibit cytokine-induced vascular cell adhesion molecule-1 expression in human endothelial cells. Circulation 1999; 99, 3125-3131.
36. Ziouzenkova O, Perrey S, Asatryan L et al. Lipolysis of triglyceride-rich lipoproteins generates PPAR ligands: evidence for an antiinflammatory role for lipoprotein lipase. Proc Natl Acad Sci U S A 2003; 100, 2730-2735.
37. Fruchart JC, Staels B, Duriez P. The role of fibric acids in atherosclerosis. Curr Atheroscler Rep 2001; 3, 83-92.
38. Kleemann R, Gervois PP, Verschuren L, Staels B, Princen HM, Kooistra T. Fibrates down-regulate IL-1-stimulated C-reactive protein gene expression in hepatocytes by reducing nuclear p50-NFkappa B-C/EBP-beta complex formation. Blood 2003; 101, 545-551.
39. Chinetti G, Lestavel S, Bocher V et al. PPAR-alpha and PPAR-gamma activators induce cholesterol removal from human macrophage foam cells through stimulation of the ABCA1 pathway. Nat Med 2001; 7, 53-58.
40. Furnsinn C, Willson TM, Brunmair B. Peroxisome proliferator-activated receptor-delta, a regulator of oxidative capacity, fuel switching and cholesterol transport. Diabetologia 2007; 50, 8-17.
41. Matsuura H, Adachi H, Smart RC, Xu X, Arata J, Jetten AM. Correlation between expression of peroxisome proliferator-activated receptor beta and squamous differentiation in epidermal and tracheobronchial epithelial cells. Mol Cell Endocrinol 1999; 147, 85-92.
42. Tanaka T, Yamamoto J, Iwasaki S et al. Activation of peroxisome proliferator-activated receptor delta induces fatty acid beta-oxidation in skeletal muscle and attenuates metabolic syndrome. Proc Natl Acad Sci U S A 2003; 100, 15924-15929.
43. Oliver WRJ, Shenk JL, Snaith MR et al. A selective peroxisome proliferator-activated receptor delta agonist promotes reverse cholesterol transport. Proc Natl Acad Sci U S A 2001; 98, 5306-5311.
44. Park BH, Vogelstein B, Kinzler KW. Genetic disruption of PPARdelta decreases the tumorigenicity of human colon cancer cells. Proc Natl Acad Sci U S A 2001; 98, 2598-2603.
45. Grimaldi PA. Regulatory functions of PPARbeta in metabolism: implications for the treatment of metabolic syndrome. Biochim Biophys Acta 2007; 1771, 983-990.
46. Mukherjee R, Jow L, Croston GE, Paterniti JRJ. Identification, characterization, and tissue distribution of human peroxisome proliferator-activated receptor (PPAR) isoforms PPARgamma2 versus PPARgamma1 and activation with retinoid X receptor agonists and antagonists. J Biol Chem 1997; 272, 8071-8076.
47. Rosen ED, Sarraf P, Troy AE et al. PPAR gamma is required for the differentiation of adipose tissue in vivo and in vitro. Mol Cell 1999; 4, 611-617.
48. Tontonoz P, Spiegelman BM. Fat and beyond: the diverse biology of PPARgamma. Annu Rev Biochem 2008; 77, 289-312.
49. Sinha R, Dufour S, Petersen KF et al. Assessment of skeletal muscle triglyceride content by (1)H nuclear magnetic resonance spectroscopy in lean and obese adolescents: relationships to insulin sensitivity, total body fat, and central adiposity. Diabetes 2002; 51, 1022-1027.

50. Okuno A, Tamemoto H, Tobe K et al. Troglitazone increases the number of small adipocytes without the change of white adipose tissue mass in obese Zucker rats. J Clin Invest 1998; 101, 1354-1361.
51. Hu E, Liang P, Spiegelman BM. AdipoQ is a novel adipose-specific gene dysregulated in obesity. J Biol Chem 1996; 271, 10697-10703.
52. Berg AH, Combs TP, Scherer PE. ACRP30/adiponectin: an adipokine regulating glucose and lipid metabolism. Trends Endocrinol Metab 2002; 13, 84-89.
53. Wellen KE, Hotamisligil GS. Inflammation, stress, and diabetes. J Clin Invest 2005; 115, 1111-1119.
54. Ricote M, Huang J, Fajas L et al. Expression of the peroxisome proliferator-activated receptor gamma (PPARgamma) in human atherosclerosis and regulation in macrophages by colony stimulating factors and oxidized low density lipoprotein. Proc Natl Acad Sci U S A 1998; 95, 7614-7619.
55. Odegaard JI, Ricardo-Gonzalez RR, Goforth MH et al. Macrophage-specific PPARgamma controls alternative activation and improves insulin resistance. Nature 2007; 447, 1116-1120.
56. Castrillo A, Tontonoz P. Nuclear receptors in macrophage biology: at the crossroads of lipid metabolism and inflammation. Annu Rev Cell Dev Biol 2004; 20, 455-480.
57. Bouhlel MA, Derudas B, Rigamonti E et al. PPARgamma activation primes human monocytes into alternative M2 macrophages with anti-inflammatory properties. Cell Metab 2007; 6, 137-143.
58. Pasceri V, Wu HD, Willerson JT, Yeh ET. Modulation of vascular inflammation in vitro and in vivo by peroxisome proliferator-activated receptor-gamma activators. Circulation 2000; 101, 235-238.
59. Li AC, Brown KK, Silvestre MJ, Willson TM, Palinski W, Glass CK. Peroxisome proliferator-activated receptor gamma ligands inhibit development of atherosclerosis in LDL receptor-deficient mice. J Clin Invest 2000; 106, 523-531.
60. Ogawa S, Lozach J, Benner C et al. Molecular determinants of crosstalk between nuclear receptors and toll-like receptors. Cell 2005; 122, 707-721.
61. Han S, Roman J. Peroxisome proliferator-activated receptor gamma: a novel target for cancer therapeutics? Anticancer Drugs 2007; 18, 237-244.
62. Banner CD, Gottlicher M, Widmark E, Sjovall J, Rafter JJ, Gustafsson JA. A systematic analytical chemistry/cell assay approach to isolate activators of orphan nuclear receptors from biological extracts: characterization of peroxisome proliferator-activated receptor activators in plasma. J Lipid Res 1993; 34, 1583-1591.
63. Bishop-Bailey D, Wray J. Peroxisome proliferator-activated receptors: a critical review on endogenous pathways for ligand generation. Prostaglandins Other Lipid Mediat 2003; 71, 1-22.
64. Yu K, Bayona W, Kallen CB et al. Differential activation of peroxisome proliferator-activated receptors by eicosanoids. J Biol Chem 1995; 270, 23975-23983.
65. Nagy L, Tontonoz P, Alvarez JG, Chen H, Evans RM. Oxidized LDL regulates macrophage gene expression through ligand activation of PPARgamma. Cell 1998; 93, 229-240.
66. Kuhn B, Hilpert H, Benz J et al. Structure-based design of indole propionic acids as novel PPARalpha/gamma co-agonists. Bioorg Med Chem Lett 2006; 16, 4016-4020.

67. Pirard B. Peroxisome proliferator-activated receptors target family landscape: a chemometrical approach to ligand selectivity based on protein binding site analysis. J Comput Aided Mol Des 2003; 17, 785-796.
68. Takada I, Yu RT, Xu HE et al. Alteration of a single amino acid in peroxisome proliferator-activated receptor-alpha (PPAR alpha) generates a PPAR delta phenotype. Mol Endocrinol 2000; 14, 733-740.
69. Ostberg T, Svensson S, Selen G et al. A new class of peroxisome proliferator-activated receptor agonists with a novel binding epitope shows antidiabetic effects. J Biol Chem 2004; 279, 41124-41130.
70. Lu IL, Huang CF, Peng YH et al. Structure-based drug design of a novel family of PPARgamma partial agonists: virtual screening, X-ray crystallography, and in vitro/in vivo biological activities. J Med Chem 2006; 49, 2703-2712.
71. Pochetti G, Godio C, Mitro N et al. Insights into the mechanism of partial agonism: crystal structures of the peroxisome proliferator-activated receptor gamma ligand-binding domain in the complex with two enantiomeric ligands. J Biol Chem 2007; 282, 17314-17324.
72. Steinhilber D, Schubert-Zsilavecz M. [Molecular pharmacology and medicinal chemistry of fibrate]. Pharm Unserer Zeit 2007; 36, 108-112.
73. Willson TM, Brown PJ, Sternbach DD, Henke BR. The PPARs: from orphan receptors to drug discovery. J Med Chem 2000; 43, 527-550.
74. Rau O, Syha Y, Zettl H, Kock M, Bock A, Schubert-Zsilavecz M. Alpha-alkyl substituted pirinixic acid derivatives as potent dual agonists of the peroxisome proliferator activated receptor alpha and gamma. Arch Pharm (Weinheim) 2008; 341, 191-195.
75. d'Atri G, Gomarasca P, Resnati G, Tronconi G, Scolastico C, Sirtori CR. Novel pyrimidine and 1,3,5-triazine hypolipidemic agents. J Med Chem 1984; 27, 1621-1629.
76. Rau O, Zettl H, Popescu L, Steinhilber D, Schubert-Zsilavecz M. The treatment of dyslipidemia--what's left in the pipeline? ChemMedChem 2008; 3, 206-221.
77. Xu Y, Mayhugh D, Saeed A et al. Design and synthesis of a potent and selective triazolone-based peroxisome proliferator-activated receptor alpha agonist. J Med Chem 2003; 46, 5121-5124.
78. Desai RC, Gratale DF, Han W et al. Aryloxazolidinediones: identification of potent orally active PPAR dual alpha/gamma agonists. Bioorg Med Chem Lett 2003; 13, 3541-3544.
79. Faucher N, Martres P, Laroze A, Pineau O, Potvain F, Grillot D. Design, synthesis and evaluation of trifluoromethane sulfonamide derivatives as new potent and selective peroxisome proliferator-activated receptor alpha agonists. Bioorg Med Chem Lett 2008; 18, 710-715.
80. Ramachandran U, Kumar R, Mittal A. Fine tuning of PPAR ligands for type 2 diabetes and metabolic syndrome. Mini Rev Med Chem 2006; 6, 563-573.
81. Oberfield JL, Collins JL, Holmes CP et al. A peroxisome proliferator-activated receptor gamma ligand inhibits adipocyte differentiation. Proc Natl Acad Sci U S A 1999; 96, 6102-6106.
82. Burgermeister E, Schnoebelen A, Flament A et al. A novel partial agonist of peroxisome proliferator-activated receptor-gamma (PPARgamma) recruits PPARgamma-coactivator-1alpha, prevents triglyceride accumulation, and potentiates insulin signaling in vitro. Mol Endocrinol 2006; 20, 809-830.

83. Einstein M, Akiyama TE, Castriota GA et al. The differential interactions of peroxisome proliferator-activated receptor gamma ligands with Tyr473 is a physical basis for their unique biological activities. Mol Pharmacol 2008; 73, 62-74.
84. Allen T, Zhang F, Moodie SA et al. Halofenate is a selective peroxisome proliferator-activated receptor gamma modulator with antidiabetic activity. Diabetes 2006; 55, 2523-2533.
85. Feldman PL, Lambert MH, Henke BR. PPAR modulators and PPAR pan agonists for metabolic diseases: the next generation of drugs targeting peroxisome proliferator-activated receptors? Curr Top Med Chem 2008; 8, 728-749.
86. Koyama H, Miller DJ, Boueres JK et al. (2R)-2-ethylchromane-2-carboxylic acids: discovery of novel PPARalpha/gamma dual agonists as antihyperglycemic and hypolipidemic agents. J Med Chem 2004; 47, 3255-3263.
87. Artis DR, Lin JJ, Zhang C et al. Scaffold-based discovery of indeglitazar, a PPAR pan-active anti-diabetic agent. Proc Natl Acad Sci U S A 2009; 106, 262-267.
88. Clofibrate in ischaemic heart disease. Br Med J 1971; 4, 765-766.
89. Brown JD, Plutzky J. Peroxisome proliferator-activated receptors as transcriptional nodal points and therapeutic targets. Circulation 2007; 115, 518-533.
90. Rubins HB, Robins SJ, Collins D et al. Gemfibrozil for the secondary prevention of coronary heart disease in men with low levels of high-density lipoprotein cholesterol. Veterans Affairs High-Density Lipoprotein Cholesterol Intervention Trial Study Group. N Engl J Med 1999; 341, 410-418.
91. Keech A, Simes RJ, Barter P et al. Effects of long-term fenofibrate therapy on cardiovascular events in 9795 people with type 2 diabetes mellitus (the FIELD study): randomised controlled trial. Lancet 2005; 366, 1849-1861.
92. Wierzbicki AS. Fibrates after the FIELD study: Some answers, more questions. Diab Vasc Dis Res 2006; 3, 166-171.
93. Rosenblatt S, Miskin B, Glazer NB, Prince MJ, Robertson KE. The impact of pioglitazone on glycemic control and atherogenic dyslipidemia in patients with type 2 diabetes mellitus. Coron Artery Dis 2001; 12, 413-423.
94. Nesto RW, Bell D, Bonow RO et al. Thiazolidinedione use, fluid retention, and congestive heart failure: a consensus statement from the American Heart Association and American Diabetes Association. October 7, 2003. Circulation 2003; 108, 2941-2948.
95. Nissen SE, Wolski K. Effect of rosiglitazone on the risk of myocardial infarction and death from cardiovascular causes. N Engl J Med 2007; 356, 2457-2471.
96. Lago RM, Singh PP, Nesto RW. Congestive heart failure and cardiovascular death in patients with prediabetes and type 2 diabetes given thiazolidinediones: a meta-analysis of randomised clinical trials. Lancet 2007; 370, 1129-1136.
97. Lincoff AM, Wolski K, Nicholls SJ, Nissen SE. Pioglitazone and risk of cardiovascular events in patients with type 2 diabetes mellitus: a meta-analysis of randomized trials. JAMA 2007; 298, 1180-1188.
98. Guan Y, Hao C, Cha DR et al. Thiazolidinediones expand body fluid volume through PPARgamma stimulation of ENaC-mediated renal salt absorption. Nat Med 2005; 11, 861-866.

99. Gerstein HC, Yusuf S, Bosch J et al. Effect of rosiglitazone on the frequency of diabetes in patients with impaired glucose tolerance or impaired fasting glucose: a randomised controlled trial. Lancet 2006; 368, 1096-1105.
100. Vosper H, Khoudoli GA, Graham TL, Palmer CN. Peroxisome proliferator-activated receptor agonists, hyperlipidaemia, and atherosclerosis. Pharmacol Ther 2002; 95, 47-62.
101. Kendall DM, Rubin CJ, Mohideen P et al. Improvement of glycemic control, triglycerides, and HDL cholesterol levels with muraglitazar, a dual (alpha/gamma) peroxisome proliferator-activated receptor activator, in patients with type 2 diabetes inadequately controlled with metformin monotherapy: A double-blind, randomized, pioglitazone-comparative study. Diabetes Care 2006; 29, 1016-1023.
102. Nissen SE, Wolski K, Topol EJ. Effect of muraglitazar on death and major adverse cardiovascular events in patients with type 2 diabetes mellitus. Jama 2005; 294, 2581-2586.
103. Fagerberg B, Edwards S, Halmos T et al. Tesaglitazar, a novel dual peroxisome proliferator-activated receptor alpha/gamma agonist, dose-dependently improves the metabolic abnormalities associated with insulin resistance in a non-diabetic population. Diabetologia 2005; 48, 1716-1725.
104. Bays H, McElhattan J, Bryzinski BS. A double-blind, randomised trial of tesaglitazar versus pioglitazone in patients with type 2 diabetes mellitus. Diab Vasc Dis Res 2007; 4, 181-193.
105. Oleksiewicz MB, Thorup I, Nielsen HS et al. Generalized cellular hypertrophy is induced by a dual-acting PPAR agonist in rat urinary bladder urothelium in vivo. Toxicol Pathol 2005; 33, 552-560.
106. Balakumar P, Rose M, Ganti SS, Krishan P, Singh M. PPAR dual agonists: are they opening Pandora's Box? Pharmacol Res 2007; 56, 91-98.
107. Zhang F, Lavan BE, Gregoire FM. Selective Modulators of PPAR-gamma Activity: Molecular Aspects Related to Obesity and Side-Effects. PPAR Res 2007; 2007, 32696.
108. Jakobsson PJ, Thoren S, Morgenstern R, Samuelsson B. Identification of human prostaglandin E synthase: a microsomal, glutathione-dependent, inducible enzyme, constituting a potential novel drug target. Proc Natl Acad Sci U S A 1999; 96, 7220-7225.
109. Jegerschold C, Pawelzik SC, Purhonen P et al. Structural basis for induced formation of the inflammatory mediator prostaglandin E2. Proc Natl Acad Sci U S A 2008; 105, 11110-11115.
110. Martinez Molina D, Wetterholm A, Kohl A et al. Structural basis for synthesis of inflammatory mediators by human leukotriene C4 synthase. Nature 2007; 448, 613-616.
111. Gillmor SA, Villasenor A, Fletterick R, Sigal E, Browner MF. The structure of mammalian 15-lipoxygenase reveals similarity to the lipases and the determinants of substrate specificity. Nat Struct Biol 1997; 4, 1003-1009.
112. Hammarberg T, Provost P, Persson B, Radmark O. The N-terminal domain of 5-lipoxygenase binds calcium and mediates calcium stimulation of enzyme activity. J Biol Chem 2000; 275, 38787-38793.
113. Pande AH, Moe D, Nemec KN, Qin S, Tan S, Tatulian SA. Modulation of human 5-lipoxygenase activity by membrane lipids. Biochemistry 2004; 43, 14653-14666.
114. Werz O, Tretiakova I, Michel A et al. Caspase-mediated degradation of human 5-lipoxygenase in B lymphocytic cells. Proc Natl Acad Sci U S A 2005; 102, 13164-13169.

115. Funk CD. Prostaglandins and leukotrienes: advances in eicosanoid biology. Science 2001; 294, 1871-1875.
116. Folco G, Murphy RC. Eicosanoid transcellular biosynthesis: from cell-cell interactions to in vivo tissue responses. Pharmacol Rev 2006; 58, 375-388.
117. Sampey AV, Monrad S, Crofford LJ. Microsomal prostaglandin E synthase-1: the inducible synthase for prostaglandin E2. Arthritis Res Ther 2005; 7, 114-117.
118. Kudo I, Murakami M. Prostaglandin E synthase, a terminal enzyme for prostaglandin E2 biosynthesis. J Biochem Mol Biol 2005; 38, 633-638.
119. Thoren S, Jakobsson PJ. Coordinate up- and down-regulation of glutathione-dependent prostaglandin E synthase and cyclooxygenase-2 in A549 cells. Inhibition by NS-398 and leukotriene C4. Eur J Biochem 2000; 267, 6428-6434.
120. Masuko-Hongo K, Berenbaum F, Humbert L, Salvat C, Goldring MB, Thirion S. Up-regulation of microsomal prostaglandin E synthase 1 in osteoarthritic human cartilage: critical roles of the ERK-1/2 and p38 signaling pathways. Arthritis Rheum 2004; 50, 2829-2838.
121. Mendez M, LaPointe MC. PPARgamma inhibition of cyclooxygenase-2, PGE2 synthase, and inducible nitric oxide synthase in cardiac myocytes. Hypertension 2003; 42, 844-850.
122. Naraba H, Yokoyama C, Tago N et al. Transcriptional regulation of the membrane-associated prostaglandin E2 synthase gene. Essential role of the transcription factor Egr-1. J Biol Chem 2002; 277, 28601-28608.
123. Bombardieri S, Cattani P, Ciabattoni G et al. The synovial prostaglandin system in chronic inflammatory arthritis: differential effects of steroidal and nonsteroidal anti-inflammatory drugs. Br J Pharmacol 1981; 73, 893-901.
124. Hardy MM, Seibert K, Manning PT et al. Cyclooxygenase 2-dependent prostaglandin E2 modulates cartilage proteoglycan degradation in human osteoarthritis explants. Arthritis Rheum 2002; 46, 1789-1803.
125. Park JY, Pillinger MH, Abramson SB. Prostaglandin E2 synthesis and secretion: the role of PGE2 synthases. Clin Immunol 2006; 119, 229-240.
126. Fitzpatrick FA, Morton DR, Wynalda MA. Albumin stabilizes leukotriene A4. J Biol Chem 1982; 257, 4680-4683.
127. Werz O. 5-lipoxygenase: cellular biology and molecular pharmacology. Curr Drug Targets Inflamm Allergy 2002; 1, 23-44.
128. Haeggstrom JZ, Wetterholm A. Enzymes and receptors in the leukotriene cascade. Cell Mol Life Sci 2002; 59, 742-753.
129. Peters-Golden M, Brock TG. 5-lipoxygenase and FLAP. Prostaglandins Leukot Essent Fatty Acids 2003; 69, 99-109.
130. Werz O, Klemm J, Samuelsson B, Radmark O. Phorbol ester up-regulates capacities for nuclear translocation and phosphorylation of 5-lipoxygenase in Mono Mac 6 cells and human polymorphonuclear leukocytes. Blood 2001; 97, 2487-2495.
131. Peters-Golden M, Henderson WRJ. Leukotrienes. N Engl J Med 2007; 357, 1841-1854.
132. Friesen RW, Mancini JA. Microsomal prostaglandin E2 synthase-1 (mPGES-1): a novel anti-inflammatory therapeutic target. J Med Chem 2008; 51, 4059-4067.

133. Riendeau D, Aspiotis R, Ethier D et al. Inhibitors of the inducible microsomal prostaglandin E2 synthase (mPGES-1) derived from MK-886. Bioorg Med Chem Lett 2005; 15, 3352-3355.
134. Cote B, Boulet L, Brideau C et al. Substituted phenanthrene imidazoles as potent, selective, and orally active mPGES-1 inhibitors. Bioorg Med Chem Lett 2007; 17, 6816-6820.
135. Xu D, Rowland SE, Clark P et al. MF63 {2-(6-chloro-1H-phenanthro[9,10-d]imidazol-2-yl)isophthalonitrile}, a selective microsomal prostaglandin E synthase 1 inhibitor, relieves pyresis and pain in preclinical models of inflammation. J Pharmacol Exp Ther 2008;
136. Koeberle A, Siemoneit U, Buhring U et al. Licofelone suppresses prostaglandin E2 formation by interference with the inducible microsomal prostaglandin E2 synthase-1. J Pharmacol Exp Ther 2008; 326, 975-982.
137. Fischer L, Hornig M, Pergola C et al. The molecular mechanism of the inhibition by licofelone of the biosynthesis of 5-lipoxygenase products. Br J Pharmacol 2007; 152, 471-480.
138. Werz O, Steinhilber D. Development of 5-lipoxygenase inhibitors--lessons from cellular enzyme regulation. Biochem Pharmacol 2005; 70, 327-333.
139. Carter GW, Young PR, Albert DH et al. 5-lipoxygenase inhibitory activity of zileuton. J Pharmacol Exp Ther 1991; 256, 929-937.
140. Werz O, Szellas D, Henseler M, Steinhilber D. Nonredox 5-lipoxygenase inhibitors require glutathione peroxidase for efficient inhibition of 5-lipoxygenase activity. Mol Pharmacol 1998; 54, 445-451.
141. Steffel J, Luscher TF, Ruschitzka F, Tanner FC. Cyclooxygenase-2 inhibition and coagulation. J Cardiovasc Pharmacol 2006; 47 Suppl 1, S15-20.
142. Jones R, Rubin G, Berenbaum F, Scheiman J. Gastrointestinal and cardiovascular risks of nonsteroidal anti-inflammatory drugs. Am J Med 2008; 121, 464-474.
143. Abdel-Tawab M, Zettl H, Schubert-Zsilavecz M. Nonsteroidal anti-inflammatory drugs: a critical review on current concepts applied to reduce gastrointestinal toxicity. Curr Med Chem 2009; 16, 2042-2063.
144. Celotti F, Laufer S. Anti-inflammatory drugs: new multitarget compounds to face an old problem. The dual inhibition concept. Pharmacol Res 2001; 43, 429-436.
145. Raynauld JP, Martel-Pelletier J, Bias P et al. Protective effects of licofelone, a 5-lipoxygenase and cyclooxygenase inhibitor, versus naproxen on cartilage loss in knee osteoarthritis: a first Multi-Centre Clinical Trial using quantitative MRI. Ann Rheum Dis 2008;
146. Zettl H, Dittrich M, Steri R et al. Novel Pirinixic Acids as PPARalpha Preferential Dual PPARalpha/gamma Agonists. QSAR & Combinatorial Science 2009; 28, 576-586.
147. Koeberle A, Zettl H, Greiner C, Wurglics M, Schubert-Zsilavecz M, Werz O. Pirinixic acid derivatives as novel dual inhibitors of microsomal prostaglandin E2 synthase-1 and 5-lipoxygenase. J Med Chem 2008; 51, 8068-8076.
148. Mandl A, Nicoletti L, Lammerhofer M, Lindner W. Quinine versus carbamoylated quinine-based chiral anion exchangers. A comparison regarding enantioselectivity for N-protected amino acids and other chiral acids. J Chromatogr A 1999; 858, 1-11.
149. Zettl H, Steri R, Lämmerhofer M, Schubert-Zsilavecz M. Discovery of a novel class of 2-mercaptohexanoic acid derivatives as highly active PPARalpha agonists. Bioorg Med Chem Lett 2009; 19, 4421-4426.

150. Aranapakam V, Grosu GT, Davis JM et al. Synthesis and structure-activity relationship of alpha-sulfonylhydroxamic acids as novel, orally active matrix metalloproteinase inhibitors for the treatment of osteoarthritis. J Med Chem 2003; 46, 2361-2375.
151. Kumar R, Ramachandran U, Raichur S, Chakrabarti R, Jain R. Synthesis and evaluation of N-acetyl-L-tyrosine based compounds as PPARalpha selective activators. Eur J Med Chem 2007; 42, 503-510.
152. Humphries PS, Do QQ, Wilhite DM. ADDP and PS-PPh3: an efficient Mitsunobu protocol for the preparation of pyridine ether PPAR agonists. Beilstein J Org Chem 2006; 2, 21.
153. Usui S, Fujieda H, Suzuki T et al. Synthesis and evaluation of 2-Nonylaminopyridine derivatives as PPAR ligands. Chem Pharm Bull (Tokyo) 2007; 55, 1053-1059.
154. Bargiggia F, Piva O. Anionic versus photochemical diastereoselective deconjugation of diacetone -glucose [alpha],[beta]-unsaturated esters. Tetrahedron: Asymmetry 2003; 14, 1819-1827.

6. Publikationsübersicht

6.1. Publikationen in *Peer-Reviewed Journals*

(1) A. Koeberle*, **H. Zettl***, C. Greiner, M.Wurglics, M. Schubert-Zsilavecz, O. Werz

Pirinixic acid derivatives as novel dual inhibitors of microsomal prostaglandin E2 synthase-1 and 5-lipoxygenase

Journal of Medicinal Chemistry 2008; 51, 8068-8076.

*beide Autoren haben in gleichem Maße zur Publikation beigetragen

eigener Beitrag: Synthese der Hälfte der beschriebenen Verbindungen, Erstellung des druckfertigen Manuskriptes (Schreiben des chemisch-synthetischen Teiles des Papers, Diskussion der Struktur-Wirkungs-Beziehungen)

(2) **H. Zettl**, M. Dittrich, R. Steri, E. Proschak, O. Rau, D. Steinhilber, G. Schneider, M. Lämmerhofer, M. Schubert-Zsilavecz

Novel pirinixic acids as PPARα preferential dual PPARα/γ agonists

QSAR & Combinatorial Science 2009; 28, 576-586.

eigener Beitrag: Konzeption und Verfassen des Papers, Synthese der vorgestellten Verbindungen mit Ausnahme der enantioselektiven Synthese (M.Dittrich)

(3) **H. Zettl**, R. Steri, M. Lämmerhofer, M. Schubert-Zsilavecz

Discovery of a novel class of 2-mercaptohexanoic acid derivatives as

highly active PPARα agonists

Bioorganic & Medicinal Chemistry Letters 2009; 19, 4421-4426.

eigener Beitrag: Konzeption und Schreiben des Papers, Synthese aller vorgestellten Verbindungen

(4) E. Proschak, **H. Zettl**, Y. Tanrikulu, M. Weisel, J. M. Kriegl, O. Rau, M. Schubert-Zsilavecz, G. Schneider

From molecular shape to potent bioactive agents I: Bioisosteric replacement of molecular fragments

ChemMedChem 2008; 4, 41-44.

eigener Beitrag: Durchführung des Luciferase-Reportergen-Assays zur biologischen Charakterisierung der Substanzen

(5) E. Proschak, K. Sander, **H. Zettl**, Y. Tanrikulu, O. Rau, P. Schneider, M. Schubert-Zsilavecz, H. Stark, G. Schneider

From molecular shape to potent bioactive agents II: Fragment-based de novo design

ChemMedChem 2008; 4, 45-48.

eigener Beitrag: Durchführung des Luciferase-Reportergen-Assays zur biologischen Charakterisierung der Substanzen, Mitwirkung bei der Syntheseplanung

(6) O. Rau, Y. Syha, **H. Zettl**, M. Kock, A. Bock, M. Schubert-Zsilavecz

alpha-Alkyl Substituted Pirinixic Acid Derivatives as Potent Dual Agonists of the Peroxisome Proliferator Activated Receptor Alpha and Gamma

Archiv der Pharmazie - Chemistry in Life Sciences 2008; 341, 191-195.

eigener Beitrag: Synthese einer Schlüsselverbindung; Schreiben des chemisch-synthetischen Teiles des Papers

6.2. Reviews in *Peer-Reviewed Journals*

(7) O. Rau, **H. Zettl**, L. Popescu, D. Steinhilber, M. Schubert-Zsilavecz

The treatment of dyslipidemia--what's left in the pipeline?

ChemMedChem 2008; 3, 206-221.

eigener Beitrag: Verfassen der Hälfte des Reviews, Implementierung aller chem. Strukturen

(8) M. Abdel-Tawab, **H. Zettl**, M. Schubert-Zsilavecz

Nonsteroidal anti-inflammatory drugs: a critical review on current analytical concepts applied to reduce gastrointestinal toxicity

Current Medicinal Chemistry 2009; 16, 2042-2063.

eigener Beitrag: Implementierung aller chem. Strukturen, Layout, Verfassen des Abschnitts zu mPGES-1-Inhibitoren

6.3. Andere Beiträge

H. Zettl, C.D. Siebert, M. Schubert-Zsilavecz

Medizinische Chemie der 5-HT_3-Rezeptor-Antagonisten

Pharmazie in unserer Zeit 2007; 36, 354-361.

H. Zettl, C.D. Siebert, M. Schubert-Zsilavecz

Medizinische Chemie der Trizyklischen Antidepressiva

Pharmazie in unserer Zeit 2008; 37, 206 - 213.

H. Zettl, M. Schubert-Zsilavecz

Medizinische Chemie der Thrombozytenaggregationshemmer

Pharmazie in unserer Zeit 2009; *in press*.

K. Sander*, **H. Zettl***, M. Schubert-Zsilavecz, H. Stark

Antitussiva und Expektorantien. Medizinisch-chemische Aspekte

Pharmazie in unserer Zeit 2007; 36, 142 - 148.

*beide Autoren haben in gleichem Maße zur Publikation beigetragen

O. Rau, **H. Zettl**, L. Popescu, D. Steinhilber, M. Schubert-Zsilavecz

Neue Targets und Wirkstoffe zur Behandlung von Fettstoffwechselstörungen: Arzneistoffe in der Pipeline

Pharmazie in unserer Zeit 2007; 36, 142 - 148.

eigener Beitrag: Verfassen der Hälfte des Reviews, Implementierung aller chem. Strukturen

7. Lebenslauf

Angaben zur Person

Name	**Heiko Zettl**
Adresse	**Ziegenleithe 4, 08304 Schönheide, Deutschland**
Staatsangehörigkeit	Deutsch
Geburtsdatum	28.05.1981
Geburtsort	Rodewisch

Schul- und Universitäre Ausbildung

• Datum (von - bis)	*seit 01.06.2006*
• Name und Art der Bildungseinrichtung	Goethe-Universität Frankfurt am Main
• Beschreibung der Tätigkeit	Wissenschaftlicher Mitarbeiter im Arbeitskreis von Prof. Manfred Schubert-Zsilavecz: Doktorand im Bereich Medizinische Chemie Praktikumsbetreuung "Pharmazeutische Chemie" 3.Semester Pharmazie

• Datum (von - bis)	*01.10.2000 - 24.09.2004*
• Name und Art der Bildungseinrichtung	Universität Leipzig
• Studienfach	Pharmazie
• Bezeichnung der erworbenen Qualifikation	Approbation als Apotheker 2. Staatsexamen (*24.09.2004*)

• Absolvierte Praktika	*19.02.2001 - 16.03.2001* Famulatur in der Stadtapotheke Rodewisch *23.07.2001 - 18.08.2001* Famulatur bei der Bayer AG/ Leverkusen im Bereich Analytik *01.03.2003 - 31.07.2003* Tätigkeit als studentische Hilfskraft am Institut für Pharmazeutische Chemie der Universität Leipzig *01.07.2003 - 15.08.2003, 11.10.2004 - 19.11.2004* Tätigkeit bei der IBFB Pharma GmbH/ Leipzig im Bereich Wirkstoffdesign/ Medizinische Chemie *25.08.2003 - 30.09.2003* Teilnahme am IPSF – Student – Exchange - Program, University of Otago und Campus Pharmacy, Dunedin, Neuseeland *01.01.2005 - 31.07.2005* Pharmaziepraktikum bei der Novartis Pharma AG, Basel im Bereich Analytical & Research Development *01.10.2005 - 31.03.2006* Pharmaziepraktikum in der Apotheke am Seepark, Freiburg
• Datum (von - bis)	*1993 - 14.07.1999*
• Name und Art der Bildungseinrichtung	J.H.Pestalozzi - Gymnasium Rodewisch
• Bezeichnung der erworbenen Qualifikation	Allgemeine Hochschulreife
• Datum (von - bis)	*1987 - 1993*
• Name und Art der Bildungseinrichtung	Grund - und Mittelschule Schönheide

Sprachkenntnisse

Muttersprache	*Deutsch*
	Englisch
• Lesen	sehr gut
• Schreiben	sehr gut
• Sprechen	sehr gut
	Französisch
• Lesen	Grundkenntnisse
• Schreiben	Grundkenntnisse
• Sprechen	Grundkenntnisse

Während der Promotionszeit besuchte Tagungen, Konferenzen und Summer/ WinterSchools

Tagungen/ Konferenzen mit Posterbeiträgen	*22.04.2007 – 25.04.2007* Pharmaceutical Sciences World Congress, Amsterdam Poster: „Structural optimization of the pirinixic acid lead structure as dual PPARα/γ-agonist“ *02.03.2008 – 05.03.2008* Frontiers in Medicinal Chemistry, Regensburg Poster: „Biphenyl pirinixic acid derivatives are PPARα preferential potent dual PPARα/γ agonists“ *31.08.2008 – 04.09.2008* International Symposium on Medicinal Chemistry, Wien Poster: „A novel series of 2-mercaptohexanoic acid derivatives adressing crucial isoleucin-interactions within the PPARα-ligand binding domain“ *08.10.2008 – 11.10.2008* EMBL Conference on Chemical Biology, Heidelberg Poster: „Pirinixic acid derivatives as dual mPGES-1/5-LO inhibitors“
Summer/ WinterSchools	*22.04.2007 – 25.04.2007* FIRST/GK 757 Summer School und Eicosanox Annual Meeting, Aigen *12.10.2008 – 17.10.2008* 8th Swiss Course on Medicinal Chemistry, Leysin *07.03.2009 – 11.03.2009* FIRST/GK 757 (Roles of Eicosanoids in Biology and Medicine) WinterSchool, Obergurgl Invited Speaker, Vortrag: „Pirinixic acid derivatives: PPAR activation & Interaction with the Arachidonic acid cascade“
Frankfurter Pharmazieschule	Winter- und Sommerschule 2008, Winter- und Sommerschule 2009 für Studenten des 4.Semesters Pharmazie Mit-Organisation und Seminar „Allgemeine und anorganische Chemie: Stoffchemie und Chemische Bindung“

Akademische Lehrer:

Dr. S.Leistner

Prof. Dr. D.Briel

Prof. Dr. K.Eger

Prof. Dr. K.Nieber

Prof. Dr. W. Süß

Prof. Dr. C.Leopold

Prof. Dr. J.W.Rauwald

Prof. Dr. M. Schubert-Zsilavecz

8. Eidesstattliche Versicherung

Ich erkläre hiermit an Eides statt, dass ich die vorliegende Arbeit selbständig angefertigt und mich anderer Hilfsmittel als der in ihr angegebenen nicht bedient habe, insbesondere, dass aus Schriften Entlehnungen, soweit sie in der Dissertation nicht ausdrücklich als solche mit Angabe der betreffenden Schrift bezeichnet sind, nicht stattgefunden haben.

Frankfurt am Main, den _____

_____

Heiko Zettl

Erklärung

Ich erkläre hiermit, dass ich mich bisher keiner Doktorprüfung unterzogen habe.

Frankfurt am Main, den _____

_____

Heiko Zettl

9. Danksagung

Mein herzlicher Dank gilt allen, die zum Gelingen der vorliegenden Arbeit beigetragen und mich während meiner Promotionszeit begleitet haben.

Besonders bedanken möchte ich mich bei meinen Eltern für ihre fortwährende Unterstützung meines Lebensweges und das Gefühl, immer ein zu Hause zu haben.

Des Weiteren möchte ich mich bedanken...

...bei meiner Freundin Martina Hieke, das zweifellos schönste Resultat meiner Promotionszeit.

...bei den Mitgliedern des AK Schubert-Zsilavecz, und zwar bei:

Laura Popescu und Dr. Oliver Rau für Ihre Hilfe beim Einstieg in die Synthese (Laura) und den PPAR-Assay (Oliver).

meiner Labornachbarin Michaela Dittrich für eine schöne und entspannte Zeit.

Ramona Steri für den Kampf mit den Zellen, die fruchtbare gemeinsame Wissenschaft, das Lesen dieser Arbeit und gemeinsame Zeit.

Dr. Mario Wurglics und Christian Ude für lustige Diskussionen und gemeinsame Sommer/Winterschulen.

Dr. Alexander Paulke, Theresa Thieme, Stefan Bihler und Astrid Kaiser.

...bei allen Kooperationspartnern, die zum Gelingen dieser Arbeit beigetragen haben, insbesondere: Prof. Dr. Oliver Werz, Prof. Dr. Gisbert Schneider, Prof. Dr. Dieter Steinhilber, Dr. Mona Abdel-Tawab und Prof Dr. Sascha Weggen.

...bei Svenja Steinbrink für alles zwischen Weinstube und Sommerschule.

...bei Dr. Ewgenij Proschak für die begeisterte Zusammenarbeit, schöne Bildchen und viele gemeinsame Kongresse.

...bei Yvonne von Coburg für die unvergessene Winterschule mit den ersten Snowboardversuchen.

...bei Kerstin Sander, Tim Kottke und Kathleen Isensee für die gemeinsamen Kongresse und die schöne gemeinsame Zeit inkl. Umtrunk.

...bei allen Kollegen aus dem OC-Praktikum.

...bei meinen Freunden Eva Kupetz, Michael Schubert, Anne Breitschuh, Frank Ebert, Heiko Fröhlich, Patrick Siegel, Claudia Bartsch und allen, die ich vergessen habe.

Schließlich bedanke ich mich sehr bei Prof. Dr. Manfred Schubert-Zsilavecz, der mir vorliegende Arbeit ermöglicht und betreut hat.

Seine umfassende Unterstützung erlaubte mir eine besondere Promotionszeit, die von vielfältigen Möglichkeiten und Erfahrungen geprägt war. Besonders hervorheben möchte ich die Teilnahme an mehreren Kongressen und Summer/WinterSchools, die Frankfurter Pharmazieschule und gemeinsame AK-Seminare. Außerdem danke ich ihm für die vielen Möglichkeiten, Forschungsprojekte mit zu koordinieren und zu deren Gelingen beizutragen, die mein Interesse und meine Begeisterung für die Wissenschaft weiter entfacht haben.

10. Anhang

10.1. Abkürzungen

5-LO	5-Lipoxygenase
AA	*arachidonic acid*
ABCA-1	*ATP-binding cassette-1*
ADDP	Azodicarbonyldipiperidid
AF-1,AF-2	*activation function-1/-2*
DBD	DNA-Bindungs-Domäne
DEAD	Diethylazodicarboxylat
DMF	Dimethylformamid
COX	Cyclooxygenase
FFS	Freie Fettsäuren
HbA_{1c}	Hämoglobin A_{1c}
HDL	*high density lipoprotein*
IL	Interleukin
LBD	Liganden-Bindungs-Domäne
LPL	Lipoproteinlipase
LT(s)	*leukotriene(s)*
mPGES-1	mikrosomale Prostaglandin E_2-Synthase-1
NF-κB	*nuclear factor κB*
NSAID(s)	*non steroidal anti-inflammatory drug(s)*
MAPEG	*membrane-associated proteins in eicosanoid and glutathione metabolism*
PG(s)	*prostaglandin(s)*
PLA_2	Phospholipase A_2

PMNL	*polymorphonuclear leukocytes*
PPAR(s)	*peroxisome proliferator-activated receptor(s)*
PPRE	*peroxisome proliferator response element*
RXR	Retinoid-X-Rezeptor
SAR	*structure-activity relationships*
sPPARγM	Selektiver PPARγ-Modulator
SRC-1	*steroid receptor coactivator-1*
T2DM	Typ 2 Diabetes mellitus
TG	Triglyceride
THF	Tetrahydrofuran
TM	Transmembranäre Helix
TNF-α	Tumornekrosefaktor-α
TPP	Triphenylphosphin
TZD	Thiazolidindion
VLDL	*very low-density lipoprotein*

10.2. Nachdrucke der Publikationen

Nachfolgend sind die als essenzielle Bestandteile dieser Arbeit veröffentlichten Publikationen inklusive der Supplemente abgedruckt.

Anhang I:

The treatment of dyslipidemia--what's left in the pipeline?

Rau O, Zettl H, Popescu L, Steinhilber D, Schubert-Zsilavecz M

ChemMedChem 2008; 3, 206-221.

Anhang II:

Novel Pirinixic Acids as PPARα Preferential Dual PPARα/γ Agonists

Zettl H, Dittrich M, Steri R, Proschak E, Rau O, Steinhilber D, Schneider G, Lämmerhofer M, Schubert-Zsilavecz M

QSAR & Combinatorial Science 2009; 28, 576-586.

Anhang III:

Discovery of a novel class of 2-mercaptohexanoic acid derivatives as highly active PPARα agonists

Zettl H, Steri R, Lämmerhofer M, Schubert-Zsilavecz M

Bioorg Med Chem Lett 2009; 19, 4421-4426.

Anhang IV:

Pirinixic Acid Derivatives as Novel Dual Inhibitors of Microsomal Prostaglandin E2 Synthase-1 and 5-Lipoxygenase

Koeberle A, Zettl H, Greiner C, Wurglics M, Schubert-Zsilavecz M, Werz O

J Med Chem 2008; 51, 8068-8076.

Anhang V:

Inanspruchnahme der Diensterfindung Thiophenoletherderivate als duale Hemmstoffe der mikrosomalen Prostaglandin-E_2-Synthase und der 5-Lipoxygenase

DOI: 10.1002/cmdc.200700165

The Treatment of Dyslipidemia—What's Left in the Pipeline?

Oliver Rau,* Heiko Zettl, Laura Popescu, Dieter Steinhilber, and Manfred Schubert-Zsilavecz[a]

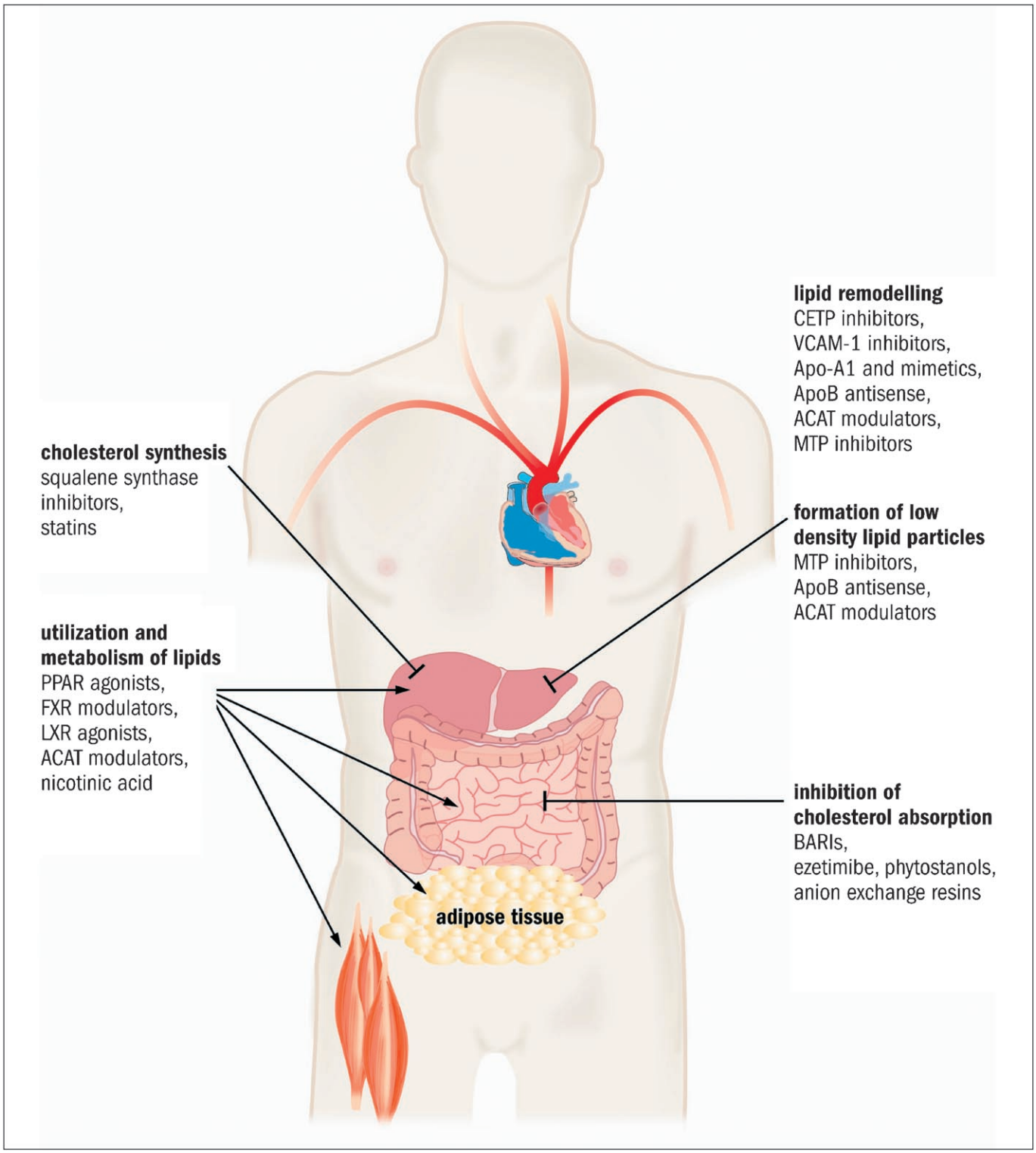

Dyslipidemia is a pathological alteration of serum lipid levels. The most common forms are either elevations of triglycerides or low density lipoprotein cholesterol associated with a reduction of high density lipoprotein cholesterol. Most frequently both forms of lipid disorders are combined. Elevations of free fatty acid blood levels are commonly not subsumed under the term dyslipidemia. However, free fatty acids should also be considered, as they are frequently associated with dyslipidemia and represent a risk factor for cardiovascular diseases. Dyslipidemias are among the major etiologic factors for arterial occlusive diseases. Resulting in fatal implications such as stroke and coronary heart disease, dyslipidemias contribute to the most prevalent causes of death. Lowering of low density lipoprotein and raising of high density lipoprotein cholesterol levels have been shown in both epidemiologic and intervention studies to decrease mortality. Established treatments of dyslipidemias are statins and fibrates. However, recent research has established some new potential therapeutic targets which are currently investigated in clinical trials. New therapeutic approaches include subtype selective, dual, and pan-agonists of the peroxisome proliferator activated receptor, inhibitors of the cholesterol ester transfer protein, Acyl-CoA-cholesterol-acyltransferase, squalene synthase, microsomal triglycerid-transfer-protein, and cholesterol absorption. Clinical implications of new drugs under investigation are discussed in this review.

Introduction

Dyslipidemia is a pathological increase of lipid and lipoprotein levels in the blood. Most prominent among these are the hyperlipidemic diseases hypercholesterolemia and hypertriglyceridemia. Elevated levels of cholesterol do mainly appear associated with low-density lipopoprotein (LDL) and less with very low-density lipoprotein (VLDL) particles in the blood, whereas elevated triglycerides are mainly related to VLDL and chylomycrones. As high-density lipoprotein (HDL) has a protective effect on the endothelium, lowered levels of those lipoprotein particles are associated with an increased risk for cardiovascular disease. Besides some rare genetically determined or familial forms, most disturbances of lipid homeostasis are associated with a more sedentary lifestyle, excessive caloric intake, and age, and do frequently appear combined with each other.[1,2] Another alteration of lipid levels, which is commonly not subsumed under the term dyslipidemia is raised levels of free fatty acids (FFA). Elevations of free fatty acid levels in the blood cause enhanced triglyceride synthesis in the liver and therefore lead to increased VLDL levels. Furthermore, free fatty acids induce insulin resistance, which is another risk factor for atherosclerosis.[3,4]

In both epidemiologic and intervention studies, lower or lowered levels of LDL and triglycerides and increased levels of HDL have been shown to be associated with a decreased risk for cardiovascular events.[5–12] Therefore the reduction of lipid levels or the increasing of HDL seems to be a valuable therapeutic approach. Indeed, several drugs (for example, statins) reduce cardiovascular events and mortality. However, lowering LDL or increasing HDL does not always seem to be an appropriate surrogate parameter for the prediction of a decreased cardiovascular mortality. Fibrates for example efficiently lower triglycerides and less extensively LDL, while increasing HDL. However, in some of the trials the overall mortality or cardiovascular mortality was not significantly lowered.[13–16]

Notably, for some of the newer drug candidates referred to in this review, it has clearly been demonstrated that they beneficially affect lipid parameters but increased mortality. In this review we give an overview about new lipid lowering agents and their targets and discuss their clinical implications and medicinal chemistry. Drugs acting by reducing food intake are not covered by this review.

Therapeutic Targets for the Treatment of Dyslipidemia

Nuclear receptors

Peroxisome proliferator-activated receptor

The peroxisome proliferator-activated receptor (PPAR) is a member of the nuclear receptor family comprising the three subtypes PPARα, PPARδ (also referred to as PPARβ), and PPARγ.

PPAR is a key-player of lipid and glucose homeostasis and therefore an appropriate target for the treatment of dyslipidemias.[17,18] Activation of PPAR leads to dimerization with the retinoid X receptor (RXR) and subsequent transactivation of the expression of target genes especially those of lipid and glucose transport and metabolism for example, lipoproteinlipase (LPL), apolipoprotein A1 (apoA1), fatty acid binding protein (FABP), fatty acid transport protein (FATP), and glucose transport proteins (GLUT).[19–23] As the PPAR subtypes bind to the same cognate response elements (PPRE) on DNA in vitro, the selectivity in vivo seems to largely depend on the tissue specific expression pattern, with PPARα mainly expressed in the liver, PPARγ in the adipose tissue, and PPARδ ubiquitously.[24,25]

Endogenous activators of PPAR are fatty acids the activity of which increases with the degree of unsatuaration. Fatty acids show only minor subtype selectivity, at most it has been suggested that PPARα has the highest affinity to less unsaturated fatty acids.[26,27] In our own observations, PPARα was activated by the mono- and diunsaturated fatty acids oleic and linoleic acid at lower concentrations than required for activation of PPARγ. Eicosanoids derived from cyclooxygenase and lipoxygenase pathways have also to be considered as endogenous

[a] *Dr. O. Rau, H. Zettl, L. Popescu, Prof. Dr. D. Steinhilber, Prof. Dr. M. Schubert-Zsilavecz*
Institute of Pharmaceutcial Chemistry/ZAFES
Johann Wolfgang Goethe University Frankfurt
Max-von-Laue-Strasse 9, 60438 Frankfurt (Germany)
Fax: (+49) 6979829332
E-mail: o.rau@em.uni-frankfurt.de

PPAR activators. As synthetic PPAR agonists mimic these natural ligands, they share the carboxyl group or a bioisosteric equivalent and a lipophilic backbone. Several structural variations have been identified that lead to increased affinity and subtype selectivity.[28,29]

There is also some prevailing preclinical evidence that PPAR activation modulates inflammatory responses, which might lead to some additional beneficial therapeutic effects for example, in endothelial dysfunction.[30,31]

Selective PPARα agonists—new fibrates?

Fibrates are well established in the therapy of dyslipidemias especially hypertriglyceridemia since the 1960s and also slightly increase HDL levels.[32–34]

A common structural element of the fibrates is the 2-hydroxy-*iso*-butyric acid residue. However in some preclinical high-affinity PPARα agonists, the oxygen linker has been replaced by sulfur.

Dr. Oliver Rau, born in 1974, graduated in pharmacy in 2003 from the Johann Wolfgang Goethe University in Frankfurt, Germany. In 2007 he completed his PhD thesis in the group of Prof. Manfred Schubert-Zsilavecz. At present he works as a postdoctoral fellow in the research group of Prof. Dieter Steinhilber.

Heiko Zettl (born in 1981); 2000–2004: study of pharmacy at the University of Leipzig; 2005: internship at Novartis Pharma AG, Basel; since June 2006: PhD student in the group of Prof. Manfred Schubert-Zsilavecz at the Johann Wolfgang Goethe University in Frankfurt, Germany.

Laura Boteanu-Popescu, born in 1968, studied chemistry at the University of Bucharest, Romania in co-operation with the University of Lille, France; 1995: master in science, organic chemistry. From 1996–1997 she was manager of the pharmaceutical production department and quality control at Les Laboratoires Holis Inc., Montréal. In 1997–1998, she was a researcher at the University of Montréal under the supervision of Prof. James Wuest; 1998–2001: quality control manager at Mosti Mondiale Inc., Montréal; 2002: manager of research and development at Packlab Products Inc., Montréal. Since April 2003 she prepared her PhD thesis in the group of Prof. Manfred Schubert-Zsilavecz at Johann Wolfgang Goethe University in Frankfurt. At present, she works as medical manager in drug development at YES Pharmaceutical Development Services GmbH, Friedrichsdorf, Germany.

Prof. Dr. Dieter Steinhilber, born in 1959, studied pharmacy at the University of Tübingen. After an assistantship there he spent a postdoctoral period with Prof. Bengt Samuelsson, Karolinska Institute, Stockholm from 1989 until 1991. In 1994 he received an associated professorship and since 2000 he has been a full professor of pharmaceutical chemistry at the Johann Wolfgang Goethe University in Frankfurt. Since 1999 he has been the director of this institute. From 1999 to 2000 he was dean of the faculty Biochemistry, Pharmacy, and Food Chemistry. Prof. Steinhilber is the speaker of the European Graduate School "Roles of Eicosanoids in Biology and Medicine" funded by DFG and Land Hessen and is a member of the board of ZAFES.

Prof. Manfred Schubert-Zsilavecz was born in Austria in 1961. He studied pharmacy at Karl-Franzens University Graz where he received his PhD in 1989. After spending his postdoctoral sojourn at Bayreuth University, he joined the faculty of chemistry at Ulm as an Erwin Schrödinger Fellowship (1992–1993). Accepting a position at the Johan Wolfgang Goethe University, Frankfurt, he has been a professor since 1997 in the pharmaceutical chemistry department and currently directs a research group of 10–15 postdoctoral and graduate students. Since 2001 Prof. Schubert-Zsilavecz has been dean of the chemical and pharmaceutical science department at Johann Wolfgang Goethe University (responsible for teaching activities). He is member of the board of ZAFES. In 2003 Prof. Schubert-Zsilavecz was appointed scientific director of the Central Laboratory of German Pharmacists and he was recently elected president of the German Pharmaceutical Society.

In vitro the fibrates are ligands of PPARα with moderate affinity displaying EC_{50} values in the micromolar range and possessing about tenfold selectivity over PPARγ. Their moderate affinity in vitro is reflected by dosages starting from one hundred milligrams. Interestingly, bezafibrate activates all three PPAR subtypes in an equipotent fashion in vitro and therefore should be considered as a pan-PPAR agonist. Bezafibrate has been proven to delay the progression of type 2 diabetes, suggesting a close relationship between diabetes and inherent PPARγ agonism.[35–37] There has been an intensive search for new high-affinity fibrates, however to our knowledge only LY518674 (Figure 1) has reached phase II trials. LY518674 is a

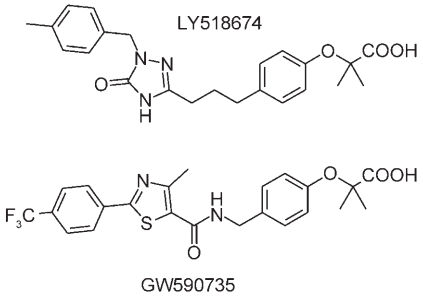

Figure 1. LY518674 and GW590735, selective agonists of PPARα.

highly selective and affine PPARα agonist with an EC_{50} of about 40 nM that displays more than 100-fold selectivity over PPARγ and PPARδ. In humanized transgenic apoA1 mice, LY518674 increased HDL levels and apoA1 synthesis. A first phase II trial with LY518674 has been completed but a subsequent trial has been suspended.[38,39]

Recently, the synthesis and structure of another selective PPARα agonist GW590735, which is currently in phase II clinical trials has been published.[40] In vitro, GW590735 showed an EC_{50} value of 4 nM for the activation of PPARα and a more than 100-fold selectivity compared to PPARγ and PPARδ. In a humanized apoA1 transgenic mouse model, GW590735 did significantly lower VLDL, LDL, and triglycerides whereas HDL was increased.

As fibrates are well established and effective in clinics, it might be questioned, whether new PPARα agonists with higher affinity and therefore presumably lower doses will show a higher therapeutic benefit and will be competitive on an economic basis. However, fibrates are essential drugs for the treatment of dyslipidemia. Fibrates are in use for more than two decades but there has been no real progress in the development of new fibrates. At least one of them, gemfibrozil is known for its strong potential for interactions, which promoted the development of rhabdomyolysis when it was combined with the cholesterol lowering drug cerivastatin. The introduction of new PPARα agonists with increased selectivity and affinity would enrich the spectrum of available fibrates and thus advance current therapies.

Selective PPARδ agonists—a new therapeutic approach

The activation of PPARδ is a rather new approach.[41] Although bezafibrate shows PPARδ agonistic activity, it is not clear at the moment whether selective PPARδ agonism is of any clinical relevance. There is preclinical evidence that PPARδ might have beneficial effects on lipid parameters.[41] GW501516 (Figure 2)

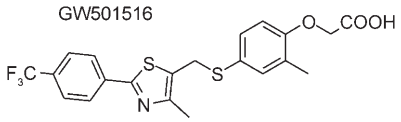

Figure 2. GW501516, a selective agonist of PPARδ.

is a highly selective and potent PPARδ agonist with an EC_{50} value of about 1 nM that displays 1000-fold selectivity over PPARα and PPARγ. GW501516 significantly reduced TG levels and increased HDL cholesterol in obese rhesus monkeys. Similar trends were observed in a small investigational study with nine healthy volunteers.[42,43] Phase II clinical trials seem to be ongoing, but have not been published so far. In addition, GW501516 led to weight loss in high fat diet-induced obese mice.[44]

However, preclinical observations also raise concerns, whether PPARδ activation might promote cancer.[45–51] Even if no such effects have been observed for the pan-agonistic bezafibrate in man, it cannot be excluded, that the selective PPARδ activation might promote angiogenesis and tumour progression.

Selective PPARγ agonists—affecting lipid levels with an antidiabetic drug

PPARγ selective glitazones are established in the treatment of type 2 diabetes.[52] However, clinical data show that the blood glucose level and lipid parameters are affected by rosiglitazone and pioglitazone.[34,53]

As PPARγ is most prominently expressed in the adipose tissue, it has to be considered as the major target organ. Activation of PPARγ leads to an enhanced uptake and storage of glucose and more relevant, free fatty acids in the adipose tissue.[19,54]

As mentioned above, glitazones, which are also referred to as thiazolidinediones (TZDs), do not only have an impact on blood glucose, but have also been shown to increase HDL, to lower TG, and for pioglitazone only, to lower LDL as well.[52]

A frequent side effect of glitazones is weight gain, which is caused by an increase of subcutaneous adipose tissue and fluid retention.[55] In a recent study, fluid retention has been suggested to be a PPARγ specific effect, caused by the increased expression of a renal sodium channel.[56] Weight gain alone is a typical side effect of antidiabetic drugs and also appears with insulin substitution and sulfonylurea therapy, although to a lesser extent. The increased incidence for edema and heart failure under glitazone therapy has lead to the con-

clusion that thiazolidinediones should not be used in patients with congestive heart failure or with edemas.[55]

Netoglitazone (MCC-555) (Figure 3), rivoglitazone (CS-011), and balaglitazone (DRF-2593) are examples of PPARγ selective agonists in clinical development, even though netoglitazone has also been suggested to affect other PPAR subtypes as well.[57–60]

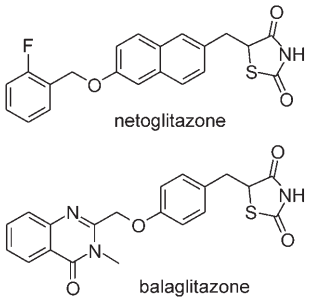

Figure 3. New glitazone type of PPARγ agonists.

A new focus in PPARγ research is the development of partial agonists such as halofenate (Figure 4). Some of these PPARγ modulators lower glucose levels as well, but might show a reduced fluid retention.[61–63] There are many factors influencing the balance between PPARγ agonism and antagonism that include the distribution of the drug in the body, the modulation of the interaction of PPARγ with co-activators and co-repressors by the drug, and the tissue distribution (kidney versus adipose tissue) of these proteins. Interestingly, recent reports have shown that some angiotensin II receptor antagonists are partial agonists of PPARγ with a moderate micromolar activity and one of them, telmisartan, is currently undergoing clinical trials to determine whether the PPARγ agonism shows any additional clinical benefit.[64,65]

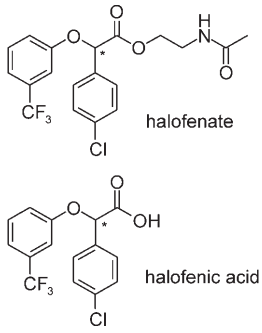

Figure 4. Halofenate and its active metabolite halofenic acid, a partial agonist of PPARγ.

Dual PPARα/γ agonists—two birds with one stone?

As hypertrigliyceridemia and type 2 diabetes are frequently associated with each other, the rationale for the combination of PPARα and PPARγ activity in one drug is obvious: PPARα agonism reduces triglyceride levels and activation of PPARγ hyperglycemia.[66–69] Hence, many efforts have been started to obtain dual agonists. However, so far, none of them has been approved although some of them have reached different stages of clinical trials up to phase III. Many of the drug candidates have been withdrawn from further trials for different reasons and there has been much controversy, whether the combined activation of PPARα and PPARγ might lead to distinct and additional toxicological problems.

The dual PPARα/γ agonist ragaglitazar (Figure 5) has been withdrawn from clinical studies after having reached phase III trials, due to the induction of bladder tumours in rats.[70,71] An animal study in rats suggests some changes in the rate of early growth response factor (EGF-1) expression in bladder urothelium, which depends on the concomitant activation of both PPARα and PPARγ. However the relevance of this observation is not clear. Interestingly, a recent publication shows that another dual PPARα/γ agonist, muraglitazar, did also lead to bladder tumours in rats, however the effect has been shown to depend on the formation of calcium and magnesium contain-

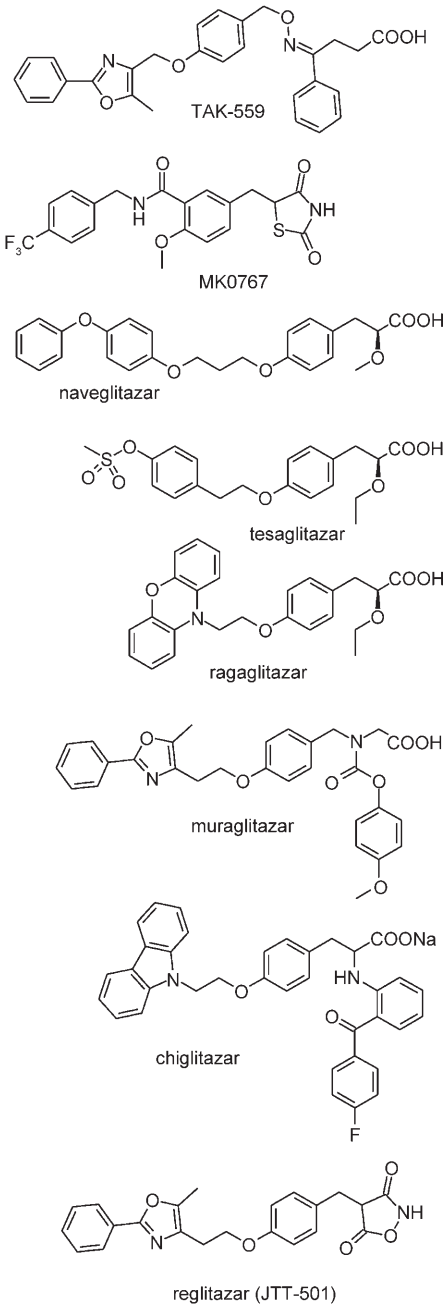

Figure 5. Dual PPARα/γ agonists.

ing precipitates and did not occur when the urine was acidified by diet, suggesting that muraglitazar is prolithogenic in rats and therefore promoting bladder tumours.[72,73] There are only two other publications in PubMed concerning bladder tumours in rodents after the administration of a PPAR activator, the PPARα agonist clofibrate.[74,75] However there is some data referred to by Samuel Cohen, which has been presented at the FDA or different symposia, suggesting that PPARγ activation might be promoting bladder tumours in rats.[76] The induction of bladder tumours by PPARγ and dual PPARα/γ agonists was exclusively observed in rats, preferentially in male ones. Cohen assumes that the bladder tumours in rats are initiated by lithiasis rather than activation of local PPARγ. That would explain why rats and especially male ones are more prone to that effect. As PPARγ activation leads to fluid retention in man (see above) and rats, this might be the triggering event for urolithiasis and subsequent tumour development in rats.

At present, it is unclear whether bladder tumour formation is relevant in man. One might argue, if the effect would be PPARγ mediated that there is a prevailing preclinical body of evidence that PPARγ is rather tumour protective.[77–79] Interestingly the PPARγ agonist rosiglitazone has recently been clinically investigated for the treatment of early stages of bladder carcinoma. The trial has been completed but not been published so far. At present, PPARγ agonistic glitazones did not show a clear benefit in clinical trials for the treatment of different types of cancer conducted so far.

Ragaglitazar is a dual agonist with a tenfold preference for PPARγ. In a 12 week dose ranging study, at single daily doses of 1 to 10 mg, ragaglitazar significantly decreased fasting plasma glucose, triglycerides, free fatty acids, LDL, total cholesterol, and glycosylated hemoglobin (HbA_{1c}) and increased HDL cholesterol compared to placebo. Reported side effects were weight gain, edema, leukopenia, and anemia.[80]

Muraglitazar is another example for a recent failure of dual PPARα/γ agonists. The new drug application (NDA) for muraglitazar had been filed to the US food and drug administration (FDA) at the end of 2005, but is still pending after the FDA has demanded additional cardiovascular safety data. The decision is related to an article by Nissen et al. in *JAMA*, where the authors analysed the data of the clinical trials and came to the conclusion that muraglitazar caused a significant excess in several composite end points including fatal events. Other combined or individual end points tended to be increased, however not significantly.[81]

It might be questioned whether the free post-hoc combination of individual endpoints and the comparison to combined control groups pioglitazone and placebo actually allows conclusion about significances. However the elevated relative risk for any of the individual end points for muraglitazar, whether significant or not, is convincing and supports the author's statement that approval should depend on additional trials concerning cardiovascular safety.

Muraglitazar is a nearly equipotent agonist of PPARα and PPARγ, with slight prevalence for PPARγ (Table 1). Muraglitazar has been investigated in phase II and III clinical trials, at dosages from 0.5 to 20 mg once a day, for its efficacy to lower lipids and glucose in the blood. At present, there are two published phase III clinical trials[82,83] and further clinical data can be extracted from the new drug application (NDA) 21-865 at the FDA homepage.[84] In CV168018, the effect of 2.5 and 5 mg muraglitazar monotherapy versus placebo over 24 weeks in three parallel groups of about 100 subjects each was studied. Muraglitazar significantly decreased fasting plasma glucose, free fatty acids, and HbA_{1c} levels but also significantly increased body weight.[82] CV168025 investigated the combined therapy of either 5 mg muraglitazar or 30 mg pioglitazone plus open-label metformin over 24 weeks in two parallel groups of over 500 subjects each with a 26 week follow-up control of weight gain, edema, cardiovascular events, and death. Muraglitazar was superior to pioglitazone in the reduction of HbA_{1c} (week 24), triglyceride, and non HDL-cholesterol (week 12) and in the increase in HDL-cholesterol (week 12).

Table 1. In vitro PPAR activation profile of dual PPARα/γ agonists.

	PPARα[a]	PPARγ[a]	Reference
ragaglitazar	0.98	0.09	[85]
tesaglitazar	1.2	1.3	[86]
muraglitazar	0.32	0.11	[87]
chiglitazar	1.2	0.08	[88]
reglitazar	5.4/1.9	0.28/0.08	[89], [90]
naveglitazar	2.86	0.36	[91]
MK0767	0.15/0.85	0.08	[90], [92]
TAK559	0.07	0.03	[93]

[a] EC_{50} values [μM] obtained in cellular transactivation assays.

Muraglitazar also showed a significantly higher weight gain and comparable rate of edema after week 50, compared to pioglitazone. The authors also provided data for cardiovascular events and deaths for both muraglitazar and pioglitazone, but no statistical analysis for these events, presumably due to low event rates that are related to the short duration of the trial.[83] What is striking is the lack of data comparing muraglitazar effects on triglycerides, non-HDL-, and HDL-cholesterol versus pioglitazone after 24 weeks, suggesting that the advantage of muraglitazar was lost.

Tesaglitazar is the third dual PPARα/γ agonist, which recently has been withdrawn because of decreased creatinine clearance and glomerular filtration rate (press release by Astra Zeneca). Tesaglitazar again is a dual PPARα/γ agonist. In a phase I study at doses of up to 1 mg per day for 12 weeks in 390 non-diabetics, tesaglitazar significantly decreased triglycerides, free fatty acids, non-HDL cholesterol, and fasting plasma glucose, and increased HDL cholesterol. At the 0.5 and 1 mg dosage, tesaglitazar also significantly increased body weight by approximately one kilogram, an effect similar to that of glitazones.[94] Another observation was increased serum creatinine levels in the first month of this study. This effect was confirmed in the yet unpublished ARMOR and GALLANT trials. This side effect and the associated reduction of the glomerular filtration rate led to the withdrawal of tesaglitazar.

Other examples of dual PPARα/γ agonists are TAK-559, KRP-297, and JTT-501, withdrawn because of unexpected toxic effects. In vitro data suggest TAK-559 to be a nearly equipotent

dual PPARα/γ agonist.[93] MK0767 has been reported to be a nearly equipotent dual PPARα/γ agonist.[92] However, other authors found that MK0767 (which has formerly been described as KRP-297) is a dual agonist with tenfold preference for PPARγ with EC_{50} values of 0.85 and 0.083 μM for PPARα and PPARγ, respectively.[90] In a recent small phase I study at doses of up to 25 mg once daily over 14 days in healthy males, MK-0767 led to significant reductions in triglycerides, free fatty acids, LDL, and total cholesterol and at the 25 mg dosage in fasting glucose.[95] The compound farglitazar, despite its name is at least in vitro a selective PPARγ agonist with a 1000-fold preference for PPARγ compared to PPARα.[96]

The development of naveglitazar is reported to be discontinued.[97] So today only chiglitazar seems to be left in clinical development. Shenzhen Chipscreen is announcing chiglitazar as a PPAR pan-agonist, suggesting that it might activate PPARδ as well, however there is no data available supporting that statement. Furthermore, Astra Zeneca reported that a PPARα/PPARγ-partial agonist has entered phase II clinical studies.

Notably, the in vitro PPAR activation profile of the referred dual PPARα/γ agonists with the exception of tesaglitzar and TAK559 shows an up to tenfold preference for PPARγ. At present, it is not clear, whether a preference in PPARα activity would lower the risk for edema and cardiovascular events.

Dual PPARα/δ agonists?

A rather new concept is the combined activation of PPARα and PPARδ, which is expected to combine the beneficial effects of PPARα and PPARδ activation on lipid metabolism, without being restricted to type 2 diabetics. However there seems to be no such compound in clinical development yet (Figure 6).

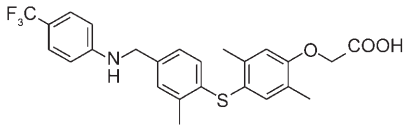

Figure 6. T0913659 a preclinical dual PPARα/δ agonist.[98]

Dual PPARγ/δ agonists?

Another concept is the simultaneous activation of PPARγ and PPARδ. The concomitant activation of both receptors is hoped to counteract the PPARγ induced weight gain. However, so far it does not seem that any compound has entered clinical trials.[99–101]

Pan-PPAR agonists

At last, when combining the activation of PPAR subtypes, then why not combine all three subtypes?[102] Well-known examples for such types of PPAR agonists are fatty acids as endogenous PPAR ligands, which are rather unselective and can be considered as pan-PPAR agonists. Another example of a pan-PPAR agonist is bezafibrate, which at least in vitro is an almost equipotent activator of all three PPAR subtypes. This drug positively influences glucose homeostasis and is well established and proven safe in decades of clinical use.[35,36,90] Bezafibrate also leads to a minor, however significant decrease in body mass index.[37] Candidates in early clinical development are GW625019, sodelglitazar (GW677954) (Figure 7), and PLX204.

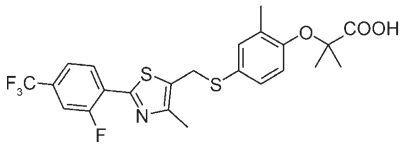

Figure 7. Sodelglitazar (GW677954).

Summary of PPAR agonists

In conclusion, today only the fibrates and the glitazones are established as PPAR agonistic drugs. Since the discovery of PPAR as the molecular target for these types of drugs in the early 1990s, there has been a lot of research on selective and combined PPAR agonists. However none of these new compounds has reached the market so far.

PPARδ seems to be a new promising approach. As it is expressed ubiquitously and its physiological effects are less understood, it might not be such a straightforward target as PPARα or PPARγ.

Dual PPARα/γ agonists seemed to be a promising strategy as well. However, there are concerns, whether dual PPARα/γ agonists might not only show the beneficial effects, but also show the combined or even superadditive toxicological profile by activating PPARα and PPARγ. So far, we cannot definitively answer this question. In the case of muraglitazar, it seems pretty likely that PPARγ specific side effects such as edema induction and an increased risk for coronary heart failure counterbalance the beneficial effects. As these effects are well known, they encourage the development of PPARγ partial agonists, also in combination with PPARα agonism. Several other dual PPARα/γ agonists failed due to toxic side effects, but so far it cannot be concluded whether these effects depend on the concomitant activation of PPARα and PPARγ or whether they are unrelated to the mode of action.

However, it has to be considered that many patients concomitantly receive fibrate and glitazone therapy, but so far there are only very limited clinical trials dealing with combination of both types of drugs.[103,104] With respect to the concern about enhanced toxicity of concomitant activation of PPARα and PPARγ, there is of course an urgent need for such a study. However, it should be kept in mind that endogenous ligands such as free fatty acids act as pan-PPAR agonists. Furthermore long experience with the pan-PPAR agonist bezafibrate does not provide evidence for such undesired events.

Agonists of the farnesoid X and the liver X receptor

The liver X receptor (LXR) and the farnesoid X receptor (FXR) are both members of the nuclear hormone receptor superfami-

ly. Activation of both receptors occurs by the formation of heterodimers with the retinoid X receptor (RXR).[31,105–107] FXR functions as a bile acid sensor and is highly expressed in tissues with high concentrations of bile acids such as liver, kidney, and small intestine.[108] FXR is an important regulator of lipid and cholesterol metabolism. FXR agonists lower serum triglyceride levels whereas FXR antagonists are predicted to lower cholesterol levels. Thus the challenge is to design FXR modulators (partial agonists).

The natural product guggulipid, an extract of the resin of *Commiphora mukul*, has been reported to lower lipid levels. The *E* and *Z* isomers of the compound guggulsterone (Figure 8), which are considered as the active ingredients, have been shown to be antagonists of FXR with an efficacy in the micromolar range.[109] However, more recent research raises doubt whether guggulsterone containing extracts are truly lowering lipid levels.[110] Furthermore it has been shown that guggulsterones do not only affect FXR but other nuclear receptors as well and even more potently.[111]

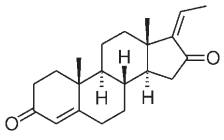

Figure 8. *Z*-guggulsterone.

The LXRs (LXRα and LXRβ) are oxysterol-activated transcription factors which play an important role in regulating the expression of the ABCA1 (ATP binding cassette A1) gene.[112] ABCA1 mediates the efflux of free cholesterol from peripheral tissues to nascent HDL. Thus, upregulation of ABCA1 expression is expected to promote reverse cholesterol transport. Several small molecule LXR agonists have been synthesized for example, the sulphonamide T0901317 and the acetic acid derivative GW3965 (Figure 9). For both compounds, preclinical studies in mice showed increased expression of ABCA1 and increased plasma HDL levels.[113,114]

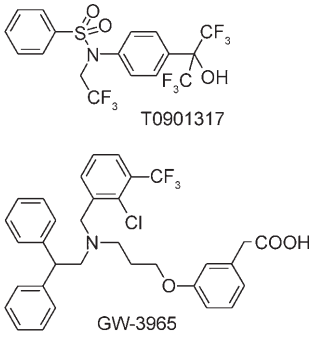

Figure 9. LXR-agonists.

CETP Inhibition

Based on the well-established inverse relation between the risk for cardiovascular disease and the level of HDL cholesterol, new pharmacological strategies to raise HDL have become interesting options.[115,116] The cholesteryl ester transfer protein (CETP) is a promising target, because the cholesteryl ester transfer process lowers HDL and contributes to an atherogenic lipoprotein profile, particularly when plasma triglycerides are high. CETP facilitates the transfer of cholesteryl ester from HDL to proatherogenic lipoproteins like LDL and VLDL with a balanced exchange of triglycerides.[117] Thus, CETP-inhibition is expected to raise HDL, lower LDL and provide a therapeutic benefit for patients with coronary heart disease (CHD). Based on results from pharmacological interference with reverse cholesterol transport, observations in animal models and CETP-deficient human populations, pro- as well as antiatherogenic effects of CETP-inhibition are still in discussion.[118] So far the most pronounced increase in HDL has been achieved by CETP inhibition.

Two substances, JTT-705 and torcetrapib (Figure 10), have been tested in phase III studies. JTT-705 is a thiol-based inhibitor.[50] To improve chemical stability and oral absorption, JTT-705 has been developed as a prodrug which shows an inhibition of CETP with an IC_{50} value of 6 μM in human plasma. An increase in activity occurs by hydrolysis of the isobutyryl thioester moiety (Figure 11), leading to the free thiol ($IC_{50} = 3$ μM) which is almost twice as potent as JTT-705. This relation in human plasma is consistent with calculated IC_{50} values in different animal species such as rabbits (1.0 μM versus 0.44 μM) and cynomolgus monkeys (2.4 μM versus 1.3 μM).[118] The suggested mechanism is the formation of a disulfide bond between the free thiol and a cysteine residue at position 13 of CETP.[119]

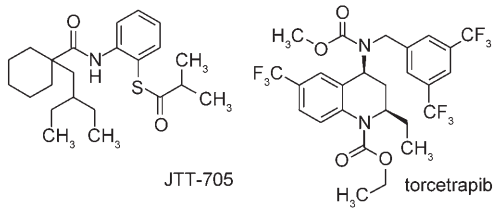

Figure 10. Structures of JTT-705 and torcetrapib.

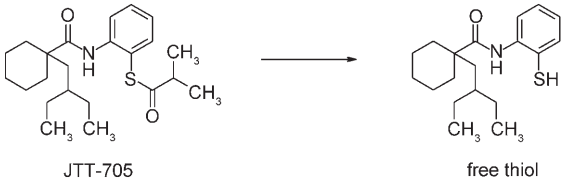

Figure 11. Bioactivation of JTT-705.

Currently, data for phase I and phase II studies of JTT-705 are published. A phase II study included 298 healthy individuals with mild dyslipidaemia, who were treated with JTT-705 at doses of 300–900 mg day^{-1} for 4 weeks.[120] The optimal dose was 600 mg day^{-1}, whereas 900 mg day^{-1} only slightly enhanced the effects. JTT-705 900 mg day^{-1} increased HDL by 34% whereas LDL was decreased by 7% and plasma triglycerides were not altered. The drug was well tolerated and the ef-

fects were readily reversible after washout. Another phase II study in which JTT-705 was combined with pravastatin 40 mg day^{-1} maintained these observations.[121] JTT-705 has been licensed in by Roche and the results of phase III studies are eagerly awaited.[122]

Torcetrapib belongs to a class of inhibitors based on 1,2,3,4-tetrahydroquinoline which shows a higher potency than JTT-705 with an IC_{50} of 0.05 μM. The molecule has two chiral centres, the 2 *R*-ethyl and 4 *S*-amino orientation was identified as optimal and thus used for further development. Torcetrapib specifically binds to CETP in an 1:1 stoichiometry and acts as a reversible inhibitor of CETP.[119] Notable physicochemical parameters are the very poor water solubility and high hydrophobicity (log*P* > 4.5) requiring atypical formulation technologies to ensure oral bioavailability.[118] The first human studies have been very promising: The maximal effect observed in a multidose study with 40 healthy subjects was an increase of HDL by 91% and a decrease of LDL by 42% with 120 mg torcetrapib twice a day. Based on these results, Pfizer decided not to await the outcome of two phase II studies but to start in parallel the large-scale phase III ILLUMINATE-trial (15000 patients) which was terminated abruptly after approximately one year and torcetrapib was withdrawn in December 2006.

Recently, the outcomes of the above mentioned phase II studies have been published.[123,124] As a parameter for the efficacy in the treatment of atherosclerosis the studies used maximum carotid intima-media thickness and normalised total atheroma volume, respectively.[123,124] The study carried out by Kastelein et. al included 850 patients with heterozygous familial hypercholesterolemia receiving either atorvastatin alone or atorvastatin combined with 60 mg torcetrapib for 2 years.[123] Despite an increase of HDL in the atorvastatin plus torcetrapib group by 54.4% (atorvastatin alone: 2.5%) and a decrease of LDL in the atorvastatin plus torcetrapib group by 14.4% (atorvastatin alone: +6.3%), both subgroups showed nearly no effect on the maximum carotid intima-media thickness as primary end point. Additionally, a slight increase in carotid intima-media thickness of the common carotid artery provided evidence of accelerated atherosclerosis in the atorvastatin plus torcetrapib group, which cannot be explained by the observed increased blood pressure of 2.8 mmHg in this group.[123] The results obtained in this study are consistent with results from the study carried out by Nissen et al. which included 1188 patients with CHD.[124] Besides the fact that mortality was raised significantly in the atorvastatin plus torcetrapib group, no additional information about the outcome of the ILLUMINATE trial is available at this point in time. There is an ongoing controversial discussion about the reasons for the failure of torcetrapib, raising the questions if torcetrapib is a "dirty drug" with several undiscovered off-target effects or if the approach of CETP-inhibition has no therapeutic benefit.[122]

Squalene Synthase Inhibitors

One of the rate limiting steps of cholesterol synthesis is the formation of squalene from trans-farnesyldiphosphate which is catalysed by the enzyme squalene synthase. An inhibition of this enzyme leads to a reduction of LDL, similar to the statins. Statins lower plasma mevalonate concentrations by the inhibition of HMG-CoA-reductase, therefore reducing cholesterol synthesis and the formation of nonsteroidal isoprenoids such as dolichol and ubiquinone.[125,126] The most important safety concern associated with statin therapy is myalgia, which might be caused by the depletion of mitochondrial ubiquinone levels.[127] Squalene synthase acts downstream of mevalonate and thus an inhibition might be able to lower LDL, avoiding the effects associated with decreased formation of nonsteroidal isoprenoids. TAK-475 (Figure 12), an orally active squalene

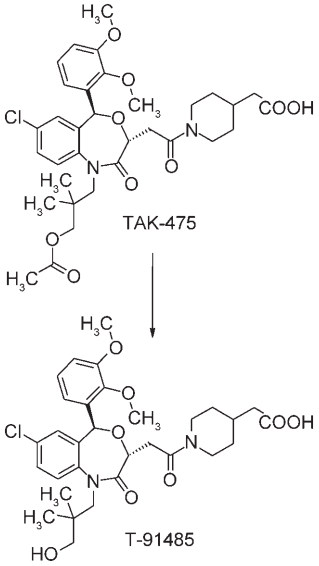

Figure 12. The squalene synthase inhibitor TAK-475 and its active metabolite T-91485.

synthase inhibitor derived from a series of 4,1-benzoxazepine-3-acetic acid derivatives is currently undergoing several phase III studies. One of these studies determining the efficacy and safety of TAK-475 compared to placebo in subjects with primary hypercholesterolemia was expected to be completed in June 2006, but no data from any human trial is available so far.[128,129]

Other ongoing studies are designed to investigate several combination regimens, for example, with atorvastatin, simvastatin, and ezetimibe.

The evaluation of TAK-475 in a variety of animal models showed a decrease in hepatic VLDL production and an increase in LDL clearance, but no influence on plasma HDL levels. The IC_{50} value of TAK-475 measured in vitro using squalene synthase from HepG2 cells is 79 nM.[130] TAK-475 is a prodrug and its pharmacologically active compound (T-91485) is generated by hydrolysis of the acetylated hydroxy group. According to the anticipated improved safety profile compared to the statins, the in vitro myotoxicity in human RD cells and skeletal myocytes was investigated. Compared to atorvastatin and simvastatin, the in vitro myotoxicity of T-91485 was at least 100- and 50-fold lower, respectively.[131]

Intestinal Cholesterol Absorption Inhibitors

Several direct approaches to inhibit the cholesterol uptake from the intestine are possible; one prominent example is ezetimibe. Currently, FM-VP4 (Figure 13) which is a water-soluble

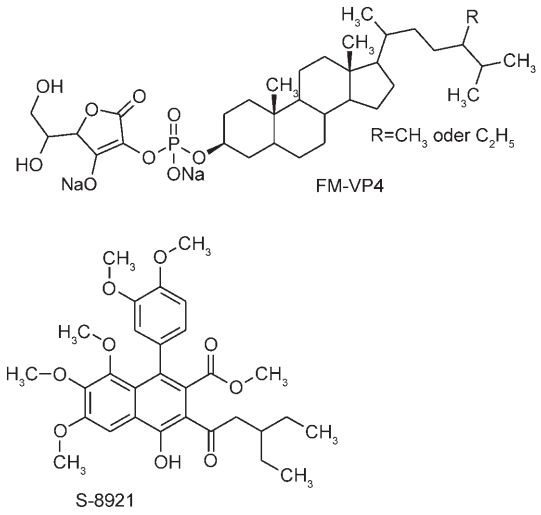

Figure 13. Cholesterol absorption inhibitors.

phytostanol analogue is under clinical investigation.[132] FM-VP4 is based on hydrogenated campesterol and sitostanol, each of them is covalently linked to ascorbic acid by a phosphodiester bond. Animal studies carried out with gerbils and apoE-deficient mice yielded very promising results. In fact, a significant decrease in both total cholesterol and total triglycerides, an increase in HDL cholesterol, and a profound effect on body weight was observed.[132] Notably, no apparent toxic effects were seen. The mechanism by which FM-VP4 prevents the absorption of cholesterol from the gastrointestinal tract is unknown. A phase II study that started in November 2005, investigating the safety and efficacy of FM-VP4 in subjects with primary hypercholesterolemia was completed, but no results have been published so far.

Another approach to treat hypercholesterolemia by modulating the cholesterol absorption process is by using bile acid reabsorption inhibitors (BARI), for example, the long established bile acid sequestrants. A new class of BARIs acts through inhibition of the ileal bile acid transporter (IBAT) which is responsible for the reabsorption of bile acids into the enterohepatic circulation.[133] In the liver, bile acids inhibit the cholesterol-7α-hydroxylase, the rate-limiting enzyme in the conversion of cholesterol to bile acids. Thus, an interruption of this circulation leads to an enhanced formation of bile acids which goes along with an upregulation of LDL-receptors and a decrease of serum LDL.[134] S-8921, a lignan derivative, is a specific IBAT-inhibitor which is currently in phase II trials.[134] Efficacy of this compound in lowering serum cholesterol and reducing atherosclerosis was shown in a variety of animal studies.[135,136] Interestingly, because of the action of BARIs at the luminal side of the intestine, these compounds do not need to be systemically available which could be advantageous with regard to the safety profile of these drugs.[134]

Vascular Protectants—VCAM-1 Inhibitors

Vascular cell adhesion molecule-1 (VCAM-1) is an early inducible inflammatory response gene which is upregulated in chronic inflammatory diseases such as atherosclerosis. Thus, besides its eligibility as a biomarker, VCAM-1 is a very promising target for the treatment of these diseases.[137] Succinobucol (AGI-1067) (Figure 14) is the monosuccinate ester of probucol,

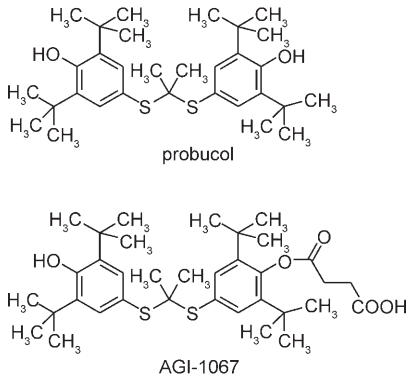

Figure 14. Vascular protectants.

an antioxidant which was discovered in the 1960s and which has been available on the US market as a lipid-lowering agent before the establishment of statins.[138] In addition to its action as an antioxidant and in contrast to probucol, succinobucol shows potent inhibitory activity on VCAM-1 expression and has improved physicochemical properties.[139] Furthermore, there have been safety concerns due to a QTc prolongation caused by probucol. In the case of succinobucol this effect is missing. A large scale phase III study (ARISE: aggressive reduction of inflammation stops events) with approximately 6600 subjects worldwide started in June 2003 and was estimated to be completed in December 2006. The aim of the study was the evaluation of the safety and efficacy of succinobucol in the treatment of vascular inflammation and atherosclerosis compared to placebo, by assessing the reduction in cardiovascular events. Results of this study are not published yet.

However, the results of a smaller study named CART-2 were recently published.[140] In this placebo-controlled, randomised trial the effects of 280 mg succinobucol per day on coronary atherosclerosis were investigated for 12 months ($n=232$). Patients treated with succinobucol showed an atherosclerosis regression of $-4.0\,mm^3$ (assessed by coronary vascular ultrasound - IVUS), although this was not statistically significant. The reason for the lack of significance might be the study size and the relatively short duration. Thus, the outcome of the ARISE study has to answer the remaining question about the efficacy of succinobucol. LDL was decreased, whereas HDL was increased significantly in the verum group of CART-2, although the clinical relevance of these changes is not clear. Notably, the

observation of reduced levels of myeloperoxidase in CART-2 supports the assigned anti-inflammatory activity of succinobucol.

ApoA1 and Mimetics

Apolipoprotein-A1 (apoA1) is the major protein component of HDL, consisting of 243 amino acids. ApoA1 is able to interact with lipids and aqueous environments because of its amphiphilic properties. Similiar to HDL, apoA1 levels are inversely correlated to the risk of atherosclerosis and other vascular diseases.[141] The protective effect of apoA1 is based on a number of mechanisms.[142] Firstly, there is a major role of apoA1 in reverse cholesterol transport, partly mediated by activation of the lecithin cholesteryl acyltransferase (LCAT), which converts cholesterol from peripheral cells to cholesteryl ester. Secondly, anti-inflammatory properties have been shown for apoA1. Several peptide and small molecule mimetics of apoA1 are currently under clinical investigation. $ApoA1_{milano}$ is a naturally occurring mutant protein which is characterized by a cysteine to arginine mutation at position 173 in the α-helix of apoA1.[143] This structural change allows the formation of homodimers and heterodimers with apoA2. A first clinical study investigating the weekly intravenous administration of a recombinant $apoA1_{milano}$/phospholipid complex (ETC-216) to patients with acute coronary syndromes has been published.[144] After 5 weeks, ETC-216 led to a significant regression of coronary atherosclerosis as measured by IVUS. In 2006, another study was published in which the relationship between atheroma regression and arterial wall remodelling after administration of ETC-216 was investigated by IVUS.[145] The authors showed a significant reduction of atheroma volume, especially in those arterial subsegments with the greatest plaque burden. The regression of atherosclerosis was accompanied by a reduction of the external elastic membrane volume, but interestingly there were no changes in luminal dimensions observed. Thus, it can be supposed that atherosclerotic plaque regression goes along with a reverse remodelling of the external elastic membrane and is achievable by infusion of $apoA1_{milano}$.

The finding that the lipid binding properties of apoA1 are largely related to its class A amphiphatic helices led to the design of synthetic 18 amino acid-peptides with a similar secondary structure.[146] D-4F is an apoA1 mimetic that exclusively contains D-amino acids and thus can be given orally. The description 4F reflects the fact that four of the 18 amino acids are phenylalanine residues. Early human clinical trials are in progress, in mice the combination of D-4F and pravastatin was able to regress already established atherosclerotic lesions.[147] Another compound which has reached clinical trials is AZD-2479 (Figure 15), a small molecule apoA1 mimetic. AZD-2479 is an orally bioavailable drug that contains a biphenylalanine residue linked with glutamate and arginine.[148]

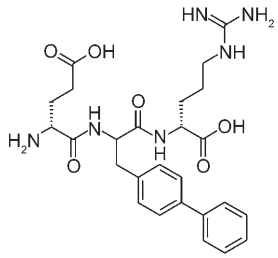

Figure 15. AZD-2479 a small molecular entity as an apoA1 mimetic.

Antisense Inhibitors of ApoB-100

Apolipoprotein-B (apoB) is the major protein component of LDL and plays a key role in LDL transport and removal. High levels of apoB seem to correlate with cardiovascular risk.[149] Thus, direct inhibition of apoB production might be an attractive therapeutic strategy. The antisense inhibitor ISIS 301012 is a 20-mer oligonucleotide, complementary to the coding region for human apoB-100 mRNA. Several clinical trials up to phase II were carried out. In 2006, the FDA granted orphan drug status to ISIS 301012 for the treatment of homozygous familial hypercholesterolemia.[150] Kastelein et al. investigated the short-term administration of ISIS 301012 to humans with mild dyslipidaemia.[151] ISIS 301012 was given weekly subcutaneous and led to a significant, prolonged, and dose dependent reduction in apoB-100 and LDL, with maximum reductions of 50% for apoB-100 and 35% for LDL reached with the largest dose of 200 mg. The most prominent side effect was mild erythema at the injection site. Further phase II studies assessing the safety and efficacy of ISIS 301012 are ongoing.

ACAT Inhibitors

Acyl-CoA cholesterol transferase (ACAT) is an intracellular enzyme which catalyzes the esterification of cholesterol with free fatty acids into cholesteryl esters. Two isoforms of ACAT are known: ACAT-1, which is expressed ubiquitously, and ACAT-2, which can be found in the liver and the small intestine.[127,152] The accumulation of cholesterol esters is a pivotal process during the formation of foam cells from macrophages and is associated with the formation of atherosclerotic plaques. Inhibition of this enzyme is supposed to reduce the accumulation and deposit of cholesterol esters in macrophages and the vessel wall. Furthermore, the clearance of free cholesterol should be increased.

Avasimibe and pactimibe (Figure 16) are nonselective ACAT inhibitors that reached phase III clinical trials. However, both compounds did not show the expected therapeutic effects and further development was discontinued in 2003 (avasimibe, Pfizer) and 2005 (pactimibe, Sankyo), respectively. In several animal studies, atherosclerotic lesions were reduced with ACAT inhibitors.[153] However, the subsequent clinical trials showed the opposite result: a proatherogenic effect was shown for avasimibe and pactimibe.[154,155] There are several issues that are discussed in the context of the failure of both compounds.[156] There have been large dosage differences between the animal and the human studies. The pharmacological explanation faces two issues: The accumulation of free cholesterol in macrophages leads to macrophage cell death, instead of an enhanced reverse cholesterol transport.[157] The other fact is

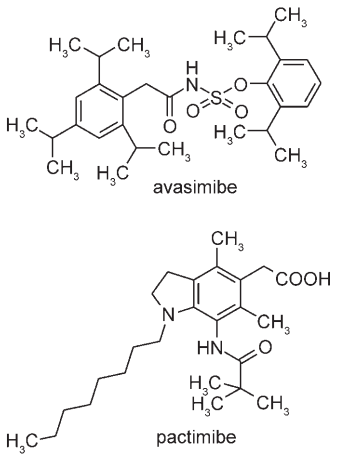

Figure 16. The ACAT inhibitors avasimibe and pactimibe.

that ACAT-1 depletion alters ABCA1 protein stability, thereby reducing reverse cholesterol transport.[158] Although the attractiveness of unspecific ACAT inhibitors in cardiovascular prevention is quite low after these findings, there are other approaches such as the design of specific ACAT-2 inhibitors and the combination of ACAT-inhibitors with drugs that stimulate reverse cholesterol transport.[156]

Novel Approaches in Nicotinic Acid Therapy?

In 1954, the Canadian pathologist Rudolf Altschul discovered that gram doses of nicotinic acid (Figure 17) lowers plasma

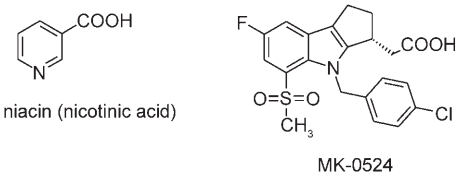

Figure 17. Structures of niacin and the prostaglandin D2 receptor antagonist, suppressing niacin induced flush.

levels of cholesterol.[159] This was the beginning of the career of one of the most effective drugs for the treatment of dyslipidemia. Niacin lowers the levels of all atherogenic lipoproteins such as VLDL, LDL, and lipoprotein A, accompanied by an increase of HDL. Notably the elevation of HDL is the most prominent among the approved drugs.[160] Beneficial effects of the combination of niacin with statins have also been proven in several clinical studies.[161] There are two major side effects associated with niacin therapy, flush and an increase of uric acid in blood. Flush is a cutaneous vasodilatation occurring rapidly after the oral administration of niacin and takes about half an hour. This very unpleasant effect limiting the clinical use could be reduced but not prevented by a prolonged release formulation of niacin.[162] As flush is induced by cyclooxygenase dependent secretion of prostaglandins by immune cells of the skin, the use of cyclooxygenase inhibitors like acetyl salicylic acid is another therapeutic option to reduce flush.[163]

The discovery that niacin-induced vasodilatation could be suppressed by antagonizing the prostaglandin D_2 receptor 1 (DP1, also called DP) by Cheng et al. has provided a new strategy for a niacin therapy with suppressed flushing.[164] MK-0524, an indole-based acetic acid derivative originally designed to treat allergic rhinitis, is a potent and selective DP receptor antagonist which inhibits the PGD_2-induced cAMP production in platelet-rich plasma with an IC_{50} of 4.0 nM.[165] In healthy subjects MK-0524 reduced niacin-induced flushing symptoms by 68% and the increase in malar skin perfusion by 76% compared to placebo when administered one hour before niacin.[164] Currently, MK-0524 is undergoing a phase III clinical trial to evaluate the efficacy to improve the tolerability of extended-release niacin therapy.

MTP Inhibitors

The microsomal triglyceride transfer protein (MTP) is one of the key enzymes in the formation of apolipoprotein B (apoB) containing lipoproteins such as chylomicrons in the intestinum and VLDL in the liver.[166] An inhibition of this enzyme showed antiatherosclerotic efficacy in animal models.[167] The first drug candidate of this class which reached clinical trials was implitapide (Figure 18), that inhibits both hepatic and intestinal MTP. In dyslipidemic subjects, implitapide decreased plasma total cholesterol, LDL and apoB. However, due to increased serum liver enzymes and gastrointestinal side effects the development of implitapide was discontinued. BMS-201038 (synonym AEGR-733) is another MTP-inhibitor which is currently undergoing clinical trials.[168] The results of a first dose-escalation study with BMS-201038 given to patients with homozygous familial hypercholesterolemia have been published recently.[169] BMS-201038 was highly effective in reducing plasma levels of all apoB containing lipoproteins. However, the therapy was associated with hepatic fat accumulation and elevated liver aminotransferase levels. A larger ongoing study for the evaluation of

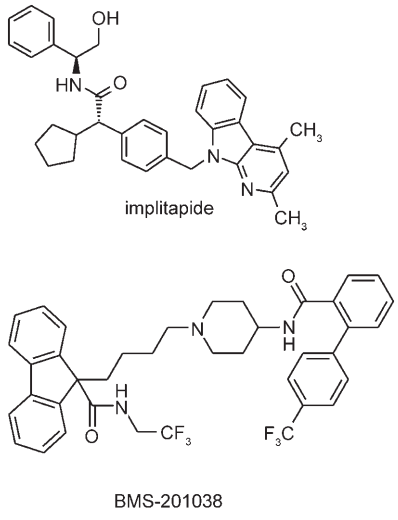

Figure 18. MTP inhibitors.

BMS-201038 and its combination with ezetimibe might deliver a more detailed picture of the safety of this drug.

Summary

In recent years a variety of potential new targets for the treatment of dyslipidemia have been discovered, including nuclear receptors and enzymes involved in lipid metabolism. For some of these targets potential drugs reached the clinic but none of these potential new drugs came on the market so far, as they have been withdrawn or failed in clinical trials. The most well developed ones for example, tesaglitzar, muraglitazar, and torcetrapib effectively modulated lipid metabolism but had toxicological problems.

Outlook

In this review, we discussed several drug candidates which seemed to be beneficial in early stages of clinical development and which significantly affected surrogate parameters. However, most of them failed in later stages of clinical development. The reasons for the withdrawals were unexpected toxic effects or discouraging outcomes in clinical endpoints such as cardiovascular events. That was the case for muraglitazar and torcetrapib, which were well effective in cholesterol lowering, but showed an increase in cardiovascular events.

This raises the question, whether the selected surrogate parameters are appropriate and sufficient for the development of safe and effective lipid lowering drugs. The data obtained from the clinical trials with compounds that address various enzymes or receptors involved in lipid metabolism underline the fact that the interplay between alterations in lipid metabolism and the modulation of disease development is complex. At present, it seems that much more work has to be done to define pharmacological profiles that lead to new, therapeutically effective lipid modulating drugs.

Abbreviations

ABCA1: ATP binding cassette A1; apoA1: apolipoprotein A1; CETP: cholesteryl ester transfer protein; CHD: coronary heart disease; EGF-1: early growth response factor 1; FA: fatty acid; FABP: fatty acid binding protein; FATP: fatty acid transport protein; FDA: Food and Drug Administration; FFA: free fatty acid; FXR: farnesoid X receptor; GFR: glomerular filtration rate; GLUT: glucose transporter; HDL: high density lipoprotein; LDL: low density lipoprotein; LXR: liver X receptor; PPAR: peroxisome proliferator-activated receptor; PPRE: PPAR response element; RXR: retinoid X receptor; TG: triglycerides; TZD: thiazoidinedione; VLDL: very low density lipoprotein.

Keywords: fatty acids · lipids · lipoproteins · PPAR

[1] S. M. Grundy, *Nat. Rev. Drug Discovery* **2006**, *5*, 295 – 309.
[2] R. Holman, *Acta Diabetol.* **2001**, *38 Suppl 1*, S9 – 14.
[3] G. F. Lewis, A. Carpentier, K. Adeli, A. Giacca, *Endocr. Rev.* **2002**, *23*, 201 – 229.
[4] J. D. McGarry, *Diabetes* **2001**, *51*, 7 – 18.
[5] D. J. Gordon, J. L. Probstfield, R. J. Garrison, J. D. Neaton, W. P. Castelli, J. D. Knoke, D. R. Jacobs, Jr., S. Bangdiwala, H. A. Tyroler, *Circulation* **1989**, *79*, 8 – 15.
[6] R. C. Turner, H. Millns, H. A. Neil, I. M. Stratton, S. E. Manley, D. R. Matthews, R. R. Holman, *Br. Med. J.* **1998**, *316*, 823 – 828.
[7] M. A. Austin, J. E. Hokanson, K. L. Edwards, *Am. J. Cardiol.* **1998**, *81*, 7B – 12B.
[8] J. E. Hokanson, M. A. Austin, *J. Cardiovasc. Risk* **1996**, *3*, 213 – 219.
[9] S. M. Grundy, J. I. Cleeman, C. N. Merz, H. B. Brewer, Jr., L. T. Clark, D. B. Hunninghake, R. C. Pasternak, S. C. Smith, Jr., N. J. Stone, *J. Am. Coll. Cardiol.* **2004**, *44*, 720 – 732.
[10] C. Baigent, A. Keech, P. M. Kearney, L. Blackwell, G. Buck, C. Pollicino, A. Kirby, T. Sourjina, R. Peto, R. Collins, R. Simes, *Lancet* **2005**, *366*, 1267 – 1278.
[11] I. Lemieux, A. Pascot, C. Couillard, B. Lamarche, A. Tchernof, N. Almeras, J. Bergeron, D. Gaudet, G. Tremblay, D. Prud'homme, A. Nadeau, J. P. Despres, *Circulation* **2000**, *102*, 179 – 184.
[12] S. J. Robins, *Am. J. Cardiol.* **2001**, *88*, 19N-23N.
[13] O. Faergeman, *Curr. Opin. Lipidol.* **2000**, *11*, 609 – 614.
[14] A. Keech, R. J. Simes, P. Barter, J. Best, R. Scott, M. R. Taskinen, P. Forder, A. Pillai, T. Davis, P. Glasziou, P. Drury, Y. A. Kesaniemi, D. Sullivan, D. Hunt, P. Colman, M. d'Emden, M. Whiting, C. Ehnholm, M. Laakso, *Lancet* **2005**, *366*, 1849 – 1861.
[15] B. Verges, *Curr. Opin. Lipidol.* **2005**, *16*, 648 – 651.
[16] G. F. Watts, S. B. Dimmitt, *Curr. Opin. Lipidol.* **1999**, *10*, 561 – 574.
[17] J. P. Berger, T. E. Akiyama, P. T. Meinke, *Trends Pharmacol. Sci.* **2005**, *26*, 244 – 251.
[18] R. M. Evans, G. D. Barish, Y. X. Wang, *Nat. Med.* **2004**, *10*, 355 – 361.
[19] B. Desvergne, W. Wahli, *Endocr. Rev.* **1999**, *20*, 649 – 688.
[20] V. Giguere, *Endocr. Rev.* **1999**, *20*, 689 – 725.
[21] H. Gronemeyer, J. A. Gustafsson, V. Laudet, *Nat. Rev. Drug Discovery* **2004**, *3*, 950 – 964.
[22] T. Lemberger, B. Desvergne, W. Wahli, *Annu. Rev. Cell Dev. Biol.* **1996**, *12*, 335 – 363.
[23] D. J. Mangelsdorf, R. M. Evans, *Cell* **1995**, *83*, 841 – 850.
[24] C. Juge-Aubry, A. Pernin, T. Favez, A. G. Burger, W. Wahli, C. A. Meier, B. Desvergne, *J. Biol. Chem.* **1997**, *272*, 25252 – 25259.
[25] T. Lemberger, O. Braissant, C. Juge-Aubry, H. Keller, R. Saladin, B. Staels, J. Auwerx, A. G. Burger, C. A. Meier, W. Wahli, *Ann. N. Y. Acad. Sci.* **1996**, *804*, 231 – 251.
[26] S. A. Kliewer, S. S. Sundseth, S. A. Jones, P. J. Brown, G. B. Wisely, C. S. Koble, P. Devchand, W. Wahli, T. M. Willson, J. M. Lenhard, J. M. Lehmann, *Proc. Natl. Acad. Sci. USA* **1997**, *94*, 4318 – 4323.
[27] B. M. Forman, J. Chen, R. M. Evans, *Proc. Natl. Acad. Sci. USA* **1997**, *94*, 4312 – 4317.
[28] S. Khanna, M. E. Sobhia, P. V. Bharatam, *J. Med. Chem.* **2005**, *48*, 3015 – 3025.
[29] B. Pirard, *J. Comput.-Aided Mol. Des.* **2003**, *17*, 785 – 796.
[30] A. Castrillo, P. Tontonoz, *Annu. Rev. Cell Dev. Biol.* **2004**, *20*, 455 – 480.
[31] M. Ricote, J. T. Huang, J. S. Welch, C. K. Glass, *J. Leukocyte Biol.* **1999**, *66*, 733 – 739.
[32] P. Lefebvre, G. Chinetti, J. C. Fruchart, B. Staels, *J. Clin. Invest.* **2006**, *116*, 571 – 580.
[33] B. Staels, J. Dallongeville, J. Auwerx, K. Schoonjans, E. Leitersdorf, J. C. Fruchart, *Circulation* **1998**, *98*, 2088 – 2093.
[34] B. Staels, J. C. Fruchart, *Diabetes* **2005**, *54*, 2460 – 2470.
[35] A. Tenenbaum, E. Z. Fisman, V. Boyko, M. Benderly, D. Tanne, M. Haim, Z. Matas, M. Motro, S. Behar, *Arch. Intern. Med.* **2006**, *166*, 737 – 741.
[36] A. Tenenbaum, M. Motro, E. Z. Fisman, Y. Adler, J. Shemesh, D. Tanne, J. Leor, V. Boyko, E. Schwammenthal, S. Behar, *Eur. Heart J.* **2005**, *26*, 2032 – 2038.
[37] A. Tenenbaum, M. Motro, E. Z. Fisman, E. Schwammenthal, Y. Adler, I. Goldenberg, J. Leor, V. Boyko, L. Mandelzweig, S. Behar, *Circulation* **2004**, *109*, 2197 – 2202.
[38] J. P. Singh, R. Kauffman, W. Bensch, G. Wang, P. McClelland, J. Bean, C. Montrose, N. Mantlo, A. Wagle, *Mol. Pharmacol.* **2005**, *68*, 763 – 768.
[39] Y. Xu, D. Mayhugh, A. Saeed, X. Wang, R. C. Thompson, S. J. Dominianni, R. F. Kauffman, J. Singh, J. S. Bean, W. R. Bensch, R. J. Barr, J. Osborne, C. Montrose-Rafizadeh, R. W. Zink, N. P. Yumibe, N. Huang, D. Luffer-Atlas, D. Rungta, D. E. Maise, N. B. Mantlo, *J. Med. Chem.* **2003**, *46*, 5121 – 5124.

[40] M. L. Sierra, V. Beneton, A. B. Boullay, T. Boyer, A. G. Brewster, F. Donche, M. C. Forest, M. H. Fouchet, F. J. Gellibert, D. A. Grillot, M. H. Lambert, A. Laroze, C. Le Grumelec, J. M. Linget, V. G. Montana, V. L. Nguyen, E. Nicodeme, V. Patel, A. Penfornis, O. Pineau, D. Pohin, F. Potvain, G. Poulain, C. B. Ruault, M. Saunders, J. Toum, H. E. Xu, R. X. Xu, P. M. Pianetti, *J. Med. Chem.* **2007**, *50*, 685 – 695.
[41] G. D. Barish, V. A. Narkar, R. M. Evans, *J. Clin. Invest.* **2006**, *116*, 590 – 597.
[42] D. L. Sprecher, C. Massien, G. Pearce, A. N. Billin, I. Perlstein, T. M. Willson, D. G. Hassall, N. Ancellin, S. D. Patterson, D. C. Lobe, T. G. Johnson, *Arterioscler. Thromb. Vasc. Biol.* **2006**, *27*, 359 – 365.
[43] W. R. Oliver, Jr., J. L. Shenk, M. R. Snaith, C. S. Russell, K. D. Plunket, N. L. Bodkin, M. C. Lewis, D. A. Winegar, M. L. Sznaidman, M. H. Lambert, H. E. Xu, D. D. Sternbach, S. A. Kliewer, B. C. Hansen, T. M. Willson, *Proc. Natl. Acad. Sci. USA* **2001**, *98*, 5306 – 5311.
[44] T. Tanaka, J. Yamamoto, S. Iwasaki, H. Asaba, H. Hamura, Y. Ikeda, M. Watanabe, K. Magoori, R. X. Ioka, K. Tachibana, Y. Watanabe, Y. Uchiyama, K. Sumi, H. Iguchi, S. Ito, T. Doi, T. Hamakubo, M. Naito, J. Auwerx, M. Yanagisawa, T. Kodama, J. Sakai, *Proc. Natl. Acad. Sci. USA* **2003**, *100*, 15924 – 15929.
[45] R. A. Gupta, D. Wang, S. Katkuri, H. Wang, S. K. Dey, R. N. DuBois, *Nat. Med.* **2004**, *10*, 245 – 247.
[46] R. L. Stephen, M. C. Gustafsson, M. Jarvis, R. Tatoud, B. R. Marshall, D. Knight, E. Ehrenborg, A. L. Harris, C. R. Wolf, C. N. Palmer, *Cancer Res.* **2004**, *64*, 3162 – 3170.
[47] D. Wang, H. Wang, Y. Guo, W. Ning, S. Katkuri, W. Wahli, B. Desvergne, S. K. Dey, R. N. DuBois, *Proc. Natl. Acad. Sci. USA* **2006**, *103*, 19069 – 19074.
[48] L. Xu, C. Han, K. Lim, T. Wu, *Cancer Res.* **2006**, *66*, 11859 – 11868.
[49] Y. Yin, R. G. Russell, L. E. Dettin, R. Bai, Z. L. Wei, A. P. Kozikowski, L. Kopelovich, R. I. Glazer, *Cancer Res.* **2005**, *65*, 3950 – 3957.
[50] A. D. Burdick, D. J. Kim, M. A. Peraza, F. J. Gonzalez, J. M. Peters, *Cell Signal* **2006**, *18*, 9 – 20.
[51] M. A. Peraza, A. D. Burdick, H. E. Marin, F. J. Gonzalez, J. M. Peters, *Toxicol. Sci.* **2006**, *90*, 269 – 295.
[52] S. E. Inzucchi, *JAMA J. Am. Med. Assoc.* **2002**, *287*, 360 – 372.
[53] H. Hauner, *Diabetes/Metab. Res. Rev.* **2002**, *18 Suppl 2*, S10 – 15.
[54] M. Lehrke, M. A. Lazar, *Cell* **2005**, *123*, 993 – 999.
[55] R. W. Nesto, D. Bell, R. O. Bonow, V. Fonseca, S. M. Grundy, E. S. Horton, M. Le Winter, D. Porte, C. F. Semenkovich, S. Smith, L. H. Young, R. Kahn, *Diabetes Care* **2004**, *27*, 256 – 263.
[56] Y. Guan, C. Hao, D. R. Cha, R. Rao, W. Lu, D. E. Kohan, M. A. Magnuson, R. Redha, Y. Zhang, M. D. Breyer, *Nat. Med.* **2005**, *11*, 861 – 866.
[57] S. Kurebayashi, X. Xu, S. Ishii, M. Shiraishi, H. Kouhara, S. Kasayama, *Atherosclerosis* **2005**, *182*, 71 – 77.
[58] K. Schimke, T. M. Davis, *Curr. Opin. Investig. Drugs* **2007**, *8*, 338 – 344.
[59] M. J. Reginato, S. T. Bailey, S. L. Krakow, C. Minami, S. Ishii, H. Tanaka, M. A. Lazar, *J. Biol. Chem.* **1998**, *273*, 32679 – 32684.
[60] B. Jamali, G. C. Theill, L. L. Sorensen, *J. Chromatogr. A* **2004**, *1049*, 183 – 187.
[61] T. Allen, F. Zhang, S. A. Moodie, L. E. Clemens, A. Smith, F. Gregoire, A. Bell, G. E. Muscat, T. A. Gustafson, *Diabetes* **2006**, *55*, 2523 – 2533.
[62] T. A. Cock, S. M. Houten, J. Auwerx, *EMBO Rep.* **2004**, *5*, 142 – 147.
[63] F. Zhang, B. E. Lavan, F. M. Gregoire, *PPAR Res.* **2007**, 32696.
[64] T. W. Kurtz, M. Pravenec, *J. Hypertens.* **2004**, *22*, 2253 – 2261.
[65] S. Yamagishi, M. Takeuchi, *Med. Hypotheses* **2005**, *64*, 476 – 478.
[66] B. Pourcet, J. C. Fruchart, B. Staels, C. Glineur, *Expert Opin. Emerging Drugs* **2006**, *11*, 379 – 401.
[67] A. Tenenbaum, M. Motro, E. Z. Fisman, *Cardiovasc. Diabetol.* **2005**, *4*, 14.
[68] T. Temelkova-Kurktschiev, M. Hanefeld, *Exp. Clin. Endocrinol. Diabetes* **2004**, *112*, 75 – 79.
[69] C. Fievet, J. C. Fruchart, B. Staels, *Curr. Opin. Pharmacol.* **2006**, *6*, 606 – 614.
[70] F. L. Egerod, H. S. Nielsen, L. Iversen, I. Thorup, T. Storgaard, M. B. Oleksiewicz, *Biomarkers* **2005**, *10*, 295 – 309.
[71] B. B. Lohray, V. B. Lohray, A. C. Bajji, S. Kalchar, R. R. Poondra, S. Padakanti, R. Chakrabarti, R. K. Vikramadithyan, P. Misra, S. Juluri, N. V. Mamidi, R. Rajagopalan, *J. Med. Chem.* **2001**, *44*, 2675 – 2678.
[72] M. A. Dominick, M. R. White, T. P. Sanderson, T. Van Vleet, S. M. Cohen, L. E. Arnold, M. Cano, S. Tannehill-Gregg, J. D. Moehlenkamp, C. R. Waites, B. E. Schilling, *Toxicol. Pathol.* **2006**, *34*, 903 – 920.
[73] T. R. Van Vleet, M. R. White, T. P. Sanderson, S. M. Cohen, M. Cano, L. L. Arnold, C. R. Waites, B. E. Schilling, J. Mitroka, M. A. Dominick, *Toxicol. Sci.* **2007**, *96*, 58 – 71.
[74] D. J. Svoboda, D. L. Azarnoff, *Cancer Res.* **1979**, *39*, 3419 – 3428.
[75] A. Hagiwara, S. Tamano, T. Ogiso, E. Asakawa, S. Fukushima, *Jpn. J. Cancer Res.* **1990**, *81*, 1232 – 1238.
[76] S. M. Cohen, *Toxicol. Sci.* **2005**, *87*, 322 – 327.
[77] C. Grommes, G. E. Landreth, M. T. Heneka, *Lancet Oncol.* **2004**, *5*, 419 – 429.
[78] L. Kopelovich, J. R. Fay, R. I. Glazer, J. A. Crowell, *Mol. Cancer Ther.* **2002**, *1*, 357 – 363.
[79] L. Michalik, B. Desvergne, W. Wahli, *Nat. Rev. Cancer* **2004**, *4*, 61 – 70.
[80] M. F. Saad, S. Greco, K. Osei, A. J. Lewin, C. Edwards, M. Nunez, R. R. Reinhardt, *Diabetes Care* **2004**, *27*, 1324 – 1329.
[81] S. E. Nissen, K. Wolski, E. J. Topol, *JAMA J. Am. Med. Assoc.* **2005**, *294*, 2581 – 2586.
[82] J. B. Buse, C. J. Rubin, R. Frederich, K. Viraswami-Appanna, K. C. Lin, R. Montoro, G. Shockey, J. A. Davidson, *Clin. Ther.* **2005**, *27*, 1181 – 1195.
[83] D. M. Kendall, C. J. Rubin, P. Mohideen, J. M. Ledeine, R. Belder, J. Gross, P. Norwood, M. O'Mahony, K. Sall, G. Sloan, A. Roberts, F. T. Fiedorek, R. A. DeFronzo, *Diabetes Care* **2006**, *29*, 1016 – 1023.
[84] I. N. U. Bristol-Myers Squibb Company, NJ (USA); Merck & Co., **2005**, available online at http://www.fda.gov.
[85] S. Ebdrup, I. Pettersson, H. B. Rasmussen, H. J. Deussen, A. Frost Jensen, S. B. Mortensen, J. Fleckner, L. Pridal, L. Nygaard, P. Sauerberg, *J. Med. Chem.* **2003**, *46*, 1306 – 1317.
[86] P. Cronet, J. F. Petersen, R. Folmer, N. Blomberg, K. Sjoblom, U. Karlsson, E. L. Lindstedt, K. Bamberg, *Structure* **2001**, *9*, 699 – 706.
[87] P. V. Devasthale, S. Chen, Y. Jeon, F. Qu, C. Shao, W. Wang, H. Zhang, M. Cap, D. Farrelly, R. Golla, G. Grover, T. Harrity, Z. Ma, L. Moore, J. Ren, R. Seethala, L. Cheng, P. Sleph, W. Sun, A. Tieman, J. R. Wetterau, A. Doweyko, G. Chandrasena, S. Y. Chang, W. G. Humphreys, V. G. Sasseville, S. A. Biller, D. E. Ryono, F. Selan, N. Hariharan, P. T. Cheng, *J. Med. Chem.* **2005**, *48*, 2248 – 2250.
[88] P. P. Li, S. Shan, Y. T. Chen, Z. Q. Ning, S. J. Sun, Q. Liu, X. P. Lu, M. Z. Xie, Z. F. Shen, *Br. J. Pharmacol.* **2006**, *148*, 610 – 618.
[89] T. Shibata, K. Matsui, K. Nagao, H. Shinkai, F. Yonemori, K. Wakitani, *Eur. J. Pharmacol.* **1999**, *364*, 211 – 219.
[90] T. M. Willson, P. J. Brown, D. D. Sternbach, B. R. Henke, *J. Med. Chem.* **2000**, *43*, 527 – 550.
[91] J. A. Martin, D. A. Brooks, L. Prieto, R. Gonzalez, A. Torrado, I. Rojo, B. Lopez de Uralde, C. Lamas, R. Ferritto, M. D. Martin-Ortega, J. Agejas, F. Parra, J. R. Rizzo, G. A. Rhodes, R. L. Robey, C. A. Alt, S. R. Wendel, T. Y. Zhang, A. Reifel-Miller, C. Montrose-Rafizadeh, J. T. Brozinick, E. Hawkins, E. A. Misener, D. A. Briere, R. Ardecky, J. D. Fraser, A. M. Warshawsky, *Bioorg. Med. Chem. Lett.* **2005**, *15*, 51 – 55.
[92] T. W. Doebber, L. J. Kelly, G. Zhou, R. Meurer, C. Biswas, Y. Li, M. S. Wu, M. C. Ippolito, Y. S. Chao, P. R. Wang, S. D. Wright, D. E. Moller, J. P. Berger, *Biochem. Biophys. Res. Commun.* **2004**, *318*, 323 – 328.
[93] J. Sakamoto, H. Kimura, S. Moriyama, H. Imoto, Y. Momose, H. Odaka, H. Sawada, *Eur. J. Pharmacol.* **2004**, *495*, 17 – 26.
[94] B. Fagerberg, S. Edwards, T. Halmos, J. Lopatynski, H. Schuster, S. Stender, G. Stoa-Birketvedt, S. Tonstad, S. Halldorsdottir, I. Gause-Nilsson, *Diabetologia* **2005**, *48*, 1716 – 1725.
[95] K. Decochez, R. K. Rippley, J. L. Miller, M. De Smet, K. X. Yan, Z. Matthijs, K. A. Riffel, H. Song, H. Zhu, H. O. Maynor, W. Tanaka, A. O. Johnson-Levonas, M. J. Davies, K. M. Gottesdiener, B. Keymeulen, J. A. Wagner, *Drugs R&D* **2006**, *7*, 99 – 110.
[96] H. E. Xu, M. H. Lambert, V. G. Montana, K. D. Plunket, L. B. Moore, J. L. Collins, J. A. Oplinger, S. A. Kliewer, R. T. Gampe, Jr., D. D. McKee, J. T. Moore, T. M. Willson, *Proc. Natl. Acad. Sci. USA* **2001**, *98*, 13919 – 13924.
[97] P. Balakumar, M. Rose, S. S. Ganti, P. Krishan, M. Singh, *Pharmacol. Res.* **2007**, *56*, 91 – 98.
[98] J. M. Wallace, M. Schwarz, P. Coward, J. Houze, J. K. Sawyer, K. L. Kelley, A. Chai, L. L. Rudel, *J. Lipid Res.* **2005**, *46*, 1009 – 1016.
[99] I. C. Gonzalez, J. Lamar, F. Iradier, Y. Xu, L. L. Winneroski, J. York, N. Yumibe, R. Zink, C. Montrose-Rafizadeh, G. J. Etgen, C. L. Broderick,

B. A. Oldham, N. Mantlo, *Bioorg. Med. Chem. Lett.* **2007**, *17*, 1052 – 1055.
[100] Y. Xu, G. J. Etgen, C. L. Broderick, E. Canada, I. Gonzalez, J. Lamar, C. Montrose-Rafizadeh, B. A. Oldham, J. J. Osborne, C. Xie, Q. Shi, L. L. Winneroski, J. York, N. Yumibe, R. Zink, N. Mantlo, *J. Med. Chem.* **2006**, *49*, 5649 – 5652.
[101] K. G. Liu, M. H. Lambert, L. M. Leesnitzer, W. Oliver, Jr., R. J. Ott, K. D. Plunket, L. W. Stuart, P. J. Brown, T. M. Willson, D. D. Sternbach, *Bioorg. Med. Chem. Lett.* **2001**, *11*, 2959 – 2962.
[102] J. L. L. Evans, J. J. Goldfine, *Curr. Diabetes Rev.* **2005**, *1*, 299 – 307.
[103] L. Normen, J. Frohlich, J. Montaner, M. Harris, T. Elliott, G. Bondy, *Diabetes Care* **2004**, *27*, 2241 – 2242.
[104] S. Seber, S. Ucak, O. Basat, Y. Altuntas, *Diabetes Res. Clin. Pract.* **2006**, *71*, 52 – 58.
[105] B. Desvergne, L. Michalik, W. Wahli, *Physiol. Rev.* **2006**, *86*, 465 – 514.
[106] A. C. Li, C. K. Glass, *J. Lipid Res.* **2004**, *45*, 2161 – 2173.
[107] B. M. Forman, E. Goode, J. Chen, A. E. Oro, D. J. Bradley, T. Perlmann, D. J. Noonan, L. T. Burka, T. McMorris, W. W. Lamph, R. M. Evans, C. Weinberger, *Cell* **1995**, *81*, 687 – 693.
[108] S. Westin, R. A. Heyman, R. Martin, *Mini-Rev. Med. Chem.* **2005**, *5*, 719 – 727.
[109] N. L. Urizar, A. B. Liverman, D. T. Dodds, F. V. Silva, P. Ordentlich, Y. Yan, F. J. Gonzalez, R. A. Heyman, D. J. Mangelsdorf, D. D. Moore, *Science* **2002**, *296*, 1703 – 1706.
[110] P. O. Szapary, M. L. Wolfe, L. T. Bloedon, A. J. Cucchiara, A. H. DerMarderosian, M. D. Cirigliano, D. J. Rader, *JAMA J. Am. Med. Assoc.* **2003**, *290*, 765 – 772.
[111] T. P. Burris, C. Montrose, K. A. Houck, H. E. Osborne, W. P. Bocchinfuso, B. C. Yaden, C. C. Cheng, R. W. Zink, R. J. Barr, C. D. Hepler, V. Krishnan, H. A. Bullock, L. L. Burris, R. J. Galvin, K. Bramlett, K. R. Stayrook, *Mol. Pharmacol.* **2004**, *67*, 948 – 954.
[112] P. Costet, Y. Luo, N. Wang, A. R. Tall, *J. Biol. Chem.* **2000**, *275*, 28240 – 28245.
[113] J. L. Collins, A. M. Fivush, M. A. Watson, C. M. Galardi, M. C. Lewis, L. B. Moore, D. J. Parks, J. G. Wilson, T. K. Tippin, J. G. Binz, K. D. Plunket, D. G. Morgan, E. J. Beaudet, K. D. Whitney, S. A. Kliewer, T. M. Willson, *J. Med. Chem.* **2002**, *45*, 1963 – 1966.
[114] N. Terasaka, A. Hiroshima, T. Koieyama, N. Ubukata, Y. Morikawa, D. Nakai, T. Inaba, *FEBS Lett.* **2003**, *536*, 6 – 11.
[115] S. A. Doggrell, *Expert Opin. Invest. Drugs* **2006**, *15*, 99 – 106.
[116] W. A. van der Steeg, J. A. Kuivenhoven, A. H. Klerkx, S. M. Boekholdt, G. K. Hovingh, J. J. Kastelein, *Curr. Opin. Lipidol.* **2004**, *15*, 631 – 636.
[117] O. Stein, Y. Stein, *Atherosclerosis* **2005**, *178*, 217 – 230.
[118] J. A. Sikorski, *J. Med. Chem.* **2006**, *49*, 1 – 22.
[119] R. W. Clark, R. B. Ruggeri, D. Cunningham, M. J. Bamberger, *J. Lipid Res.* **2005**, *47*, 537 – 552.
[120] G. J. de Grooth, J. A. Kuivenhoven, A. F. Stalenhoef, J. de Graaf, A. H. Zwinderman, J. L. Posma, A. van Tol, J. J. Kastelein, *Circulation* **2002**, *105*, 2159 – 2165.
[121] J. A. Kuivenhoven, G. J. de Grooth, H. Kawamura, A. H. Klerkx, F. Wilhelm, M. D. Trip, J. J. Kastelein, *Am. J. Cardiol.* **2005**, *95*, 1085 – 1088.
[122] A. R. Tall, L. Y. van-Charvet, N. Wang, *Arterioscler. Thromb. Vasc. Biol.* **2006**, *27*, 257 – 260.
[123] J. J. Kastelein, S. I. van Leuven, L. Burgess, G. W. Evans, J. A. Kuivenhoven, P. J. Barter, J. H. Revkin, D. E. Grobbee, W. A. Riley, C. L. Shear, W. T. Duggan, M. L. Bots, *N. Engl. J. Med.* **2007**, *356*, 1620 – 1630.
[124] S. E. Nissen, J. C. Tardif, S. J. Nicholls, J. H. Revkin, C. L. Shear, W. T. Duggan, W. Ruzyllo, W. B. Bachinsky, G. P. Lasala, E. M. Tuzcu, *N. Engl. J. Med.* **2007**, *356*, 1304 – 1316.
[125] J. Davignon, M. Montigny, R. Dufour, *Can. J. Cardiol.* **1992**, *8*, 843 – 864.
[126] G. C. Ness, Z. Zhao, R. K. Keller, *Arch. Biochem. Biophys.* **1994**, *311*, 277 – 285.
[127] A. S. Wierzbicki, *Int. J. Clin. Pract.* **2004**, *58*, 1063 – 1072.
[128] J. R. Burnett, *Curr. Opin. Investig. Drugs* **2006**, *7*, 850 – 856.
[129] T. Miki, M. Kori, H. Mabuchi, R. Tozawa, T. Nishimoto, Y. Sugiyama, K. Teshima, H. Yukimasa, *J. Med. Chem.* **2002**, *45*, 4571 – 4580.
[130] T. Nishimoto, Y. Amano, R. Tozawa, E. Ishikawa, Y. Imura, H. Yukimasa, Y. Sugiyama, *Br. J. Pharmacol.* **2003**, *139*, 911 – 918.
[131] T. Nishimoto, R. Tozawa, Y. Amano, T. Wada, Y. Imura, Y. Sugiyama, *Biochem. Pharmacol.* **2003**, *66*, 2133 – 2139.
[132] A. W. Ng, T. Lukic, P. H. Pritchard, K. M. Wasan, *Cardiovasc. Drug Rev.* **2003**, *21*, 151 – 168.
[133] D. Y. Hui, P. N. Howles, *Semin. Cell Dev. Biol.* **2005**, *16*, 183 – 192.
[134] W. Kramer, H. Glombik, *Curr. Med. Chem.* **2006**, *13*, 997 – 1016.
[135] S. Hara, J. Higaki, K. Higashino, M. Iwai, N. Takasu, K. Miyata, K. Tonda, K. Nagata, Y. Goh, T. Mizui, *Life Sci.* **1997**, *60*, PL365 – 370.
[136] J. Higaki, S. Hara, N. Takasu, K. Tonda, K. Miyata, T. Shike, K. Nagata, T. Mizui, *Arterioscler. Thromb. Vasc. Biol.* **1998**, *18*, 1304 – 1311.
[137] K. Peter, U. Weirich, T. K. Nordt, J. Ruef, C. Bode, *Thromb. Haemostasis* **1999**, *82 Suppl 1*, 38 – 43.
[138] J. C. Tardif, *Am. J. Cardiol.* **2003**, *91*, 41A – 49A.
[139] M. A. Wasserman, C. L. Sundell, C. Kunsch, D. Edwards, C. Q. Meng, R. M. Medford, *Am. J. Cardiol.* **2003**, *91*, 34 A – 40 A.
[140] J. C. Tardif, J. Gregoire, L. L'Allier, P. R. Ibrahim, T. J. Anderson, F. Reeves, L. M. Title, E. Schampaert, M. Lemay, J. Lesperance, R. Scott, M. C. Guertin, M. L. Brennan, S. L. Hazen, O. F. Bertrand, *Atherosclerosis* **2007**, DOI: 10.1016/j.atherosclerosis.2006.11.039.
[141] E. M. Rubin, R. M. Krauss, E. A. Spangler, J. G. Verstuyft, S. M. Clift, *Nature* **1991**, *353*, 265 – 267.
[142] D. W. Garber, S. P. Handattu, G. Datta, V. K. Mishra, H. Gupta, C. R. White, G. M. Anantharamaiah, *Curr. Pharm. Biotechnol.* **2006**, *7*, 235 – 240.
[143] G. Chiesa, C. R. Sirtori, *Curr. Opin. Lipidol.* **2003**, *14*, 159 – 163.
[144] S. E. Nissen, T. Tsunoda, E. M. Tuzcu, P. Schoenhagen, C. J. Cooper, M. Yasin, G. M. Eaton, M. A. Lauer, W. S. Sheldon, C. L. Grines, S. Halpern, T. Crowe, J. C. Blankenship, R. Kerensky, *JAMA J. Am. Med. Assoc.* **2003**, *290*, 2292 – 2300.
[145] S. J. Nicholls, E. M. Tuzcu, I. Sipahi, P. Schoenhagen, T. Crowe, S. Kapadia, S. E. Nissen, *J. Am. Coll. Cardiol.* **2006**, *47*, 992 – 997.
[146] G. M. Anantharamaiah, *Methods Enzymol.* **1986**, *128*, 627 – 647.
[147] M. Navab, G. M. Anantharamaiah, S. Hama, G. Hough, S. T. Reddy, J. S. Frank, D. W. Garber, S. Handattu, A. M. Fogelman, *Arterioscler. Thromb. Vasc. Biol.* **2005**, *25*, 1426 – 1432.
[148] M. Pal, S. Pillarisetti, *Curr. Med. Chem. Cardiovasc. Hematol. Agents* **2007**, *5*, 55 – 66.
[149] G. Walldius, I. Jungner, I. Holme, A. H. Aastveit, W. Kolar, E. Steiner, *Lancet* **2001**, *358*, 2026 – 2033.
[150] J. R. Burnett, *Curr. Opin. Mol. Ther.* **2006**, *8*, 461 – 467.
[151] J. J. Kastelein, M. K. Wedel, B. F. Baker, J. Su, J. D. Bradley, R. Z. Yu, E. Chuang, M. J. Graham, R. M. Crooke, *Circulation* **2006**, *114*, 1729 – 1735.
[152] C. Leon, J. S. Hill, K. M. Wasan, *Pharm. Res.* **2005**, *22*, 1578 – 1588.
[153] D. J. Delsing, E. H. Offerman, W. van Duyvenvoorde, H. van Der Boom, E. C. de Wit, M. J. Gijbels, A. van Der Laarse, J. W. Jukema, L. M. Havekes, H. M. Princen, *Circulation* **2001**, *103*, 1778 – 1786.
[154] S. E. Nissen, E. M. Tuzcu, H. B. Brewer, I. Sipahi, S. J. Nicholls, P. Ganz, P. Schoenhagen, D. D. Waters, C. J. Pepine, T. D. Crowe, M. H. Davidson, J. E. Deanfield, L. M. Wisniewski, J. J. Hanyok, L. M. Kassalow, *N. Engl. J. Med.* **2006**, *354*, 1253 – 1263.
[155] J. C. Tardif, J. Gregoire, P. L. L'Allier, T. J. Anderson, O. Bertrand, F. Reeves, L. M. Title, F. Alfonso, E. Schampaert, A. Hassan, R. McLain, M. L. Pressler, R. Ibrahim, J. Lesperance, J. Blue, T. Heinonen, J. Rodes-Cabau, *Circulation* **2004**, *110*, 3372 – 3377.
[156] M. C. Meuwese, R. Franssen, E. S. Stroes, J. J. Kastelein, *Curr. Opin. Lipidol.* **2006**, *17*, 426 – 430.
[157] G. J. Warner, G. Stoudt, M. Bamberger, W. J. Johnson, G. H. Rothblat, *J. Biol. Chem.* **1995**, *270*, 5772 – 5778.
[158] Y. R. Su, D. E. Dove, A. S. Major, A. H. Hasty, B. Boone, M. F. Linton, S. Fazio, *Circulation* **2005**, *111*, 2373 – 2381.
[159] R. Altschul, I. H. Herman, *Arch. Biochem. Biophys.* **1954**, *51*, 308 – 309.
[160] L. A. Carlson, *J. Intern. Med.* **2005**, *258*, 94 – 114.
[161] A. J. Taylor, L. E. Sullenberger, H. J. Lee, J. K. Lee, K. A. Grace, *Circulation* **2004**, *110*, 3512 – 3517.
[162] L. A. Carlson, *Int. J. Clin. Pract.* **2004**, *58*, 706 – 713.
[163] H. Oberwittler, M. Baccara-Dinet, *Int. J. Clin. Pract.* **2006**, *60*, 707 – 715.
[164] K. Cheng, T. J. Wu, K. K. Wu, C. Sturino, K. Metters, K. Gottesdiener, S. D. Wright, Z. Wang, G. O'Neill, E. Lai, M. G. Waters, *Proc. Natl. Acad. Sci. USA* **2006**, *103*, 6682 – 6687.
[165] C. F. Sturino, G. O'Neill, N. Lachance, M. Boyd, C. Berthelette, M. Labelle, L. Li, B. Roy, J. Scheigetz, N. Tsou, Y. Aubin, K. P. Bateman, N. Chauret, S. H. Day, J. F. Levesque, C. Seto, J. H. Silva, L. A. Trimble, M. C. Carriere, D. Denis, G. Greig, S. Kargman, S. Lamontagne, M. C. Mathieu, N.

Sawyer, D. Slipetz, W. M. Abraham, T. Jones, M. McAuliffe, H. Piechuta, D. A. Nicoll-Griffith, Z. Wang, R. Zamboni, R. N. Young, K. M. Metters, *J. Med. Chem.* **2007**, *50*, 794 – 806.
[166] J. R. Burnett, G. F. Watts, *Expert Opin. Ther. Targets* **2007**, *11*, 181 – 189.
[167] J. R. Wetterau, R. E. Gregg, T. W. Harrity, C. Arbeeny, M. Cap, F. Connolly, C. H. Chu, R. J. George, D. A. Gordon, H. Jamil, K. G. Jolibois, L. K. Kunselman, S. J. Lan, T. J. Maccagnan, B. Ricci, M. Yan, D. Young, Y. Chen, O. M. Fryszman, J. V. Logan, C. L. Musial, M. A. Poss, J. A. Robl, L. M. Simpkins, W. A. Slusarchyk, R. Sulsky, P. Taunk, D. R. Magnin, J. A. Tino, R. M. Lawrence, J. K. Dickson, Jr., S. A. Biller, *Science* **1998**, *282*, 751 – 754.
[168] R. Sulsky, J. A. Robl, S. A. Biller, T. W. Harrity, J. Wetterau, F. Connolly, K. Jolibois, L. Kunselman, *Bioorg. Med. Chem. Lett.* **2004**, *14*, 5067 – 5070.
[169] M. Cuchel, L. T. Bloedon, P. O. Szapary, D. M. Kolansky, M. L. Wolfe, A. Sarkis, J. S. Millar, K. Ikewaki, E. S. Siegelman, R. E. Gregg, D. J. Rader, *N. Engl. J. Med.* **2007**, *356*, 148 – 156.

Received: July 12, 2007
Revised: September 11, 2007
Published online on October 26, 2007

QSAR & Combinatorial Science QCS

Novel Pirinixic Acids as PPARα Preferential Dual PPARα/γ Agonists

Heiko Zettl[a], Michaela Dittrich[a], Ramona Steri[a], Ewgenij Proschak[b], Oliver Rau[a], Dieter Steinhilber[a], Gisbert Schneider[b], Michael Lämmerhofer[c], and Manfred Schubert-Zsilavecz*[a]

[a] Goethe-University Frankfurt, Institute of Pharmaceutical Chemistry/ZAFES/LiFF, Max-von-Laue-Str. 9, D-60348 Frankfurt/M., Germany, Fax: (+) 49-69-79829352
*E-mail: Schubert-zsilavecz@pharmchem.uni-frankfurt.de
[b] Goethe-University Frankfurt, Beilstein Endowed Chair for Cheminformatics/LiFF, Institute of Organic Chemistry & Chemical Biology, Siesmayerstr. 70, D-60323 Frankfurt/M., Germany
[c] University of Vienna, Institute for Analytical Chemistry & Food Chemistry, Währinger Str. 38, A-1090 Vienna, Austria

Keywords: Chirality, Medicinal chemistry, Drug design, Molecular modeling, Structure-activity relationships, PPAR

Received: November 26, 2008; Accepted: January 3, 2009

DOI: 10.1002/qsar.200860163

Abstract

Pirinixic acid is a moderate agonist of both the alpha and the gamma subtype of the peroxisome proliferator activated receptor (PPAR). Previously, we have shown that α-alkyl substitution leads to balanced low micromolar-active dual agonists of PPARα and PPARγ. Taking α-hexyl pirinixic acid as a new scaffold, we further optimized PPAR activity by enlargement of the lipophilic backbone by substituting the 2,3-dimethylphenyl with biphenylic moieties. Such a substitution pattern had only minor impact on PPARγ activity but further increased PPARα activity leading to nanomolar activities. Supporting docking studies proposed that the (*R*)-enantiomer should fit the PPARα ligand-binding pocket better and thus be more active than the (*S*)-enantiomer. Single enantiomers of selected active analogues were then prepared by enantio-selective synthesis and enantio-selective preparative HPLC, respectively. Biological data for the distinct enantiomers fully corroborated the docking experiments and substantiate a stereochemical impact on PPAR activation.

1 Introduction

The peroxisome proliferator activated receptor (PPAR) is among the most prominent targets for the treatment of metabolic disorders [1, 2]. PPARα agonistic fibrate-type drugs are currently in clinical use for the treatment of several forms of dyslipidemia, particularly hypertriglyceridemia. With the exception of bezafibrate, all clinically used fibrates show a 10-fold in vitro preference for PPARα over PPARγ [3].

The PPARγ agonistic glitazone-type drugs are in use for the treatment of type 2 diabetes. Notably, a positive impact on lipid parameters has also been shown for glitazones [4]. As diabetic patients frequently exhibit associated lipid alterations, it is a current approach to combine the therapeutic effects of both PPARα and PPARγ in one drug [5]. However, the farthest developed dual PPARα/γ agonist muraglitazar, which showed a preference towards PPARγ activation, failed approval due to increased cardiovascular events [6]. It is a well-known side effect of PPARγ agonists to induce edema resulting in an increased incidence of coronary heart failure. Thus, one could reason that preferential PPARα agonists with minor PPARγ activity might avoid these undesired side effects.

Pirinixic acid (Table 1) has been established as an experimental PPARα agonist with micromolar activity and some inherent PPARγ activity. In previous studies we demonstrated that aliphatic substitution in α-position to the carboxylic acid head group of pirinixic acid improves both PPARα and PPARγ activity and leads to balanced dual PPARα/γ agonists in the lower micromolar range, with α-hexyl pirinixic acid (**3**) as the most active compound [7]. In the present study we were interested in fur-

Supporting information for this article is available on the WWW under www.qcs.wiley-vch.de

ther improvement of α-hexyl pirinixic acid in particular with regard to PPARα activity by substituting the 2,3-dimethylaniline residue. The presented series of α-alkyl substituted derivatives of pirinixic acid, namely those with a lipophilic backbone enlarged by biphenylic moieties instead of the 2,3-dimethylaniline, show a noteworthy increase in PPARα activity with no further induction of PPARγ agonism. These compounds are dual PPARα/γ agonists with a significant PPARα preference. Due to the introduction of the α-alkyl chain to our scaffold, a stereocenter is created with impact on PPAR activity as suggested by our docking studies as well as by comparison with other α-substituted carboxylic acids described in the literature [8, 9]. To scrutinize this hypothesis, individual enantiomers of selected active analogues were prepared by an enantio-selective synthesis approach and enantio-selective HPLC on a preparative scale. The results of the in vitro tests on all three PPAR subtypes (α, β, γ) fully corroborate the modeling studies and are presented here.

2 Results and Discussion

2.1 Chemistry

Synthesis of reference compounds **1**–**3** was published recently [7]. Compounds **4**–**11** (Table 1) were synthesized in a four step reaction modified from d'Atri et al. as shown in Scheme 1 [10]. Reaction of thiobarbituric acid with the appropriate α-bromoalkanoic acid ethylesters (step a) led to the respective thioether derivatives. The introduction of the *n*-butyl and *n*-hexyl chain succeeds easier with triethylamine as conjugated base in DMF rather than with NaOH in H_2O/EtOH. Aromatic nucleophilic substitution with $POCl_3$ (b) gave the 4,6-dichloro-substituted pyrimidine derivative. Subsequent treatment with the appropriate primary amine using triethylamine in refluxed EtOH (c) yielded the respective substituted pyrimidine derivatives. The resultant esters were hydrolyzed by LiOH in EtOH (d) to give the desired carboxylic acids (**4**–**11**).

The synthetic route of the enantio-selective preparation is outlined in Scheme 2. For validation of our synthetic concept we have chosen to prepare the enantiomers of α-propyl pirinixic acid. They were synthesized employing the established method of the Evan's auxiliary [11]. Firstly, the (*R*)- or (*S*)-enantiomer of benzyloxazolidinone was converted into its *N*-pentanoyl derivative (step e). By coupling with the chlorinated disulfide of thiobarbituric acid a diastereoselective reaction took place (f). Substitution of one chlorine with 2,3-dimethylaniline in the presence of *N*-ethyl diisopropyl amine in THF afforded the aminated precursor (g). Finally, removal of the chiral auxiliary with LiOH at 0 °C yielded the desired pirinixic acid derivatives (h).

For example, by starting with (*R*)-benzyloxazolidinone diastereoface selection in the course of α-alkylation at the *N*-acylated intermediate is directed by the forward-oriented (relative to the plane spanned by the oxazolidinone ring) benzyl residue to take place from the backside leading in the present case to primarily (*R*)-configured intermediates and end products, respectively (see Scheme 2) [11]. Thereby, (*R*)-**1** could be obtained from (*R*)-benzyloxazolidinone with enantiomeric excess (*ee*) of about 80% as determined by enantio-selective HPLC (vide infra) (Fig. 1). On the other hand, (*S*)-**1** was synthesized from (*S*)-benzyloxazolidinone by the same procedure with enantiomeric purity of 87% *ee*. The assignment of the absolute configurations were confirmed by enantio-selective HPLC via elution orders as described below.

2.2 Analytical and Preparative Enantio-Selective HPLC

The chromatographic enantiomer separations of the chiral 2-(2-pyrimidinyl)thioalkanoic acid derivatives (**1**, **2**, and **11**) were carried out on a chiral anion-exchanger based on *O*-9-(*tert*-butylcarbamoyl)quinidine selector which provid-

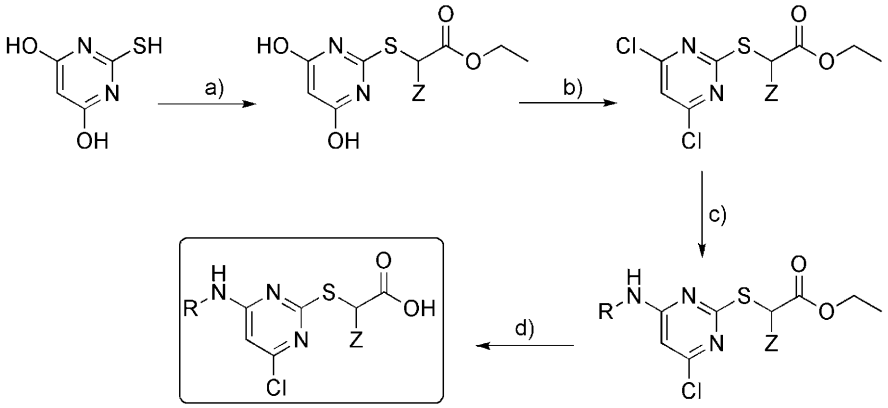

Scheme 1. Reagents and conditions: a) (Z = H): thiobarbituric acid, ethyl bromoacetate, NaOH, H_2O, EtOH, 60 °C, 2 h; (Z = *n*Hex): thiobarbituric acid, ethyl bromocaprylate, triethylamine, DMF, 80 °C, 1.5 h; b) $POCl_3$, *N*,*N*-diethylaniline, reflux., 2–3.5 h; c) R-NH_2, triethylamine, EtOH, reflux., 4–96 h; d) LiOH, EtOH, r.t., 24 h.

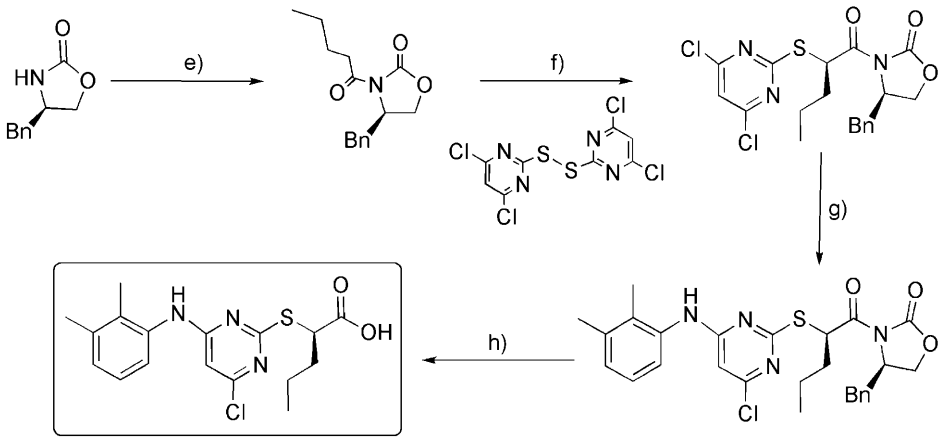

Scheme 2. Reagents and conditions: e) potassium-*tert*-butoxide, pentanoyl chloride, abs. THF, 0 °C, 1 h; f) LDA, abs. THF, −78 °C, 3 h; g) 2,3-dimethylaniline, *N*-ethyl diisopropyl amine, THF, reflux., 3.5 d; h) LiOH, THF, H_2O, 0° → r.t., 3 h.

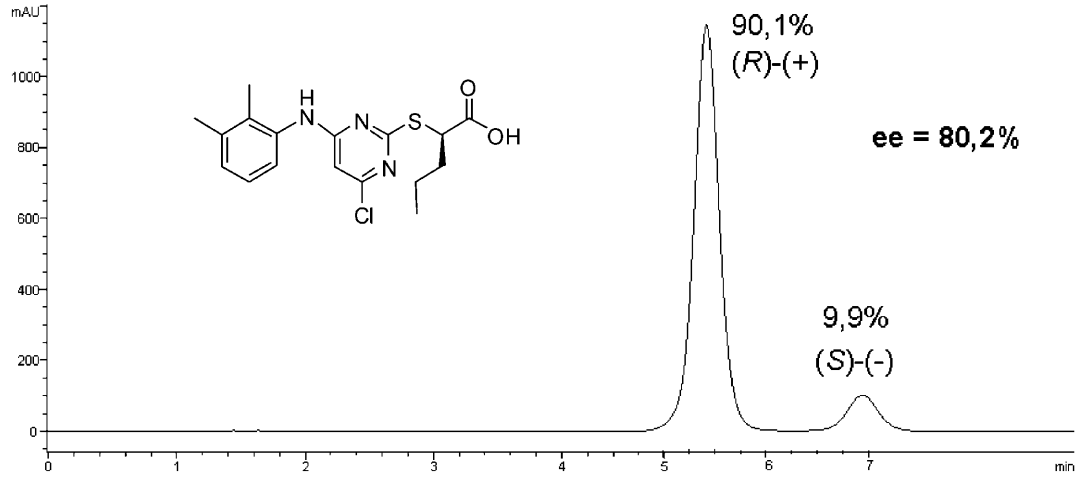

Figure 1. Enantiomeric excess of (*R*)-**1**: The determination of the enantiomeric excess (*ee*) was carried out by enantio-selective HPLC with an anion-exchange type chiral stationary phase. Column: Chiralpak QD-AX; column dimension: 150 × 4 mm ID; eluent: methanol-glacial acetic acid-ammonium acetate (98:2:0.5; v/v/w); flow rate: 1 mL/min; temperature: 25 °C; Detection: UV 254 nm.

ed excellent separation factors for all of the investigated solutes [12]. This allowed for straightforward liquid chromatographic determination of the enantiomeric excess (*ee*) of the synthesized enantiomers. An exemplary separation is shown in Figure 1. With the given mobile phase, the (+)-enantiomer of 1 eluted before the (−)-enantiomer providing a means to pinpoint the identity of the prepared or isolated enantiomers. Since optical rotation may change with solvent or substitution, other stereochemical descriptors are therefore preferred. It has been found that carboxylic acids of the type Ar-X-CH(R^1)-COOH with X being −O− or −S− show a consistent binding and chiral recognition mechanism at the quinidine carbamate selector moiety [13]. This allows for the indirect assignment of absolute configurations of the present 2-arylthio-alkanoic acids. On the quinidine carbamate-based chiral stationary phase, the *R*-enantiomer of carboxylic acids of the Ar-X-CH(R^1)-COOH elutes earlier than the *S*-enantiomer being fully in agreement with the assignment from the diastereoselective alkylation preference with the Evans' auxiliary. Some care must be taken if substituents such as additional acidic groups are present in the solute that might disturb the chiral recognition mechanism of the chiral quinidine selector. This is, however, not the case for the given α-alkyl substituted pirinixic acid derivatives used in our study. Nevertheless, since the assignment was mainly based on elution order of single enantiomers of 2-aryloxyalkanoic acid type reference solutes rather than 2-alkylthioalkanoic acids, enantiomeric 2-(2-pyrimidinylthio)propionic acids were synthesized from (*R*)- and (*S*)-2-bromo-propionic acid by nucleophilic substitution (SN_2) with pyrimidine-2-thiol. Considering the inversion of the stereoconfiguration in the course of SN_2, it turned out that the elution order of 2-arylthioalkanoic acids is the same as for aryloxycarboxylic

acids. More details on the chromatographic separation and indirect assignment of absolute configurations are published elsewhere (M. Lämmerhofer, H. Zettl, M. Schubert-Zsilavecz, W. Lindner, Chirality, in preparation).

The quinidine-derived chiral anion-exchanger also constitutes a tool to obtain rapid access to both of the enantiomers for in vitro tests by performing the separations on a preparative scale. Mass loadings of around 10 mg per injections onto an analytical column of the dimension 150 × 4 mm *i.d.* allowed to produce 10's of mg of individual enantiomers on an analytical HPLC system with little method development efforts. Fractionation was performed in such a way that a high enantiomeric excess is assured. This guarantees reliable results for the assessment of the receptor-subtype stereoselectivity. The *ee*-values of the enantiomeric products, which were subjected to the in vitro tests, are specified in Table 1.

2.3 Docking Experiments

A PPARα-binding mode of compound (*R*)-**1**, which was proposed by an automated ligand docking experiment, might explain the different EC_{50}-values between the two enantiomers. Figure 2 shows that the left proximal pocket of PPARα can be occupied by the alkyl chain in α-position of the carboxylic acid in case of the (*R*)-enantiomer (PPARα EC_{50} 2.2 μM). In contrast, the (*S*)-enantiomer (EC_{50} 9.7 μM) would cause a steric clash with helix H3. The effect increases with the size of the α-substituent. PPARγ, which possesses more space to accommodate the carboxyl group and the α-substituent due to the fact that Tyr314 is exchanged by His323 is comparatively less effected.

2.4 Discussion

α-Hexyl substituted pirinixic acid (**3**) was selected from our previously published series as a preferred scaffold of dual PPARα/γ agonists [7]. We replaced the 2,3-dimethylaniline residue of pirinixic acid by 2-phenethylamine or 2-phenoxyethylamine (Table 1, compound **5** and **7**). The in vitro activity data confirm the beneficial effect of α-substitution on PPARα/γ agonism as compared to the nonsubstituted analogs **4** and **6** (R^1 = H). The insertion of an ethylene (**4, 5**) or ethylene-oxy (**6, 7**) linker between nitrogen and the phenylic backbone was unfavorable and decreased both PPARα and PPARγ agonism compared to starting compound (**3**). Inspired by other known potent PPARα/γ

Table 1. In vitro activities on human PPARs. $EC_{50} \pm SD$ values were calculated using SigmaPlot2001 based on the mean values of at least three determinations. Values in brackets give the relative activation compared to the positive control. For compounds where there is given no EC_{50} value, the given value represents the highest activation observed at 100 μM or concentration indicated. Positive controls were 100 μM WY14643 for PPARα, pioglitazone for PPARγ and L165041 for PPARβ each at 1 μM.

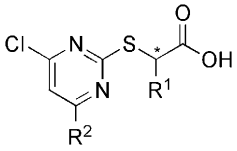

Compound	R^1	R^2	EC_{50} (μM) ± *SD* (rel. activation compared to control means ± *SD*) PPARα	PPARβ	PPARγ
Pirinixic acid	H	2,3-Dimethylaniline	39.8 ± 0.7 (100%)	(17 ± 3%)	53.7 ± 0.8 (79 ± 10%)
1 [7]	*n*Pr	2,3-Dimethylaniline	7.0 ± 0.6 (134 ± 44%)	ia [a]	5.5 ± 0.7 (106 ± 21%)
(*R*)-**1** *ee*% = 94.4	*n*Pr	2,3-Dimethylaniline	2.2 ± 0.1 (151 ± 4%)	ia [b]	8.7 ± 2.2 (192 ± 21%)
(*S*)-**1** *ee*% = 93.4	*n*Pr	2,3-Dimethylaniline	9.7 ± 0.3 (147 ± 3%)	ia [b]	2.9 ± 0.4 (118 ± 11%)
2 [7]	*n*Bu	2,3-Dimethylaniline	1.2 ± 0.2 (132 ± 7%)	ia [a]	3.0 ± 0.1 (120 ± 35%)
(*R*)-**2** *ee*% = 91.1	*n*Bu	2,3-Dimethylaniline	0.5 ± 0.2 (159 ± 26%)	ia [b]	3.5 ± 0.3 (149 ± 7%)
(*S*)-**2** *ee*% = 93.0	*n*Bu	2,3-Dimethylaniline	5.61 ± 0.7 (166 ± 14%)	ia [b]	2.8 ± 0.4 (156 ± 17%)
3 [7]	*n*Hex	2,3-Dimethylaniline	1.0 ± 0.2 (146 ± 13%)	ia [a]	3.6 ± 0.2 (139 ± 35%)
4	H	2-Phenethylamine	ia	ia	(17 ± 6%)
5	*n*Hex	2-Phenethylamine	12.9 ± 0.5 (279 ± 208%)	ia [a]	12.4 ± 0.7 (315 ± 237%)
6	H	2-Phenoxyethylamine	(26 ± 6%)	ia	ia
7	*n*Hex	2-Phenoxyethylamine	6.7 ± 1.5 (125 ± 107%)	ia [b]	6.1 ± 0.2 (93 ± 12%)
8	*n*Hex	4-Phenylbenzylamine	6.0 ± 17.2 (71 ± 8%)	(82 ± 33%) [a]	12.2 ± 3.2 (225 ± 128%)
9	*n*Hex	4-Aminobiphenyl	0.32 ± 0.01 (141 ± 24%)	ia [b]	2.4 ± 0.1 (130 ± 42%)
10	*n*Hex	5-Methoxy-2-methylbiphenyl-4-amine	0.63 ± 0.2 (138 ± 20%)	ia [b]	3.1 ± 0.5 (176 ± 3%)
11	*n*Hex	4-(4-Amino-phenyl)benzonitrile	0.19 ± 0.04 (155 ± 24%)	ia [b]	1.5 ± 0.1 (134 ± 2%)
(*R*)-**11** *ee*% = 98.8	*n*Hex	4-(4-Amino-phenyl)benzonitrile	0.03 ± 0.005 (113 ± 4%)	ia [b]	1.1 ± 0.07 (123 ± 2%)
(*S*)-**11** *ee*% = 96.8	*n*Hex	4-(4-amino-phenyl)benzonitrile	2.2 ± 0.4 (147 ± 13%)	ia [b]	3.4 ± 0.02 (143 ± 3%)
Pioglitazone	–	–	(26 ± 6%) [b]	ia [b]	0.27 ± 0.1 (100%)

ia: inactive at 100 μM or at concentration indicated: [a] at 30 μM, [b] at 10 μM.

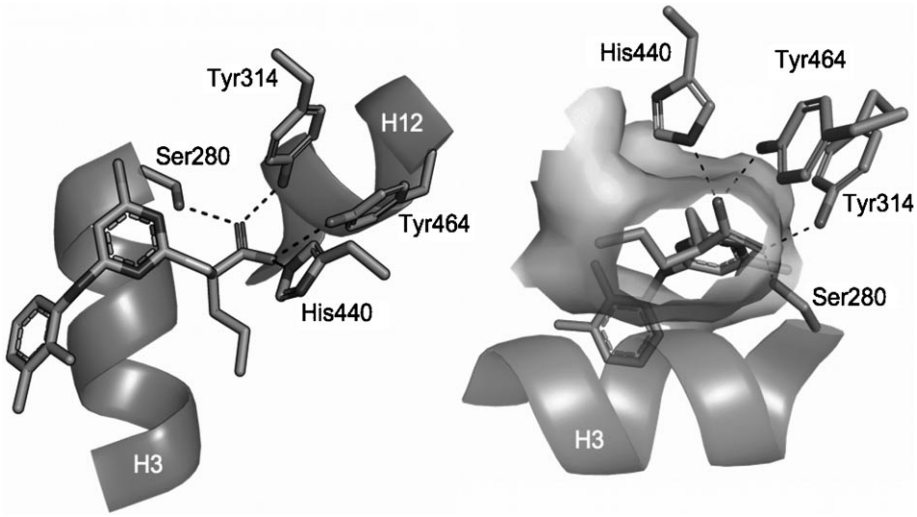

Figure 2. Compound (*R*)-**1** docked to the ligand-binding domain of PPARα. The *n*-propyl chain in α-position to the carboxylic acid might occupy the left proximal pocket of PPARα (right panel).

agonists, we decided to elucidate the effect of biphenyl moieties on PPAR activity (compounds **8**–**11**). Direct linkage of the biphenylic moiety to the exocyclic nitrogen of the pyrimidine core (**9**–**11**) improved PPARα agonism by a factor of five while PPARγ agonism was only marginally affected. In contrast, the additional methylene group in the biphenyl methylamine derivative (**8**) decreased both PPARα and PPARγ activity compared to compound (**3**). The selective improvement of PPARα agonism by the biphenyl substitution resulted in dual PPARα/γ activators with an approximately five-fold preference for PPARα. The additional cyano group in *para*-position of the biphenyl residue yielded the most active compound (**11**), which was selected for enantiomeric separation. By combining the *n*-hexyl substitution in α-position with biphenylic substitution at the pyrimidine core we achieved a 200-fold enhancement of PPARα activity and a more than 30-fold increase of PPARγ activity compared to pirinixic acid.

Concerning the investigation of the stereochemical impact of the substituent in α-position of the carboxylic acid head group, we were able to fully confirm the preference of the (*R*)-enantiomers as suggested by docking results especially for longer alkyl chains like *n*-butyl and *n*-hexyl (compounds **2** and **11**). For the *n*-propyl-substituted compound **1**, we observe a twofold preference of the (*R*)-enantiomer for PPARα compared to the racemate, whereas the (*S*)-enantiomer yields a better EC_{50} for PPARγ. This might be explained by the size of the *n*-propyl chain, which is too short to occupy the relatively large left proximal binding pocket in PPARγ. This hypothesis is supported by the observed (*R*)-preference of PPARα, as this PPAR subtype has a narrower left proximal pocket. Additionally, these results are in line with those of comparable *n*-propyl substituted fibrate analogues published by Pinelli et al. [9]. The *n*-butyl substituted compound **2** shows similar results with a twofold improvement for (*R*) and five-fold deterioration for (*S*) regarding PPARα and no notable differences for PPARγ. The most impressive enantiomeric impact is observed for compound **11.** This compound contains an *n*-hexyl chain, which represents the α-substituent with the highest steric demand from our series. (*R*)-**11** is a low nanomolar PPARα activator with an EC_{50} of 30 nM displaying a six-fold higher activity than the racemate, whereas (*S*)-**11** is remarkably less active. Even for PPARγ (*R*)-**11** shows a slightly improvement and (*S*)-**11** a twofold attenuation.

3 Conclusions

We have demonstrated that the variation of the backbone of pirinixic acid derivatives has an impact not only on their activity, but also on PPAR subtype selectivity. A biphenyl substitution especially improved PPARα agonism. We have also shown that the (*R*)-enantiomers are more potent activators of PPARα than the (*S*)-enantiomers. This effect increases with the elongation of the α-alkyl chain. Notably, PPARγ activation is merely affected. The use of (*R*)-enantiomers of α-alkyl substituted carboxylic acids might provide a means to shift the selectivity profile of dual PPAR agonists towards PPARα.

The racemic biphenyl-substituted compounds **9**–**11** show an about five-fold preference for PPARα over PPARγ and therefore fall in between fibrate type of drugs with an about 10-fold preference for PPARα and typical glitazar type PPARα/γ dual agonists which are equipotent or preferentially activate PPARγ. PPARγ specific side effects might be causative for an increase of cardiovascular events in the case of the dual PPARα/γ agonist muraglitazar and have also been observed for the PPARγ selective

rosiglitazone [14]. However, the PPARα specific agonist gemfibrozil as well as PPARγ specific agonist pioglitazone were proven to reduce mortality [15, 16]. Thus, a nonglitazar like dual PPARα/γ agonist with a marked preference for PPARα – like compound (**11**) – might represent a more favorable approach combining the therapeutical benefits of PPARα and PPARγ activation.

4 Experimental

4.1 General

All commercial chemicals and solvents are of reagent grade and were used without further purification unless otherwise specified. ^{1}H NMR and ^{13}C NMR spectra were measured on a Bruker ARX 300 (^{1}H NMR) and AC 200 E (^{13}C NMR) spectrometer. Chemical shifts are reported in parts per million (ppm) using tetramethylsilane (TMS) as internal standard. Mass spectra were obtained on a Fissous Instruments VG Platform 2 spectrometer measuring in the positive or negative ion mode (ESI – MS system). Elemental analysis has been performed by the Microanalytical Laboratory of the Institute of Organic Chemistry and Chemical Biology, University of Frankfurt, on a Foss Heraeus CHN–O–rapid elemental analyzer.

4.2 Synthesis of Novel Pirinixic Acid Derivatives 4 – 11

The respective intermediates were prepared as shown in Scheme 1.

4.2.1 Step a)

(Z = H)

To an ethanolic suspension of 2-thiobarbituric acid (1 eq) was added a solution of NaOH (1.17 eq) in water. After adding dropwise ethyl bromoacetate (1.08 eq), the reaction mixture was heated 2 h at 60 °C. The suspension was filtered and the resulting filtrate was cooled in a refrigerator over night. Refiltering the obtained precipitate, washing with water and diethyl ether, and drying under vacuum yielded in the respective thioether.

(Z = nHex)

2-Thiobarbituric acid (1 eq) was dissolved under heating in DMF/triethylamine (3 eq) and ethyl bromocaprylate (1.5 eq) was added dropwise. After 2 h the reaction mixture was quenched with 4 parts of water and extracted with ethyl acetate. The organic phase was concentrated under reduced pressure and the obtained residue was recrystallized from ethyl acetate/n-hexane.

4.2.2 Step b)

To a solution of the thioether resulting from step a) (1 eq) in $POCl_3$ (18 eq) *N,N*-diethylaniline (1 eq) was added. After refluxing the solution at 110 °C for 2 – 3.5 h (Z = H and Z = *n*Hex, respectively), the excessive $POCl_3$ was distilled and the oily residue was poured upon crushed ice. The aqueous solution was extracted with ethyl acetate; combined organic layers were washed with diluted HCl, with saturated $NaHCO_3$ solution and brine. The organic layer was dried over Na_2SO_4, filtered and evaporated under reduced pressure. Purifying the resulting oil by column chromatography (*n*-hexane/ethyl acetate) gave the chlorinated pyrimidine derivatives.

4.2.3 Step c)

A mixture of the chlorinated pyrimidine (1 eq) obtained from step b), the according aniline/amine derivative (1.05 equiv), triethylamine (3 eq) and EtOH was prepared and heated at reflux (4 – 96 h) under TLC control. The reaction mixture was evaporated under reduced pressure. The residue was dissolved in ethyl acetate and the organic layer was washed with diluted HCl, saturated $NaHCO_3$ solution and brine. After drying over $MgSO_4$, the solvent was evaporated under reduced pressure and the residue was purified by column chromatography (*n*-hexane/ethyl acetate).

4.2.4 Step d)

The esters (1 eq) from step c) were dissolved in EtOH and LiOH (3 eq) was added. After stirring for 24 h, EtOH was removed and the residue was dissolved in water (under heating, if necessary low amounts of MeOH were added). This solution was acidified with diluted hydrochloric acid and the precipitate was filtered, washed to neutrality with water and then with *n*-hexane. Recrystallization from *n*-hexane/ethyl acetate gave the carboxylic acids **4 – 11.**

2-(4-Chloro-6-(phenethylamino)pyrimidin-2-ylthio)acetic acid (4). mp = 115 °C. ^{1}H NMR (300.13 MHz, $(CD_3)_2SO$): δ 2.79 (t, 2H, Ph-C*H*$_2$, J = 7.2 Hz), 3.54 (q, 2H, C*H*$_2$-NH, J = 6.6 Hz), 3.85 (s, 2H, S-C*H*$_2$), 6.20 (s, 1H, Pyr 5-*H*), 7.16 – 7.31 (m, 5H, Ph-*H*), 7.89 (t, 1H, -N*H*, J = 5.4 Hz). ^{13}C NMR (75.45 MHz, $(CD_3)_2SO$): δ 33.1 (S-*C*H$_2$), 34.7 (Ph-*C*H$_2$), 41.6 (*C*H$_2$-NH), 99.3 (Pyr-*C*$_5$), 126.1 (Ph-*C*$_4$), 128.3 (2C, Ph-*C*$_2$ + -*C*$_6$), 128.7 (2C, Ph-*C*$_3$ + -*C*$_5$), 139.2 (Ph-*C*$_1$), 156.3 (Pyr-*C*$_4$), 162.4 (Pyr-*C*$_2$), 169.9 (Pyr-*C*$_6$), 170.1 (*C*OOH). MS (ESI –): *m/e* = 323.9 (M – 1). Anal. ($C_{14}H_{14}ClN_3O_2S$) C, H, N: Calc. C 51.93 H 4.36 N 12.98, Found C 51.96 H 4.59 N 12.75. yield 60%.

2-(4-Chloro-6-(phenethylamino)pyrimidin-2-ylthio)-octanoic acid (5). mp = 88 °C. ^{1}H NMR (300.13 MHz, $(CD_3)_2SO$): δ 0.82 (t, 3H, C*H*$_3$-Hex, J = 6.5 Hz), 1.21 – 1.28 (m, 6H, C*H*$_2$-Hex), 1.31 – 1.36 (m, 2H, C*H*$_2$-Hex), 1.74 – 1.89 (m, 2H, C*H*$_2$-Hex), 2.80 (t, 2H, Ph-C*H*$_2$, J = 7.4 Hz),

3.54 (q, 2H, CH_2-NH, J = 5.9 Hz), 4.31 (t, 1H, S-CH, J = 7.2 Hz), 6.21 (s, 1H, Pyr 5-H), 7.17 – 7.31 (m, 5H, Ph-H), 7.91 (br s, 1H, -NH). ^{13}C NMR (75.45 MHz, $(CD_3)_2SO$): δ 14.2 (*C*H_3-Hex), 21.9 (*C*H_2-Hex), 26.6 (*C*H_2-Hex), 28.1 (*C*H_2-Hex), 30.9 (*C*H_2-Hex), 31.5 (*C*H_2-Hex), 34.7 (Ph-*C*H_2), 41.6 (*C*H_2-NH), 47.1 (S-*C*H), 99.5 (Pyr-C_5), 126.1 (Ph-C_4), 128.3 (2C, Ph-C_2 + -C_6), 128.7 (2C, Ph-C_3 + -C_5), 139.1 (Ph-C_1), 156.3 (Pyr-C_4), 162.4 (Pyr-C_2), 169.7 (Pyr-C_6), 172.7 (*C*OOH). MS (ESI –): *m*/*e* = 406.1 (M – 1). Anal. ($C_{20}H_{26}ClN_3O_2S$) C, H, N: Calc. C 58.88 H 6.42 N 10.30, Found C 58.68 H 6.42 N 10.18. yield 53%.

2-(4-Chloro-6-(2-phenoxyethylamino)pyrimidin-2-ylthio)-acetic acid (6). mp = 105 °C. ^{1}H NMR (300.13 MHz, $(CD_3)_2$ SO): δ 3.67 (t, 2H, CH_2-NH, J = 5.1 Hz), 3.82 (s, 2H, S-CH_2), 4.05 (t, 2H, Ph-O-CH_2, J = 5.1 Hz), 6.28 (s, 1H, Pyr-5H), 6.92 (t, 3H, Ph-2H + – 4H + – 6H, J = 7.7 Hz), 7.27 (t, 2H, Ph-3H + – 5H, J = 8.0 Hz), 8.11 (br s, 1H, -NH). ^{13}C NMR (75.45 MHz, $(CD_3)_2SO$): δ 33.4 (S-*C*H_2), 39.8 (*C*H_2-NH), 65.9 (Ph-O-*C*H_2), 99.4 (Pyr-C_5), 114.4 (2C, Ph-C_2 + -C_6), 120.7 (Ph-C_4), 129.5 (2C, Ph-C_3 + -C_5), 156.5 (Ph-C_1), 158.3 (Pyr-C_4), 162.5 (Pyr-C_2), 170.1 (2C, Pyr-C_6, *C*OOH). MS (ESI –): *m*/*e* = 339.9 (M-1). Anal. ($C_{14}H_{14}ClN_3O_3S$) C, H, N: Calc. C 49.49 H 4.15 N 12.37, Found C 49.24 H 4.21 N 12.27. yield 86%.

2-(4-Chloro-6-(2-phenoxyethylamino)pyrimidin-2-ylthio)-octanoic acid (7). yellow oil. ^{1}H NMR (300.13 MHz, $(CD_3)_2SO$): δ 0.82 (t, 3H, CH_3-Hex, J = 6.8 Hz), 1.14 – 1.36 (m, 8H, CH_2-Hex), 1.77 – 1.90 (m, 2H, CH_2-Hex), 3.69 (t, 2H, CH_2-NH, J = 4.2 Hz), 4.06 (t, 2H, Ph-O-CH_2, J = 5.4 Hz), 4.25 (t, 1H, S-CH, J = 7.2 Hz), 6.29 (s, 1H, Pyr-5H), 6.92 (t, 3H, Ph-2H + – 4H + – 6H, J = 7.0 Hz), 7.28 (t, 2H, Ph-3H + – 5H, J = 8.0 Hz), 8.11 (br s, 1H, -NH). ^{13}C NMR (75.45 MHz, $(CD_3)_2SO$): δ 13.8 (*C*H_3-Hex), 22.0 (*C*H_2-Hex), 26.6 (*C*H_2-Hex), 28.3 (*C*H_2-Hex), 31.0 (*C*H_2-Hex), 32.0 (*C*H_2-Hex), 39.8 (*C*H_2-NH), 47.3 (S*C*H), 65.9 (Ph-O-*C*H_2), 99.4 (Pyr-C_5), 114.4 (2C, Ph-C_2 + -C_6), 120.7 (Ph-C_4), 129.5 (2C, Ph-C_3 + -C_5), 156.5 (Ph-C_1), 158.3 (Pyr-C_4), 162.6 (Pyr-C_2), 170.3 (Pyr-C_6), 173.1 (*C*OOH). MS (ESI –): *m*/*e* = 422.0 (M-1). Anal. ($C_{20}H_{26}ClN_3O_3S$) C, H, N: Calc. C 56.66 H 6.18 N 9.91, Found C 56.42 H 6.34 N 9.65. yield 59%.

2-(4-(Biphenyl-4-ylmethylamino)-6-chloropyrimidin-2-ylthio)-octanoic acid (8). mp = 110 °C. ^{1}H NMR (300.13 MHz, $(CD_3)_2SO$): δ 0.77 (t, 3H, CH_3-Hex, J = 6.3 Hz), 1.14 – 1.28 (m, 8H, CH_2-Hex), 1.66 – 1.84 (m, 2H, CH_2-Hex), 4.23 (t, 1H, S-CH, J = 7.1 Hz), 4.49 (dd, 1H, CH_{2A}-NH, J_1 = 5.4 Hz, J_2 = 15.5 Hz), 4.65 (dd, 1H, CH_{2B}-NH, J_1 = 5.6 Hz, J_2 = 15 Hz), 6.31 (s, 1H, Pyr-5H), 7.31 – 7.47 (m, 5H, Ph-H + Ph′-H), 7.61 (d, 2H, Ph-3H + Ph-5H, J = 1.8 Hz), 7.64 (d, 2H, Ph′-2H + Ph-6H, J = 1.2 Hz), 8.39 (t, 1H, -NH, J = 4.8 Hz). ^{13}C NMR (75.45 MHz, $(CD_3)_2$ SO): δ 13.8 (*C*H_3-Hex), 21.9 (*C*H_2-Hex), 26.5 (*C*H_2-Hex), 28.1 (*C*H_2-Hex), 31.0 (*C*H_2-Hex), 31.4 (*C*H_2-Hex), 43.3 (*C*H_2-NH), 47.3 (S-*C*H), 99.5 (Pyr-C_5), 126.5 (2C, Ph-C_3 + -C_5), 126.7 (2C, Ph′-C_2 + -C_6), 127.3 (Ph′-C_4), 127.9 (2C, Ph-C_2 + -C_6), 128.9 (2C, Ph′-C_3 + -C_5), 138.0 (Ph-C_4), 138.9 (Ph′-C_1), 139.8 (Ph-C_1), 156.6 (Pyr-C_6), 162.4 (Pyr-C_4), 169.8 (Pyr-C_2), 172.7 (*C*OOH). MS (ESI +): *m*/*e* = 470.1 $[M + H]^+$. Anal. ($C_{25}H_{28}ClN_3O_2S$) C, H, N: Calc. C 63.88 H 6.00 N 8.94, Found C 63.65 H 6.01 N 8.76. yield 78%.

2-(4-(Biphenyl-4-ylamino)-6-chloropyrimidin-2-ylthio)-octanoic acid (9). mp = 127 °C. ^{1}H NMR (300.13 MHz, $(CD_3)_2SO$): δ 0.78 (t, 3H, CH_3-Hex, J = 6.6 Hz), 1.14 – 1.36 (m, 8H, CH_2-Hex), 1.79 – 1.92 (m, 2H, CH_2-Hex), 4.38 (t, 1H, S-CH, J = 6.9 Hz), 6.54 (s, 1H, Pyr-5H), 7.33 (t, 1H, Ph′-4H, J = 7.4 Hz), 7.45 (t, 2H, Ph-2H + 6H, J = 7.5 Hz), 7.63 – 7.66 (m, 6H, Ph-H + Ph′-H), 10.04 (s, 1H, -NH). ^{13}C NMR (75.45 MHz, $(CD_3)_2SO$): δ 13.8 (*C*H_3-Hex), 21.9 (*C*H_2-Hex), 26.5 (*C*H_2-Hex), 28.1 (*C*H_2-Hex), 31.0 (*C*H_2-Hex), 31.7 (*C*H_2-Hex), 47.1 (S-*C*H), 101.2 (Pyr-C_5), 120.9 (2C, Ph-C_2 + -C_6), 126.2 (2C, Ph′-C_2 + -C_6), 127.0 (2C, Ph-C_3 + -C_5), 127.1 (Ph′-C_4), 128.9 (2C, Ph′-C_3 + -C_5), 135.2 (Ph-C_4), 138.0 (Ph′-C_1), 139.6 (Ph-C_1), 157.4 (Pyr-C_6), 160.5 (Pyr-C_2), 170.0 (Pyr-C_4), 172.4 (*C*OOH). MS (ESI –): *m*/*e* = 454.2 (M – 1). Anal. ($C_{24}H_{26}ClN_3O_2S$) C, H, N: Calc. C 63.21 H 5.75 N 9.21, Found C 63.01 H 5.78 N 9.08. yield 62%.

2-(4-Chloro-6-(5-methoxy-2-methylbiphenyl-4-ylamino)-pyrimidin-2-ylthio) octanoic acid (10). mp = 101 °C. ^{1}H NMR (300.13 MHz, $(CD_3)_2SO$): δ 0.78 (t, 3H, CH_3-Hex, J = 6.9 Hz), 1.16 – 1.30 (m, 8H, CH_2-Hex), 1.69 – 1.86 (m, 2H, CH_2-Hex), 2.17 (s, 3H, Ph-CH_3), 3.82 (s, 3H, Ph-O-CH_3), 4.39 (t, 1H, S-CH, J = 7.1 Hz), 6.61 (s, 1H, Pyr-5H), 6.88 (s, 1H, Ph-6H), 7.33 – 7.47 (m, 5H, Ph-H + Ph′-H), 7.69 (s, 1H, Ph-3H), 9.36 (s, 1H, -NH). ^{13}C NMR (75.45 MHz, $(CD_3)_2SO$): δ 13.8 (*C*H_3-Hex), 19.3 (Ph-*C*H_3), 21.9 (*C*H_2-Hex), 26.3 (*C*H_2-Hex), 28.1 (*C*H_2-Hex), 30.9 (*C*H_2-Hex), 31.8 (*C*H_2-Hex), 46.8 (S-*C*H), 55.8 (Ph-O-*C*H_3), 100.7 (Pyr-C_5), 112.9 (Ph-C_6), 125.3 (Ph-C_3), 125.8 (Ph′-C_4), 126.2 (Ph-C_1), 126.9 (Ph-C_2), 128.2 (2C, Ph′-C_2 + -C_6), 129.0 (2C, Ph′-$C3$ + -C_5), 138.2 (Ph-C_4), 141.0 (Ph′-C_1), 149.3 (Ph-C_5), 157.4 (Pyr-C_4), 161.2 (Pyr-C_2), 169.5 (Pyr-C_6), 172.5 (*C*OOH). MS (ESI –): *m*/*e* = 498.2 (M – 1) Anal. ($C_{26}H_{30}ClN_3O_3S$) C, H, N: Calc. C 62.45 H 6.05 N 8.40, Found C 62.30 H 6.01 N 8.39. yield 65%.

2-(4-Chloro-6-(4'-cyanobiphenyl-4-ylamino)pyrimidin-2-ylthio)-octanoic acid (11). mp = 111 °C. ^{1}H NMR (300.13 MHz, $(CD_3)_2SO$): δ 0.77 (t, 3H, CH_3-Hex, J = 6.5 Hz), 1.17 – 1.36 (m, 8H, CH_2-Hex), 1.77 – 1.94 (m, 2H, CH_2-Hex), 4.37 (t, 1H, S-CH, J = 7.1 Hz), 6.56 (s, 1H, Pyr-5H), 7.70 – 7.77 (m, 4H, Ph-H), 7.85 – 7.92 (m, 4H, Ph′-H), 10.13 (s, 1H, -NH). ^{13}C NMR (75.45 MHz, $(CD_3)_2SO$): δ 13.8 (*C*H_3-Hex), 21.9 (*C*H_2-Hex), 26.5 (*C*H_2-Hex), 28.1 (*C*H_2-Hex), 30.9 (*C*H_2-Hex), 31.6 (*C*H_2-Hex), 47.1 (S*C*H), 101.4 (Pyr-C_5), 109.5 (Ph′-C_4), 118.9 (-*C*N), 120.8 (2C, Ph-C_2 + -C_6), 126.9 (2C, Ph′-C_2 + – C_6), 127.5 (2C, Ph-C_3 + -C_5), 132.8 (2C, Ph′-C_3 + -C_5), 139.3 (Ph′-C_1), 144.0 (Ph-C_1), 157.5 (Pyr-C_6), 160.4 (Pyr-C_2), 170.0 (Pyr-C_4), 172.4 (*C*OOH). MS (ESI +): *m*/*e* = 481.0 $[M + H]^+$. Anal. ($C_{25}H_{25}ClN_4O_2S$) C, H, N: Calc. C 62.42 H 5.24 N 11.65, Found C 62.26 H 5.33 N 11.49. yield 59%.

4.3 Enantio-Selective Synthesis of (R)-1 and (S)-1

Synthesis was following the procedure as displayed in Scheme 2.

The respective (*S*)-configurated products were synthesized under same conditions with (*S*)-4-benzyloxazolidin-2-one as starting material (step e).

4.3.1 Step e)

(R-configurated)

To a solution of potassium-*tert*-butoxide (1.1 eq) in abs. THF (*R*)-4-benzyloxazolidin-2-one (1 eq) in abs. THF was added under cooling to 0 °C. After stirring for 30 min under cooling (ice) pentanoylchloride in abs. THF was added drop wise. The reaction mixture was stirred for 1 h and quenched with a saturated solution of NH_4Cl. After extraction with ethyl acetate the organic layer was washed with H_2O, saturated $NaHCO_3$ solution and brine. Afterwards the organic layer was dried over $MgSO_4$, concentrated under reduced pressure and the crude product was purified by column chromatography (*n*-hexane/ethyl acetate).

(*R*)-4-Benzyl-3-pentanoyloxazolidin-2-one. ^{1}H NMR (300.13 MHz, $CDCl_3$): δ 0.96 (t, 3H, C*H*$_3$-Pent, J = 7.3 Hz), 1.42 (m, 2H, C*H*$_2$-Pent), 1.68 (m, 2H, C*H*$_2$-Pent), 2.77 (dd, 1H, C*H*$_2$-Benzyl, J = 9.4/13.5 Hz), 2.94 (m, 2H, COC*H*$_2$), 3.30 (dd, 1H, C*H*$_2$-Benzyl, J = 3.3/13.3 Hz), 4.18 (m, 2H, C*H*$_2$-Oxazolid.), 4.68 (m, 1H, C*H*-Oxazolid.), 7.19 – 7.37 (m, 5H, Ph-C*H*). ^{13}C NMR (75.45 MHz, $CDCl_3$): δ 13.8 (*C*H$_3$-Bu), 22.3 (*C*H$_2$-Bu), 26.4 (*C*H$_2$-Bu), 35.2 (CO-*C*H$_2$-Bu), 37.9 (*C*H$_2$-Benzyl), 55.1 (*C*H-Oxazolid.), 66.1 (*C*H$_2$-Oxazolid.), 127.3 (Ph-C_4), 128.9 (2C, Ph-C_3 + -C_5), 129.4 (2C, Ph-C_2 + -C_6), 135.3 (Ph-C_1), 153.4 (*C*O-Oxazolid.), 173.4 (*C*ON). MS (ESI+): *m/e* = 261.9 $[M+H]^+$. yield 71%.

(*S*)-4-Benzyl-3-pentanoyloxazolidin-2-one. ^{1}H-NMR (300.13 MHz, $CDCl_3$): δ 0.96 (t, 3H, C*H*$_3$-Pent, J = 7.3 Hz,), 1.42 (m, 2H, C*H*$_2$-Pent), 1.68 (m, 2H, C*H*$_2$-Pent), 2.76 (dd, 1H, C*H*$_2$-Benzyl, J = 9.6/13.3 Hz), 2.94 (m, 2H, COC*H*$_2$), 3.30 (dd, 1H, C*H*$_2$-Benzyl, J = 3.3/13.4 Hz), 4.18 (m, 2H, C*H*$_2$-Oxazolid.), 4.68 (m, 1H, C*H*$_2$-Oxazolid.), 7.19 – 7.37 (m, 5H, Ph-C*H*). ^{13}C NMR (75.45 MHz, $CDCl_3$): δ 13.8 (*C*H$_3$-Bu), 22.2 (*C*H$_2$-Bu), 26.4 (*C*H$_2$-Bu), 35.2 (*C*O-CH$_2$-Bu), 37.9 (*C*H$_2$-Benzyl), 55.1 (*C*H-Oxazolid.), 66.1 (*C*H$_2$-Oxazolid.), 127.3 (Ph-C_4), 128.9 (2C, Ph-C_3 + -C_5), 129.4 (2C, Ph-C_2 + -C_6), 135.4 (Ph-C_1), 153.4 (*C*O-Oxazolid.), 173.4 (*C*ON). MS (ESI+): *m/e* = 262.0 $[M+H]^+$. yield 97%.

4.3.2 Step f)

Chlorinated Disulfide of Thiobarbituric Acid

2-Thiobarbituric acid (1 eq) was dissolved in $POCl_3$ and *N,N*-diethylaniline (2.3 eq) was added. After refluxing the mixture for 1.5 h, the excess of $POCl_3$ was distilled and the remaining residue was poured upon crushed ice. After melting of the ice the obtained precipitate was filtered, washed with H_2O, and recrystallized from dichloromethane.

1,2-Bis(4,6-dichloropyrimidin-2-yl)disulfane. ^{1}H NMR (300.13 MHz, $CDCl_3$): δ 7.18 (s, 2H, Pyr-C*H*). ^{13}C NMR (75.45 MHz, $CDCl_3$): δ 118.3 (2C, Pyr-C_5), 162.3 (4C, Pyr-C_4 + -C_6), 170.4 (2C, Pyr-C_2). MS (ESI+): *m/e* = 360.7 $[M+H]^+$. yield 55%.

(R-configurated)

(*R*)-4-benzyl-3-pentanoyloxazolidin-2-one (1 eq) was dissolved in abs. THF and cooled to −78 °C. A 2 molar solution of LDA (1.1 eq) in THF was added dropwise followed by stirring for 30 min at −78 °C. Subsequently a solution of bis-(4,6-dichloropyrimidin-2-yl)disulfide (1 eq) in abs. THF was added dropwise. After stirring for more 3 h the reaction mixture was quenched with saturated NH_4Cl solution and extracted with ethyl acetate. The organic layer was washed with brine and H_2O. The organic layer was dried over $MgSO_4$, concentrated under reduced pressure and the crude product was purified by column chromatography (*n*-hexane/ethyl acetate).

(*R*)-4-Benzyl-3-((*R*)-2-(4,6-dichloropyrimidin-2-ylthio)-pentanoyl)-oxazolidin-2-one. ^{1}H NMR (300.13 MHz, $CDCl_3$): δ 0.99 (t, 3H, C*H*$_3$-Pr, J = 7.4 Hz), 1.49 – 1.72 (m, 2H, C*H*$_2$-Pr), 1.79 – 2.07 (m, 2H, C*H*$_2$-Pr), 2.74 (dd, 1H, C*H*$_2$-Benzyl, J = 11.0/13.2 Hz), 3.41 (dd, 1H, C*H*$_2$-Benzyl, J = 3.3/13.2 Hz), 4.22 (d, 2H, C*H*$_2$-Oxazolid., J = 4.9 Hz), 4.63 – 4.73 (m, 1H, C*H*-Oxazolid.), 5.81 (dd, 1H, SC*H*, J = 5.6/8.6 Hz), 7.04 (s, 1H, Pyr-C*H*), 7.21 – 7.37 (m, 5H, Ph-C*H*). ^{13}C NMR (75.45 MHz, $CDCl_3$): δ 13.7 (*C*H$_3$-Pr), 20.4 (*C*H$_2$-Pr), 32.8 (*C*H$_2$-Pr), 38.0 (*C*H$_2$-Benzyl), 47.8 (S-*C*H), 56.3 (*C*H-Oxazolid.), 66.3 (*C*H$_2$-Oxazolid.), 116.4 (Pyr-C_5), 127.3 (Ph-C_4), 129.0 (2C, Ph-C_3 + -C_5), 129.4 (2C, Ph-C_2 + -C_6), 135.6 (Ph-C_1), 153.0 (*C*O-Oxazolid.), 161.4 (2C, Pyr-C_4 + -C_6), 172.0 (Pyr-C_2), 173.0 (*C*ON). MS (ESI+): *m/e* = 440.1 $[M+H]^+$. yield 55%.

(*S*)-4-Benzyl-3-((*S*)-2-(4,6-dichloropyrimidin-2-ylthio)-pentanoyl)-oxazolidin-2-one. ^{1}H NMR (300.13 MHz, $CDCl_3$): δ 0.99 (t, 3H, C*H*$_3$-Pr, J = 7.4 Hz), 1.35 – 1.74 (m, 2H, C*H*$_2$-Pr), 1.79 – 2.04 (m, 2H, C*H*$_2$-Pr), 2.74 (dd, 1H, C*H*$_2$-Benzyl, J = 11.1/13.3 Hz), 3.41 (dd, 1H, C*H*$_2$-Benzyl, J = 3.2/13.2 Hz), 4.22 (d, 2H, C*H*$_2$-Oxazolid., J = 5.2 Hz), 4.63 – 4.73 (m, 1H, C*H*-Oxazolid.), 5.80 (dd, 1H, SC*H*, J = 5.7/8.8 Hz), 7.04 (s, 1H, Pyr-C*H*), 7.19 – 7.37 (m, 5H, Ph-C*H*). ^{13}C NMR (75.45 MHz, $CDCl_3$): δ 13.7 (*C*H$_3$-Prop), 20.4 (*C*H$_2$-Prop), 32.8 (*C*H$_2$-Prop), 37.6 (*C*H$_2$-Benzyl), 47.7 (S-*C*H), 56.3 (*C*H-Oxazolid.), 66.3 (*C*H$_2$-Oxazolid.), 116.4 (Pyr-C_5), 127.3 (Ph-C_4), 129.0 (2C, Ph-C_3 + -C_5), 129.4 (2C, Ph-C_2 + -C_6), 135.6 (Ph-C_1), 153.0 (*C*O-Oxazolid.), 161.4 (2C, Pyr-C_4 + -C_6), 172.0 (Pyr-C_2), 173.0 (*C*ON). MS (ESI+): *m/e* = 440.0 $[M+H]^+$. yield 79%.

4.3.3 Step g)

(R-configurated)

To a solution of (*R*)-4-benzyl-3-((*R*)-2-(4,6-dichloropyrimidin-2-ylthio)pentanoyl)-oxazolidin-2-one (1 eq) in abs. THF 2,3-dimethylaniline (1.2 eq) and *N*-ethyl diisopropyl amine (1.2 eq) was added. After refluxing for 3d the solvent was removed and the oily residue was dissolved in ethyl acetate. The organic layer was washed with diluted HCl, H_2O, and brine. After drying over $MgSO_4$ and removing the solvent under reduced pressure the crude product was obtained, which was purified by column chromatography (*n*-hexane/ethyl acetate).

(*R*)-4-Benzyl-3-((*R*)-2-(4-chloro-6-(2,3-dimethylphenylamino)-pyrimidin-2-ylthio)pentanoyl)oxazolidin-2-one. ^{1}H NMR (300.13 MHz, $CDCl_3$): δ 0.99 (t, 3H, CH_3-Pr, J = 7.5 Hz), 1.49 – 1.63 (m, 2H, CH_2-Pr), 1.82 – 1.96 (m, 1H, CH_2-Pr), 1.96 – 2.09 (m, 1H, CH_2-Pr), 2.20 (s, 3H, NH-Ph-2-CH_3), 2.33 (s, 3H, NH-Ph-3-CH_3), 2.71 (dd, 1H, CH_2-Benzyl, J = 10.8/13.3 Hz), 3.42 (dd, 1H, CH_2-Benzyl, J = 3.2/13.4 Hz), 4.23 (d, 2H, CH_2-Oxazolid., J = 5.1 Hz), 4.63 – 4.73 (m, 1H, C*H*-Oxazolid.), 5.88 (dd, 1H, SC*H*, J = 5.4/8.7 Hz), 6.15 (s, 1H, Pyr-C*H*), 7.00 – 7.06 (m, 1H, NH-Ph-6*H*), 7.13 – 7.21 (m, 2H, NH-Ph-4*H* + − 5*H*), 7.21 – 7.38 (m, 5H, Ph-C*H*). ^{13}C NMR (62.9 MHz, $CDCl_3$): δ 13.6 (Ph-2-CH_3), 14.3 (*C*H_3-Pr), 20.4 (Ph-3-CH_3), 20.5 (*C*H_2-Pr), 32.6 (*C*H_2-Pr), 37.6 (*C*H_2-Benzyl), 48.6 (S*C*H), 56.3 (*C*H-Oxazolid.), 66.4 (*C*H_2-Oxazolid.), 99.6 (Pyr-C_5), 123.5 (Ph-C_6), 126.8 (Ph-C_4), 127.4 (Ph-C_4-Oxazolid.), 129.0 (2C, Ph-$C_3 + C_5$-Oxazolid.), 129.3 (2C, Ph-$C_2 + C_6$-Oxazolid.), 130.8 (Ph-C_5), 133.5 (Ph-C_2), 135.3 (Ph-C_3), 135.7 (Ph-C_1-Oxazolid.), 139.6 (Ph-C_1), 152.9 (*C*O-Oxazolid.), 157.0 (Pyr-C_4), 161.5 (Pyr-C_2), 170.3 (Pyr-C_6), 171.9 (*C*ON). MS (ESI +): *m*/*e* = 525.2 $[M+H]^+$. yield 42%.

(*S*)-4-Benzyl-3-((*S*)-2-(4-chloro-6-(2,3-dimethylphenylamino)-pyrimidin-2-ylthio)pentanoyl)oxazolidin-2-one. ^{1}H NMR (300.13 MHz, $CDCl_3$): δ 0.99 (t, 3H, CH_3-Pr, J = 7.3 Hz), 1.49 – 1.66 (m, 2H, CH_2-Pr), 1.81 – 1.93 (m, 1H, CH_2-Pr), 1.93 – 2.09 (m, 1H, CH_2-Pr), 2.18 (s, 3H, NH-Ph-2-CH_3), 2.33 (s, 3H, NH-Ph-3-CH_3), 2.71 (dd, 1H, CH_2-Benzyl, J = 10.9/13.4 Hz), 3.43 (dd, 1H, CH_2-Benzyl, J = 3.2/13.4 Hz), 4.22 (d, 2H, CH_2-Oxazolid., J = 5.0 Hz), 4.63 – 4.73 (m, 1H, C*H*-Oxazolid.), 5.87 (dd, 1H, SC*H*, J = 5.3/8.6 Hz), 6.10 (s, 1H, Pyr-C*H*), 7.00 – 7.06 (m, 1H, NH-Ph-6*H*), 7.13 – 7.20 (m, 2H, NH-Ph-4*H* + − 5*H*), 7.20 – 7.38 (m, 5H, Ph-C*H*). ^{13}C NMR (75.45 MHz, $CDCl_3$): δ 13.6 (Ph-2-CH_3), 14.2 (*C*H_3-Pr), 20.4 (Ph-3-CH_3), 20.4 (*C*H_2-Pr), 32.7 (*C*H_2-Pr), 37.6 (*C*H_2-Benzyl), 48.1 (S*C*H), 56.2 (*C*H-Oxazolid.), 66.4 (*C*H_2-Oxazolid.), 99.1 (Pyr-C_5), 123.7 (Ph-C_6), 126.7 (Ph-C_4), 127.3 (Ph-C_4-Oxazolid.), 129.0 (2C, Ph-$C_3 + C_5$-Oxazolid.), 129.3 (2C, Ph-$C_2 + C_6$-Oxazolid.), 130.2 (Ph-C_5), 133.4 (Ph-C_2), 135.5 (Ph-C_3), 135.7 (Ph-C_1-Oxazolid.), 139.3 (Ph-C_1), 152.9 (*C*O-Oxazolid.), 158.9 (Pyr-C_4), 160.9 (Pyr-C_2), 171.2 (Pyr-C_6), 171.9 (*C*ON). MS (ESI +): *m*/*e* = 525.2 $[M+H]^+$. yield 36%.

4.3.4 Step h)

(R-configurated)

(*R*)-4-benzyl-3-((*R*)-2-(4-chloro-6-(2,3-dimethylphenylamino)-pyrimidin-2-ylthio)pentanoyl)oxazolidin-2-one (1 eq) was dissolved in THF. After cooling the mixture to 0 °C, LiOH (2 eq) in H_2O was added. The reaction mixture was stirred for 3 h at 0 °C. The solvent was removed under reduced pressure and the residue was dissolved in water. The solution was acidified with diluted hydrochloric acid and extracted with ethyl acetate. Afterwards, the organic layer was dried over $MgSO_4$. Removing the solvent under reduced pressure and purification by column chromatography (*n*-hexane/ethyl acetate) yielded the desired carboxylic acid.

(R)-1

(*R*)-2-(4-Chloro-6-(2,3-dimethylphenylamino)pyrimidin-2-ylthio)pentanoic acid. ^{1}H NMR (300.13 MHz, $(CD_3)_2SO$): δ 0.81 (t, 3H, CH_3-Pr, J = 7.3 Hz), 1.19 – 1.32 (m, 2H, CH_2-Pr), 1.59 – 1.85 (m, 2H, CH_2-Pr), 2.05 (s, 3H, NH-Ph-2-CH_3), 2.25 (s, 3H, Ph-3-CH_3), 4.15 – 4.25 (m, 1H, SC*H*), 6.19 (s, 1H, Pyr-C*H*), 7.09 – 7.13 (m, 3H, Ph-*H*), 9.48 (br s, 1H, N*H*). ^{13}C NMR (75.45 MHz, $CDCl_3$): δ 13.4 (Ph-2-*C*H_3), 14.0 (*C*H_3-Pr), 19.8 (*C*H_2-Pr), 20.0 (Ph-3-*C*H_3), 34.1 (*C*H_2-Pr), 46.8 (S*C*H), 98.8 (Pyr-C_5), 124.0 (Ph-C_6), 125.7 (Ph-C_4), 127.9 (Ph-C_5), 132.4 (Ph-C_2), 135.6 (Ph-C_3), 137.6 (Ph-C_1), 157.7 (Pyr-C_4), 162.2 (Pyr-C_2), 169.7 (Pyr-C_6), 172.5 (*C*OOH). MS (ESI −): *m*/*e* = 364.0 (M − 1). yield 55%. *ee* = 80.2%.

(S)-1

(*S*)-2-(4-Chloro-6-(2,3-dimethylphenylamino)pyrimidin-2-ylthio)pentanoic acid. ^{1}H NMR (300.13 MHz, $(CD_3)_2$ SO): δ 0.81 (t, 3H, CH_3-Pr, J = 7.6 Hz), 1.20 – 1.35 (m, 2H, CH_2-Pr), 1.59 – 1.86 (m, 2H, CH_2-Pr), 2.05 (s, 3H, Ph-2-CH_3), 2.26 (s, 3H, Ph-3-CH_3), 4.16 – 4.27 (m, 1H, SC*H*), 6.19 (s, 1H, Pyr-C*H*), 7.06 – 7.14 (m, 3H, Ph-*H*), 9.49 (br s, 1H, N*H*). ^{13}C NMR (75.45 MHz, $CDCl_3$): δ 13.4 (Ph-2-*C*H_3), 14.0 (*C*H_3-Pr), 19.8 (*C*H_2-Pr), 20.0 (Ph-3-*C*H_3), 34.1 (*C*H_2-Pr), 46.8 (S*C*H), 98.9 (Pyr-C_5), 124.0 (Ph-C_6), 125.7 (Ph-C_4), 127.9 (Ph-C_5), 132.4 (Ph-C_2), 135.6 (Ph-C_3), 137.6 (Ph-C_1), 157.7 (Pyr-C_4), 162.2 (Pyr-C_2), 169.7 (Pyr-C_6), 172.5 (*C*OOH). MS (ESI +): *m*/*e* = 365.8 $[M+H]^+$. yield 55%. *ee* = 87.4%.

4.4 In Vitro Transactivation Assays, Cell Culture and Transfection, Plasmids and Propagation of the Luciferase Assay

These topics have been described previously [17, 18]. In short: Cos7 cells were grown in DMEM supplemented with FCS, sodium pyruvate, penicillin, and streptomycine at 37 °C and 5% CO_2. The pH of the medium was adjusted to that concentration of CO_2 by adding hydrochloric acid. Cells were seeded in 96-well plates at a density of 30000 per well the day before transfection. Cells were transfected with Lipofectamine2000 according to the manufacturer's

protocol with pFR-Luc (Stratagene), pRL-SV40 (Promega) and the respective receptor expression plasmid pFA-CMV-hPPAR-α/β/γ-LBD or pFA-CMV-hPPARγ-LBD. After transfection, medium was changed to DMEM without phenol red and FCS, containing appropriate concentrations of test compounds. Each concentration was tested in triplicate wells and each determination was repeated at least three times.

4.4.1 Luciferase Assay

Following overnight incubation with the test compounds Luciferase assay was carried out using Dual-Glo Luciferase Assay System (Promega) according to the manufacturer's protocol. Luminescence was measured with a GENios Pro luminometer (Tecan).

4.4.2 Compounds

All compounds were dissolved in DMSO and diluted 1:1000 upon addition to the cells. Normalization for transfection efficacy and cell growth was done by renilla luciferase data. Activation factors were obtained by dividing by DMSO control. EC_{50} and standard deviation (*SD*) values were calculated with mean values of at least three determinations by SigmaPlot 2001 (SPSS Inc) using four parameter logistic regression. All active compounds were evaluated to act as full agonists by comparison of the achieved maximum effect to that of reference compounds named in Table 1. For the determination of the PPAR activities the enantiomeric compounds were prepared or at least polished by preparative HPLC to obtain sufficiently high *ee*-products and reliable activity data. The *ee*-values of the enantiomers subjected to the in vitro tests can be found in Table 1.

4.5 Enantio-selective HPLC [12, 13]

The chromatographic experiments were carried out on a VWR EliteChrom HPLC System equipped with a quaternary gradient pump, a UV detector, a manual injector from Rheodyne with a 20 μL sample loop for analytical runs and a 500 μL loop for preparative runs. In some preliminary runs an optical rotation detector OR-990 from Jasco (Gross-Umstadt, Germany) was coupled in series to monitor the sign of optical rotation for the individual enantiomers. The data were acquired and processed by EZ-Chrom software. The column was a 150 × 4 mm i.d. CHIRALPAK QD-AX (120 Å pore size; 5 μm diameter particles) from Chiral Technologies Europe (Illkirch, France). The separations were performed at 25 °C or room temperature employing an eluent consisting of a mixture of methanol-acetic acid-ammonium acetate (98:2:0.5; v/v/w) and a flow rate of 1 mL/min. The detection wavelength was 250 nm. For analytical separations the sample was dissolved in methanol at a concentration of about 0.5 mg/mL and an aliquot of 2 μL was injected. For preparative scale separations, the 20 μL loop was replaced by a 500 μL sample loop and the sample was dissolved in methanol at a concentration of about 20 mg/mL. Depending on the type of solute and separation factor, about 5 to 10 mg sample masses were injected onto the analytical 150 × 4 mm *i.d.* column per run. The peaks corresponding to the individual enantiomers were collected separately, the combined fractions evaporated to dryness. The residues were extracted from slightly HCl-acidic saturated brine solution into ethylacetate. The combined organic phases were dried over Na_2SO_4, filtrated and evaporated to dryness yielding the final enantiomeric products. For *ee*-values see Table 1.

4.6 Docking

Docking experiments were performed with GOLD 4.0 software [19]. The structure of the ligand-binding domain of PPARα (PDB code 1i7g [20]) was prepared for docking by adding explicit hydrogens with MOE 2007.09 (Chemical Computing Group, Montreal, Canada) using the Protonate 3D algorithm. Default options and Goldscore scoring function were used to propose ten potential binding modes from which the one with an interaction pattern of the carboxylic group most similar to the co-crystallized ligand AZ242 was selected by visual inspection.

5 Acknowledgement

We gratefully acknowledge financial support from the Else-Kroener-Fresenius-Stiftung (FIRST).

References

[1] S. M. Grundy, *Nat. Rev. Drug. Discov.* **2006**, *5*, 295.
[2] S. Kersten, B. Desvergne, W. Wahli, *Nature* **2000**, *405*, 421.
[3] T. M. Willson, P. J. Brown, D. D. Sternbach, B. R. Henke, *J. Med. Chem.* **2000**, *43*, 527.
[4] O. Rau, H. Zettl, L. Popescu, D. Steinhilber, M. Schubert-Zsilavecz, *ChemMedChem* **2008**, *3*, 206.
[5] J. P. Berger, T. E. Akiyama, P. T. Meinke, *Trends Pharmacol. Sci.* **2005**, *26*, 244.
[6] S. E. Nissen, K. Wolski, E. J. Topol, *Jama* **2005**, *294*, 2581.
[7] O. Rau, Y. Syha, H. Zettl, M. Kock, A. Bock, M. Schubert-Zsilavecz, *Arch. Pharm. (Weinheim)* **2008**, *341*, 191.
[8] M. Nomura, T. Tanase, T. Ide, M. Tsunoda, M. Suzuki, H. Uchiki, K. Murakami, H. Miyachi, *J. Med. Chem.* **2003**, *46*, 3581.
[9] A. Pinelli, C. Godio, A. Laghezza, N. Mitro, G. Fracchiolla, V. Tortorella, A. Lavecchia, E. Novellino, J. C. Fruchart, B. Staels, M. Crestani, F. Loiodice, *J Med Chem* **2005**, *48*, 5509.
[10] G. d'Atri, P. Gomarasca, G. Resnati, G. Tronconi, C. Scolastico, C. R. Sirtori, *J. Med. Chem.* **1984**, *27*, 1621.
[11] D. A. Evans, M. D. Ennis, D. J. Mathre, *J. Am. Chem. Soc.* **1982**, *104*, 1737.

[12] M. Lammerhofer, W. Lindner, *J. Chromatogr. A* **1996**, *741*, 33.
[13] A. Mandl, L. Nicoletti, M. Lammerhofer, W. Lindner, *J. Chromatogr. A* **1999**, *858*, 1.
[14] S. E. Nissen, K. Wolski, *N. Engl. J. Med.* **2007**, *356*, 2457.
[15] H. B. Rubins, S. J. Robins, D. Collins, C. L. Fye, J. W. Anderson, M. B. Elam, F. H. Faas, E. Linares, E. J. Schaefer, G. Schectman, T. J. Wilt, J. Wittes, *N. Engl. J. Med.* **1999**, *341*, 410.
[16] J. A. Dormandy, B. Charbonnel, D. J. Eckland, E. Erdmann, M. Massi-Benedetti, I. K. Moules, A. M. Skene, M. H. Tan, P. J. Lefebvre, G. D. Murray, E. Standl, R. G. Wilcox, L. Wilhelmsen, J. Betteridge, K. Birkeland, A. Golay, R. J. Heine, L. Koranyi, M. Laakso, M. Mokan, A. Norkus, V. Pirags, T. Podar, A. Scheen, W. Scherbaum, G. Schernthaner, O. Schmitz, J. Skrha, U. Smith, J. Taton, *Lancet* **2005**, *366*, 1279.
[17] O. Rau, M. Wurglics, A. Paulke, J. Zitzkowski, N. Meindl, A. Bock, T. Dingermann, M. Abdel-Tawab, M. Schubert-Zsilavecz, *Planta Med.* **2006**, *72*, 881.
[18] S. Ulrich, S. M. Loitsch, O. Rau, A. von Knethen, B. Brune, M. Schubert-Zsilavecz, J. M. Stein, *Cancer Res.* **2006**, *66*, 7348.
[19] M. L. Verdonk, J. C. Cole, M. J. Hartshorn, C. W. Murray, R. D. Taylor, *Proteins* **2003**, *52*, 609.
[20] P. Cronet, J. F. Petersen, R. Folmer, N. Blomberg, K. Sjoblom, U. Karlsson, E. L. Lindstedt, K. Bamberg, *Structure* **2001**, *9*, 699.

Supporting Information

Supporting Information

Novel pirinixic acids as PPARα preferential dual PPARα/γ agonists

Heiko Zettl, Michaela Dittrich, Ramona Steri, Ewgenij Proschak, Oliver Rau, Dieter Steinhilber, Gisbert Schneider, Michael Lämmerhofer, and Manfred Schubert-Zsilavecz*

Synthesis of novel pirinixic acid derivatives **4-11** as shown in **Scheme 1** (modified from [1]):

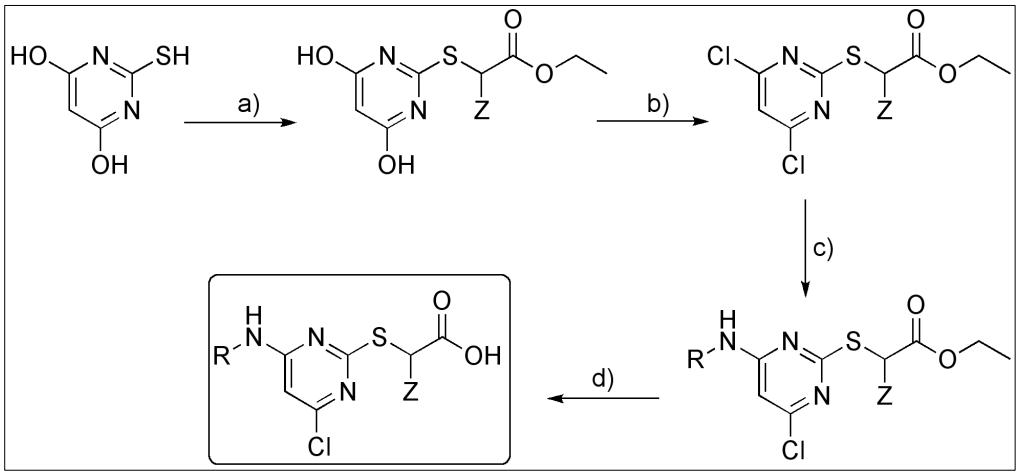

Scheme 1. Reagents and conditions: **a) (Z=H):** thiobarbituric acid, ethyl bromoacetate, NaOH, H_2O, EtOH, 60°C, 2h **(Z=*n*Hex):** thiobarbituric acid, ethyl bromocaprylate, triethylamine, DMF, 80°C, 1.5h **b)** $POCl_3$, *N*,*N*-diethylaniline, reflux., 2-3.5h **c)** R-NH_2, triethylamine, EtOH, reflux., 4-96h **d)** corresponding ester, LiOH, EtOH, r.t., 24h

Structures of the intermediates (steps **a**)-**c**)) confirmed by ^{1}H-NMR and mass spectrometry (ESI) as follows:

Step **a)**

(Z=H)

ethyl 2-(4,6-dihydroxypyrimidin-2-ylthio)acetate ^{1}H NMR (300.13 MHz, $(CD_3)_2SO$): δ 1.17 (t, 3H, C*H*$_3$, J=7.2Hz), 3.99 (s, 2H, S-C*H*$_2$), 4.10 (q, 2H, O-C*H*$_2$, J=7.2Hz), 5.19 (s, 1H, Pyr-5*H*), 11.78 (br s, 2H, O*H*). [1]

(Z=*n*Hex)

ethyl 2-(4,6-dihydroxypyrimidin-2-ylthio)octanoate ^{1}H NMR (300.13 MHz, $(CD_3)_2SO$): δ 0.83 (t, 3H, C*H*$_3$-Hex, J=6.9Hz), 1.17 (t, 3H, C*H*$_3$, J=7.1Hz), 1.23-1.30 (m, 8H, C*H*$_2$-Hex), 1.76-1.88 (m, 2H, C*H*$_2$-Hex), 4.11 (q, 2H, O-C*H*$_2$, J=7.1Hz), 4.50 (t, 1H, S-C*H*, J=7.1Hz), 5.22 (s, 1H, Pyr-5*H*), 11.79 (br s, 2H, O*H*). ^{13}C NMR (50.32 MHz, $(CD_3)_2SO$): δ 13.8 (*C*H$_3$-Hex), 13.9 (*C*H$_3$), 21.9 (*C*H$_2$-Hex), 26.3 (*C*H$_2$-Hex), 28.1 (*C*H$_2$-Hex), 30.9 (*C*H$_2$-Hex), 31.6 (*C*H$_2$-Hex), 46.5 (S*C*H), 61.1 (O*C*H$_2$), 85.7 (Pyr-*C*$_5$), 162.7 (Pyr-*C*$_2$), 167.8 (2C, Pyr-C$_4$ + -*C*$_6$), 170.9 (*C*OO). MS (ESI+): *m/e* = 315.1 $[M+H]^+$. yield 50%.

Step **b)**

(Z=H)

ethyl 2-(4,6-dichloropyrimidin-2-ylthio)acetate ^{1}H NMR (300.13 MHz, $CDCl_3$): δ 1.29 (t, 3H, C*H*$_3$, J=7.1Hz), 3.90 (s, 2H, S-C*H*$_2$), 4.23 (q, 2H, O-C*H*$_2$, J=7.1Hz), 7.06 (s, 1H, Pyr-5*H*). [1]

(Z=*n*Hex)

ethyl 2-(4,6-dichloropyrimidin-2-ylthio)octanoate ^{1}H NMR (300.13 MHz, $CDCl_3$): δ 0.87 (t, 3H, C*H*$_3$-Hex, J=6.8Hz), 1.28 (t, 3H, C*H*$_3$, J=7.1Hz), 1.26-1.36 (m, 6H, C*H*$_2$-Hex), 1.43-1.49 (m, 2H, C*H*$_2$-Hex), 1.86-1.98 (m, 2H, C*H*$_2$-Hex), 4.20 (q, 2H, O-C*H*$_2$, J=7.1Hz), 4.38 (t, 1H, S-C*H*, J=7.2Hz), 7.03 (s, 1H, Pyr-5*H*). ^{13}C NMR (50.32 MHz, $CDCl_3$): δ 14.00 (*C*H$_3$-Hex), 14.2 (*C*H$_3$), 22.5 (*C*H$_2$-Hex), 27.0 (*C*H$_2$-Hex), 28.7 (*C*H$_2$-Hex), 31.0 (*C*H$_2$-Hex), 31.2 (*C*H$_2$-Hex), 48.6 (S*C*H), 61.6 (O*C*H$_2$), 116.3 (Pyr-*C*$_5$), 161.4 (2C, Pyr-C$_4$ + *C*$_6$), 171.4 (Pyr-*C*$_2$), 172.8 (*C*OO). MS (ESI+): *m/e* = 350.9 $[M+H]^+$. yield 85%.

Step **c)**

ethyl 2-(4-chloro-6-(phenethylamino)pyrimidin-2-ylthio)acetate (compound 4-ester) ^{1}H NMR (300.13 MHz, $(CD_3)_2SO$): δ 1.07 (t, 3H, C*H*$_3$, J=7.1Hz), 2.79 (t, 2H, Ph-C*H*$_2$, J=7.4Hz), 3.49 (q, 2H, C*H*$_2$-NH, J=6.7MHz), 3.91 (s, 1H, S-C*H*$_2$), 4.02 (q, 2H, O-C*H*$_2$, J=7.1Hz), 6.20 (s, 1H, Pyr-5*H*), 7.17-7.31 (m, 5H, Ph-*H*, J=7.2MHz), 7.75 (t, 1H, -N*H*, J=5.3MHz). ^{13}C NMR (75.45 MHz, $(CD_3)_2SO$) δ 13.9 (*C*H$_3$), 32.9 (S*C*H$_2$), 34.7 (Ph-*C*H$_2$), 41.6 (*C*H$_2$-NH), 60.9 (O*C*H$_2$), 99.4 (Pyr-*C*$_5$), 126.2 (Ph-*C*$_4$), 128.3 (2C, Ph-*C*$_2$ + -*C*$_6$), 128.7 (2C, Ph-*C*$_3$ + -*C*$_5$), 139.1 (Ph-*C*$_1$), 156.3 (Pyr-*C*$_4$), 162.4 (Pyr-*C*$_2$), 168.9 (Pyr-*C*$_6$), 169.5 (*C*OO). MS (ESI−): *m/e* = 352.0 (M−1). yield 80%.

ethyl 2-(4-chloro-6-(phenethylamino)pyrimidin-2-ylthio)octanoate (5-ester) ^{1}H NMR (300.13 MHz, $CDCl_3$): δ 0.89 (t, 3H, C*H*$_3$-Hex, J=3.3Hz), 1.25 (t, 3H, C*H*$_3$, J=6.3Hz), 1.27-1.29 (m, 6H, C*H*$_2$-Hex), 1.33-1.47 (m, 2H, C*H*$_2$-Hex), 1.87-1.93 (m, 2H, C*H*$_2$-Hex), 2.90 (t, 2H, Ph-C*H*$_2$, J=8.5Hz), 3.58 (br s, 1H, -N*H*), 4.11-4.22 (m, 4H, O-C*H*$_2$ + C*H*$_2$-NH), 4.37 (t, 1H, S-C*H*, J=7.4Hz), 5.99 (s, 1H, Pyr-5*H*), 7.19-7.36 (m, 5H, Ph-*H)*. ^{13}C NMR (75.45 MHz, $CDCl_3$): δ 14.0 (*C*H$_3$), 14.2 (*C*H$_3$-Hex), 22.6 (*C*H$_2$-Hex), 27.1 (*C*H$_2$-Hex), 28.8 (*C*H$_2$-Hex), 31.5 (*C*H$_2$-Hex), 31.6 (*C*H$_2$-Hex), 35.3 (Ph-*C*H$_2$), 42.4 (*C*H$_2$-NH), 47.9 (S*C*H), 61.3 (O*C*H$_2$), 99.0 (Pyr-*C*$_5$), 126.8 (Ph-*C*$_4$), 128.7 (2C, Ph-*C*$_2$ + -*C*$_6$), 128.8 (2C, Ph-*C*$_3$ + -*C*$_5$), 138.2 (Ph-*C*$_1$), 158.8 (Pyr-*C*$_4$), 162.6 (Pyr-*C*$_2$), 170.7 (Pyr-*C*$_6$), 172.4 (*C*OO). MS (ESI+): *m/e* = 436.2 $[M+H]^+$. yield 40%.

ethyl 2-(4-chloro-6-(2-phenoxyethylamino)pyrimidin-2-ylthio)acetate (6-ester) ^{1}H NMR (300.13 MHz, $(CD_3)_2SO$): δ 1.15 (t, 3H, C*H*$_3$, J=7.2Hz), 3.65 (d, 2H, C*H*$_2$-NH, J=5.4Hz), 3.88 (s, 2H, S-C*H*$_2$), 4.03 (q, 2H, O-C*H*$_2$, J=5.6MHz), 4.09 (t, 2H, Ph-O-C*H*$_2$, J=7.1Hz), 6.29 (s, 1H, Pyr-5*H*), 6.92 (t, 3H, Ph-2*H* + 4*H* + 6*H*, J=6.9Hz), 7.28 (t, 2H, Ph-3*H* + 5*H*, J=8.0Hz), 8.08 (br s,1H, -N*H*). ^{13}C NMR (75.45 MHz, $(CD_3)_2SO$): δ 14.0 (*C*H$_3$), 32.9 (S*C*H$_2$), 39.6 (*C*H$_2$-NH), 60.9 (O*C*H$_2$), 65.7 (Ph-O-*C*H$_2$), 99.6 (Pyr-*C*$_5$), 114.4 (2C, Ph-*C*$_2$ + -*C*$_6$), 120.7 (Ph-*C*$_4$), 129.8 (2C, Ph-*C*$_3$ + -*C*$_5$), 156.5 (Ph-*C*$_1$), 158.2 (Pyr-*C*$_4$), 162.6 (Pyr-*C*$_2$), 168.9 (Pyr- *C*$_6$), 169.6 (*C*OO). MS (ESI−): *m/e* = 368.0 (M−1). yield 88%.

ethyl 2-(4-chloro-6-(2-phenoxyethylamino)pyrimidin-2-ylthio)octanoate (7-ester) ^{1}H NMR (300.13 MHz, $(CD_3)_2SO$): δ 0.82 (t, 3H, C*H*$_3$-Hex, J=6.9Hz), 1.12-1.19 (m, 5H, C*H*$_3$ + C*H*$_2$-Hex), 1.22-1.35 (m, 6H, C*H*$_2$-Hex), 1.73-1.87 (m, 2H, C*H*$_2$-Hex), 3.67 (t, 2H, C*H*$_2$-NH, J=5.7Hz), 4.03-4.15 (m, 4H, O-C*H*$_2$ + Ph-O-C*H*$_2$), 4.29 (t, 1H, S-C*H*, J=7.2Hz), 6.30 (s, 1H, Pyr-5*H*), 6.93 (t, 3H, Ph-2*H* + -4*H* + -6*H*, J=5.7Hz*)*, 7.28 (t, 2H, Ph-3*H* + -5*H*, J=8.0Hz), 8.11 (br s,1H, -N*H*). ^{13}C NMR (75.45 MHz, $(CD_3)_2SO$): δ 13.8 (*C*H$_3$), 13.9 (*C*H$_3$-Hex), 21.9 (*C*H$_2$-Hex), 26.5 (*C*H$_2$-Hex), 28.1 (*C*H$_2$-Hex), 30.9 (*C*H$_2$-Hex), 31.1 (*C*H$_2$-Hex), 39.7 (*C*H$_2$-NH), 47.0 (S*C*H), 60.9 (O*C*H$_2$), 65.8 (Ph-O-*C*H$_2$), 99.8 (Pyr-*C*$_5$), 114.4 (2C, Ph-*C*$_2$ + -*C*$_6$), 120.7 (Ph-*C*$_4$), 129.5 (2C, Ph-*C*$_3$ + -*C*$_5$), 156.5 (Ph-*C*$_1$), 158.2 (Pyr-*C*$_4$), 162.6 (Pyr-*C*$_2$), 169.4 (Pyr-*C*$_6$), 171.4 (*C*OO). MS (ESI+): *m/e* = 452.0 $[M+H]^+$. yield 37%.

ethyl 2-(4-(biphenyl-4-ylmethylamino)-6-chloropyrimidin-2-ylthio) octanoate (8-ester) ^{1}H-NMR (300.13 MHz, $(CD_3)_2SO$) δ 0.82 (t, 3H, C*H*$_3$-Hex, J=7.9Hz), 1.10-1.23 (m, 11H, C*H*$_3$ + C*H*$_2$-Hex), 1.71-1.80 (m, 2H, C*H*$_2$-Hex), 4.07 (q, 2H, O-C*H*$_2$, J=7.2Hz), 4.26 (t, 1H, S-C*H*, J=7.2Hz), 4.56 (dd, 2H, C*H*$_2$-NH, J_1=5.6Hz, J_2=15Hz), 6.32 (s, 1H, Pyr-5*H*), 7.32-7.47 (m, 5H, Ph-*H* + Ph'-*H)*, 7.63 (m, 4H, Ph-*H* + Ph'-*H*), 8.42 (t,1H, -N*H*, J=6.0Hz). ^{13}C NMR (75.45 MHz, $(CD_3)_2SO$): δ 13.8 (*C*H$_3$-Hex), 13.9 (*C*H$_3$), 21.9 (*C*H$_2$-Hex), 26.4 (*C*H$_2$-Hex), 28.0 (*C*H$_2$-Hex), 30.9 (*C*H$_2$-Hex), 31.1 (*C*H$_2$-Hex), 43.2 (*C*H$_2$-NH), 47.0 (S*C*H), 60.9 (O*C*H$_2$), 99.7 (Pyr-*C*$_5$), 126.5 (2C, Ph-*C*$_3$ + -*C*$_5$), 126.7 (2C, Ph'-*C*$_2$ + -*C*$_6$), 127.3 (Ph'-*C*$_4$), 127.8 (2C, Ph-*C*$_2$ + -*C*$_6$), 128.9 (2C, Ph'-*C*$_3$ + -*C*$_5$), 138.0 (Ph-*C*$_4$), 138.9 (Ph'-*C*$_1$), 139.8 (Ph-*C*$_1$), 156.6 (Pyr-*C*$_6$), 162.4 (Pyr-*C*$_4$), 169.5 (Pyr-*C*$_2$), 171.4 (*C*OO). MS (ESI+): *m/e* = 498.3 $[M+H]^+$. yield 40%.

ethyl 2-(4-(biphenyl-4-ylamino)-6-chloropyrimidin-2-ylthio)octanoate (9-ester) ^{1}H NMR (300.13 MHz, $(CD_3)_2SO$): δ 0.79 (t, 3H, C*H*$_3$-Hex, J=6.5Hz), 1.14 (t, 3H, C*H*$_3$, J=7.1Hz), 1.19-1.35 (m, 8H, C*H*$_2$-Hex), 1.76-1.94 (m, 2H, C*H*$_2$-Hex), 4.10 (q, 2H, O-C*H*$_2$, J=7.2Hz), 4.43 (t, 1H, S-C*H*, J=7.4Hz), 6.54 (s, 1H, Pyr-5*H*), 7.33 (t, 1H, Ph'-4*H*, J=7.2Hz), 7.45 (t, 2H, Ph-2*H* + 6*H*, J=7.5Hz), 7.63-7.70 (m, 6H, Ph-*H* + Ph'-*H*), 10.05 (s, 1H, -N*H*). ^{13}C NMR (75.45 MHz, $(CD_3)_2SO$): δ 13.8 (*C*H$_3$-Hex), 13.9 (*C*H$_3$), 21.9 (*C*H$_2$-Hex), 26.4 (*C*H$_2$-Hex), 28.0 (*C*H$_2$-Hex), 30.9 (*C*H$_2$-Hex), 31.6 (*C*H$_2$-Hex), 46.8 (S*C*H), 61.0 (O*C*H$_2$), 101.3 (Pyr-*C*$_5$), 121.0 (2C, Ph-*C*$_2$ + -*C*$_6$), 126.2 (2C, Ph'-*C*$_2$ + -*C*$_6$), 127.0 (2C, Ph-*C*$_3$ + -*C*$_5$), 127.1 (Ph'-*C*$_4$), 128.9 (2C, Ph'-*C*$_3$ + -*C*$_5$), 135.3 (Ph-*C*$_4$), 137.9 (Ph'-*C*$_1$), 139.5 (Ph-*C*$_1$), 157.4 (Pyr-*C*$_6$), 160.5 (Pyr-*C*$_2$), 169.6 (Pyr-*C*$_4$), 171.1 (*C*OO). MS (ESI+): *m/e* = 484.2 $[M+H]^+$. yield 59%.

ethyl 2-(4-chloro-6-(5-methoxy-2-methylbiphenyl-4-ylamino)pyrimidin-2-ylthio) octanoate (10-ester) ^{1}H NMR (300.13 MHz, $(CD_3)_2SO$): δ 0.79 (t, 3H, C*H*$_3$-Hex, J=6.8Hz), 1.12 (t, 3H, C*H*$_3$, J=7.2Hz), 1.16-1.28 (m, 8H, C*H*$_2$-Hexyl), 1.68-1.88 (m, 2H, C*H*$_2$-Hexyl), 2.17 (s, 3H, Ph-C*H*$_3$), 3.82 (s, 3H, Ph-O-C*H*$_3$), 4.10 (q, 2H, O-C*H*$_2$, J=7.0Hz), 4.42 (t, 1H, S-C*H*, J=7.2Hz), 6.61 (s, 1H, Pyr-5*H*), 6.89 (s, 1H, Ph-6*H*), 7.33-7.47 (m, 5H, Ph-*H* + Ph'-*H*), 7.67 (s, 1H, Ph-3*H*), 9.37 (s, 1H, -N*H*). ^{13}C NMR (75.45 MHz, $(CD_3)_2SO$): δ 13.8 (*C*H$_3$-Hex), 13.9 (*C*H$_3$), 19.3 (Ph-*C*H$_3$), 21.8 (*C*H$_2$-Hex), 26.3 (*C*H$_2$-Hex), 28.0 (*C*H$_2$-Hex), 30.9 (*C*H$_2$-Hex), 31.5 (*C*H$_2$-Hex), 46.7 (S*C*H), 55.8 (Ph-O-*C*H$_3$), 60.9 (O*C*H$_2$), 100.9 (Pyr-*C*$_5$), 112.9 (Ph-*C*$_6$), 125.2 (Ph-*C*$_3$), 125.9 (Ph'-*C*$_4$), 126.2 (Ph-*C*$_1$), 126.9 (Ph-*C*$_2$), 128.2 (2C, Ph'-*C*$_2$ + -*C*$_6$), 129.0 (2C, Ph'-*C*$_3$ + -*C*$_5$), 138.3 (Ph-*C*$_4$), 141.0 (Ph'-*C*$_1$), 149.4 (Ph-*C*$_5$), 157.4 (Pyr-*C*$_4$), 161.3 (Pyr-*C*$_2$), 169.1 (Pyr-*C*$_6$), 171.2 (*C*OO). MS (ESI+): *m/e* = 528.2 $[M+H]^+$. yield 41%.

ethyl 2-(4-chloro-6-(4'-cyanobiphenyl-4-ylamino)pyrimidin-2-ylthio) octanoate (11-ester) ^{1}H NMR (300.13 MHz, $(CD_3)_2SO$): δ 0.78 (t, 3H, C*H*$_3$-Hex, J=6.3Hz), 1.14 (t, 3H, C*H*$_3$, J=6.9Hz), 1.17-1.37 (m, 8H, C*H*$_2$-Hex), 1.76-1.91 (m, 2H, C*H*$_2$-Hex), 4.10 (q, 2H, O-C*H*$_2$, J=7.2Hz), 4.43 (t, 1H, S-C*H*, J=7.2Hz), 6.56 (s, 1H, Pyr-5*H*), 7.67-7.77 (m, 4H, Ph-*H*), 7.84-7.91 (m, 4H, Ph'-*H*), 10.13 (s, 1H, -N*H*). ^{13}C NMR (75.45 MHz, $(CD_3)_2SO$): δ 13.8 (*C*H$_3$-Hex), 13.9 (*C*H$_3$), 21.9 (*C*H$_2$-Hex), 26.4 (*C*H$_2$-Hex), 28.0 (*C*H$_2$-Hex), 30.9 (*C*H$_2$-Hex), 31.3 (*C*H$_2$-Hex), 46.9 (S*C*H), 61.0 (O*C*H$_2$), 101.6 (Pyr-*C*$_5$), 109.5 (Ph'-*C*$_4$),

118.9 (-*C*N), 120.8 (2C, Ph-C_2 + -C_6), 126.9 (2C, Ph'-C_2 + -C_6), 127.5 (2C, Ph-C_3 + -C_5), 132.8 (2C, Ph'-C_3 + -C_5), 139.2 (Ph'-C_1), 144.0 (Ph-C_1), 157.5 (Pyr-C_6), 160.4 (Pyr-C_2), 169.6 (Pyr-C_4), 171.1 (*C*OO). MS (ESI+): *m/e* = 509.2 $[M+H]^+$. yield 60%.

Compounds **(*R*)-1**, **(*S*)-1**, **(*R*)-2**, **(*S*)-2**, and **(*R*)-11**, **(*S*)-11** were obtained by preparative HPLC of **1**[2], **2**[2], and **11**, respectively, under following conditions:

chiral stationary phase: Chiralpak QD-AX (Column dimension, 150 x 4 mm ID)

eluent: methanol-glacial acetic acid-ammonium acetate (98:2:0.5; v/v/w)

flow rate: 1 mL/min; temperature, 25°; detection, UV 250 nm

Compound	**Molecular Formula**	**Enantiomeric Excess (ee)**	**Purity**	**Impurity Tracings**
(*R*)-1	$C_{17}H_{19}ClN_3O_2S$	80.2%	90.1%	9.9%
(*S*)-1	$C_{17}H_{19}ClN_3O_2S$	87.4%	93.7%	6.3%
(*R*)-2	$C_{18}H_{22}ClN_3O_2S$	91.1%	95.6%	4.4%
(*S*)-2	$C_{18}H_{22}ClN_3O_2S$	93.0%	96.5%	3.5%
(*R*)-11	$C_{25}H_{25}ClN_4O_2S$	98.8%	99.4%	0.6%
(*S*)-11	$C_{25}H_{25}ClN_4O_2S$	96.8%	98.4%	1.6%

Enantiomeric purity determination of **(*R*)-1**:

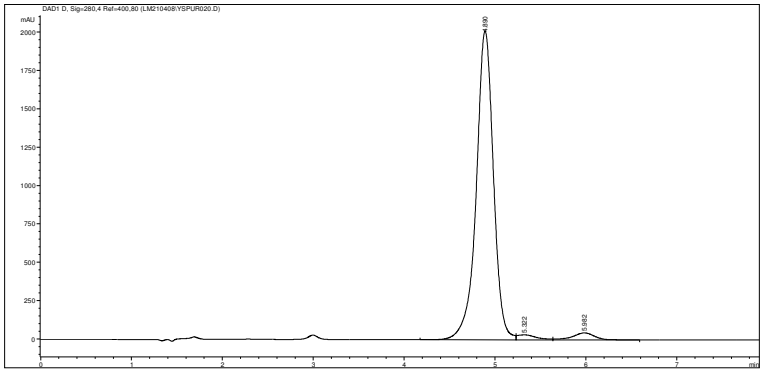

Enantiomeric purity determination of **(*S*)-1**:

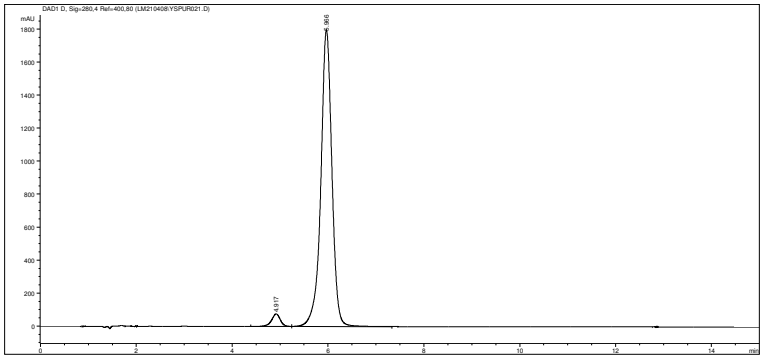

Enantiomeric purity determination of (***R***)**-2**:

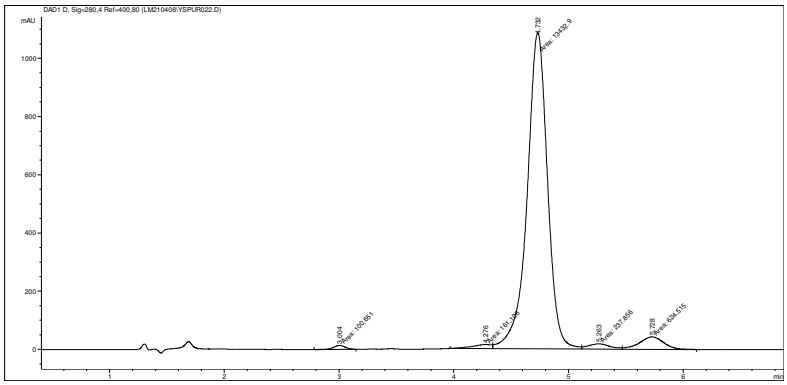

Enantiomeric purity determination of (***S***)**-2**:

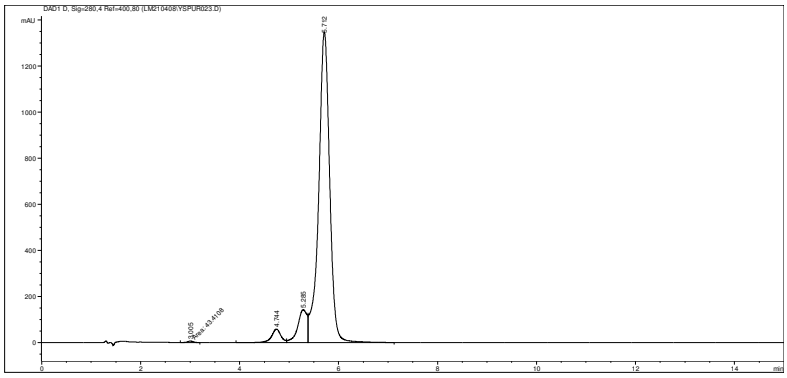

Enantiomeric purity determination of (***R***)**-11**:

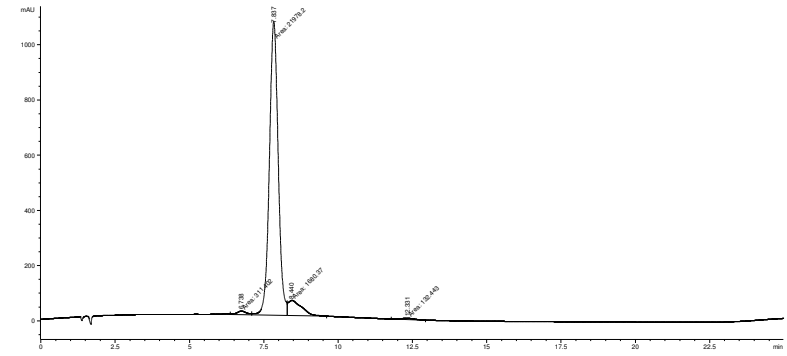

Enantiomeric purity determination of (***S***)**-11**:

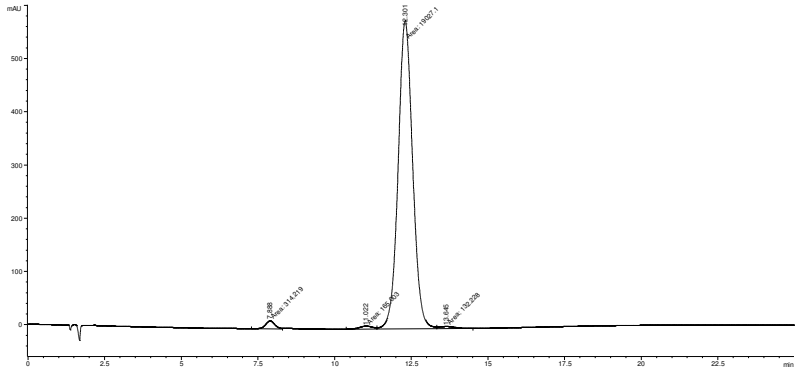

Docking

Docking was performed using GOLD 4.0 software [3]. Crystal structure of PPARα ligand binding domain, co-crystallized with agonist AZ 242 (PDB code 1I7G) [4] was prepared in a way described in the experimental section. GOLD configuration file is given below. Docking experiments were performed with compounds (*R*)-1, (*S*)-1, (*R*)-11 and (*S*)-11. Ten binding modes per compound were proposed by the GOLD software and were inspected manually. None of the binding modes of compound (*S*)-1 and (*S*)-11 was exhibiting the H-bond pattern typical for potent PPARα agonists, namely simultaneous interaction with Ser280, Tyr314, His440 and Tyr464. In contrary, the proposed binding modes of compounds (*R*)-1 and (*R*)-11 exhibited the mentioned interaction pattern.

GOLD CONFIGURATION FILE with

generated by gold front end (GOLD v4.0)

POPULATION
popsiz = 100
select_pressure = 1.1
n_islands = 5
maxops = 100000
niche_siz = 2

GENETIC OPERATORS
pt_crosswt = 95
allele_mutatewt = 95
migratewt = 10

FLOOD FILL
radius = 10
origin = 0 0 0
do_cavity = 1
floodfill_atom_no = 0
cavity_file = AZ2.mol2

floodfill_center = cavity_from_ligand

DATA FILES

protein_datafile = 1I7G.mol2

ligand_data_file compound1_r.MOL 10

ligand_data_file compound1_s.MOL 10

ligand_data_file compound11_r.MOL 10

ligand_data_file compound11_s.MOL 10

param_file = DEFAULT

set_ligand_atom_types = 0

set_protein_atom_types = 1

directory = .

tordist_file = DEFAULT

make_subdirs = 0

save_lone_pairs = 1

fit_points_file = fit_pts.mol2

read_fitpts = 0

FLAGS

display = 0

internal_ligand_h_bonds = 0

n_ligand_bumps = 0

flip_free_corners = 0

flip_amide_bonds = 0

flip_planar_n = 1 flip_ring_NRR flip_ring_NHR

flip_pyramidal_n = 0

rotate_carboxylic_oh = flip

use_tordist = 1

TERMINATION

early_termination = 0

n_top_solutions = 3

rms_tolerance = 1.5

CONSTRAINTS

force_constraints = 0

COVALENT BONDING

covalent = 0

SAVE OPTIONS

save_score_in_file = 1

save_protein_torsions = 1

concatenated_output = /home/eugen/Modelling/HZ64/HZ56_gold_solutions_GoldScore.sdf

clean_up_option delete_all_solutions

clean_up_option delete_rank_file

clean_up_option delete_all_log_files

clean_up_option delete_redundant_log_files

clean_up_option delete_empty_directories

output_file_format = MACCS

FITNESS FUNCTION SETTINGS

initial_virtual_pt_match_max = 2.5

relative_ligand_energy = 0

score_param_file = DEFAULT

start_vdw_linear_cutoff = 2.5

References:

[1] G. d'Atri, P. Gomarasca, G. Resnati, G. Tronconi, C. Scolastico, C. R. Sirtori, J Med Chem 1984, 27, 1621.

[2] O. Rau, Y. Syha, H. Zettl, M. Kock, A. Bock, M. Schubert-Zsilavecz, Arch Pharm (Weinheim) 2008, 341, 191.

[3] M. L. Verdonk, J. C. Cole, M. J. Hartshorn, C. W. Murray, R. D. Taylor, *Proteins* 2003, 52, 609.

[4] P. Cronet, J. F. Petersen, R. Folmer, N. Blomberg, K. Sjoblom, U. Karlsson, E. L. Lindstedt, K. Bamberg, *Structure* 2001, 9, 699.

Bioorganic & Medicinal Chemistry Letters 19 (2009) 4421–4426

Contents lists available at ScienceDirect

Bioorganic & Medicinal Chemistry Letters

journal homepage: www.elsevier.com/locate/bmcl

Discovery of a novel class of 2-mercaptohexanoic acid derivatives as highly active PPARα agonists

Heiko Zettl [a], Ramona Steri [a], Michael Lämmerhofer [b], Manfred Schubert-Zsilavecz [a,*]

[a] Goethe-University Frankfurt, Institute of Pharmaceutical Chemistry/ZAFES/LiFF, Max-von-Laue-Str. 9, D-60348 Frankfurt/M., Germany
[b] University of Vienna, Department for Analytical Chemistry and Food Chemistry, Währinger Str. 38, A-1090 Vienna, Austria

ARTICLE INFO

Article history:
Received 17 April 2009
Revised 13 May 2009
Accepted 14 May 2009
Available online 18 May 2009

Keywords:
PPAR
2-Mercaptohexanoic acid
SAR
PPARα agonists

ABSTRACT

A novel and robust scaffold for highly active PPARα agonists based on the 2-mercaptohexanoic acid substructure is presented. Systematic structural variation of the substitution pattern of the phenolic backbone yielded detailed SAR especially of *ortho* and *meta* substituents. We corroborated the importance of the sulfur atom as well as of the *n*-butyl chain for PPARα activity in the 2-mercaptohexanoic acid head group by preparation of carbon analogs and α-unsubstituted derivatives. Compound **10** represents a low nano molar active PPARα activator with excellent selectivity towards PPARγ.

The peroxisome proliferator-activated receptors (PPARs) are among today's most prominent targets for antidiabetic and antilipidemic drugs. Activation of different PPAR subtypes (α, β, γ) leads to elevated expression of apolipoproteins and cellular glucose transporters, resulting in enhanced clearance of lipids and glucose from the blood. PPARα-selective fibrates are well established drugs for the treatment of dyslipidemias, whereas PPARγ-selective glitazones have been proven as valuable drugs for the treatment of type 2 diabetes.[1]

PPARα is mainly expressed in tissues with a high rate of fatty acid catabolism such as liver and skeletal muscle. Its activation by fibrates has been proven to be efficient in lowering triglyceride levels accompanied by a moderate elevation of HDL–cholesterol. The clinical benefits are nevertheless limited, as several large clinical trials failed to show a reduction in cardiovascular mortality.[2,3] In respect to their pharmacological profiles, these drugs have some significant detrimental properties: Exhibiting EC_{50} values in the micro molar range, they are neither very potent PPARα agonists nor highly selective versus other PPAR subtypes.[1] Thus, the question remains if highly active and selective PPARα agonists would provide better clinical prospects.[4] State-of-the-art compounds, such as the recently reported 1,3-dioxane-2-carboxylic acid derivative NS220, display nano molar PPARα activity in vitro and very promising hypolipidemic properties in mice models.[5]

Synthetic PPAR agonists commonly share a general structure mimicking those of fatty acids, which serve as endogenous ligands.[6] In general, the structural features include an acidic head group combined with a large lipophilic backbone. Subtype selectivity may be influenced by two means: either by the introduction of a lipophilic α-substituent or by varying size and branching of the backbone of the molecule (Fig. 1).[7]

In previous studies, we used pirinixic acid (WY14,643; **1**) as a scaffold for structural optimization. By introducing alkyl chains in α-position of the carboxylic acid we achieved an enhanced activity for both PPARα and PPARγ and identified an optimal chain length of 4–6 carbons, represented by *n*-butyl-substituted derivative **2**.[8]

For this study, we replaced the central pyrimidine ring of **2** by benzene and the amine linker by a larger propane-1,3-diol moiety. We maintained the 2-mercaptohexanoic acid substructure as the acidic head group for the first series (Fig. 2), and systematically varied the cyclic tail of the molecule in order to evaluate the SAR of various alkyl and alkoxy substituents in *ortho* and *meta* positions. The 2,3-dimethylphenyl-moiety has been retained in the second series (Fig. 3) to evaluate the influence of the α-*n*-butyl-chain (by preparing the α-unsubstituted analogs) and of the sulfur (by replacement with a methylene group).

The 2-mercaptohexanoic acid derivatives **6**–**21** were synthesized starting with 4-mercaptophenol and ethyl 2-bromohexanoate as shown in Scheme 1. Ethyl 2-bromoacetate was used as the ester component for the preparation of **21**. Nucleophilic substitution with the α-bromoester first yielded the thioether derivatives **3a** and **3b**.[9] Two equal synthetic pathways could then be used to

* Corresponding author. Tel.: +49 69 79829339; fax: +49 69 79829332.
E-mail address: Schubert-zsilavecz@pharmchem.uni-frankfurt.de (M. Schubert-Zsilavecz).

0960-894X/$ - see front matter © 2009 Elsevier Ltd. All rights reserved.
doi:10.1016/j.bmcl.2009.05.057

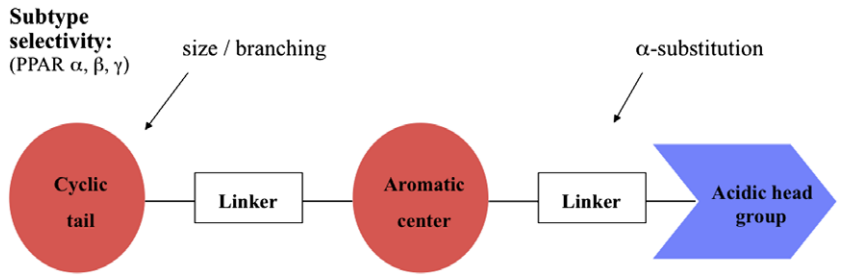

Figure 1. General structure of synthetic PPAR agonists.

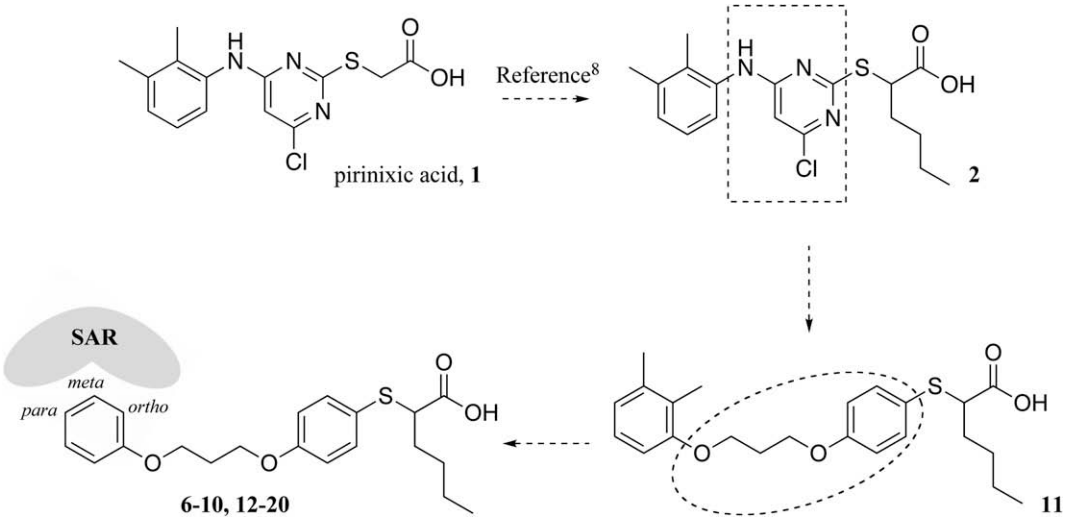

Figure 2. Structural development of presented compounds according to previous studies.[8,15]

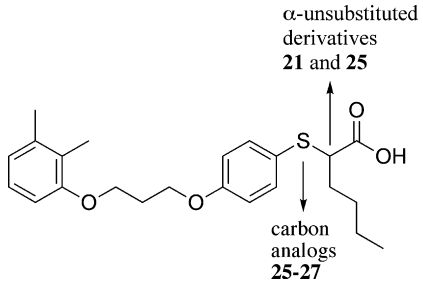

Figure 3. SAR-investigation of the 2-mercaptohexanoic acid head group based on compound **11**.

introduce the propylene spacer via a *Williamson*-like ether synthesis with 3-bromopropan-1-ol (step b): either by direct coupling to **3a** to yield **4** or by reaction with the commercially available phenol derivatives to yield the precursors **5a**–**5e**. Subsequent arrangement of the second ether function was achieved by a *Mitsunobu* reaction (**6a**–**21a**).[10,11] Finally, hydrolysis with lithium hydroxide gave the desired carboxylic acids **6**–**21**.

The carbon analogs of **11** were prepared starting with the conversion of ethyl 2-bromohexanoate into its phosphonate derivative **22** by an *Arbuzov* reaction (Scheme 2).[12] This was coupled via a *Wittig–Horner* reaction to the aldehyde group of the precursor **24**, which was synthesized based on 4-hydroxybenzaldehyde.[13] The resulting ester **26a** could be directly hydrolyzed to yield **26** or

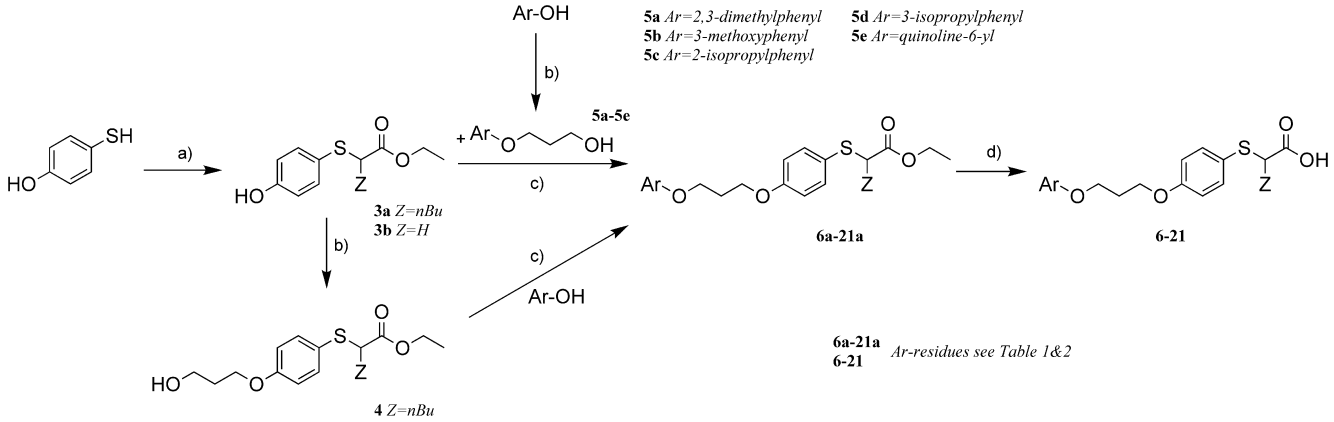

Scheme 1. Reagents and conditions: (a) ethyl-2-bromoacetate ($Z = H$) or ethyl-2-bromohexanoate ($Z = nBu$), Et_3N, $CHCl_3$, reflux, 1 h; (b) 3-bromopropanol, K_2CO_3, ACN, reflux, 24-48 h; (c) DEAD or ADDP, TPP, THF, rt, 4–48 h; (d) LiOH, MeOH, H_2O, 40 °C, 2 h.

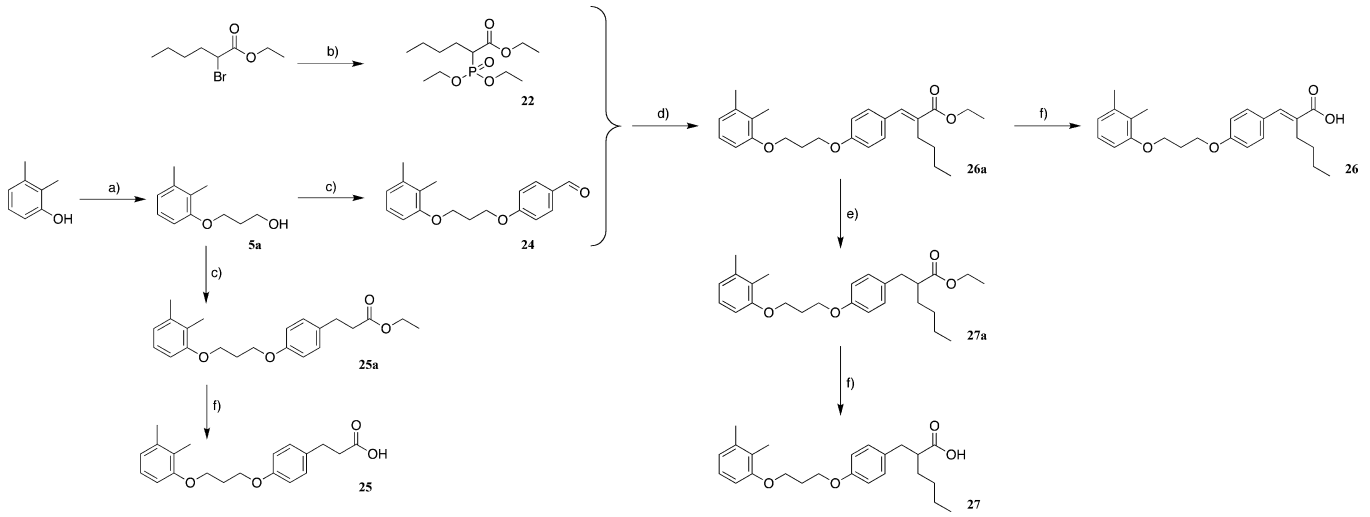

Scheme 2. Reagents and conditions: (a) 3-bromopropanol, K_2CO_3, ACN, reflux, 24 h; (b) triethylphosphite, reflux, overnight; (c) 4-hydroxybenzaldehyde or ethyl 3-(4-hydroxyphenyl)propanoate, DEAD, TPP, THF, rt, 4 h; (d) NaH, THF, rt, 24 h; (e) Pd/C, H_2, EtOH, rt, 24 h; (f) LiOH, MeOH, H_2O, reflux, 8–20 h.

hydrogenated and afterwards hydrolyzed to yield **27**. Only two steps (*Mitsunobu* condensation and hydrolysis) were needed for the preparation of the α-unsubstituted carbon analog **25** as the precursor molecule ethyl 3-(4-hydroxyphenyl)propanoate was commercially available.

The final compounds were tested in vitro for PPAR transactivation (EC_{50} values are given in Tables 1 and 2).[14] The structural reference used as the starting point was the phenyl-unsubstituted 2-(4-(3-phenoxypropoxy)-phenylthio)hexanoic acid **6** (Table 1). This compound itself is already a nano molar active PPARα-agonist with an EC_{50} of 0.29 μM and a ninefold selectivity versus PPARγ. This compound and all other 2-mercaptohexanoic acid derivatives presented are PPARβ-inactive. The *ortho*(**7**)-, *meta*(**8**)- and *para*(**9**)-methyl analogs were prepared based on **6**. SAR revealed a significant improvement for the *meta* and *para*-methyl substituted compounds shifting EC_{50} values to the double-digit nanomolar range (PPARα **8**: EC_{50} 0.09 μM, **9**: EC_{50} 0.085 μM), whereas no improvement could be observed for the *ortho*-methyl derivative. Comparison of the selectivity profile of *meta* and *para*-methyl derivatives (PPARγ **8**: EC_{50} 3.1 μM, **9**: EC_{50} 0.93 μM) revealed that *meta*-methyl substitution was able to selectively enhance PPARα activity whereas *para*-methyl substitution enhanced PPARα and PPARγ activity equally.

Two vicinal methyl groups were introduced next, yielding the 3,4-dimethyl (**10**) and 2,3-dimethyl (**11**) derivatives. Both compounds were able to further enhance PPARα activity compared with the mono methyl-substituted analogs. As indicated by the activity of the *meta* and *para*-methyl analogs, the combination 3,4-dimethyl represents the most active racemic compound within this series (PPARα **10**: EC_{50} 0.021 μM). It was noted with interest that the 2,3-dimethyl moiety also showed significant improvement of PPARα activity (EC_{50} 0.056 μM). In regard to PPARγ, selectivity increased by the introduction of two methyl groups from factor nine for unsubstituted phenyl (**6**) to factor 54 for compound **11**. According to previous studies,[8] this substructure is of particular interest (see Fig. 2). We thus maintained **11** as a scaffold for the investigation of the stereochemistry (**(*R*)-11** and **(*S*)-11**) as well as for the SAR of the acidic head group of our series (**21** and **25–27**).

Bridging of the 2,3-dimethyl substructure of **11** yielded the tetrahydronaphthyl derivative **12**, which showed a slight decrease in PPARα activity compared to **11**. We decided to further elucidate SAR of the *ortho* and *meta* position by introducing larger substituents based on the various methyl analogs. We thus prepared methoxy and isopropyl *ortho* and *meta* analogs. Both *ortho*-substituted compounds (**13** and **15**) showed decreased PPARα activity. The most significant loss was observed for the largest substituent (**15**; isopropyl). *meta*-Methoxy substituted **14** was able to further enhance PPARα activity (EC_{50} 0.049 μM) compared to *meta*-methyl substituted **8** whereas the *meta*-isopropyl substitution (**16**) did not cause any further improvement.

As the *meta*-substitution turned out to be the most eligible tool to selectively improve PPARα activity, we replaced the methyl group of **8** by a trifluoromethyl to yield compound **17**. This modification was the most successful structural modification of the *meta*-position with a PPARα EC_{50} of 0.025 μM and excellent selectivity towards PPARγ (EC_{50} 4.6 μM). It was noted with interest that the additional *para*-chloro substituent of **18** decreased both PPARα and PPARγ activity.

Compounds **19** and **20** represent a larger structural modification and could be described as PPARα-preferential dual PPARα/γ agonists. Biphenyl-substituted **19** is the most potent synthesized compound in regard to PPARγ (EC_{50} 0.54 μM) with an approx. fivefold remaining selectivity for PPARα. Compound **20**, which bears a quinoline-6-yl moiety, shows a very promising PPARγ modulating profile (EC_{50} 1.3 μM, maximal relative activation of 49%) combined with a sixfold selectivity for PPARα.

We recently showed the impact of the stereocentre in α-position of α-*n*-hexyl substituted pirinixic acid derivatives on PPAR activity emphasized by in silico studies.[15] Encouraged by these results and by examples found in literature,[16] we separated **11** by enantio-selective preparative HPLC into its distinct enantiomers.[15,17,18] In vitro data of **(*R*)-11** and **(*S*)-11** are in line with previous observations: **(*R*)-11** (PPARα EC_{50} 0.011 μM) displays superior biological activity and was shown to be approx. five times more potent than the racemic mixture and approx. 140 times more potent than the (*S*)-enantiomer. **(*R*)-11** is the most potent PPARα activator in this series with the highest selectivity versus PPARγ.

We again chose the 2,3-dimethyl substitution pattern of compound **11** for the investigation of the SAR (Table 2) of the linker between the acidic head group and the central aromatic ring (Fig. 1). We first prepared the α-unsubstituted analog **21**. This modification led to an attenuation of PPARα selectivity compared to **11**; nevertheless, it showed an interesting PPAR-*pan*-agonistic profile with a slight preference for PPARα. Obviously, PPARβ activity was gained by removal of the α-substitution. Finally, the sulfur atom was re-

Table 1
In vitro transactivation activities for compounds **6**–**20** on human PPARs

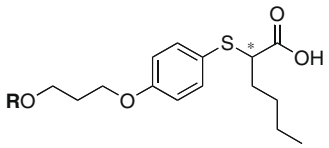

Compound	R	Transactivation EC_{50} (μM) ± SD (% activation compared to control)		
		PPARα	PPARβ	PPARγ
6		**0.29**$^{\pm 0.04}$ (76%)	ia	**2.6**$^{\pm 0.35}$ (83%)
7	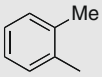	**0.25**$^{\pm 0.05}$ (64%)	ia	**2.3**$^{\pm 0.5}$ (114%)
8	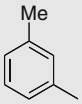	**0.09**$^{\pm 0.02}$ (80%)	ia	**3.0**$^{\pm 0.41}$ (96%)
9	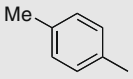	**0.085**$^{\pm 0.03}$ (91%)	(31% at 10 μM)	**0.93**$^{\pm 0.12}$ (87%)
10	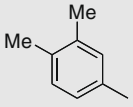	**0.021**$^{\pm 0.01}$ (72%)	ia	**3.5**$^{\pm 0.1}$ (61%)
11	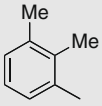	**0.056**$^{\pm 0.019}$ (113%)	ia	**3.0**$^{\pm 0.22}$ (82%)
(***R***)-**11**		**0.011**$^{\pm 0.004}$ (115%)	ia	**3.9**$^{\pm 0.83}$ (125%)
(***S***)-**11**		**1.7**$^{\pm 0.18}$ (94%)	ia	**9.9**$^{\pm 1.44}$ (77%)
12	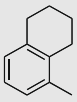	**0.19**$^{\pm 0.04}$ (101%)	ia	**8.1**$^{\pm 0.5}$ (107%)
13	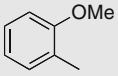	**0.55**$^{\pm 0.03}$ (92%)	ia	**1.6**$^{\pm 0.41}$ (85%)
14	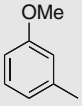	**0.049**$^{\pm 0.02}$ (85%)	ia	**1.2**$^{\pm 0.16}$ (85%)
15	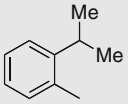	**2.0**$^{\pm 0.43}$ (89%)	ia	**4.1**$^{\pm 0.32}$ (92%)
16	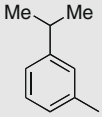	**0.15**$^{\pm 0.02}$ (98%)	ia	**5.3**$^{\pm 0.3}$ (91%)
17	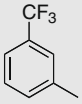	**0.025**$^{\pm 0.02}$ (75%)	ia	**4.6**$^{\pm 0.19}$ (68%)

Table 1 (*continued*)

Compound	R	Transactivation EC_{50} (μM) ± SD (% activation compared to control)		
		PPARα	PPARβ	PPARγ
18	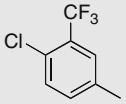	**0.39**$^{\pm 0.02}$ (65%)	ia	**7.8**$^{\pm 0.4}$ (96%)
19	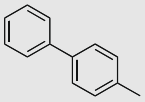	**0.11**$^{\pm 0.01}$ (125%)	ia	**0.54**$^{\pm 0.06}$ (108%)
20	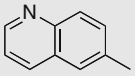	**0.22**$^{\pm 0.04}$ (95%)	ia	**1.3**$^{\pm 0.9}$ (49%)

EC_{50}/SD values were calculated using SigmaPlot2001 based on the mean values of at least three determinations. Values in brackets give the relative activation compared to the positive control. Positive controls were GW7647 for PPARα, pioglitazone for PPARγ and L165,041 for PPARβ, each at 1 μM; ia: inactive at 10 μM. Rand X are typed in bold as these entities display the varied substructure of the respective scaffold.

Table 2
In vitro transactivation activities for compounds **21** and **25**–**27** on human PPARs

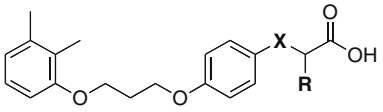

Compound	X	R	Transactivation EC_{50} (μM) ± SD (% activation compared to control)		
			PPARα	PPARβ	PPARγ
21	–S–	H	**0.60**$^{\pm 0.12}$ (81%)	**1.4**$^{\pm 0.38}$ (52%)	**3.8**$^{\pm 0.34}$ (77%)
25	$-CH_2-$	H	**13.8**$^{\pm 3.4}$ (63%)	**11.2**$^{\pm 0.45}$ (72%)	**15.7**$^{\pm 0.77}$ (54%)
26	–CH=	*n*-Bu	ia	ia	ia
27	$-CH_2-$	*n*-Bu	**1.5**$^{\pm 0.25}$ (73%)	ia	**4.2**$^{\pm 0.53}$ (120%)

EC_{50}/SD values were calculated using SigmaPlot2001 based on the mean values of at least three determinations. Values in brackets give the relative activation compared to the positive control. Positive controls were GW7647 for PPARα, pioglitazone for PPARγ and L165,041 for PPARβ, each at 1 μM; ia: inactive at 10 μM. Rand X are typed in bold as these entities display the varied substructure of the respective scaffold.

placed by a methylene group and the α-unsubstituted (**25**) as well as the α-*n*-butyl-substituted (**27**) analog was synthesized. Methin-analog **26** was obtained during synthesis. Interestingly, rigidization by the additional exocyclic double bond caused a complete loss of PPAR activity. Methylene analog **25** revealed an attenuated activity for all PPAR subtypes compared to **21**, whereas for *n*-butyl-substituted **27** an impressive loss could be observed only for PPARα activity. Regarding the 2-mercaptohexanoic acid substructure, these findings suggest a strong impact of the sulfur atom as well as of the α-*n*-butyl chain for PPARα but not for PPARγ activity.

In summary, we successfully established a novel and robust scaffold for highly active PPARα agonists based on the 2-mercaptohexanoic acid substructure. By systematic structural variation, we were able to cover a broad selectivity profile from PPARα-preferential dual PPARα/γ agonists to selective and nano molar active PPARα agonists. By preparation of carbon analogs and α-unsubstituted derivatives, we corroborated the importance of the sulfur atom as well as of the *n*-butyl chain of our 2-mercaptohexanoic acid head group for PPAR activity. Regarding the phenolic backbone of our scaffold, SAR revealed that especially substituents in *meta*-position (e.g., –Me, $-CF_3$, –OMe) were able to selectively improve PPARα activity. Encouraged by these promising in vitro results, we are planning further profiling of an eligible candidate in vivo in the near future.

Acknowledgement

We gratefully acknowledge financial support from the Else-Kroener-Fresenius-Stiftung (FIRST).

Supplementary data

Supplementary data (detailed synthetic procedure and analytical characterization of the compounds) associated with this article can be found, in the online version, at doi:10.1016/j.bmcl.2009.05.057.

References and notes

1. Rau, O.; Zettl, H.; Popescu, L.; Steinhilber, D.; Schubert-Zsilavecz, M. *ChemMedChem* **2008**, *3*, 206.
2. Keech, A.; Simes, R.; Barter, P.; Best, J.; Scott, R.; Taskinen, M.; Forder, P.; Pillai, A.; Davis, T.; Glasziou, P.; Drury, P.; Kesaniemi, Y.; Sullivan, D.; Hunt, D.; Colman, P.; d'Emden, M.; Whiting, M.; Ehnholm, C.; Laakso, M. *Lancet* **2005**, *366*, 1849.
3. *Circulation* **2000**, *102*, 21.
4. Staels, B.; Maes, M.; Zambon, A. *Nat. Clin. Pract. Cardiovasc. Med.* **2008**, *5*, 542.
5. Asaki, T.; Aoki, T.; Hamamoto, T.; Sugiyama, Y.; Ohmachi, S.; Kuwabara, K.; Murakami, K.; Todo, M. *Bioorg. Med. Chem.* **2008**, *16*, 981.
6. Kuhn, B.; Hilpert, H.; Benz, J.; Binggeli, A.; Grether, U.; Humm, R.; Marki, H.; Meyer, M.; Mohr, P. *Bioorg. Med. Chem. Lett.* **2006**, *16*, 4016.
7. Feldman, P. L.; Lambert, M. H.; Henke, B. R. *Curr. Top. Med. Chem.* **2008**, *8*, 728.
8. Rau, O.; Syha, Y.; Zettl, H.; Kock, M.; Bock, A.; Schubert-Zsilavecz, M. *Arch. Pharm. (Weinheim)* **2008**, *341*, 191.
9. Aranapakam, V.; Grosu, G. T.; Davis, J. M.; Hu, B.; Ellingboe, J.; Baker, J. L.; Skotnicki, J. S.; Zask, A.; DiJoseph, J. F.; Sung, A.; Sharr, M. A.; Killar, L. M.; Walter, T.; Jin, G.; Cowling, R. *J. Med. Chem.* **2003**, *46*, 2361.
10. Humphries, P. S.; Almaden, J. V.; Barnum, S. J.; Carlson, T. J.; Do, Q. Q.; Fraser, J. D.; Hess, M.; Kim, Y. H.; Ogilvie, K. M.; Sun, S. *Bioorg. Med. Chem. Lett.* **2006**, *16*, 6116.
11. Humphries, P. S.; Do, Q. Q.; Wilhite, D. M. *Beilstein J. Org. Chem.* **2006**, *2*, 21.
12. Bargiggia, F.; Piva, O. *Tetrahedron: Asymmetry* **2003**, *14*, 1819.
13. Usui, S.; Fujieda, H.; Suzuki, T.; Yoshida, N.; Nakagawa, H.; Ogura, M.; Makishima, M.; Miyata, N. *Chem. Pharm. Bull. (Tokyo)* **2007**, *55*, 1053.
14. Cell culture, transfection and Gal4-transactivation-assay: Cos7 cells were grown in DMEM, supplemented with FCS, sodium pyruvate and penicillin/

streptomycine at 37 °C and 5% CO_2. The day before transfection, cells were seeded in 96-well plates in a density of 30,000 cells/well. Transfection was carried out by Lipofectamine™ 2000 reagent (Invitrogen) according to the manufacturer's protocol with pFR-Luc (Stratagene), pRL-SV40 (Promega) and the Gal4-fusion receptor plasmids (pFA-CMV-hPPAR-LBD) of the respective subtype. 5 h after transfection, medium was changed to DMEM without FCS, containing 0.1% DMSO and the respective concentrations of the test compounds. Following overnight incubation with the test compounds, cells were assayed for reportergene activity using Dual-Glo™ Luciferase Assay System (Promega) according to the manufacturer's protocol. Luminescence was measured with a GENios Pro luminometer (Tecan).

Each concentration of the compounds was tested in triplicate wells and each experiment was repeated independently at least three times.

15. Zettl, H.; Dittrich, M.; Steri, R.; Proschak, E.; Rau, O.; Steinhilber, D.; Schneider, G.; Lämmerhofer, M.; Schubert-Zsilavecz, M. *QSAR Combinatorial Sci.* **2009**, *28*, 576.
16. Pinelli, A.; Godio, C.; Laghezza, A.; Mitro, N.; Fracchiolla, G.; Tortorella, V.; Lavecchia, A.; Novellino, E.; Fruchart, J. C.; Staels, B.; Crestani, M.; Loiodice, F. *J. Med. Chem.* **2005**, *48*, 5509.
17. Mandl, A.; Nicoletti, L.; Lammerhofer, M.; Lindner, W. *J. Chromatogr., A* **1999**, *858*, 1.
18. Lämmerhofer, M.; Pell, R.; Richter, M.; Schiesel, S.; Mahut, M.; Zettl, H.; Dittrich, M.; Schubert-Zsilavecz, M.; Lindner, W. *Chirality*, in preparation.

Supporting information

Discovery of a novel class of 2-mercaptohexanoic acid derivatives as highly active PPARα agonists

Heiko Zettl, Ramona Steri, Michael Lämmerhofer, and Manfred Schubert-Zsilavecz

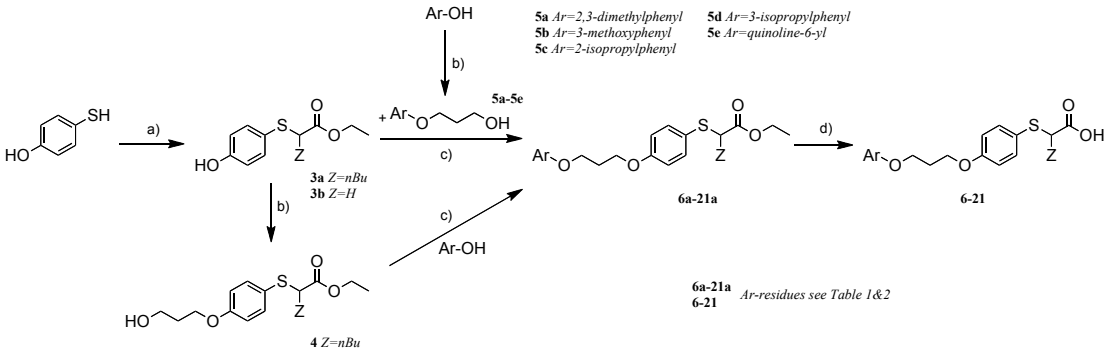

Scheme 1: Synthesis of compounds **6-21**
Reagents and conditions: a) ethyl-2-bromoacetate (*Z=H*) or ethyl-2-bromohexanoate (*Z=nBu*), Et_3N, $CHCl_3$, reflux, 1h; b) 3-bromopropanol, K_2CO_3, ACN, reflux, 24-48h; c) DEAD or ADDP, TPP, THF, rt, 4-48h; d) LiOH, MeOH, H_2O, 40°C, 2h.

ethyl 2-(4-hydroxyphenylthio)hexanoate **3a**
Commercially available 4-hydroxy thiophenol (1 equiv.), 2-bromoethyl hexanoate (1 equiv.) and triethyl amine (1.5 equiv.) were refluxed in $CHCl_3$ for 1h. The solvent was removed and the residue was purified by column chromatography (*n*-hexane/ethyl acetate 5:1).
^{1}H NMR (300.13 MHz, $(CD_3)_2SO$): δ 0.83 (t, 3H, Bu-C*H*$_3$, J=6.9Hz); 1.08 (t, 3H, -C*H*$_3$, J=7.0Hz); 1.23-1.35 (m, 4H, Bu-C*H*$_2$); 1.56-1.66 (m, 2H, Bu-C*H*$_2$); 3.48 (t, 1H, SC*H*, J=8.1Hz); 4.02 (t, 2H, OC*H*$_2$, J=7.2Hz); 6.72 (dd, 2H, Ph-3*H* + -5*H*, J_1=1.8Hz, J_2=8.4Hz); 7.24 (dd, 2H, Ph-2*H* + -6*H*, J_1=2.7Hz, J_2=11.4Hz); 9.75 (s, 1H, -O*H*). MS (ESI-): *m/e* = 266.9 (M-1). yield 90%.

ethyl 2-(4-(3-hydroxypropoxy)phenylthio)hexanoate **4**
A solution of **3a** (1 equiv.), 3-bromopropanol (1.5 equiv.) and K_2CO_3 (2 equiv.) in ACN was refluxed for 48h. After filtration, the solvent was removed and the residue was purified by column chromatography (*n*-hexane/ethyl acetate 5:1).
^{1}H NMR (300.13 MHz, $(CD_3)_2SO$): δ 0.82 (t, 3H, Bu-C*H*$_3$, J=6.9Hz); 1.08 (t, 3H, -C*H*$_3$, J=7.1Hz); 1.23-1.30 (m, 4H, Bu-C*H*$_2$); 1.57-1.67 (m, 2H, Bu-C*H*$_2$); 1.84 (quint, 2H, -C*H*$_2$-, J=6.3Hz); 3.54 (t, 1H, SC*H*, J=6.6Hz); 3.97-4.04 (m, 4H, Ph-OC*H*$_2$+C*H*$_2$-OH); 6.90 (d, 2H, Ph-3*H* + -5*H*, J=9.9Hz); 7.33 (d, 2H, Ph-2*H* + -6*H*, J=9.9Hz). MS (ESI-): *m/e* = 325.1 (M-1). yield 81.7%.

3-(2,3-dimethylphenoxy)propan-1-ol **5a**
A solution of 2,3-dimethylphenol (1 equiv.), 3-bromopropanol (1.2 equiv.) and K_2CO_3 (2 equiv.) in ACN was refluxed for 48h. After removal of the solvent, the residue was dissolved in ethyl acetate and washed with diluted hydrochloric acid, saturated $NaHCO_3$-solution and brine. Removal of the organic solvent yielded the crude product.
^{1}H NMR (300.13 MHz, $(CD_3)_2SO$): δ 1.86 (quint, 2H, -C*H*$_2$-, J=6.3Hz); 2.05 (s, 3H, Ph-2-C*H*$_3$); ; 2.19 (s, 3H, Ph-3-C*H*$_3$); 3.57 (q, 2H, C*H*$_2$-OH, J=5.7Hz); 3.98 (t, 2H, Ph-OC*H*$_2$, J=6.3Hz); 6.71-6.77 (t, 2H, Ph-4*H* + -6*H*); 7.00 (t, 1H, Ph-5*H*, J=7.8Hz). MS (ESI+): *m/e* = 180.8 $[M+H]^+$. yield 84%.

3-(3-methoxyphenoxy)propan-1-ol **5b**
prepared as **5a**
^{1}H NMR (300.13 MHz, $(CD_3)_2SO$): δ 1.83 (quint, 2H, -C*H*$_2$-, J=6.2Hz); 3.53 (q, 2H, C*H*$_2$-OH, J=6.0Hz); 3.71 (s, 3H, Ph-OC*H*$_3$); 3.97 (t, 2H, Ph-OC*H*$_2$, J=6.4Hz); 6.45-6.50 (m, 3H, Ph-2*H* + -4*H* + -6*H*); 7.15 (t, 1H, Ph-5*H*, J=8.1Hz). MS (ESI+): *m/e* = 180.9 $[M+H]^+$. yield 89%.

3-(2-isopropylphenoxy)propan-1-ol **5c**
prepared as **5a**
^{1}H NMR (300.13 MHz, $(CD_3)_2SO$): δ 1.14 (d, 6H, Isopr-C*H*$_3$, J=6.8Hz); 1.86 (quint, 2H, -C*H*$_2$-, J=6.2Hz); 3.17-3.27 (m, 1H, Isopr-C*H*); 3.56 (q, 2H, C*H*$_2$-OH, J=6.0Hz); 4.01 (t, 2H, Ph-OC*H*$_2$, J=6.2Hz); 6.83-6.91 (m, 2H, Ph-5*H* + -6*H*); 7.09-7.17 (m, 2H, Ph-3*H* + -4*H*). MS (ESI-): *m/e* = 193.8 (M-1). yield 81%.

3-(3-isopropylphenoxy)propan-1-ol **5d**
prepared as **5a**
^{1}H NMR (300.13 MHz, $(CD_3)_2SO$): δ 1.16 (d, 6H, Isopr-C*H*$_3$, J=7.2Hz); 1.83 (quint, 2H, -C*H*$_2$-, J=6.4Hz); 2.78-2.87 (m, 1H, Isopr-C*H*); 3.53 (q, 2H, C*H*$_2$-OH, J=6.0Hz); 3.99 (t, 2H, Ph-OC*H*$_2$, J=6.4Hz); 6.70-6.79 (m, 3H, Ph-2*H* + -5*H* + -6*H*); 7.16 (t, 1H, Ph-5*H*, J=7.7Hz). MS (ESI-): *m/e* = 193.7 (M-1). yield 77%.

3-(quinolin-6-yloxy)propan-1-ol **5e**
prepared as **5a**
^{1}H NMR (300.13 MHz, $(CD_3)_2SO$): δ 1.93 (quint, 2H, -C*H*$_2$-, J=6.3Hz); 3.59 (q, 2H, C*H*$_2$-OH, J=6.0Hz); 4.16 (t, 2H, Quin-OC*H*$_2$, J=6.3Hz); 4.18 (t, 1H, -O*H*, J=5.1Hz); 7.36-7.47 (m, 3H, Quin-*H*); 7.89 (d, 1H, Quin-8*H*, J=8.7Hz); 8.23 (d, 1H, Quin-4*H*, J=5.7Hz); 8.71 (d, 1H, Quin-2*H*, J=5.7Hz). MS (ESI+): *m/e* = 203.8 $[M+H]^+$.
yield 60%

ethyl 2-(4-(3-phenoxypropoxy)phenylthio)hexanoate **6a**
4 (1.1 equiv.), phenol (1 equiv.) and TPP (1.5 equiv.) were dissolved in abs. THF and a solution of DEAD (1.5 equiv.) in abs. THF was added. The solution was stirred 48h under Argon. After removal of the solvent, the residue was purified by column chromatography (*n*-hexane/ethyl acetate 10:1).
^{1}H NMR (300.13 MHz, $(CD_3)_2SO$): δ 0.82 (t, 3H, Bu-C*H*$_3$, J=6.9Hz); 1.06 (t, 3H, -C*H*$_3$, J=7.2Hz); 1.22-1.35 (m, 4H, Bu-C*H*$_2$); 1.57-1.70 (m, 2H, Bu-C*H*$_2$); 2.15 (quint, 2H, -C*H*$_2$-, J=6.0Hz); 3.55 (t, 1H, SC*H*, J=7.4Hz); 4.00 (q, 2H, OC*H*$_2$, J=7.2Hz); 4.11 (q, 4H, Ph-OC*H*$_2$, Ph'-OC*H*$_2$, J=6.3Hz); 6.88-6.95 (m, 5H, Ph-2*H* + -6*H*, Ph'-2*H* + -4*H* + -6*H*); 7.26 (t, 2H, Ph'-3*H* + -5*H*, J=7.7Hz); 7.34 (d, 2H, Ph-3*H* + -5*H*, J=8.4Hz). MS (ESI+): *m/e* = 403.3 $[M+H]^+$. yield 27%.

2-(4-(3-phenoxypropoxy)phenylthio)hexanoic acid **6**
6a was dissolved in MeOH and LiOH (10 equiv.) in H_2O (MeOH:H_2O=5:1) was added. The solution was stirred for 4h at 40°C. After removal of the solvent, the residue was dissolved in hot H_2O (if necessary, small amounts of MeOH were added) and the carboxylic acid was precipitated by adding diluted hydrochloric acid. The obtained residue was purified by by column chromatography (*n*-hexane/ethyl acetate 1:1).
^{1}H NMR (300.13 MHz, $(CD_3)_2SO$): δ 0.82 (t, 3H, Bu-C*H*$_3$, J=7.1Hz); 1.21-1.35 (m, 4H, Bu-C*H*$_2$); 1.51-1.68 (m, 2H, Bu-C*H*$_2$); 2.15 (quint, 2H, -C*H*$_2$-, J=6.1Hz); 3.47 (t, 1H, SC*H*, J=7.3Hz); 4.08-4.14 (m, 4H, Ph-OC*H*$_2$, Ph'-OC*H*$_2$); 6.88-6.94 (m, 5H, Ph-2*H* + -6*H*, Ph'-2*H* + -4*H* + -6*H*); 7.26 (t, 2H, Ph'-3*H* + -5*H*, J=8.0Hz); 7.35 (d, 2H, Ph-3*H* + -5*H*, J=8.6Hz). ^{13}C NMR (75.45 MHz, $(CD_3)_2SO$): δ 13.69 (Bu-*C*H$_3$); 21.69 (Bu-*C*H$_2$); 28.56 (Bu-*C*H$_2$); 28.69 (-*C*H$_2$-); 30.79 (Bu-*C*H$_2$); 50.84 (S*C*H); 63.99 (Ph-O*C*H$_2$); 64.38 (Ph'-O*C*H$_2$); 114.43 (2C, Ph'-C_2 + –C_6); 115.11 (2C, Ph-C_3 + –C_5); 120.53 (Ph'-C_4); 123.31 (Ph-C_1); 129.44 (2C, Ph'-C_3 + –

C_5); 135.13 (2C, Ph-C_2 + –C_6); 158.41 (Ph'-C_1); 158.67 (Ph-C_4); 172.91 (*C*OO). MS (ESI-): *m/e* = 373.1 (M-1).
Anal. ($C_{21}H_{26}O_4S$ [374.49]) C, H: calc C 67.35 H 7.00 found C 67.12 H 6.92. yield 70%.

ethyl 2-(4-(3-(*o*-tolyloxy)propoxy)phenylthio)hexanoate **7a**
prepared as **6a**, instead of DEAD ADDP was used.
^{1}H NMR (300.13 MHz, $(CD_3)_2SO$): δ 0.84 (t, 3H, Bu-C*H*$_3$, J=7.1Hz); 1.07 (t, 3H, -C*H*$_3$, J=7.2Hz); 1.24-1.40 (m, 4H, Bu-C*H*$_2$); 1.59-1.71 (m, 2H, Bu-C*H*$_2$); 2.14 (s, 3H, Ph'-C*H*$_3$); 2.18 (quint, 2H, -C*H*$_2$-, J=6.2Hz); 3.57 (t, 1H, SC*H*, J=7.5Hz); 4.01 (q, 2H, OC*H*$_2$, J=6.0Hz); 4.09-4.19 (m, 4H, Ph-OC*H*$_2$, Ph'-OC*H*$_2$); 6.80-6.97 (m, 4H, Ph-2*H* + -6*H*, Ph'-4*H* + -6*H*); 7.11-7.18 (m, 2H, Ph'-3*H* + -5*H*); 7.36 (d, 2H, Ph-3*H* + -5*H*, J=7.0Hz). MS (ESI+): *m/e* = 417.0 $[M+H]^+$. yield 80%.

2-(4-(3-(*o*-tolyloxy)propoxy)phenylthio)hexanoic acid **7**
prepared as **6**
^{1}H NMR (300.13 MHz, $(CD_3)_2SO$): δ 0.82 (t, 3H, Bu-C*H*$_3$, J=7.0Hz); 1.21-1.35 (m, 4H, Bu-C*H*$_2$); 1.54-1.68 (m, 2H, Bu-C*H*$_2$); 2.13 (s, 3H, Ph'-C*H*$_3$); 2.17 (quint, 2H, -C*H*$_2$-, J=6.3Hz); 3.47 (t, 1H, SC*H*, J=7.3Hz); 4.08-4.17 (m, 4H, Ph-OC*H*$_2$, Ph'-OC*H*$_2$); 6.81 (t, 1H, Ph'-5*H*, J=7.3Hz) 6.91-6.94 (m, 3H, Ph'-3*H* + 4*H* + -6*H*); 7.10 (d, 2H, Ph-2*H* + -6*H*, J=7.6Hz); 7.35 (d, 2H, Ph-3*H* + -5*H*, J=8.9Hz). ^{13}C NMR (75.45 MHz, $(CD_3)_2SO$): δ 13.69 (Bu-*C*H$_3$); 15.85 (Ph'-*C*H$_3$); 21.69 (Bu-*C*H$_2$); 28.68 (2C, Bu-*C*H$_2$, -*C*H$_2$-); 30.80 (Bu-*C*H$_2$); 50.85 (S*C*H); 64.07 (Ph-O*C*H$_2$); 64.46 (Ph'-O*C*H$_2$); 111.25 (Ph'-C_6); 115.08 (2C, Ph-C_3 + –C_5); 120.19 (Ph'-C_4); 123.31 (Ph-C_1); 125.72 (Ph'-C_5); 126.91 (Ph'-C_2); 130.33 (Ph'-C_3); 135.12 (2C, Ph-C_2 + –C_6); 156.45 (Ph'-C_1); 158.68 (Ph-C_4); 172.91 (*C*OOH). MS (ESI-): *m/e* = 387.1 (M-1).
Anal. ($C_{22}H_{28}O_4S$ [388.52]) C, H: calc C 68.01 H 7.26 found C 68.06 H 7.15. yield 59%.

ethyl 2-(4-(3-(*m*-tolyloxy)propoxy)phenylthio)hexanoate **8a**
prepared as **6a**
^{1}H NMR (300.13 MHz, $(CD_3)_2SO$): δ 0.84 (t, 3H, Bu-C*H*$_3$, J=7.1Hz); 1.08 (t, 3H, -C*H*$_3$, J=7.2Hz); 1.24-1.37 (m, 4H, Bu-C*H*$_2$); 1.57-1.71 (m, 2H, Bu-C*H*$_2$); 2.15 (quint, 2H, -C*H*$_2$-, J=6.3Hz); 2.26 (s, 3H, Ph'-C*H*$_3$); 3.57 (t, 1H, SC*H*, J=7.5Hz); 4.01 (q, 2H, OC*H*$_2$, J=7.2Hz); 4.07-4.15 (m, 4H, Ph-OC*H*$_2$, Ph'-OC*H*$_2$); 6.72-6.76 (m, 3H, Ph'-2*H* + -4*H* + -6*H*); 6.95 (d, 2H, Ph-2*H* + -6*H*, J=8.7Hz); 7.15 (t, 1H, Ph'-5*H*, J=7.8Hz); 7.35 (d, 2H, Ph-3*H* + -5*H*, J=8.7Hz). MS (ESI+): *m/e* = 417.1 $[M+H]^+$. yield 22%.

2-(4-(3-(*m*-tolyloxy)propoxy)phenylthio)hexanoic acid **8**
prepared as **6**
^{1}H NMR: (300.13 MHz, $(CD_3)_2SO$): δ 0.82 (t, 3H, Bu-C*H*$_3$, J=7.0Hz); 1.23-1.35 (m, 4H, Bu-C*H*$_2$); 1.54-1.68 (m, 2H, Bu-C*H*$_2$); 2.13 (quint, 2H, -C*H*$_2$-, J=6.3Hz); 2.15 (s, 3H, Ph'-C*H*$_3$); 3.47 (t, 1H, SC*H*, J=7.5Hz); 4.06-4.13 (m, 4H, Ph-OC*H*$_2$, Ph'-OC*H*$_2$); 6.71-6.75 (m, 3H, Ph'-2*H* + -4*H* + -6*H*); 6.92 (d, 2H, Ph-2*H* + -6*H*, J=8.8Hz); 7.13 (t, 1H, Ph'-5*H*, J=7.8Hz); 7.35 (d, 2H, Ph-3*H* + -5*H*, J=8.6Hz). ^{13}C NMR (75.45 MHz, $(CD_3)_2SO$): δ 13.69 (Bu-*C*H$_3$); 21.03 (Ph'-*C*H$_3$); 21.69 (Bu-*C*H$_2$); 28.58 (Bu-*C*H$_2$); 28.69 (-*C*H$_2$-); 30.78 (Bu-*C*H$_2$); 50.83 (S*C*H); 63.91 (Ph-O*C*H$_2$); 64.37 (Ph'-O*C*H$_2$); 111.45 (Ph'-C_6); 115.08 (Ph'-C_4); 115.10 (2C, Ph-C_3 + –C_5); 121.27 (Ph'-C_2); 123.29 (Ph-C_1); 129.16 (Ph'-C_5); 135.13 (2C, Ph-C_2 + –C_6); 138.93 (Ph'-C_3); 158.44 (Ph'-C_1); 158.67 (Ph-C_4); 172.90 (*C*OOH). MS (ESI+): *m/e* = 417.1 $[M+H]^+$.
Anal. ($C_{22}H_{28}O_4S$ [388.52]) C, H: calc C 68.01 H 7.26 found C 67.79 H 7.45.
yield 48%.

ethyl 2-(4-(3-(*p*-tolyloxy)propoxy)phenylthio)hexanoate **9a**
prepared as **6a**
^{1}H NMR (300.13 MHz, $(CD_3)_2SO$): δ 0.83 (t, 3H, Bu-C*H*$_3$, J=7.1Hz); 1.07 (t, 3H, -C*H*$_3$, J=7.1Hz); 1.23-1.39 (m, 4H, Bu-C*H*$_2$); 1.58-1.70 (m, 2H, Bu-C*H*$_2$); 2.13 (quint, 2H, -C*H*$_2$-, J=6.3Hz); 2.21 (s, 3H, Ph'-C*H*$_3$); 3.55 (t, 1H, SC*H*, J=7.2Hz); 3.99-4.13 (m, 6H, OC*H*$_2$, Ph-

OCH_2, Ph'-OCH_2); 6.81 (d, 2H, Ph'-2*H* + -6*H*, J=7.8Hz); 6.93 (d, 2H, Ph'-3*H* + -5*H*, J=8.7Hz); 7.06 (d, 2H, Ph-2H + -6*H*, J=8.4Hz); 7.34 (d, 2H, Ph-3*H* + -5*H*, J=8.7Hz). MS (ESI+): *m/e* = 417.2 $[M+H]^+$.

2-(4-(3-(*p*-tolyloxy)propoxy)phenylthio)hexanoic acid **9**
prepared as **6**
^{1}H NMR (300.13 MHz, $(CD_3)_2SO$): δ 0.82 (t, 3H, Bu-CH_3, J=7.0Hz); 1.21-1.35 (m, 4H, Bu-CH_2); 1.55-1.69 (m, 2H, Bu-CH_2); 2.13 (quint, 2H, -CH_2-, J=6.2Hz); 2.21 (s, 3H, Ph'-CH_3); 3.47 (t, 1H, SC*H*, J=7.2Hz); 3.98-4.13 (m, 6H, Ph-OCH_2, Ph'-OCH_2); 6.81 (d, 2H, Ph'-2*H* + -6*H*, J=8.7Hz); 6.92 (d, 2H, Ph'-3*H* + -5*H*, J=8.7Hz); 7.06 (d, 2H, Ph-2H + -6*H*, J=8.4Hz); 7.35 (d, 2H, Ph-3*H* + -5*H*, J=8.7Hz). ^{13}C NMR (75.45 MHz, $(CD_3)_2SO$): δ 13.69 (Bu-*C*H_3); 20.01 (Ph'-*C*H_3); 21.69 (Bu-*C*H_2); 28.60 (Bu-*C*H_2); 28.69 (-*C*H_2-); 30.80 (Bu-*C*H_2); 50.85 (S*C*H); 64.09 (Ph-O*C*H_2); 64.41 (Ph'-O*C*H_2); 114.31 (2C, Ph'-C_2+C_6); 115.11 (2C, Ph-C_3 + –C_5); 123.32 (Ph-C_1); 129.16 (Ph'-C_4); 129.76 (2C, Ph'-C_3 + -C_5); 135.12 (2C, Ph-C_2 + –C_6); 156.32 (Ph'-C_1); 158.68 (Ph-C_4); 172.89 (*C*OOH). MS (ESI-): *m/e* = 387.2 (M-1).
Anal. ($C_{22}H_{28}O_4S$ [388.52]) C, H: calc C 68.01 H 7.26 found C 67.85 H 7.37.

ethyl 2-(4-(3-(3,4-dimethylphenoxy)propoxy)phenylthio)hexanoate **10a**
prepared as **6a**, instead of DEAD ADDP was used.
^{1}H NMR (300.13 MHz, $(CD_3)_2SO$) δ 0.83 (t, 3H, Bu-CH_3, J=7.0Hz); 1.07 (t, 3H, -CH_3, J=7.1Hz); 1.23-1.36 (m, 4H, Bu-CH_2); 1.57-1.70 (m, 2H, Bu-CH_2); 2.11 (s, 3H, Ph'-4-CH_3); 2.15-2.20 (m, 5H, Ph'-3-CH_3 + -CH_2-); 3.55 (t, 1H, SC*H*, J=7.2Hz); 3.99-4.13 (m, 6H, OCH_2 + Ph-OCH_2 + Ph'-OCH_2); 6.64 (d, 1H, Ph'-6*H*, J=8.1Hz); 6.73 (s, 1H, Ph'-2*H*); 6.93 (d, 2H, Ph-2*H* + -6*H*, J=8.7Hz); 6.99 (d, 1H, Ph'-5*H*, J=8.4Hz); 7.34 (d, 2H, Ph-3*H* + -5*H*, J=8.6Hz). MS (ESI+): *m/e* = 431.0 $[M+H]^+$. yield 78%.

2-(4-(3-(3,4-dimethylphenoxy)propoxy)phenylthio)hexanoic acid **10**
prepared as **6**
^{1}H NMR (300.13 MHz, $(CD_3)_2SO$): δ 0.82 (t, 3H, Bu-CH_3, J=6.9Hz); 1.16-1.30 (m, 4H, Bu-CH_2); 1.52-1.71 (m, 2H, Bu-CH_2); 2.11 (s, 3H, Ph'-4-CH_3); 2.12-2.18 (m, 5H, Ph'-3-CH_3 + -CH_2-); 3.46 (t, 1H, SC*H*, J=7.0Hz); 4.05 (t, 2H, Ph-OCH_2, J=6.3Hz); 4.10 (t, 2H, Ph'-OCH_2, J=6.2Hz); 6.64 (d, 1H, Ph'-6*H*, J=8.4Hz); 6.73 (s, 1H, Ph'-2*H*); 6.92 (d, 2H, Ph-2*H* + 6*H*, J=8.7Hz); 6.99 (d, 1H, Ph'-5*H*, J=8.4Hz); 7.35 (d, 2H, Ph-3*H* + -5*H*, J=8.7Hz). ^{13}C-NMR (75.45 MHz, $(CD_3)_2SO$) δ 13.74 (Bu-*C*H_3); 18.38 (Ph'-4-*C*H_3); 19.56 (Ph'-3-*C*H_3); 21.73 (Bu-*C*H_2); 28.61 (Bu-*C*H_2); 28.71 (-*C*H_2-); 30.79 (Bu-*C*H_2); 50.81 (S*C*H); 63.93 (Ph-O*C*H_2); 64.36 (Ph'-O*C*H_2); 111.40 (Ph'-C_6); 115.08 (2C, Ph-C_3 + –C_5); 115.80 (Ph'-C_2); 123.24 (Ph-C_1); 127.94 (Ph'-C_4); 130.13 (Ph'-C_5); 135.17 (2C, Ph-C_2 + –C_6); 137.21 (Ph'-C_3); 156.52 (Ph'-C_1); 158.68 (Ph-C_4); 172.94 (*C*OOH). MS (ESI-): *m/e* = 401.3 (M-1).
Anal. ($C_{23}H_{30}O_4S$ [402.55]) C, H: calc C 68.62 H 7.51; found C 68.88 H 7.55.
yield 79%.

ethyl 2-(4-(3-(2,3-dimethylphenoxy)propoxy)phenylthio)hexanoate **11a**
3a (1.0 equiv.), **5a** (1.1 equiv.) and TPP (1.5 equiv.) were dissolved in abs. THF and a solution of DEAD (1.5 equiv.) in abs. THF was added. The solution was stirred 48h under Argon. After removal of the solvent, the residue was purified by column chromatography (*n*-hexane/ethyl acetate 10:1).
^{1}H NMR (300.13 MHz, $(CD_3)_2SO$) δ 0.83 (t, 3H, Bu-CH_3, J=7.0Hz); 1.06 (t, 3H, -CH_3, J=7.1Hz); 1.23-1.36 (m, 4H, Bu-CH_2); 1.57-1.70 (m, 2H, Bu-CH_2); 2.05 (s, 3H, Ph'-2-CH_3); 2.05-2.20 (m, 5H, Ph'-3-CH_3 + -CH_2-); 3.55 (t, 1H, SC*H*, J=7.6Hz); 4.01 (q, 2H, OCH_2, J=6.9Hz); 4.07 (t, 2H, Ph-OCH_2, J=6.2Hz); 4.15 (t, 2H, Ph'-OCH_2, J=6.3Hz); 6.73 (d, 1H, Ph'-6*H*, J=7.5Hz); 6.78 (d, 1H, Ph'-4*H*, J=8.4Hz); 6.92-7.02 (m, 3H, Ph-2*H* + -6*H*, Ph'-5*H*); 7.35 (d, 2H, Ph-3*H* + -5*H*, J=8.4Hz). MS (ESI+): *m/e* = 431.0 $[M+H]^+$. yield 55%.

2-(4-(3-(2,3-dimethylphenoxy)propoxy)phenylthio)hexanoic acid **11**
prepared as **6**
^{1}H NMR (300.13 MHz, $(CD_3)_2SO$): δ 0.82 (t, 3H, Bu-C*H*$_3$, J=6.9Hz); 1.21-1.35 (m, 4H, Bu-C*H*$_2$); 1.52-1.71 (m, 2H, Bu-C*H*$_2$); 2.05 (s, 3H, Ph'-2-C*H*$_3$); 2.12-2.18 (m, 5H, Ph'-3-C*H*$_3$ + -C*H*$_2$-); 3.47 (t, 1H, SC*H*, J=7.6Hz); 4.07 (t, 2H, Ph-OC*H*$_2$, J=6.0Hz); 4.15 (t, 2H, Ph'-OC*H*$_2$, J=6.0Hz); 6.73 (d, 1H, Ph'-6*H*, J=7.2Hz); 6.78 (d, 1H, Ph'-4*H*, J=8.4Hz); 6.91-7.03 (m, 3H, Ph-2*H* + -6*H*, Ph'-5*H*); 7.36 (d, 2H, Ph-3*H* + -5*H*, J=8.7Hz). ^{13}C-NMR (75.45 MHz, $(CD_3)_2SO$) δ 11.33 (Ph'-2-*C*H$_3$); 13.68 (Bu-*C*H$_3$); 19.63 (Ph'-3-*C*H$_3$); 21.69 (Bu-*C*H$_2$); 28.69 (Bu-*C*H$_2$); 28.73 (-*C*H$_2$-); 30.79 (Bu-*C*H$_2$); 50.84 (S*C*H); 64.38 (Ph-O*C*H$_2$); 64.52 (Ph'-O*C*H$_2$); 109.26 (Ph'-*C*$_6$); 115.08 (2C, Ph-*C*$_3$ + –*C*$_5$); 122.05 (Ph'-*C*$_4$); 123.30 (Ph-*C*$_1$); 124.19 (Ph'-*C*$_2$); 125.85 (Ph'-*C*$_5$); 135.13 (2C, Ph-*C*$_2$ + –*C*$_6$); 137.17 (Ph'-*C*$_3$); 156.25 (Ph'-*C*$_1$); 158.70 (Ph-*C*$_4$); 172.89 (*C*OOH). MS (ESI-): *m/e* = 401.1 (M-1).
Anal. ($C_{23}H_{30}O_4S$ [402.55]) C, H: calc C 68.62 H 7.51; found C 68.35 H 7.43.
yield 75%.

ethyl 2-(4-(3-(5,6,7,8-tetrahydronaphthalen-1-yloxy)propoxy)phenylthio)-hexanoate **12a**
prepared as **6a**
^{1}H NMR (300.13 MHz, $(CD_3)_2SO$): δ 0.83 (t, 3H, Bu-C*H*$_3$, J=6.9Hz); 1.07 (t, 3H, -C*H*$_3$, J=7.2Hz); 1.23-1.34 (m, 4H, Bu-C*H*$_2$); 1.58-1.67 (m, 6H, Bu-C*H*$_2$ + Tetrahydronaph-6C*H*$_2$ + -7C*H*$_2$); 2.15 (q, 2H, -C*H*$_2$-, J=6.0Hz); 2.50-2.54 (m, 2H, Tetrahydronaph-5C*H*$_2$); 2.65-2.67 (m, 2H, Tetrahydronaph-8C*H*$_2$); 3.56 (t, 1H, SC*H*, J=7.5Hz); 4.00 (q, 2H, OC*H*$_2$, J=7.2Hz); 4.07 (t, 2H, Ph-OC*H*$_2$, J=6.0Hz); 4.14 (t, 2H, Tetrahydronaph-OC*H*$_2$, J=6.3Hz); 6.62 (d, 1H, Tetrahydronaph-2*H*, J=7.5Hz); 6.71 (d, 1H, Tetrahydronaph-4*H*, J=8.1Hz); 6.92-7.03 (m, 3H, Ph-2*H* + -6*H*, Tetrahydronaph-3*H*); 7.35 (d, 2H, Ph-3*H* + -5*H*, J=8.7Hz). MS (ESI+): *m/e* = 457.2 $[M+H]^+$. yield 15%.

2-(4-(3-(5,6,7,8-tetrahydronaphthalen-1-yloxy)propoxy)phenylthio)hexanoic acid **12**
prepared as **6**
^{1}H NMR (300.13 MHz, $(CD_3)_2SO$): δ 0.82 (t, 3H, Bu-C*H*$_3$, J=6.8Hz); 1.22-1.35 (m, 4H, Bu-C*H*$_2$); 1.54-1.67 (m, 6H, Bu-C*H*$_2$ + Tetrahydronaph-6C*H*$_2$ + -7C*H*$_2$); 2.15 (q, 2H, -C*H*$_2$-, J=6.0Hz); 2.52-2.65 (m, 4H, Tetrahydronaph-5C*H*$_2$ + -8C*H*$_2$); 3.47 (t, 1H, SC*H*, J=7.2Hz); 4.07 (t, 2H, Ph-OC*H*$_2$, J=6.0Hz); 4.14 (t, 2H, Tetrahydronaph-OC*H*$_2$, J=6.0Hz); 6.62 (d, 1H, Tetrahydronaph-2*H*, J=7.5Hz); 6.71 (d, 1H, Tetrahydronaph-4*H*, J=8.1Hz); 6.91-7.03 (m, 3H, Ph-2*H* + -6*H*, Tetrahydronaph-3*H*); 7.35 (d, 2H, Ph-3*H* + -5*H*, J=8.4Hz). ^{13}C NMR (75.45 MHz, $(CD_3)_2SO$): δ 13.69 (Bu-*C*H$_3$); 21.69 (Bu-*C*H$_2$); 22.30 (2C, Tetrahydronaph-*C*$_6$ + -*C*$_7$); 22.33 (Tetrahydronaph-*C*$_8$); 22.61 (Tetrahydronaph-*C*$_5$); 28.68 (Bu-*C*H$_2$); 28.97 (-*C*H$_2$-); 30.80 (Bu-*C*H$_2$); 50.86 (S*C*H); 63.89 (Ph-O*C*H$_2$); 64.48 (Tetrahydronaph-O*C*H$_2$); 108.03 (Tetrahydronaph-*C*$_2$); 115.08 (2C, Ph-*C*$_3$ + –*C*$_5$); 121.11 (Tetrahydronaph-*C*$_4$); 123.30 (Tetrahydronaph-*C*$_{8a}$); 125.00 (Tetrahydronaph-*C*$_3$); 125.73 (Ph-*C*$_1$); 135.12 (2C, Ph-*C*$_2$ + –*C*$_6$); 137.73 (Tetrahydronaph-*C*$_{4a}$); 156.00 (Tetrahydro-naph-*C*$_1$); 158.68 (Ph-*C*$_4$); 172.91 (*C*OOH). MS (ESI-): *m/e* = 427.2 (M-1).
Anal. ($C_{25}H_{32}O_4S$ [428.58]) C, H: calc C 70.06 H 7.53; found C 70.27 H 7.68.
yield 67%.

ethyl 2-(4-(3-(2-methoxyphenoxy)propoxy)phenylthio)hexanoate **13a**
prepared as **13a**
^{1}H NMR (300.13 MHz, $(CD_3)_2SO$): δ 0.83 (t, 3H, Bu-C*H*$_3$, J=7.0Hz); 1.07 (t, 3H, -C*H*$_3$, J=7.1Hz); 1.23-1.36 (m, 4H, Bu-C*H*$_2$); 1.58-1.71 (m, 2H, Bu-C*H*$_2$); 2.14 (quint, 2H, -C*H*$_2$-, J=6.2Hz); 3.56 (t, 1H, SC*H*, J=7.5Hz); 3.72 (s, 3H, Ph'-OC*H*$_3$); 4.02 (q, 2H, OC*H*$_2$, J=7.3Hz); 4.06-4.15 (m, 4H, Ph-OC*H*$_2$, Ph'-OC*H*$_2$); 6.82-6.89 (m, 2H, Ph'-3*H* + -6*H*); 6.90-6.98 (m, 4H, Ph-2*H* + -6*H*, Ph'-4*H* + -5*H*); 7.36 (d, 2H, Ph-3*H* + -5*H*, J=8.7Hz). MS (ESI+): *m/e* = 433.3 $[M+H]^+$.
yield 16.6%.

2-(4-(3-(2-methoxyphenoxy)propoxy)phenylthio)hexanoic acid **13**
prepared as **6**
^{1}H NMR (300.13 MHz, $(CD_3)_2SO$): δ 0.82 (t, 3H, Bu-CH_3, J=7.1Hz); 1.21-1.35 (m, 4H, Bu-CH_2); 1.56-1.69 (m, 2H, Bu-CH_2); 2.14 (quint, 2H, -CH_2-, J=6.2Hz); 3.47 (t, 1H, SC*H*, J=7.4Hz); 3.72 (s, 3H, Ph'-OCH_3); 4.06-4.14 (m, 4H, Ph-OCH_2, Ph'-OCH_2); 6.85-6.96 (m, 6H, Ph-2*H* + -6*H*, Ph'-*H*); 7.35 (d, 2H, Ph-3*H* + -5*H*, J=8.7Hz). ^{13}C-NMR (75.45 MHz, $(CD_3)_2SO$) δ 13.69 (Bu-*C*H$_3$); 21.70 (Bu-*C*H$_2$); 28.69 (2C, Bu-*C*H$_2$, -*C*H$_2$-); 30.84 (Bu-*C*H$_2$); 50.95 (S*C*H); 55.52 (Ph'-O*C*H$_3$); 64.41 (Ph-O*C*H$_2$); 65.04 (Ph'-O*C*H$_2$); 112.38 (Ph'-C_3); 113.74 (Ph'-C_6); 115.11 (2C, Ph-C_3 + –C_5); 120.73 (Ph'-C_4); 121.10 (Ph'-C_5); 123.42 (Ph-C_1); 135.05 (2C, Ph-C_2 + –C_6); 147.99 (Ph'-C_2); 149.22 (Ph'-C_1); 158.65 (Ph-C_4); 172.92 (*C*OOH). MS (ESI-): *m/e* = 403.2 (M-1).
Anal. ($C_{22}H_{28}O_5S$ [404.52]) C, H: calc C 65.32 H 6.98 found C 65.08 H 7.00.
yield 73.3%.

ethyl 2-(4-(3-(3-methoxyphenoxy)propoxy)phenylthio)hexanoate **14a**
prepared as **11a** (using **5b** instead of **5a**)
^{1}H NMR (300.13 MHz, $(CD_3)_2SO$): δ 0.83 (t, 3H, Bu-CH_3, J=6.8Hz); 1.07 (t, 3H, -CH_3, J=7.1Hz); 1.23-1.38 (m, 4H, Bu-CH_2); 1.57-1.70 (m, 2H, Bu-CH_2); 2.14 (quint, 2H, -CH_2-, J=6.2Hz); 3.56 (t, 1H, SC*H*, J=7.5Hz); 3.71 (s, 3H, Ph'-OCH_3); 4.01 (q, 2H, OCH_2, J=7.0Hz); 4.07-4.14 (m, 4H, Ph-OCH_2, Ph'-OCH_2); 6.48-6.53 (m, 3H, Ph'-2*H* + -4*H* + -6*H*); 6.94 (d, 2H, Ph-2*H* + -6*H*, J=8.7Hz); 7.15 (t, 1H, Ph'-5*H*, J=8.3Hz); 7.35 (d, 2H, Ph-3*H* + -5*H*, J=8.7Hz). MS (ESI+): *m/e* = 433.1 $[M+H]^+$.

2-(4-(3-(3-methoxyphenoxy)propoxy)phenylthio)hexanoic acid **14**
prepared as **6**
^{1}H NMR (300.13 MHz, $(CD_3)_2SO$): δ 0.82 (t, 3H, Bu-CH_3, J=6.9Hz); 1.16-1.35 (m, 4H, Bu-CH_2); 1.54-1.69 (m, 2H, Bu-CH_2); 2.14 (quint, 2H, -CH_2-, J=6.2Hz); 3.47 (t, 1H, SC*H*, J=7.3Hz); 3.71 (s, 3H, Ph'-OCH_3); 4.07-4.13 (m, 4H, Ph-OCH_2, Ph'-OCH_2); 6.48-6.53 (m, 3H, Ph'-2*H* + -4*H* + -6*H*); 6.93 (d, 2H, Ph-2*H* + -6*H*, J=8.7Hz); 7.15 (t, 1H, Ph'-5*H*, J=8.6Hz); 7.36 (d, 2H, Ph-3*H* + -5*H*, J=8.7Hz). ^{13}C-NMR (75.45 MHz, $(CD_3)_2SO$) δ 13.69 (Bu-*C*H$_3$); 21.70 (Bu-*C*H$_2$); 28.55 (Bu-*C*H$_2$); 28.69 (-*C*H$_2$-); 30.80 (Bu-*C*H$_2$); 50.86 (S*C*H); 55.03 (Ph'-O*C*H$_3$); 64.13 (Ph-O*C*H$_2$); 64.37 (Ph'-O*C*H$_2$); 100.70 (Ph'-C_2); 106.40 (Ph'-C_4); 106.59 (Ph'-C_6); 115.11 (2C, Ph-C_3 + –C_5); 123.35 (Ph-C_1); 129.91 (Ph'-C_5); 135.11 (2C, Ph-C_2 + –C_6); 158.66 (Ph-C_4); 159.70 (Ph'-C_1); 160.49 (Ph'-C_3); 172.90 (*C*OOH). MS (ESI-): *m/e* = 403.2 (M-1).
Anal. ($C_{22}H_{28}O_5S$ [404.52]) C, H: calc C 65.32 H 6.98 found C 65.15 H 7.03.
yield 59.6%

ethyl 2-(4-(3-(2-isopropylphenoxy)propoxy)phenylthio)hexanoate **15a**
prepared as **11a** (using **5c** instead of **5a**)
^{1}H NMR (250.13 MHz, $(CD_3)_2SO$): δ 0.82 (t, 3H, Bu-CH_3, J=7.0Hz); 1.03-1.14 (m, 9H, Isopr-CH_3, -CH_3); 1.22-1.37 (m, 4H, Bu-CH_2); 1.52-1.75 (m, 2H, Bu-CH_2); 2.18 (quint, 2H, -CH_2-, J=6.1Hz); 3.15-3.31 (m, 1H, Isopr-C*H*); 3.57 (t, 1H, SC*H*, J=7.5Hz); 4.00 (q, 2H, OCH_2, J=7.1Hz); 4.08-4.19 (m, 4H, Ph-OCH_2, Ph'-OCH_2); 6.84-6.95 (m, 4H, Ph-2*H* + -6*H*, Ph'-5*H* + -6*H*); 7.06-7.18 (m, 2H, Ph'-3*H* + -4*H*); 7.35 (d, 2H, Ph-3*H* + -5*H*, J=8.7Hz).
yield 36.2%.

2-(4-(3-(2-isopropylphenoxy)propoxy)phenylthio)hexanoic acid **15**
prepared as **6**
^{1}H NMR (300.13 MHz, $(CD_3)_2SO$): δ 0.82 (t, 3H, Bu-CH_3, J=7.1Hz); 1.12 (d, 6H, Isopr-CH_3, J=7.2Hz); 1.23-1.30 (m, 4H, Bu-CH_2); 1.52-1.76 (m, 2H, Bu-CH_2); 2.18 (quint, 2H, -CH_2-, J=6.1Hz); 3.21-3.28 (m, 1H, Isopr-C*H*); 3.47 (t, 1H, SC*H*, J=7.5Hz); 4.11 (t, 2H, Ph-OCH_2, J=6.1Hz); 4.16 (t, 2H, Ph'-OCH_2, J=6.3Hz); 6.85-6.94 (m, 4H, Ph-2*H* + -6*H*, Ph'-5*H* + -6*H*); 7.09-7.17 (m, 2H, Ph'-3*H* + -4*H*); 7.35 (d, 2H, Ph-3*H* + -5*H*, J=8.7Hz). ^{13}C-NMR (75.45 MHz, $(CD_3)_2SO$) δ 13.73 (Bu-*C*H$_3$); 21.73 (Bu-*C*H$_2$); 22.50 (2C, Isopr-*C*H$_3$); 26.31 (Isopr-

*C*H); 28.70 (2C, Bu-*C*H$_2$, -*C*H$_2$-); 30.80 (Bu-*C*H$_2$); 50.84 (S*C*H); 64.15 (Ph-O*C*H$_2$); 64.47 (Ph'-O*C*H$_2$); 111.56 (Ph'-C_6); 115.03 (2C, Ph-C_3 + –C_5); 120.51 (Ph'-C_4); 123.29 (Ph-C_1); 125.74 (Ph'-C_5); 126.68 (Ph'-C_3); 135.15 (2C, Ph-C_2 + –C_6); 136.04 (Ph'-C_2); 155.50 (Ph'-C_1); 158.68 (Ph-C_4); 172.98 (*C*OOH). MS (ESI-): *m/e* = 415.2 (M-1).
Anal. ($C_{24}H_{32}O_4S$ [416.57]) C, H: calc C 69.20 H 7.74 found C 68.95 H 7.77.
yield 84%.

ethyl 2-(4-(3-(3-isopropylphenoxy)propoxy)phenylthio)hexanoate **16a**
prepared as **11a** (using **5d** instead of **5a**)
^{1}H NMR (300.13 MHz, $(CD_3)_2SO$): δ 0.83 (t, 3H, Bu-C*H*$_3$, J=7.0Hz); 1.07-1.15 (m, 9H, Isopr-C*H*$_3$, -C*H*$_3$); 1.17-1.38 (m, 4H, Bu-C*H*$_2$); 1.51-1.75 (m, 2H, Bu-C*H*$_2$); 2.14 (quint, 2H, -C*H*$_2$-, J=6.2Hz); 2.79-2.84 (m, 1H, Isopr-C*H*); 3.55 (t, 1H, SC*H*, J=7.5Hz); 4.01 (q, 2H, OC*H*$_2$, J=7.1Hz); 4.07-4.14 (m, 4H, Ph-OC*H*$_2$, Ph'-OC*H*$_2$); 6.70-6.80 (m, 3H, Ph'-2*H* + -4*H* + -6*H*); 6.94 (d, 2H, Ph-2*H* + -6*H*, J=8.7Hz); 7.17 (t, 1H, Ph'-5*H*, J=8.1Hz); 7.35 (d, 2H, Ph-3*H* + -5*H*, J=8.7Hz). MS (ESI+): *m/e* = 445.3 $[M+H]^+$.

2-(4-(3-(3-isopropylphenoxy)propoxy)phenylthio)hexanoic acid **16**
prepared as **6**
^{1}H NMR (300.13 MHz, $(CD_3)_2SO$): δ 0.82 (t, 3H, Bu-C*H*$_3$, J=7.1Hz); 1.16 (d, 6H, Isopr-C*H*$_3$, J=7.2Hz); 1.23-1.35 (m, 4H, Bu-C*H*$_2$); 1.57-1.71 (m, 2H, Bu-C*H*$_2$); 2.14 (quint, 2H, -C*H*$_2$-, J=6.2Hz); 2.77-2.86 (m, 1H, Isopr-C*H*); 3.47 (t, 1H, SC*H*, J=7.4Hz); 4.07-4.14 (m, 4H, Ph-OC*H*$_2$, Ph'-OC*H*$_2$); 6.72-6.80 (m, 3H, Ph'-2*H* + -4*H* + -6*H*); 6.93 (d, 2H, Ph-2*H* + -6*H*, J=8.7Hz); 7.17 (t, 1H, Ph'-5*H*, J=8.1Hz); 7.36 (d, 2H, Ph-3*H* + -5*H*, J=8.7Hz). ^{13}C-NMR (75.45 MHz, $(CD_3)_2SO$) δ 13.69 (Bu-*C*H$_3$); 21.69 (Bu-*C*H$_2$); 23.75 (2C, Isopr-*C*H$_3$); 28.63 (Bu-*C*H$_2$); 28.69 (-*C*H$_2$-); 30.80 (Bu-*C*H$_2$); 33.39 (Isopr-*C*H); 50.86 (S*C*H); 63.94 (Ph-O*C*H$_2$); 64.41 (Ph'-O*C*H$_2$); 111.52 (Ph'-C_6); 112.68 (Ph'-C_2); 115.11 (2C, Ph-C_3 + –C_5); 118.57 (Ph'-C_4); 123.34 (Ph-C_1); 129.23 (Ph'-C_5); 135.11 (2C, Ph-C_2 + –C_6); 150.08 (Ph'-C_3); 158.51 (Ph'-C_1); 158.67 (Ph-C_4); 172.89 (*C*OOH). MS (ESI-): *m/e* = 415.3 (M-1).
Anal. ($C_{24}H_{32}O_4S$ [416.57]) C, H: calc C 69.20 H 7.74 found C 69.01 H 7.75.
yield 69.3%.

ethyl 2-(4-(3-(3-(trifluoromethyl)phenoxy)propoxy)phenylthio)hexanoate **17a**
prepared as **6a**
^{1}H NMR (300.13 MHz, $(CD_3)_2SO$): δ 0.83 (t, 3H, Bu-C*H*$_3$, J=7.0Hz); 1.07 (t, 3H, -C*H*$_3$, J=7.1Hz); 1.21-1.36 (m, 4H, Bu-C*H*$_2$); 1.58-1.71 (m, 2H, Bu-C*H*$_2$); 2.18 (quint, 2H, -C*H*$_2$-, J=6.2Hz); 3.56 (t, 1H, SC*H*, J=7.4Hz); 4.00 (q, 2H, OC*H*$_2$, J=7.2Hz); 4.14 (t, 2H, Ph-OC*H*$_2$, J=6.2Hz); 4.21 (t, 2H, Ph'-OC*H*$_2$, J=6.3Hz); 6.94 (d, 2H, Ph-2*H* + -6*H*, J=8.9Hz); 7.25-7.29 (m, 3H, Ph'-2*H* + -4*H* + -6*H*); 7.35 (d, 2H, Ph-3*H* + -5*H*, J=8.9Hz); 7.51 (t, 1H, Ph'-5*H*, J=7.9Hz). MS (ESI+): *m/e* = 471.2 $[M+H]^+$.
yield 25%.

2-(4-(3-(3-(trifluoromethyl)phenoxy)propoxy)phenylthio)hexanoic acid **17**
prepared as **6**
^{1}H NMR (300.13 MHz, $(CD_3)_2SO$): δ 0.82 (t, 3H, Bu-C*H*$_3$, J=7.0Hz); 1.20-1.35 (m, 4H, Bu-C*H*$_2$); 1.51-1.68 (m, 2H, Bu-C*H*$_2$); 2.17 (quint, 2H, -C*H*$_2$-, J=6.2Hz); 3.47 (t, 1H, SC*H*, J=7.4Hz); 4.13 (t, 2H, Ph-OC*H*$_2$, J=6.2Hz); 4.20 (t, 2H, Ph'-OC*H*$_2$, J=6.2Hz); 6.93 (d, 2H, Ph-2*H* + -6*H*, J=8.8Hz); 7.25-7.29 (m, 3H, Ph'-2*H* + -4*H* + -6*H*); 7.35 (d, 2H, Ph-3*H* + -5*H*, J=8.7Hz); 7.50 (t, 1H, Ph'-5*H*, J=7.7Hz). ^{13}C NMR (75.45 MHz, $(CD_3)_2SO$): δ 13.68 (Bu-*C*H$_3$); 21.69 (Bu-*C*H$_2$); 28.40 (Bu-*C*H$_2$); 28.68 (-*C*H$_2$-); 30.81 (Bu-*C*H$_2$); 50.88 (S*C*H); 64.27 (Ph-O*C*H$_2$); 64.76 (Ph'-O*C*H$_2$); 110.98 (Ph'-C_2); 115.11 (2C, Ph-C_3 + –C_5); 117.05 (Ph'-C_4); 118.73 (Ph'-C_6); 123.41 (Ph-C_1); 125.77 (-*C*F$_3$); 130.09 (Ph'-C_3); 130.68 (Ph'-C_5); 135.08 (2C, Ph-C_2 + –C_6); 158.62 (Ph'-C_1); 158.75 (Ph-C_4); 172.90 (*C*OOH). MS (ESI-): *m/e* = 441.2 (M-1).
Anal. ($C_{22}H_{25}F_3O_4S$ [442.49]) C, H: calc C 59.72 H 5.69 found C 59.63 H 5.87.
yield 68%.

ethyl 2-(4-(3-(4-chloro-3-(trifluoromethyl)phenoxy)propoxy)phenylthio)-hexanoate **18a**
prepared as **6a**
^{1}H NMR (300.13 MHz, $(CD_3)_2SO$): δ 0.82 (t, 3H, Bu-CH_3, J=6.9Hz); 1.06 (t, 3H, -CH_3, J=7.2Hz); 1.22-1.35 (m, 4H, Bu-CH_2); 1.57-1.70 (m, 2H, Bu-CH_2); 2.16 (quint, 2H, -CH_2-, J=6.3Hz); 3.55 (t, 1H, SC*H*, J=7.6Hz); 4.12 (t, 2H, Ph-OCH_2, J=6.3Hz); 4.20 (t, 2H, Ph'-OCH_2, J=6.4Hz); 6.93 (d, 2H, Ph-2*H* +-6*H*, J=8.6Hz); 7.27-7.36 (m, 4H, Ph'-2*H* + -6*H*, Ph-3*H* +-5*H*); 7.60 (d, 1H, Ph'-5*H*, J=8.8Hz). MS (ESI+): *m/e* = 505.2 $[M+H]^+$.
yield 54.5%.

2-(4-(3-(4-chloro-3-(trifluoromethyl)phenoxy)propoxy)phenylthio)hexanoic acid **18**
prepared as **6**
^{1}H NMR (300.13 MHz, $(CD_3)_2SO$): δ 0.82 (t, 3H, Bu-CH_3, J=7.2Hz); 1.26-1.32 (m, 4H, Bu-CH_2); 1.54-1.65 (m, 2H, Bu-CH_2); 2.16 (quint, 2H, -CH_2-, J=6.3Hz); 3.46 (t, 1H, SC*H*, J=7.2Hz); 4.12 (t, 2H, Ph-OCH_2, J=6.3Hz); 4.21 (t, 2H, Ph'-OCH_2, J=6.3Hz); 6.92 (d, 2H, Ph-2*H* +-6*H*, J=9.0Hz); 7.26-7.37 (m, 4H, Ph-3*H* + -5*H*, Ph'-2*H* +-6*H*); 7.60 (d, 1H, Ph'-5*H*, J=9.0Hz). ^{13}C NMR (75.45 MHz, $(CD_3)_2SO$): δ 13.69 (Bu-*C*H_3); 21.69 (Bu-*C*H_2); 28.31 (Bu-*C*H_2); 28.68 (-*C*H_2-); 30.79 (Bu-*C*H_2); 50.87 (S*C*H); 64.19 (Ph-O*C*H_2); 65.23 (Ph'-O*C*H_2); 114.11 (-*C*F_3); 114.17 (Ph'-C_2); 115.11 (2C, Ph-C_3 + –C_5); 119.83 (Ph'-C_6); 122.58 (Ph'-C_4); 124.40 (Ph-C_1); 127.60 (Ph'-C_3); 132.70 (Ph'-C_5); 135.09 (2C, Ph-C_2 + –C_6); 157.31 (Ph'-C_1); 158.59 (Ph-C_4); 172.90 (*C*OOH). MS (ESI-): *m/e* = 475.2 (M-1).
Anal. ($C_{22}H_{24}ClF_3O_4S$ [476.94]) C, H: calc C 55.40 H 5.07; found C 55.59 H 5.19.
yield 42%.

ethyl 2-(4-(3-(biphenyl-4-yloxy)propoxy)phenylthio)hexanoate **19a**
prepared as **6a**
^{1}H NMR (300.13 MHz, $(CD_3)_2SO$): δ 0.82 (t, 3H, Bu-CH_3, J=6.9Hz); 1.07 (t, 3H, -CH_3, J=6.9Hz); 1.23-1.38 (m, 4H, Bu-CH_2); 1.57-1.67 (m, 2H, Bu-CH_2); 2.18 (q, 2H, -CH_2-, J=6.1Hz); 3.56 (t, 1H, SC*H*, J=6.6Hz); 4.00 (q, 2H, OCH_2, J=7.2Hz); 4.12-4.18 (m, 4H, Ph-OCH_2 + Ph'-OCH_2); 6.95 (d, 2H, Ph'-2*H*+ -6*H*, J=8.7Hz); 7.02 (d, 2H, Ph-2*H* + -6*H*, J=9.0Hz); 7.26-7.44 (m, 5H, Ph''-*H*); 7.56-7.61 (m, 4H, Ph-3*H* + -5*H*, Ph'-3*H* +-5*H*). MS (ESI+): *m/e* = 479.0 $[M+H]^+$.
yield 73%.

2-(4-(3-(biphenyl-4-yloxy)propoxy)phenylthio)hexanoic acid **19**
prepared as **6**
^{1}H NMR (300.13 MHz, $(CD_3)_2SO$): δ 0.82 (t, 3H, Bu-CH_3, J=6.9Hz); 1.20-1.35 (m, 4H, Bu-CH_2); 1.57-1.69 (m, 2H, Bu-CH_2); 2.18 (q, 2H, -CH_2-, J=6.2Hz); 3.48 (t, 1H, SC*H*, J=7.4Hz); 4.12-4.18 (m, 4H, Ph-OCH_2 + Ph'-OCH_2); 6.94 (d, 2H, Ph'-2*H*+ -6*H*, J=8.7Hz); 7.03 (d, 2H, Ph-2*H* + -6*H*, J=8.7Hz); 7.35-7.45 (m, 5H, Ph''-*H*); 7.56-7.60 (m, 4H, Ph-3*H* + -5*H*, Ph'-3*H* +-5*H*). ^{13}C NMR (75.45 MHz, $(CD_3)_2SO$): δ 13.70 (Bu-*C*H_3); 21.70 (Bu-*C*H_2); 28.53 (Bu-*C*H_2); 28.68 (-*C*H_2-); 30.78 (Bu-*C*H_2); 50.82 (S*C*H); 64.23 (Ph-O*C*H_2); 64.34 (Ph'-O*C*H_2); 114.89 (2C, Ph-C_3 + –C_5); 115.10 (2C, Ph'-C_2 + –C_6); 123.31 (Ph-C_1); 126.11 (2C, Ph''-C_2 + –C_6); 126.65 (Ph''-C_4); 127.71 (2C, Ph''-C_3 + –C_5); 128.79 (2C, Ph'-C_3 + –C_5); 132.58 (Ph'-C_4); 135.13 (2C, Ph-C_2 + –C_6); 139.76 (Ph''-C_1); 158.06 (Ph'-C_1); 158.65 (Ph-C_4); 172.91 (*C*OOH). MS (ESI-): *m/e* = 449.2 (M-1).
Anal. ($C_{27}H_{30}O_4S$ [450.59]) C, H: calc C 71.72 H 6.71; found C 71.97 H 6.71.
yield 50%.

ethyl 2-(4-(3-(quinolin-6-yloxy)propoxy)phenylthio)hexanoate **21a**
prepared as **11a** (using **5e** instead of **5a**)
^{1}H NMR (300.13 MHz, $(CD_3)_2SO$): δ 0.82 (t, 3H, Bu-CH_3, J=6.9Hz); 1.06 (t, 3H, -CH_3, J=7.1Hz); 1.16-1.30 (m, 4H, Bu-CH_2); 1.57-1.67 (m, 2H, Bu-CH_2); 2.26 (quint, 2H, -CH_2-, J=6.1Hz); 3.56 (t, 1H, SC*H*, J=7.5Hz); 4.00 (q, 2H, OCH_2, J=6.6Hz); 4.18 (t, 2H, Ph-OCH_2, J=6.0Hz); 4.26 (t, 2H, Quin-OCH_2, J=6.2Hz); 6.96 (d, 2H, Ph-2*H* + -6*H*, J=8.7Hz); 7.34-7.48

(m, 5H, Ph-3*H* + -5*H*, Quin-3*H* + -5*H* + -7*H*); 7.90 (d, 1H, Quin-8*H*, J=8.4Hz); 8.22 (d, 1H, Quin-4*H*, J=8.4Hz); 8.72 (d, 1H, Quin-2*H*, J=3.0Hz). MS (ESI+): *m/e* = 453.8 $[M+H]^+$.
yield 29%

2-(4-(3-(quinolin-6-yloxy)propoxy)phenylthio)hexanoic acid **21**
prepared as **6**
^{1}H NMR (300.13 MHz, $(CD_3)_2SO$): δ 0.82 (t, 3H, Bu-CH_3, J=6.9Hz); 1.24-1.35 (m, 4H, Bu-CH_2); 1.46-1.68 (m, 2H, Bu-CH_2); 2.25 (quint, 2H, -CH_2-, J=6.2Hz); 3.47 (t, 1H, SC*H*, J=7.3Hz); 4.17 (t, 2H, Ph-OCH_2, J=6.2Hz); 4.27 (t, 2H, Quin-OCH_2, J=6.2Hz); 6.95 (d, 2H, Ph-2*H* + -6*H*, J=8.7Hz); 7.35-7.50 (m, 5H, Ph-3*H* + -5*H*, Quin-3*H* + -5*H* + -7*H*); 7.91 (d, 1H, Quin-8*H*, J=9.9Hz); 8.24 (d, 1H, Quin-4*H*, J=8.1Hz); 8.73 (d, 1H, Quin-2*H*, J=2.7Hz). ^{13}C NMR (75.45 MHz, $(CD_3)_2SO$): δ 13.70 (Bu-*C*H_3); 21.70 (Bu-*C*H_2); 28.47 (Bu-*C*H_2); 28.69 (-*C*H_2-); 30.77 (Bu-*C*H_2); 50.80 (S*C*H); 64.37 (Ph-O*C*H_2); 64.69 (Quin-O*C*H_2); 106.52 (Quin-C_5); 115.12 (2C, Ph-C_3 + –C_5); 121.61 (Quin-C_3); 122.30 (Quin-C_7); 123.32 (Ph-C_1); 129.05 (Quin-C_{4a}); 130.04 (Quin-C_8); 135.10 (Quin-C_4); 135.16 (2C, Ph-C_2 + –C_6); 143.37 (Quin-C_{8a}); 147.69 (Quin-C_2); 156.40 (Ph-C_4); 158.66 (Quin-C_6); 172.90 (*C*OOH). MS (ESI-): *m/e* = 424.1 (M-1).
Anal. ($C_{24}H_{27}NO_4S$ [425.54]) C, H, N: calc C 67.74 H 6.40 N 3.29; found C 67.47 H 6.62 N 3.11.
yield 53%.

ethyl 2-(4-(3-(2,3-dimethylphenoxy)propoxy)phenylthio)acetate **21a**
prepared as **11a** with ethyl 2-(4-hydroxyphenylthio)acetate **3b**[1] instead of **3a**
^{1}H NMR (300.13 MHz, $(CD_3)_2SO$): δ 1.09 (t, 3H, -CH_3, J=7.1Hz); 2.05 (s, 3H, Ph'-2-CH_3); 2.15 (quint, 2H, -CH_2-, J=6.1Hz); 2.18 (s, 3H, Ph'-3-CH_3); 3.66 (s, 2H, SC*H*); 3.99-4.08 (m, 4H, OCH_2, Ph-OCH_2); 4.14 (t, 2H, Ph'-OCH_2, J=6.2Hz); 6.72 (d, 1H, Ph'-6*H*, J=7.6Hz); 6.77 (d, 1H, Ph'-4*H*, J=8.4Hz); 6.92 (d, 2H, Ph-2*H* + -6*H*, J=8.7Hz); 7.00 (t, 1H, Ph'-5*H*, J=7.6Hz); 7.34 (d, 2H, Ph-3*H* + -5*H*, J=8.6Hz). MS (ESI+): *m/e* = 375.1 $[M+H]^+$.
yield 65.2%.

2-(4-(3-(2,3-dimethylphenoxy)propoxy)phenylthio)acetic acid **21**
prepared as **6**
^{1}H NMR (300.13 MHz, $(CD_3)_2SO$): δ 2.05 (s, 3H, Ph'-2-CH_3); 2.15 (quint, 2H, -CH_2-, J=6.3Hz); 2.18 (s, 3H, Ph'-3-CH_3); 3.62 (s, 2H, SC*H*); 4.07 (t, 2H, Ph-OCH_2, J=6.1Hz); 4.13 (t, 2H, Ph'-OCH_2, J=6.3Hz); 6.73 (d, 1H, Ph'-6*H*, J=7.7Hz); 6.77 (d, 1H, Ph'-4*H*, J=7.9Hz); 6.92 (d, 2H, Ph-2*H* + -6*H*, J=9.0Hz); 7.00 (t, 1H, Ph'-5*H*, J=8.0Hz); 7.32 (d, 2H, Ph-3*H* + -5*H*, J=9.1Hz). ^{13}C NMR (75.45 MHz, $(CD_3)_2SO$): δ 11.33 (Ph'-2-*C*H_3); 19.63 (Ph'-3-*C*H_3); 28.73 (-*C*H_2-); 37.12 (S*C*H); 64.37 (Ph-O*C*H_2); 64.51 (Ph'-O*C*H_2); 109.25 (Ph'-C_6); 115.22 (2C, Ph-C_3 + –C_5); 122.04 (Ph'-C_4); 124.19 (Ph'-C_2); 125.49 (Ph-C_1); 125.85 (Ph'-C_5); 132.00 (2C, Ph-C_2 + –C_6); 137.18 (Ph'-C_3); 156.24 (Ph'-C_1); 157.84 (Ph-C_4); 170.67 (*C*OOH). MS (ESI-): *m/e* = 344.9 (M-1).
Anal. ($C_{19}H_{22}O_4S$ [346.44]) C, H: calc C 65.87 H 6.40; found C 65.62 H 6.64.
yield 85%.

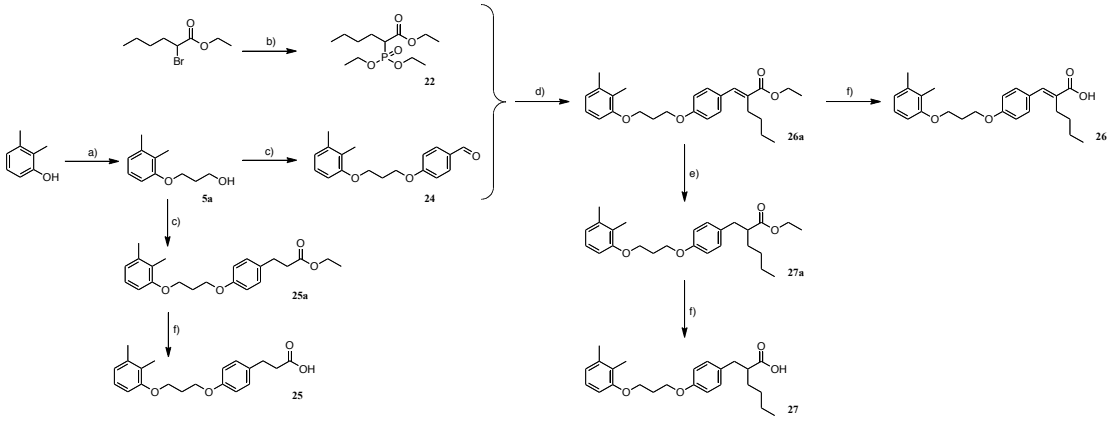

Scheme 2: Synthesis of compounds **25-27**.
Reagents and conditions: a) 3-bromopropanol, K_2CO_3, ACN, RF, 24h; b) triethylphosphite, reflux, overnight; c) 4-hydroxybenzaldehyde or ethyl 3-(4-hydroxyphenyl)propanoate, DEAD, TPP, THF, rt, 4h; d) NaH, THF, rt, 24h; e) Pd/C, H_2, EtOH, rt, 24h; f) LiOH, MeOH, H_2O, reflux, 8-20h.

4-(3-(2,3-dimethylphenoxy)propoxy)benzaldehyde **24**
4-hydroxybenzaldehyde (1 equiv.), **5a** (1.1 equiv.) and TPP (1.5 equiv.) were dissolved in abs. THF and a solution of DEAD (1.5 equiv.) in abs. THF was added. The solution was stirred for 96h under Argon. After removal of the solvent, the residue was purified by column chromatography (*n*-hexane/ethyl acetate 15:1).
^{1}H NMR (300.13 MHz, $(CD_3)_2SO$): δ 2.06 (s, 3H, Ph'-2-C*H*$_3$); 2.15-2.25 (m, 5H, -C*H*$_2$-, Ph'-3-C*H*$_3$); 4.09 (t, 2H, Ph'-OC*H*$_2$, J=6.1Hz); 4.28 (t, 2H, Ph-OC*H*$_2$, J=6.2Hz); 6.73 (d, 1H, Ph'-6*H*, J=7.6Hz); 6.79 (d, 1H, Ph'-4*H*, J=8.1Hz); 7.00 (t, 1H, Ph'-5*H*, J=7.9Hz); 7.14 (d, 2H, Ph-3*H* + -5*H*, J=8.6Hz); 7.85 (d, 2H, Ph-2*H* + -6*H*, J=8.7Hz); 9.85 (s, 1H, C*H*O). MS (ESI+): *m/e* = 285.0 $[M+H]^+$.

ethyl 3-(4-(3-(2,3-dimethylphenoxy)propoxy)phenyl)propanoate **25a**
ethyl 4-hydroxyhydrocinnamate (1 equiv.), **5a** (1.1 equiv.) and TPP (1.5 equiv.) were dissolved in abs. THF and a solution of ADDP (1.5 equiv.) in abs. THF was added. The solution was stirred for 8h under Argon. After removal of the solvent, the residue was purified by column chromatography (*n*-hexane/ethyl acetate 10:1).
^{1}H NMR (300.13 MHz, $(CD_3)_2SO$): δ 1.13 (t, 3H, -C*H*$_3$, J=7.2Hz); 2.05 (s, 3H, Ph'-2-C*H*$_3$); 2.10-2.18 (m, 5H, -C*H*$_2$-, Ph'-3-C*H*$_3$); 2.54 (t, 2H, -C*H*$_2$-COO, J=7.5Hz); 2.76 (t, 2H, Ph-C*H*$_2$, J=7.5Hz); 3.98-4.13 (m, 6H, OC*H*$_2$, Ph-OC*H*$_2$, Ph'-OC*H*$_2$); 6.73 (d, 1H, Ph'-6*H*, J=7.5Hz); 6.78 (d, 1H, Ph'-4*H*, J=8.3Hz); 6.84 (d, 2H, Ph-3*H* + -5*H*, J=8.7Hz); 6.99 (t, 1H, Ph'-5*H*, J=7.9Hz); 7.11 (d, 2H, Ph-2*H* + -6*H*, J=8.6Hz). MS (ESI+): *m/e* = 357.1 $[M+H]^+$.
yield 67.1%.

3-(4-(3-(2,3-dimethylphenoxy)propoxy)phenyl)propanoic acid **25**
prepared as **6**
^{1}H NMR (300.13 MHz, $(CD_3)_2SO$): δ 2.05 (s, 3H, Ph'-2-C*H*$_3$); 2.10-2.17 (m, 2H, -C*H*$_2$-); 2.18 (s, 3H, Ph'-3-C*H*$_3$); 2.44 (t, 2H, -C*H*$_2$-COO, J=7.5Hz); 2.73 (t, 2H, Ph-C*H*$_2$, J=7.5Hz); 4.05-4.13 (m, 4H, Ph-OC*H*$_2$, Ph'-OC*H*$_2$); 6.73 (d, 1H, Ph'-6*H*, J=7.5Hz); 6.78 (d, 1H, Ph'-4*H*, J=8.2Hz); 6.84 (d, 2H, Ph-3*H* + -5*H*, J=8.7Hz); 7.00 (t, 1H, Ph'-5*H*, J=7.9Hz); 7.11 (d, 2H, Ph-2*H* + -6*H*, J=8.5Hz). ^{13}C NMR (75.45 MHz, $(CD_3)_2SO$): δ 11.33 (Ph'-2-*C*H$_3$); 19.64 (Ph'-3-*C*H$_3$); 28.83 (-*C*H$_2$-); 29.56 (Ph-*C*H$_2$); 35.74 (*C*H$_2$-COO); 64.25 (Ph-O*C*H$_2$); 64.42 (Ph'-O*C*H$_2$); 109.23 (Ph'-C_6); 114.25 (2C, Ph-C_3 + –C_5); 122.02 (Ph'-C_4); 124.17 (Ph'-C_2); 125.85 (Ph'-C_5); 129.15 (2C, Ph-C_2 + –C_6); 132.94 (Ph-C_1); 137.16 (Ph'-C_3); 156.26 (Ph'-C_1); 156.77 (Ph-C_4); 173.80 (*C*OOH). MS (ESI-): *m/e* = 327.2 (M-1).
Anal. ($C_{20}H_{24}O_4$ [328.40]) C, H: calc C 73.15 H 7.37; found C 72.92 H 7.37.
yield 95%.

ethyl 2-(4-(3-(2,3-dimethylphenoxy)propoxy)benzylidene)hexanoate **26a**

To a suspension of sodium hydride (1.2 equiv.) in abs. THF under Argon and ice cooling, a solution of ethyl 2-(diethoxyphosphoryl)hexanoate **22**[2] was added dropwise and the mixture was stirred for 1h. Afterwards, a solution of **24** (1 equiv.) in abs. THF was added and the cooling was removed. The mixture was stirred for 24h at room temperature. After removal of the solvent, the residue was poured into H_2O and extracted with ethyl acetate. The organic layer was dried over $MgSO_4$, the solvent was removed and the residue was purified by column chromatography (*n*-hexane/ethyl acetate 15:1).

^{1}H NMR (300.13 MHz, $(CD_3)_2SO$): δ 0.87 (t, 3H, Bu-C*H*$_3$, J=7.3Hz); 1.25 (t, 3H, -C*H*$_3$, J=7.2Hz); 1.29-1.47 (m, 4H, Bu-C*H*$_2$); 2.06 (s, 3H, Ph'-2-C*H*$_3$); 2.16-2.20 (m, 5H, Ph'-3-C*H*$_3$, -C*H*$_2$-); 2.44-2.49 (m, 2H, Bu-C*H*$_2$); 4.08 (t, 2H, Ph-OC*H*$_2$, J=6.5Hz); 4.13-4.22 (m, 4H, OC*H*$_2$, Ph'-OC*H*$_2$); 6.73 (d, 1H, Ph'-6*H*, J=7.6Hz); 6.78 (d, 1H, Ph'-4*H*, J=8.2Hz); 6.98-7.03 (m, 3H, Ph-3*H* + -5*H*, Ph'-5*H*); 7.39 (d, 2H, Ph-2*H* + -6*H*, J=8.7Hz); 7.50 (s, 1H, Ph-C*H*=). MS (ESI+): *m/e* = 411.2 $[M+H]^+$.

2-(4-(3-(2,3-dimethylphenoxy)propoxy)benzylidene)hexanoic acid **26**

26a was dissolved in MeOH/THF and LiOH (10 equiv.) in H_2O (MeOH:THF:H_2O=5:2:1) was added. The solution was refluxed for 20h. After removal of the solvent, the residue was dissolved in hot H_2O (if necessary, small amounts of MeOH were added) and the free carboxylic acid was precipitated by adding diluted hydrochloric acid. The obtained crude product was recrystallized from *n*-hexane/ethyl acetate.

^{1}H NMR (300.13 MHz, $(CD_3)_2SO$): δ 0.87 (t, 3H, Bu-C*H*$_3$, J=7.2Hz); 1.29-1.44 (m, 4H, Bu-C*H*$_2$); 2.06 (s, 3H, Ph'-2-C*H*$_3$); 2.16-2.20 (m, 5H, Ph'-3-C*H*$_3$, -C*H*$_2$-); 2.40-2.48 (m, 2H, Bu-C*H*$_2$); 4.08 (t, 2H, Ph-OC*H*$_2$, J=6.0Hz); 4.19 (t, 2H, Ph'-OC*H*$_2$, J=6.2Hz); 6.73 (d, 1H, Ph'-6*H*, J=7.5Hz); 6.78 (d, 1H, Ph'-4*H*, J=8.4Hz); 6.98-7.02 (m, 3H, Ph-3*H* + -5*H*, Ph'-5*H*); 7.36 (d, 2H, Ph-2*H* + -6*H*, J=8.6Hz); 7.48 (s, 1H, Ph-C*H*=). ^{13}C NMR (75.45 MHz, $(CD_3)_2SO$): δ 11.33 (Ph'-2-*C*H$_3$); 13.67 (Bu-*C*H$_3$); 19.63 (Ph'-3-*C*H$_3$); 22.26 (Bu-*C*H$_2$); 26.67 (Bu-*C*H$_2$); 28.72 (-*C*H$_2$-); 30.68 (Bu-*C*H$_2$); 64.35 (Ph'-O*C*H$_2$); 64.45 (Ph-O*C*H$_2$); 109.24 (Ph'-*C*$_6$); 114.61 (2C, Ph-*C*$_3$ + –*C*$_5$); 122.04 (Ph'-*C*$_4$); 124.17 (Ph'-*C*$_2$); 125.86 (Ph'-*C*$_5$); 127.78 (Ph-*C*$_1$); 130.89 (2C, Ph-*C*$_2$ + –*C*$_6$); 131.67 (CH=*C*); 137.10 (Ph-*C*H); 137.17 (Ph'-*C*$_3$); 156.24 (Ph'-*C*$_1$); 158.65 (Ph-*C*$_4$); 169.35 (*C*OOH). MS (ESI-): *m/e* = 381.3 (M-1).

Anal. ($C_{24}H_{30}O_4$ [382.49]) C, H: calc C 75.36 H 7.91; found C 75.60 H 7.88.

yield 58.6%.

ethyl 2-(4-(3-(2,3-dimethylphenoxy)propoxy)benzyl)hexanoate **27a**

To a solution of **26a** (1 equiv.) in EtOH 10% Pd/C was added. The reaction mixture was stirred under H_2 for 24h. The catalyst was removed by Celite filtration and the solvent was evaporated to yield the pure product.

^{1}H NMR (300.13 MHz, $(CD_3)_2SO$): δ 0.81 (t, 3H, Bu-C*H*$_3$, J=6.9Hz); 1.04 (t, 3H, -C*H*$_3$, J=7.1Hz); 1.18-1.21 (m, 4H, Bu-C*H*$_2$); 1.42-1.60 (m, 2H, Bu-C*H*$_2$); 2.05 (s, 3H, Ph'-2-C*H*$_3$); 2.12-2.18 (m, 5H, Ph'-3-C*H*$_3$, -C*H*$_2$-); 2.50-2.70 (m, 3H, Ph-C*H*$_2$, -C*H*COO); 3.95 (q, 2H, OC*H*$_2$, J=7.0Hz); 4.04-4.12 (m, 4H, Ph-OC*H*$_2$, Ph'-OC*H*$_2$); 6.71-6.84 (m, 4H, Ph-3*H* + -5*H*, Ph'-4*H*, Ph'-6*H*); 6.97-7.06 (m, 3H, Ph-2*H* + -6*H*, Ph'-5*H*). MS (ESI+): *m/e* = 413.3 $[M+H]^+$.

yield 95%.

2-(4-(3-(2,3-dimethylphenoxy)propoxy)benzyl)hexanoic acid **27**

27a was dissolved in MeOH/THF and LiOH (10 equiv.) in H_2O (MeOH:THF:H_2O=5:2:1) was added. The solution was refluxed for 8h. After removal of the solvent, the residue was dissolved in hot H_2O (if necessary, small amounts of MeOH were added) and the free carboxylic acid was precipitated by adding diluted hydrochloric acid. The mixture was extracted with $CHCl_3$, the solvent was removed and the remaining residue was dissolved in petrolether. Storage in the refrigerator overnight allowed crystallization.

^{1}H NMR (300.13 MHz, $(CD_3)_2SO$): δ 0.82 (t, 3H, Bu-C*H*$_3$, J=6.8Hz); 1.18-1.29 (m, 4H, Bu-C*H*$_2$); 1.41-1.55 (m, 2H, Bu-C*H*$_2$); 2.05 (s, 3H, Ph'-2-C*H*$_3$); 2.11-2.18 (m, 2H, -C*H*$_2$-); 2.18 (s, 3H, Ph'-3-C*H*$_3$); 2.40-2.49 (m, 1H, -C*H*COO); 2.55-2.76 (m, 2H, Ph-C*H*$_2$); 4.07 (t, 2H,

Ph-OCH_2, J=6.0Hz); 4.10 (t, 2H, Ph'-OCH_2, J=6.3Hz); 6.73 (d, 1H, Ph'-6H, J=7.5Hz); 6.78 (d, 1H, Ph'-4H, J=8.4Hz); 6.83 (d, 2H, Ph-3H + -5H, J=8.7Hz); 7.00 (t, 1H, Ph'-5H, J=7.8Hz); 7.06 (d, 2H, Ph-2H + -6H, J=8.4Hz). ^{13}C NMR (75.45 MHz, $(CD_3)_2SO$): δ 11.33 (Ph'-2-CH_3); 13.75 (Bu-CH_3); 19.63 (Ph'-3-CH_3); 22.00 (Bu-CH_2); 28.84 (Bu-CH_2); 28.92 (-CH_2-); 31.15 (Bu-CH_2); 36.91 (Ph-CH_2); 47.02 (-CHCOO); 64.22 (Ph-OCH_2); 64.43 (Ph'-OCH_2); 109.23 (Ph'-C_6); 114.14 (2C, Ph-C_3 + –C_5); 122.02 (Ph'-C_4); 124.17 (Ph'-C_2); 125.85 (Ph'-C_5); 129.71 (2C, Ph-C_2 + –C_6); 131.57 (Ph-C_1); 137.16 (Ph'-C_3); 156.26 (Ph'-C_1); 156.85 (Ph-C_4); 176.31 (COOH). MS (ESI-): *m/e* = 383.2 (M-1).
Anal. ($C_{24}H_{32}O_4$ [384.51]) C, H: calc C 74.97 H 8.39; found C 74.70 H 8.52.
yield 83%.

Compounds **(*R*)-11** and **(*S*)-11** were obtained by preparative HPLC of **11** under following conditions:
Chiral stationary phase: Chiralpak AD-H (Chiral Technologies, Illkirch, France)
Column dimension: 250 x 4 mm ID
Eluent: heptane - 2-propanol – trifluoroacetic acid (80:20:0.1; v/v/v)
flow rate: 1 mL/min
temperature: ambient
detection: UV 250 nm

Enantiomeric purity determination of **(*R*)-11**

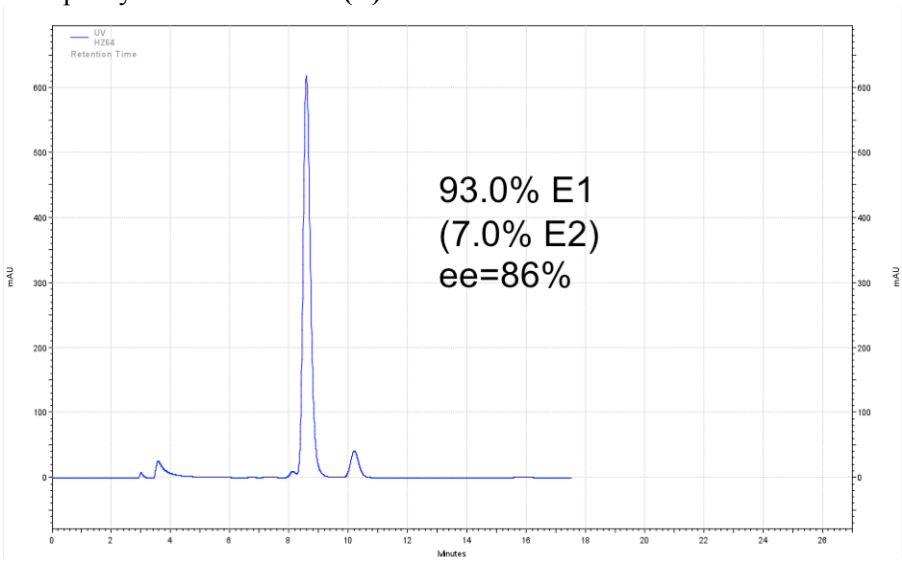

Enantiomeric purity determination of **(*S*)-11**

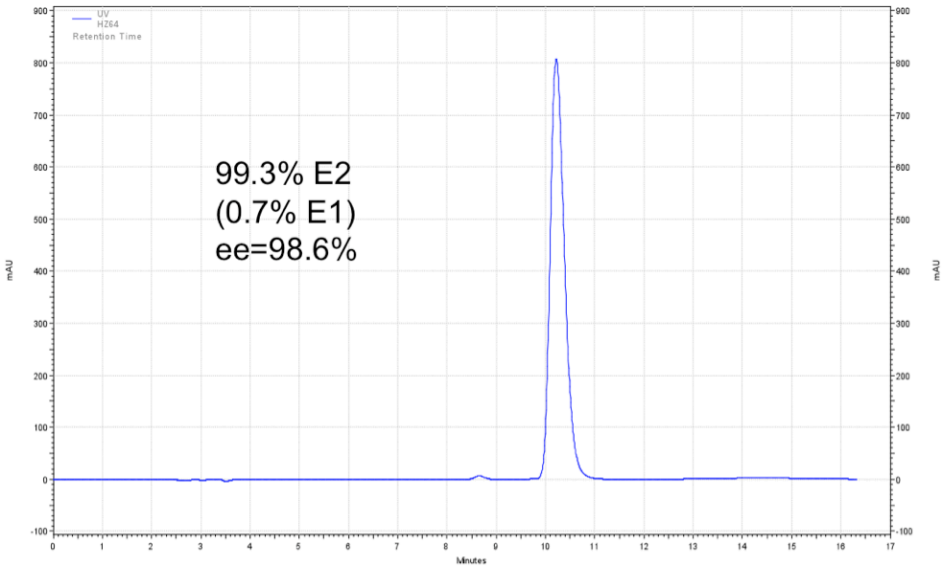

Assignment of absolute configurations[3]:

Chiral stationary phase, Chiralpak QD-AX (Chiral Technologies)
Column dimension, 150 x 4 mm ID
Eluent, methanol-acetonitrile-glacial acetic acid-ammonium acetate (20:80:0.2:0.05; v/v/w)
flow rate, 0.5 mL/min; temperature, ambient;
detection, UV 250 nm

The first eluted enantiomer on Chiralpak QD-AX (quinidine carbamate based chiral anion-exchanger) has *R*-configuration, while the second eluted enantiomer has *S*-configuration. The enantiomer that was eluted first from the Chiralpak AD-H column (E1) was the first eluted enantiomer on Chiralpak QD-AX (chiral anion-exchanger) and therefore assigned with *R*-configuration. The second eluted enantiomer on Chiralpak AD-H (E2) was stronger retained on Chiralpak QD-AX (chiral anion-exchanger) and therefore determined to be the *S*-enantiomer. More details on this chromatographic absolute configuration assignment can be found in ref. 3.

References:

1. Furnsinn, C.; Willson, T.; Brunmair, B. *Diabetologia* **2007,** *50*, 8.
2. Bargiggia, F.; Piva, O. *Tetrahedron: Asymmetry* **2003,** *14*, 1819.
3. Lämmerhofer, M.; Pell, R.; Richter, M.; Schiesel, S.; Mahut, M.; Zettl, H.; Dittrich, M.; Schubert-Zsilavecz, M.; Lindner, W. *Chirality* **2009**, in preparation.

Pirinixic Acid Derivatives as Novel Dual Inhibitors of Microsomal Prostaglandin E_2 Synthase-1 and 5-Lipoxygenase

Andreas Koeberle,[†,‡] Heiko Zettl,[†,§] Christine Greiner,[‡] Mario Wurglics,[§] Manfred Schubert-Zsilavecz,[§] and Oliver Werz*[,‡]

Department of Pharmaceutical Analytics, Pharmaceutical Institute, Eberhard-Karls-University Tuebingen, Auf der Morgenstelle 8, D-72076 Tuebingen, Germany, and Institute of Pharmaceutical Chemistry, ZAFES, LIFF, Goethe-University Frankfurt, Max-von-Laue-Strasse 9, D-60438 Frankfurt, Germany

Received September 1, 2008

Dual inhibition of the prostaglandin (PG) and leukotriene (LT) biosynthetic pathway is supposed to be superior over single interference, both in terms of efficacy and side effects. Here, we present a novel class of dual microsomal PGE_2 synthase-1/5-lipoxygenase (5-LO) inhibitors based on the structure of pirinixic acid [PA, 2-(4-chloro-6-(2,3-dimethylphenylamino)pyrimidin-2-ylthio)acetic acid, compound **1**]. Target-oriented structural modification of **1**, particularly α substitution with extended *n*-alkyl or bulky aryl substituents and concomitant replacement of the 2,3-dimethylaniline by a biphenyl-4-yl-methane-amino residue, resulted in potent suppression of mPGES-1 and 5-LO activity, exemplified by 2-(4-(biphenyl-4-ylmethylamino)-6-chloropyrimidin-2-ylthio)octanoic acid (**7b**, IC_{50} = 1.3 and 1 μM, respectively). Select compounds also potently reduced PGE_2 and 5-LO product formation in intact cells. Importantly, inhibition of cyclooxygenases-1/2 was significantly less pronounced. Taken together, these pirinixic acid derivatives constitute a novel class of dual mPGES-1/5-LO inhibitors with a promising pharmacologial profile and a potential for therapeutic use.

Introduction

Prostaglandins (PGs)[a] and leukotrienes (LTs) are synthesized from arachidonic acid (AA) by the initial actions of the key enzymes cyclooxygenase (COX) and 5-lipoxygenase (5-LO), respectively.[1] Pathological conditions, such as inflammation, pain, fever, anorexia, atherosclerosis, stroke, and tumorigenesis, are related to elevated levels of PGE_2.[2] Accordingly, pharmacological inhibitors of COX isoenzymes [i.e., nonsteroidal anti-inflammatory drugs (NSAIDs) or COX-2-selective coxibs] are used to treat respective disorders.[1] However, other PGs (e.g., PGI_2 and $PGF_{2\alpha}$) are needed to maintain homeostasis, and thus, inhibition of the synthesis of these PGs by NSAIDs is likely responsible for gastrointestinal and renal side effects.[3] Although coxibs have a lower risk of gastrointestinal damage, they exert cardiovascular side effects presumably by altering the balance between PGI_2 and thromboxanes.[4]

PGE_2 is synthesized from the COX product PGH_2 by three terminal isoforms of PGE_2 synthases (PGES). Increasing evidence suggests that the microsomal PGE_2 synthase-1 (mPGES-1), which is induced by pro-inflammatory stimuli and functionally coupled to COX-2, provides elevated PGE_2 levels during inflammation, fever, and pain.[2] Thus, mPGES-1 may constitute a potential target for therapeutic intervention,[5] but only a few mPGES-1 inhibitors have been described thus far. Compound **9** [MK-886, 3-(3-(*tert*-butylthio)-1-(4-chlorobenzyl)-5-isopropyl-1*H*-indol-2-yl)-2,2-dimethylpropanoic acid, IC_{50} = 2.4 μM[6]] and structural derivatives[7] potently inhibit mPGES-1 *in vitro*, but they are afflicted to high plasma protein binding. Recently, phenanthrene imidazoles have been identified as selective and orally active mPGES-1 inhibitors (IC_{50} = 1.3 μM in whole blood[8]) that effectively relieve both pyresis and inflammatory pain in preclinical models of inflammation.[9]

LTs are important mediators of inflammatory and allergic diseases but also play roles in cardiovascular disease and cancer.[10] Anti-LT therapy is used in asthma therapy and may possess therapeutic potential also for other LT-related disorders. It was found that dual inhibition of both the PG and LT biosynthetic pathway, for example, by 2-(6-(4-chlorophenyl)-2,2-dimethyl-7-phenyl-2,3-dihydro-1*H*-pyrrolizin-5-yl) acetic acid (licofelone), is superior over single interference, not only in terms of anti-inflammatory effectiveness but also because of a lower incidence of gastrointestinal toxicity, typically related to COX inhibition.[11,12] We have recently shown that licofelone suppresses PGE_2 formation primarily by interference with mPGES-1, whereas COX-2 was hardly affected.[13] It is speculated that drugs that selectively suppress PGE_2 formation combined with reduction of LT biosynthesis may lack the detrimental cardiovascular side effects, implying an alternative pharmacological strategy for intervention with inflammation.[5,14]

Recently, we have shown that aliphatic α substitution of pirinixic acid [PA, 2-(4-chloro-6-(2,3-dimethylphenylamino)pyrimidin-2-ylthio)acetic acid, compound **1**] enhanced both peroxisome proliferator-activated receptor (PPAR)α and PPARγ agonism[15] and enables these derivatives to inhibit cellular LT formation (IC_{50} = 0.6 μM).[16] Here, we address the effectiveness of **1** and its derivatives for inhibition of PGE_2 synthesis and interaction with mPGES-1, 5-LO, and COX-1/2. Although **1** itself failed to suppress PGE_2 formation, we present α-substi-

* To whom correspondence should be addressed: Department of Pharmaceutical Analytics, Pharmaceutical Institute, Eberhard-Karls-University Tuebingen, Auf der Morgenstelle 8, D-72076 Tuebingen, Germany. Telephone: ++49-7071-2978793. Fax: ++49-7071-294565. E-mail: oliver.werz@uni-tuebingen.de.

† Both authors contributed equally to this work.

‡ Eberhard-Karls-University Tuebingen.

§ Goethe-University Frankfurt.

[a] Abbreviations: AA, arachidonic acid; COX, cyclooxygenase; cPGES, cytosolic prostaglandin E_2 synthase; ELISA, enzyme-linked immunosorbent assay; FLAP, 5-LO-activating protein; 12-HHT, 12(*S*)-hydroxy-5-*cis*-8,10-*trans*-heptadecatrienoic acid; IL, interleukin; 5-LO, 5-lipoxygenase; LT, leukotriene; mPGES, microsomal prostaglandin E_2 synthase; NSAID, nonsteroidal anti-inflammatory drug; PBS, phosphate-buffered saline; PPAR, peroxisome proliferator-activated receptor; PA, pirinixic acid; PMNL, polymorphonuclear leukocyte; PG, prostaglandin.

10.1021/jm801085s CCC: $40.75
Published on Web 11/19/2008

Scheme 1. General Synthesis of Compounds **5a**−**7e**[a]

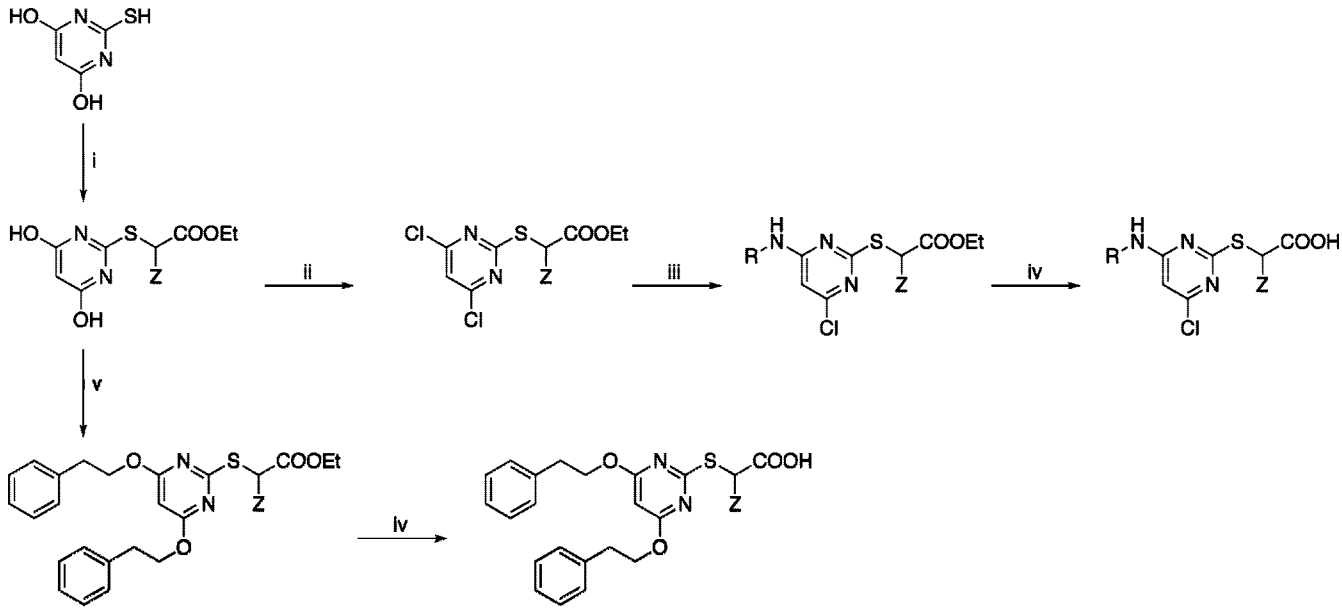

[a] Reagents and conditions: (i) (Z = H), thiobarbituric acid, 2-bromoethylester (1.17 equiv), NaOH (1.08 equiv), H_2O/EtOH (1:1), 60 °C, 2 h; (Z = *n*-Bu), (Z = *n*-Hex), thiobarbituric acid, 2-bromoethylester (1.5 equiv), triethylamine (3.0 equiv), DMF, 80 °C, 1.5−3 h; (ii) $POCl_3$ (18 equiv), *N*,*N*-diethylaniline (1 equiv), RF, 2−3.5 h; (iii) R-NH_2 (1.2 equiv), triethylamine (3 equiv), EtOH, RF, 3.5−96 h; (iv) LiOH (3 equiv), EtOH, RT, 24 h; (v) (2-bromoethyl)benzene (2 equiv), K_2CO_3 (3 equiv), DMF, 80 °C, 5−9 h.

tuted derivatives as potent dual mPGES-1/5-LO inhibitors in cellular and cell-free systems.

Results and Discussion

Chemistry. The presented compounds were generally synthesized in a four-step reaction, which was modified from the synthesis of **1** published by D'Atri et al.[17] Compounds **2a**−**4** were synthesized as previously reported.[15,18] The synthesis of compounds **5a**−**7e** is presented in Scheme 1. First, the thiol group of thiobarbituric acid was etherified with the appropriate α-bromoethylester (i). The introduction of alkyl chains longer than four carbons succeeds easier with triethylamine as a conjugated base in DMF instead of NaOH in H_2O/EtOH.[17] Aromatic nucleophilic substitution with $POCl_3$ (ii) gave the chlorinated pyrimidine derivatives. In the following step, treatment with the appropriate primary amine employing triethylamine in refluxed EtOH (iii) resulted in monoamination of the pyrimidine core. These compounds were hydrolyzed with LiOH in EtOH (iv) to give the desired carboxylic acids. A side path via a Williamson-like ether synthesis (v) led to symmetrically substituted 3,5-bis-ether pyrimidine derivatives, which were hydrolyzed to the corresponding carboxylic acids as described (iv).

Screening for Dual 5-LO and mPGES-1 Inhibitors Derived from Prinixic Acid. We have previously shown that target-oriented structural modification of **1** led to potent inhibitors of 5-LO product formation in intact polymorphonuclear leukocytes (PMNL) and to a minor extent also in cell-free assays.[16] In particular, esterification of the carboxylic acid group, replacement of the 2,3-dimethylaniline by 6-aminoquinoline, and alkylation in the α position of the carboxylic acid group yielded compound **3b** (IC_{50} = 0.6 μM in intact PMNL) as the most potent derivative out of the structures **1**−**3d** (Table 1 and ref 16). Because dual inhibition of both the LT and the PG biosynthetic pathway might be advantageous over single interference,[11] potent inhibitors that dually interfere with 5-LO product and PGE_2 formation would be desirable. Accordingly, we pursued our search for improved 5-LO inhibitors with the core structure of **1** and also addressed their effectiveness for inhibition of mPGES-1. To initially screen for dual inhibitors of 5-LO and mPGES-1, compound **1** and its derivatives (at 10 μM) were analyzed for their ability to inhibit the conversion of PGH_2 to PGE_2 mediated by mPGES-1 in microsomes of IL-1β-treated A549 cells.[13] Focus was placed on derivatives that are substituted in the α position of the carboxyl group. The representatives **2d**, **2e**, **2g**, and **3a**−**3d** out of this series were already shown to inhibit 5-LO product synthesis in human PMNL, and values given in Table 1 are referenced.[16] Thus, only for novel derivatives **2f**, **2h**, and **4**−**7e**, the 5-LO inhibitory potential was assessed in the first screening round. The 5-LO inhibitor **8** [BWA4C, (*E*)-*N*-hydroxy-*N*-(3-(3-phenoxyphenyl)-allyl)acetamide][19] and the mPGES-1 inhibitor **9** were used as reference compounds, respectively.

In accordance with the literature,[6,7,13] compound **9** concentration-dependently blocked PGE_2 formation with an IC_{50} = 2.1 μM, and 26 ± 3% activity remained at a concentration of 10 μM. Compound **1** itself did not inhibit mPGES-1 activity. Introduction of one (**2a**) or two (**2b**) methyl groups or a *n*-butyl residue (**2c**) in the α position of the carboxyl group of **1** was without effect. However, elongation of the *n*-alkyl chain [*n*-hexyl (**2d**) and *n*-octyl (**2f**)] yielded potent inhibitors of mPGES-1 (Table 1). The α-phenyl-substituted **2g** was hardly active, but introduction of a naphthyl moiety (**2h**) clearly enhanced the efficacy against mPGES-1, comparable to the *n*-octyl-substituted **2f**. Together, *n*-hexyl, *n*-octyl, or naphthyl substitution of **1** in the α position leads to mPGES-1 inhibition, implying a requirement of bulky lipophilic substituents. Note that the novel derivatives **2h** and **2f**, which are carboxylic acids possessing bulky α-substituents, also efficiently inhibited 5-LO product synthesis in PMNL (Table 1), suggesting that similar SARs are applicable for both mPGES-1 and 5-LO. The effectiveness of the free carboxylic acids against 5-LO is surprising because, for interference with 5-LO product formation in PMNL, the corresponding esters have been found to be generally superior

Table 1. Inhibition of PGE_2 Formation in Microsomal Preparations of A549 Cells and Inhibition of 5-LO Product Formation in PMNL by Test Compounds[d]

comp.	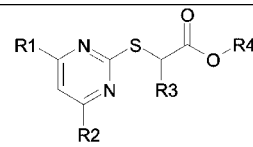 R1	R2	R3	R4	cell-free mPGES-1 activity (percentage of control) at 10 μM	PMNL 5-LO activity (percentage of control) at 10 μM
1	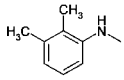	-Cl	-H	-H	n.i.[a]	n.i.[b]
2a	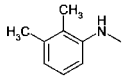	-Cl	$-CH_3$	-H	n.i.	n.i.[b]
2b	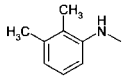	-Cl	$-(CH_3)_2$	-H	83.8 (± 7.4)	n.i.[b]
2c	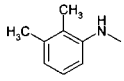	-Cl	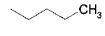	-H	n.i.	n.i.[b]
2d	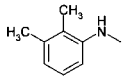	-Cl	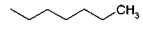	-H	31.9 (± 5.6)***	28.9 (± 14.3)***b
2e	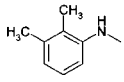	-Cl	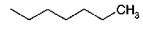	$-C_2H_5$	n.i.	30.5 (± 2.8)***b
2f	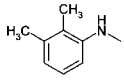	-Cl	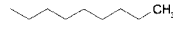	-H	29.8 (± 7.1)***	7.0 (± 2.3)***
2g	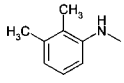	-Cl		-H	74.6 (± 1.9)	n.i.[b]
2h	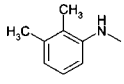	-Cl		-H	39.6 (± 5.2)***	16.8 (± 9.6)***
3a	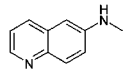	-Cl	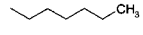	-H	59.0 (± 6.5)**	20.1 (± 1.9)***b
3b	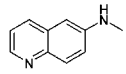	-Cl	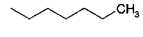	$-C_2H_5$	39.1 (± 5.8)***	4.0 (± 1.2)***b
3c	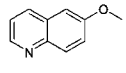	-Cl	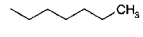	-H	67.4 (± 7.3)*	10.7 (± 2.7)***b
3d	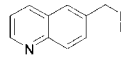	-Cl	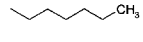	-H	85.7 (± 8.9)	26.7 (± 2.2)***b
4	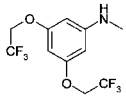	-Cl	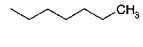	-H	26.7 (± 1.8)***	8.0 (± 4.0)***
5a	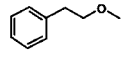	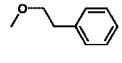	-H	-H	66.4 (± 2.4)*	40.6 (± 10.0)***

Table 1. Continued

comp.	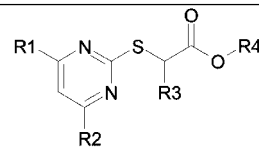 R1	R2	R3	R4	cell-free mPGES-1 activity (percentage of control) at 10 μM	PMNL 5-LO activity (percentage of control) at 10 μM
5b	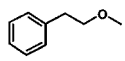	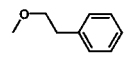	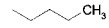	-H	43.1 (± 5.4)***	2.7 (± 0.2)***
5c	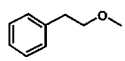	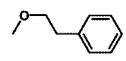	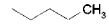	$-C_2H_5$	n.i.	80.1 (± 9.1)
6a	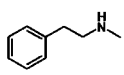	-Cl		-H	70.0 (± 9.4)	16.07 (± 6.3)***
6b	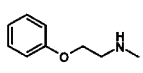	-Cl		-H	79.9 (± 6.2)	28.0 (± 8.0)***
6c	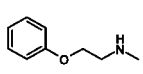	-Cl		$-C_2H_5$	80.7 (± 8.0)	37.1 (± 4.9)***
7a	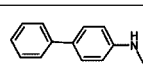	-Cl		-H	21.7 (± 2.9)***	4.1 (± 1.1)***
7b	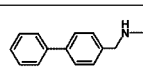	-Cl		-H	21.8 (± 4.2)***	3.0 (± 2.3)***
7c	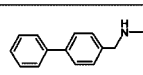	-Cl	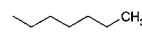	$-C_2H_5$	n.i.	80.2 (± 9.9)
7d	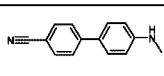	-Cl	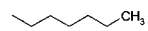	-H	26.1 (± 8.0)***	2.7 (± 0.8)***
7d(S)	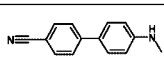	-Cl		-H	23.0 (± 5.9)***	2.8 (± 1.7)***
7d(R)	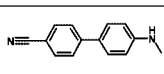	-Cl		-H	36.8 (± 4.7)***	2.8 (± 1.5)***
7e	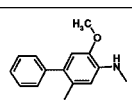	-Cl	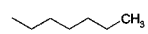	-H	24.9 (± 1.2)***	3.1 (± 0.6)***
8	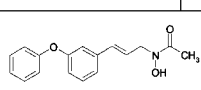				n.i.	3.3 (± 0.5)***c
9	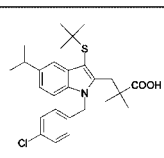				25.5 (± 2.8)***	n.i.

[a] n.i. = no inhibition. [b] Published by Werz et al.[16] [c] Inhibition at 1 μM. [d] Mean values ($n = 3-4$) and standard error estimates are given: (*) $p < 0.05$, (**) $p < 0.01$, and (***) $p < 0.001$.

over the free acids.[16] Here, we find that the need for esterification was abolished by insertion of long and bulky alkyl/aryl residues in the α position of the carboxylic group, reflected by the high efficacy of the α-naphthyl derivative **2h** and the α-(*n*-octyl)-analogue **2f** against 5-LO.

Replacement of the 2,3-dimethylphenyl residue by a quinoline moiety (**3a**−**3d**), regardless of the bridging atom (N or O), was shown to significantly improve inhibition of 5-LO product formation.[16] Although this derivatization did not enhance the potency of the α-(*n*-hexyl)-substituted free acids **3a**, **3c**, and

3d toward mPGES-1, compound **3b**, the esterified analogue of **3a**, was quite efficient and remarkably superior over its 2,3-dimethylphenyl analogue **2e**. Therefore, the presence of a quinoline residue apparently overcomes the necessity of the free carboxylic group, whereas all other esters tested were rather poor inhibitors of mPGES-1. For example, **2e**, the ethyl ester of **2d** (that potently inhibited mPGES-1), failed to suppress PGE_2 formation, suggesting that the free carboxylic group governs mPGES-1 inhibition. Why the ester **3b** was superior over the free acid as inhibitor of mPGES-1 is not readily understood and requires more detailed analysis.

Also, the exchange of the 2,3-dimethylaniline by more bulky lipophilic substituents at C6 of the pyrimidine, for example, by 3,5-bis(2,2,2-trifluoroethoxy)-aniline (**4**), led to derivatives that were similarly active on mPGES-1 as compared to **2d**. Of interest, the carboxylic acid **4** also potently inhibited 5-LO product synthesis. Hence, bulky lipohilic substituents not only in the α position but also linked to the pyrimidine ring may allow the free acid analogues to inhibit cellular 5-LO product formation. Along these lines, replacement of the 2,3-dimethylaniline moiety and the chlorine at the pyrimidine ring of **1** by phenylethoxy residues led to compound **5a** and its α-butyl analogue **5b**, free acids that moderately (**5a**) or potently (**5b**) blocked 5-LO product synthesis in PMNL, respectively. Both compounds also inhibited mPGES-1, and again, the corresponding ester of **5b**, namely, compound **5c**, was not (mPGES-1) or hardly (5-LO) active.

In view of the SARs regarding mPGES-1 apparent thus far, bulky lipophilic substituents at C6 of the pyrimidine ring could basically increase the efficacy. Whereas exchange of the 2,3-dimethylaniline by phenethylamine (**6a**) or phenoxyethylamine (**6b** or **6c**) failed to increase the potency versus **2d**, introduction of a biphenyl-4-amine (**7a**) or a biphenyl-4-methane amine moiety (**7b**) yielded derivatives that potently inhibited mPGES-1 as well as 5-LO. The corresponding esters (exemplified by **7c**) failed to interfere with mPGES-1 and also were hardly active against 5-LO. Moreover, substitutions of the biphenyl-4-amino moiety were tolerated, because introduction of a cyano group in position 4′ (**7d**) or methyl and methoxy substitutents at the biphenyl (**7e**) did not hamper the interference with either mPGES-1 or 5-LO. Finally, we investigated whether or not the absolute configuration of the α-C atom next to the carboxyl group influences the potencies of the compounds. The two enantiomeric forms of the *n*-hexyl-substituted derivative **7d**, namely, **7d**(*R*) and **7d**(*S*) were separated and tested for inhibition of 5-LO and mPGES-1. Neither for inhibition of 5-LO (intact cells or cell-free assay) nor for mPGES-1 was a marked discrepancy in the efficacies (mPGES-1, $IC_{50} = 1.6$ and 2.1 μM, respectively, and cell-free 5-LO, $IC_{50} = 0.8$ and 1.5 μM, respectively) determined, implying that the absolute configuration is essentially negligible. Taken together, two structural modifications of the parental inactive compound **1**, namely, (I) introduction of an *n*-hexyl residue in the α position and (II) replacement of the 2,3-dimethylaniline at the C6 of the pyrimidine ring by a biphenyl-4-yl-methanamine residue yield efficient dual mPGES-1/5-LO inhibitors, including **7a**, **7b**, **7d**, and **7e**, with about equal efficacies for both enzymes.

Detailed Analysis of Selected Test Compounds on mPGES-1, 5-Lipoxygenase, and Cyclooxygenases. As stated above and shown in Table 2, there is obviously a strong correlation between the efficiency against mPGES-1 and 5-LO, and all eight representatives chosen block both enzymes similarly well with comparable IC_{50} values in the range of 1.3−5.6 μM for mPGES-1 and in the range of 0.4−5 μM for 5-LO in PMNL. Compound **7b** turned out to be the most potent mPGES-1 inhibitor, with an $IC_{50} = 1.3$ μM, being even somewhat superior over **9** [$IC_{50} = 2.1$ (Table 2) and 2.4 μM[6]]. Compound **7d** was the most active inhibitor of 5-LO in intact PMNL and purified 5-LO ($IC_{50} = 0.4$ and 1.5 μM, respectively), with similar potency as 1-(1-(benzo[*b*]thiophen-2-yl)ethyl)-1-hydroxyurea (zileuton, Zyflo), the most advanced 5-LO inhibitor under comparable conditions ($IC_{50} = 0.5$ to 1 μM[20]). Importantly, the reported discrepancy between the potency regarding 5-LO inhibition in cell-based assays (high efficacy) and cell-free systems (low efficacy) that was originally apparent for the ester **3b** and other esterified derivatives of **1**[16] is not evident for the free acids. Thus, the α-(*n*-hexyl)-substituted acids bearing a bulky lipophilic residue at C6 of the pyrimidine ring also potently inhibit 5-LO in cell-free assays, with IC_{50} values in the range of 1.5−6.5 μM, and can thus be designated direct 5-LO inhibitors.

Ideally, the preferred pharmacological dynamics of a lead compound for intervention with chronic inflammatory diseases, CVD, or cancer without typical side effects of NSAIDs and coxibs could comprise a potent and dually suppressive effect on mPGES-1 and 5-LO without inhibiting COX isoenzymes.[13] Accordingly, selected potent dual mPGES-1/5-LO inhibitors from the first screening round were investigated for their pharmacological profile in more detail. Because lipophilic acids, such as **1** and its derivatives mimicking AA, are likely to act on COX enzymes and because the active lead compounds inhibit the COX-related mPGES-1 and 5-LO about equally well, it appeared reasonable to address if the compounds may also interfere with COX-1/2. The effects of selected compounds on the activities of isolated ovine COX-1 and human recombinant COX-2 [using the COX metabolite 12(*S*)-hydroxy-5-*cis*-8,10-*trans*-heptadecatrienoic acid (12-HHT) as a biomarker[21]] were determined. With the exception of compounds **2h** and **4**, all selected derivatives were only moderate inhibitors of COX-1 and COX-2, with IC_{50} values > 10 μM. In control experiments, 2-[1-(4-chlorobenzoyl)-5-methoxy-2-methyl-1*H*-indol-3-yl]acetic acid (indomethacin, 10 μM) suppressed the activity of COX-1 and 4-(5-(4-methylphenyl)-3-(trifluoromethyl)pyrazol-1-yl)benzenesulfonamide (celecoxib, 5 μM) inhibited the activity of COX-2 with 19 ± 2 and 21 ± 3% remaining activity, respectively. Therefore, we conclude that COX inhibition by the lead compounds is markedly less pronounced as compared to interference with 5-LO and mPGES-1.

Effectiveness of the PA Derivatives on PGE_2 Formation in Intact A549 Cells. In contrast to the convenient cell-based assay applied for the evaluation of 5-LO inhibitors, assessment of mPGES-1 inhibitors in intact cell assays is laborious.[13] Hence, we analyzed only select compounds (i.e., **2d**, **4**, and **7b**) for inhibition of PGE_2 formation in IL-1β-stimulated A549 cells. For PGE_2 biosynthesis in intact cells, phospholipases A_2 liberate AA as a substrate for COX isoenzymes to produce PGH_2 that is eventually transformed by selective PG or thromboxane synthases to various structurally related eicosanoids. In IL-1β-treated A549 cells, PGH_2 is provided by highly expressed COX-2 and converted by mPGES-1,[22] whereas COX-1 could not be detected.[23] After 48 h of treatment with IL-1β and preincubation (10 min) with test compounds, cells were activated via massive intracellular Ca^{2+} influx using 2.5 μM Ca^{2+} ionophore A23187 [5-methylamino-2-(2*S*,3*R*,5*R*,8*S*,9*S*)-3,5,9-trimethyl-2-(1-oxo-1-(1*H*-pyrrol-2-yl)propan-2-yl)-1,7-dioxaspiro(5.5)undecan-8-yl)methyl)benzooxazole-4-carboxylic acid]. Simultaneously, exogenous AA [1 μM AA and 18.4 kBq [^{3}H]AA] was provided to initiate PGH_2 formation and

Table 2. IC_{50} Values for mPGES-1 in Microsomal Preparations of A549 Cells, 5-LO Activity in PMNL, and Purified 5-LO in a Cell-Free Assay[c]

comp.	structure	mPGES-1 (IC_{50} [μM]) cell-free	5-LO (IC_{50} [μM]) PMNL	5-LO (IC_{50} [μM]) pur. 5-LO	COX (remaining activity at 10 μM) COX-1	COX (remaining activity at 10 μM) COX-2
2h	R1 = 2,3-dimethylaniline R2 = naphthyl R3 = -H	5.1	5.0	n.d.[a]	42.2 (±11.4)***	32.5 (± 7.3)***
2d	R1 = 2,3-dimethylaniline R2 = *n*-hexyl R3 = -H	3.9	4.1	6.5	75.2 (± 8.9)	62.0 (± 5.6)*
3b	R1 = 6-aminoquinoline R2 = *n*-hexyl R3 = $-C_2H_5$	5.6	0.6	19.0	69.5 (± 1.9)	61.7 (± 9.3)*
4	R1 = 3,5-bis(2,2,2-trifluoroethoxy)aniline R2 = *n*-hexyl R3 = -H	2.6	1.5	3.0	40.0 (± 8.9)***	70.4 (± 9.3)
7a	R1 = biphenyl-4-amine R2 = *n*-hexyl R3 = -H	1.6	0.7	1.5	52.3 (± 0.9)**	57.1 (± 5.1)**
7b	R1 = biphenyl-4-yl-methan-amine R2 = *n*-hexyl R3 = -H	1.3	1.0	2.0	67.3 (± 1.2)	61.3 (± 3.7)**
7d	R1 = 4'-cyanobiphenyl-4-ylamine R2 = *n*-hexyl R3 = -H	1.7	0.4	1.5	66.0 (± 8.3)*	61.2 (± 3.6)**
7e	R1 = 5-methoxy-2-methyl-biphenyl-4-amine R2 = *n*-hexyl R3 = -H	2.1	0.5	2.0	71.2 (± 1.0)	53.7 (± 3.8)**
8	*N*-(3-phenoxycinnamyl)-acetohydroxamic acid	n.i.[b]	0.11	0.16	n.d.	n.d.
9	3-[1-(4-chlorobenzyl)-3-t-butyl-thio-5-isopropylindol-2-yl]-2,2-dimethylpropanoic acid	2.1	0.09	n.i.[b]	n.d.	n.d.

[a] n.d. = not determined. [b] n.i. = no significant inhibition at 10 μM. [c] Inhibition of isolated ovine COX-1 and human recombinant COX-2 by selected compounds given as remaining activity at 10 μM. Mean values ($n = 3$) and standard error estimates are given: (*) $p < 0.05$, (**) $p < 0.01$, and (***) $p < 0.001$.

circumvent the need for release of endogenous AA by phospholipases. ^{3}H-labeled PGE_2 was separated by RP-HPLC from other eicosanoids and quantified by liquid scintillation counting. As expected, PGE_2 formation was almost completely suppressed by the COX inhibitors indomethacin (10 μM, data not shown) or celecoxib (5 μM) (Figure 1). Inhibition of mPGES-1 in intact A549 cells by **9** (33 μM) reduced PGE_2 formation by only 63%. Compounds **2d** and **7b** concentration-dependently inhibited PGE_2 formation, with apparent IC_{50} values of 12 and 6 μM, respectively (Figure 1). However, inhibition of PGE_2 formation already started at effective concentrations ≥1−3 μM, but neither **2d**, **4**, or **7b** nor the mPGES-1 inhibitor **9** completely inhibited PGE_2 synthesis. Compound **4** was markedly less potent, and inhibition of PGE_2 formation started first at 10 μM, with the apparent IC_{50} value being >30 μM (Figure 2).

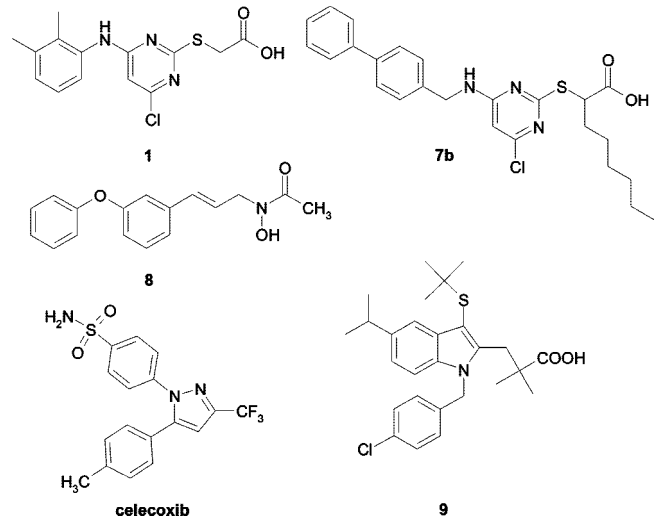

Figure 1. Chemical structures of selected inhibitors.

Conclusions

Here, we present the design of compounds that combine a potent suppression of PGE_2 formation by inhibiting mPGES-1 with a potent 5-LO inhibitory action, leading to reduced levels of LTs, but lack pronounced interference with both COX-1 and COX-2. In particular, the biphenylic derivatives of **1** (e.g., **7b**) were most potent, but also **2d** and **4** are efficient dual inhibitors of mPGES-1 and 5-LO in cell-free assay and cell-based systems. However, in contrast to the COX inhibitors celecoxib and indomethacin, PGE_2 formation was not completely suppressed in A549 cells by the derivatives of **1** as well as by **9**, with 30−40% PGE_2 still remaining, probably related to the action of other PGE_2 synthases not affected by the compounds. Dual inhibitors of COX/5-LO are superior over compounds interfering

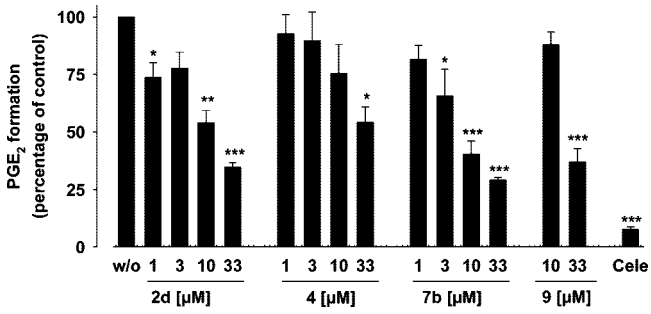

Figure 2. Effects of test compounds on the formation of PGE_2 in intact A549 cells. A549 cells (4×10^6/mL) were pre-incubated with test compounds or vehicle (DMSO) for 10 min, and then cellular PGE_2 synthesis was elicited by addition of 2.5 μM Ca^{2+} ionophore A23187 plus 1 μM AA and [^{3}H]AA (18.4 kBq). After 15 min at 37 °C, formed [^{3}H]PGE_2 was analyzed by RP-HPLC and liquid scintillation counting as described in the Materials and Methods. Data are given as mean ± standard error (SE). $n = 3$. (∗) $p < 0.05$, (∗∗) $p < 0.01$, or (∗∗∗) $p < 0.001$ versus vehicle (0.1% DMSO) control. ANOVA + Tukey HSD posthoc tests. Cele = celecoxib, 5 μM.

with only COX enzymes (i.e., NSAIDs and coxibs) in terms of anti-inflammatory effectiveness associated with a lower incidence of gastrointestinal and cardiovascular toxicity.[11] This might be attributable to the accompanied suppression of pro-inflammatory LTs,[24] which significantly contribute to gastric epithelial injury and atherogenesis.[10] For example, licofelone that blocks mPGES-1, LT formation, and COX-1 without inhibiting COX-2[13] exhibits a significantly superior gastric tolerability and a lower incidence of ulcers compared to (*S*)-2-(6-methoxynaphthalen-2-yl)propanoic acid (naproxen) in healthy humans,[25] and in contrast to COX-2-selective inhibitors, licofelone reduced neointimal formation and inflammation in an atherosclerotic model.[26] To our knowledge, no dual mPGES-1/5-LO inhibitor has been reported, although MK-886 and licofelone inhibit mPGES-1[6,13] and the 5-LO-activating protein,[27,28] also leading to suppression of PGE_2 and LT formation. Future experiments aiming to resolve the detailed interference of these compounds presented here with mPGES-1 and the 5-LO enzyme as well as studies addressing the effectiveness *in vivo* using animal models of inflammation, fever, pain, cancer, or atherosclerosis are necessary and may reveal the therapeutic potential of PA derivatives for intervention with mPGES-1- and 5-LO-related diseases.

Materials and Methods

Compounds and Chemistry. Compound **1** was purchased from Sigma-Aldrich (Deisenhofen, Germany). The structures of previously reported compounds **2a**−**4** were confirmed by ^{1}H and ^{13}C NMR, as well as by mass spectrometry (ESI); the purity (>98%) was checked by combustion analysis as described.[15,18]

Compounds **5a**−**7e** were synthesized as described in Scheme 1. The synthesis is modified from the method reported from D'Atri et al.[17] All commercial chemicals and solvents are of reagent grade and were used without further purification, unless otherwise specified. ^{1}H and ^{13}C NMR spectra were measured in DMSO-d_6 or $CDCl_3$ on a Bruker ARX 300 (^{1}H NMR) and AC 200 E (^{13}C NMR) spectrometer. Chemical shifts are reported in parts per million (ppm) using tetramethylsilane (TMS) as an internal standard. Mass spectra were obtained on a Fissous Instruments VG Platform 2 spectrometer measuring in the positive- or negative-ion mode (ESI−MS system). Elemental analysis has been performed by the Microanalytical Laboratory of the Institute of Organic Chemistry and Chemical Biology, Goethe-University Frankfurt, on a Foss Heraeus CHN-O-rapid elemental analyzer (for details see the Supporting Information).

The synthetic procedure is exemplified by the following description of the synthesis of key compounds **7b** and **7d**.

Step (i) (Z = *n*-Hexyl). 2-Thiobarbituric acid (1 equiv) was dissolved under heating in DMF/triethylamine (3 equiv), and ethyl-2-bromooctyl acetate (1.5 equiv) was added dropwise. After 2 h, the reaction mixture was quenched with 4 parts of water and extracted with ethyl acetate. The residue obtained from the organic phase was recrystallized from ethyl acetate/*n*-hexane to give ethyl 2-(4,6-dihydroxypyrimidin-2-ylthio)octanoate (50%).

Step (ii). To a solution of the thioether resulting from step (i) (1 equiv) in $POCl_3$ (18 equiv), *N*,*N*-diethylaniline (1 equiv) was added. After refluxing the solution at 110 °C for 3.5 h, the excessive $POCl_3$ was distilled *in vacuo* and the oily residue was poured upon crushed ice. The aqueous solution was extracted with ethyl acetate, and combined organic layers were washed with diluted HCl, saturated $NaHCO_3$ solution, and brine. The organic layer was dried over $MgSO_4$, filtered, and evaporated under reduced pressure. Purifying the resulting oil by column chromatography (*n*-hexane/ethyl acetate) gave ethyl 2-(4,6-dichloropyrimidin-2-ylthio)octanoate (85%).

Step (iii). A mixture of the chlorinated pyrimidine (1 equiv) obtained from step (ii), the appropriate aniline/amine derivate (1.05 equiv), triethylamine (3 equiv), and EtOH was prepared and heated under reflux (**7b**-ester, 6 h; **7d**-ester, 96 h). The reaction mixture was evaporated under reduced pressure. The residue was dissolved in ethyl acetate, and the organic layer was extracted with diluted HCl, saturated $NaHCO_3$ solution, and brine. After drying over $MgSO_4$, the solvent was evaporated under reduced pressure and the residue was purified by column chromatography (*n*-hexane/ethyl acetate) to give ethyl 2-(4-(biphenyl-4-ylmethylamino)-6-chloropyrimidin-2-ylthio)octanoate (**7b**-ester, 40%) and ethyl 2-(4-chloro-6-(4′-cyanobiphenyl-4-ylamino)pyrimidin-2-ylthio)-octanoate (**7d**-ester, 60%), respectively.

Step (iv). The respective ester (1 equiv) from step (iii) was dissolved in EtOH, and LiOH (3 equiv) was added. After stirring for 24 h at room temperature, EtOH was removed and the residue was dissolved in water (under heating, if necessary, low amounts of MeOH were added). This solution was acidified with diluted hydrochloric acid, and the precipitate was filtered, washed to neutrality with water and then with *n*-hexane. Recrystallization from *n*-hexane/ethyl acetate gave the carboxylic acids.

2-(4-(Biphenyl-4-ylmethylamino)-6-chloropyrimidin-2-ylthio)octanoic Acid (7b). mp = 110 °C. ^{1}H NMR (300.13 MHz, $(CD_3)_2SO$) δ: 0.77 (t, 3H, C*H*$_3$−Hex, $J = 6.3$ Hz), 1.14−1.28 (m, 8H, C*H*$_2$−Hex), 1.66−1.84 (m, 2H, C*H*$_2$−Hex), 4.23 (t, 1H, S−C*H*, $J = 7.1$ Hz), 4.49 (dd, 1H, C*H*$_2$−NH, $J_1 = 5.4$ Hz, $J_2 = 15.5$ Hz), 4.65 (dd, 1H, C*H*$_{2B}$−NH, $J_1 = 5.6$ Hz, $J_2 = 15$ Hz), 6.31 (s, 1H, Pyr−5*H*), 7.31−7.47 (m, 5H, Ph−*H* + Ph′−*H*), 7.61 (d, 2H, Ph−3*H* + Ph−5*H*, $J = 1.8$ Hz), 7.64 (d, 2H, Ph′−2*H* + Ph−6*H*, $J = 1.2$ Hz), 8.39 (t,1H, −N*H*, $J = 4.8$ Hz). ^{13}C NMR (75.45 MHz, $(CD_3)_2SO$) δ: 13.80 (*C*H$_3$−Hex), 21.89 (*C*H$_2$−Hex), 26.50 (*C*H$_2$−Hex), 28.13 (*C*H$_2$−Hex), 30.95 (*C*H$_2$−Hex), 31.39 (*C*H$_2$−Hex), 43.29 (*C*H$_2$−NH), 47.26 (S−*C*H), 99.54 (Pyr−C_5), 126.50 (2C, Ph−C_3 + −C_5), 126.67 (2C, Ph′−C_2 + −C_6), 127.32 (Ph′−C_4), 127.89 (2C, Ph−C_2 + −C_6), 128.85 (2C, Ph′−C_3 + −C_5), 138.04 (Ph−C_4), 138.91 (Ph′−C_1), 139.82 (Ph−C_1), 156.57 (Pyr−C_6), 162.40 (Pyr−C_4), 169.76 (Pyr−C_2), 172.72 (*C*OOH). MS (ESI+): *m/e* 470.1 $[M + H]^+$. Anal. Calcd ($C_{25}H_{28}ClN_3O_2S$): C, H, N. Yield: 80%.

2-(4-Chloro-6-(4′-cyanobiphenyl-4-ylamino)pyrimidin-2-ylthio)octanoic Acid (7d). mp = 111 °C. ^{1}H NMR (300.13 MHz, $(CD_3)_2SO$) δ: 0.77 (t, 3H, C*H*$_3$−Hex, $J = 6.5$ Hz), 1.17−1.36 (m, 8H, C*H*$_2$−Hex), 1.77−1.94 (m, 2H, C*H*$_2$−Hex), 4.37 (t, 1H, S−C*H*, $J = 7.1$ Hz), 6.56 (s, 1H, Pyr−5*H*), 7.70−7.77 (m, 4H, Ph−*H*), 7.85−7.92 (m, 4H, Ph′−*H*), 10.13 (s,1H, −N*H*). ^{13}C NMR (75.45 MHz, $(CD_3)_2SO$) δ: 13.77 (*C*H$_3$−Hex), 21.87 (*C*H$_2$−Hex), 26.49 (*C*H$_2$−Hex), 28.08 (*C*H$_2$−Hex), 30.93 (*C*H$_2$−Hex), 31.61 (*C*H$_2$−Hex), 47.13 (S−*C*H), 101.44 (Pyr−C_5), 109.50 (Ph′−C_4), 118.88 (−*C*N), 120.77 (2C, Ph−C_2 + −C_6), 126.92 (2C, Ph′−C_2 + −C_6), 127.50 (2C, Ph−C_3 + −C_5), 132.80 (2C, Ph′−C_3 + −C_5), 139.27 (Ph′−C_1), 143.97 (Ph−C_1), 157.48 (Pyr−C_6), 160.43

(Pyr−C_2), 170.02 (Pyr−C_4), 172.38 (*C*OOH). MS (ESI+): *m/e* 481.0 $[M + H]^+$. Anal. Calcd ($C_{25}H_{25}ClN_4O_2S$): C, H, N. Yield: 60%.

Assay Systems. Materials. DMEM/high glucose (4.5 g/L) medium, penicillin, streptomycin, and trypsin/EDTA solution were obtained from PAA (Coelbe, Germany). PGH_2 was obtained from Larodan (Malmö, Sweden). 11β-PGE_2, PGB_1, MK-886, human recombinant COX-2, and ovine isolated COX-1 were obtained from Cayman Chemical (Ann Arbor, MI). [5,6,8,9,11,12,14,15-^{3}H] AA ([^{3}H]AA) was obtained from BioTrend Chemicals GmbH (Cologne, Germany). Ultima Gold XR was obtained from Perkin-Elmer (Boston, MA). All other chemicals were obtained from Sigma-Aldrich (Deisenhofen, Germany), unless stated otherwise.

Cells and Cell Viability Assay. Blood cells were freshly isolated from leukocyte concentrates obtained at the Blood Center of the University Hospital Tuebingen (Germany) as described.[29] In brief, venous blood was taken from healthy adult donors that did not take any medication for at least 7 days, and leukocyte concentrates were prepared by centrifugation (4000*g*, 20 min, 20 °C). Cells were immediately isolated by dextran sedimentation and centrifugation on Nycoprep cushions (PAA, Coelbe, Germany). For incubations with solubilized compounds, methanol or DMSO was used as vehicle, never exceeding 1% (v/v). PMNL were immediately isolated from the pellet after centrifugation on Nycoprep cushions, and hypotonic lysis of erythrocytes was performed as described.[30] Cells were finally resuspended in phosphate-buffered saline (PBS) at pH 7.4, containing 1 mg/mL glucose and 1 mM $CaCl_2$ (PGC buffer) (purity > 96−97%).

A549 cells were cultured in DMEM/high glucose (4.5 g/L) medium supplemented with heat-inactivated fetal calf serum (10%, v/v), penicillin (100 units/mL), and streptomycin (100 μg/mL) at 37 °C and 5% CO_2. After 3 days, confluent cells were detached using 1× trypsin/EDTA solution and reseeded at 2×10^6 cells in 20 mL of medium. Cell viability was measured using the colorimetric thiazolyl blue tetrazolium bromide (MTT) dye reduction assay as described.[31] A549 cells (4×10^4 cells/100 μL of medium) were plated into a 96-well microplate and incubated at 37 °C and 5% CO_2 for 16 h. Then, test compounds or solvent (DMSO) were added, and the samples were incubated for another 5 h. MTT (20 μL, 5 mg/mL) was added, and the incubations were continued for 4 h. The formazan product was solubilized with sodium dodecylsulfate [10% (w/v), in 20 mM HCl], and the absorbance of each sample was measured at 595 nm relative to that of vehicle (DMSO)-treated control cells using a multiwell scanning spectrophotometer (Victor^3 plate reader, Perkin-Elmer, Rodgau-Juegesheim, Germany). Compounds **1**, **2d**, **4**, and **7b** did not significantly reduce cell viability within 5 h at 10 μM (data not shown), excluding possible acute cytotoxic effects of the compound in the cellular assays.

Determination of 5-LO Product Formation in Intact Cells. For assays of intact cells, 5×10^6 freshly isolated PMNL were resuspended in 1 mL of PGC buffer. After pre-incubation with the test compounds (15 min, RT), 5-LO product formation was started by addition of 2.5 μM Ca^{2+}-ionophore A23187 plus 20 μM AA. After 10 min at 37 °C, the reaction was stopped with 1 mL of methanol and 30 μL of 1 N HCl, 200 ng of prostaglandin B_1, and 500 μL of PBS were added. Formed 5-LO metabolites were extracted and analyzed by HPLC as described.[30] 5-LO product formation is expressed as nanograms of 5-LO products per 10^6 cells, which includes LTB_4 and its all-*trans* isomers, and 5(*S*)-hydro(p-ero)xy-6-*trans*-8,11,14-*cis*-eicosatetraenoic acid. Cysteinyl LTs C_4, D_4, and E_4 were not detected, and oxidation products of LTB_4 were not determined.

Expression and Purification of Human Recombinant 5-LO from *Escherichia coli.* *E. coli* MV1190 was transformed with pT3-5LO plasmid, and recombinant 5-LO protein was expressed at 27 °C as described.[32] Cells were lysed by incubation in 50 mM triethanolamine/HCl at pH 8.0, 5 mM EDTA, soybean trypsin inhibitor (60 μg/mL), 1 mM phenylmethylsulfonyl fluoride (PMSF), and lysozyme (500 μg/mL), homogenized by sonication (3 × 15 s), and centrifuged at 100000*g* for 70 min at 4 °C. The resulting 100000*g* supernatants were applied to an ATP-agarose column (Sigma A2767, Deisenhofen, Germany), and the column was eluted as described previously.[33] Partially purified 5-LO was immediately used for *in vitro* activity assays.

Determination of 5-LO Activity of Semi-purified 5-LO. Partially purified 5-LO was added to 1 mL of a 5-LO reaction mix (PBS at pH 7.4, 1 mM EDTA, and 1 mM ATP). Samples were pre-incubated with the test compounds for 10 min at 4 °C and prewarmed for 30 s at 37 °C, and 2 mM $CaCl_2$ and 20 μM AA were added to start 5-LO product formation. The reaction was stopped after 10 min at 37 °C by the addition of 1 mL ice-cold methanol, and the formed metabolites were analyzed as described for intact cells.

Induction of mPGES-1 in A549 Cells and Isolation of Microsomes. Preparation of A549 cells was performed as described.[22] In brief, cells (2×10^6 cells) in 20 mL of DMEM/high glucose (4.5 g/L) medium containing FCS (2%, v/v) were incubated for 16 h at 37 °C and 5% CO_2. Subsequently, the culture medium was replaced by fresh medium; IL-1β (1 ng/mL) was added; and cells were incubated for another 72 h. Thereafter, cells were detached with trypsin/EDTA, washed with PBS, and frozen in liquid nitrogen. Ice-cold homogenization buffer (0.1 M potassium phosphate buffer at pH 7.4, 1 mM PMSF, 60 μg/mL soybean trypsin inhibitor, 1 μg/mL leupeptin, 2.5 mM glutathione, and 250 mM sucrose) was added, and after 15 min, cells were resuspended and sonicated on ice (3 × 20 s). The homogenate was subjected to differential centrifugation at 10000*g* for 10 min and 174000*g* for 1 h at 4 °C. The pellet (microsomal fraction) was resuspended in 1 mL of homogenization buffer, and the protein concentration was determined by the Coomassie protein assay.

Determination of PGE_2 Synthase Activity in Microsomes of A549 Cells. Microsomal membranes of A549 cells were diluted in potassium phosphate buffer (0.1 M, pH 7.4) containing 2.5 mM glutathione (100 μL total volume), and test compounds or vehicle (DMSO) was added. After 15 min, PGE_2 formation was initiated by the addition of PGH_2 (20 μM, final concentration). After 1 min at 4 °C, the reaction was terminated with 100 μL of stop solution (40 mM $FeCl_2$, 80 mM citric acid, and 10 μM of 11β-PGE_2), and PGE_2 was separated by solid-phase extraction on reversed-phase (RP) C18 material using acetonitrile (200 μL) as an eluent and analyzed by RP-HPLC [30% acetonitrile aqueous + 0.007% TFA (v/v), Nova-Pak C18 column, 5 × 100 mm, 4 μm particle size, flow rate of 1 mL/min], with UV detection at 195 nm. 11β-PGE_2 was used as an internal standard to quantify PGE_2 product formation by integration of the area under the peaks.

Determination of PGE_2 Formation in Intact A549 Cells. A549 cells (2×10^6), treated with IL-1β for 72 h as described above, were resuspended in 0.5 mL of PBS containing 1 mM $CaCl_2$ and pre-incubated with the indicated compounds at 37 °C for 10 min, and PGE_2 formation was started by the addition of Ca^{2+}-ionophore A23187 (2.5 μM), AA (1 μM), and [^{3}H]AA (18.4 kBq). The reaction was stopped after 15 min at 37 °C, and the samples were put on ice. After centrifugation (800*g*, 5 min, 4 °C), the supernatant was acidified to pH 3 by the addition of citric acid (20 μL, 2 M) and the internal standard 11β-PGE_2 (2 nmol) was added. PGE_2 was separated by solid-phase extraction and RP-HPLC as described above. The amount of 11β-PGE_2 was quantified by integration of the area under the eluted peaks. For quantification of radiolabeled PGE_2, fractions (0.5 mL) were collected and mixed with Ultima Gold XR (2 mL) for liquid scintillation counting in a LKB Wallac 1209 Rackbeta liquid scintillation counter.

Activity Assays of Isolated COX-1 and COX-2. Inhibition of the activities of isolated ovine COX-1 and human COX-2 was performed as described.[21,34] Although the purified COX-1 is not of human origin, ovine COX-1 is generally used for inhibitor studies when examining the effectiveness of compounds on the activity of isolated COX-1 enzyme.[34] Briefly, purified COX-1 (ovine, 50 units) or COX-2 (human recombinant, 20 units) were diluted in 1 mL reaction mixture containing 100 mM Tris buffer at pH 8, 5 mM glutathione, 5 μM hemoglobin, and 100 μM EDTA at 4 °C and pre-incubated with the test compounds for 5 min. Samples were prewarmed for 60 s at 37 °C, and AA (5 μM for COX-1 and 2 μM

for COX-2) was added to start the reaction. After 5 min at 37 °C, the COX product 12-HHT was extracted and then analyzed by HPLC as described.[29]

Statistics. Data are expressed as mean ± SE. The IC_{50} values were analyzed using GraphPad Prism. The program Graphpad Instat (Graphpad Software, Inc., San Diego, CA) was used for statistical comparisons. Statistical evaluation of the data was performed by one-way ANOVAs for independent or correlated samples followed by Tukey HSD posthoc tests. A p value of <0.05 (*) was considered significant.

Acknowledgment. We thank Gertrud Kleefeld and Bianca Jazzar for expert technical assistance. This work was supported by the LOEWE Lipid Signaling Forschungszentrum Frankfurt (LiFF).

Supporting Information Available: Chemical synthesis and routine analytics by ^1H and ^{13}C NMR, mass spectrometry (ESI−), and elemental analysis. This material is available free of charge via the Internet at http://pubs.acs.org.

References

(1) Funk, C. D. Prostaglandins and leukotrienes: Advances in eicosanoid biology. *Science* **2001**, *294*, 1871–1875.
(2) Samuelsson, B.; Morgenstern, R.; Jakobsson, P. J. Membrane prostaglandin E synthase-1: A novel therapeutic target. *Pharmacol. Rev.* **2007**, *59*, 207–224.
(3) Rainsford, K. D. Anti-inflammatory drugs in the 21st century. *Subcell. Biochem.* **2007**, *42*, 3–27.
(4) McGettigan, P.; Henry, D. Cardiovascular risk and inhibition of cyclooxygenase: a systematic review of the observational studies of selective and nonselective inhibitors of cyclooxygenase 2. *J. Am. Med. Assoc.* **2006**, *296*, 1633–1644.
(5) Friesen, R. W.; Mancini, J. A. Microsomal prostaglandin E2 synthase-1 (mPGES-1): A novel anti-inflammatory therapeutic target. *J. Med. Chem.* **2008**, *51*, 4059–4067.
(6) Claveau, D.; Sirinyan, M.; Guay, J.; Gordon, R.; Chan, C. C.; Bureau, Y.; Riendeau, D.; Mancini, J. A. Microsomal prostaglandin E synthase-1 is a major terminal synthase that is selectively up-regulated during cyclooxygenase-2-dependent prostaglandin E2 production in the rat adjuvant-induced arthritis model. *J. Immunol.* **2003**, *170*, 4738–4744.
(7) Riendeau, D.; Aspiotis, R.; Ethier, D.; Gareau, Y.; Grimm, E. L.; Guay, J.; Guiral, S.; Juteau, H.; Mancini, J. A.; Methot, N.; Rubin, J.; Friesen, R. W. Inhibitors of the inducible microsomal prostaglandin E2 synthase (mPGES-1) derived from MK-886. *Bioorg. Med. Chem. Lett.* **2005**, *15*, 3352–3355.
(8) Cote, B.; Boulet, L.; Brideau, C.; Claveau, D.; Ethier, D.; Frenette, R.; Gagnon, M.; Giroux, A.; Guay, J.; Guiral, S.; Mancini, J.; Martins, E.; Masse, F.; Methot, N.; Riendeau, D.; Rubin, J.; Xu, D.; Yu, H.; Ducharme, Y.; Friesen, R. W. Substituted phenanthrene imidazoles as potent, selective, and orally active mPGES-1 inhibitors. *Bioorg. Med. Chem. Lett.* **2007**, *17*, 6816–6820.
(9) Xu, D.; Rowland, S. E.; Clark, P.; Giroux, A.; Cote, B.; Guiral, S.; Salem, M.; Ducharme, Y.; Friesen, R. W.; Methot, N.; Mancini, J.; Audoly, L.; Riendeau, D. MF63 {2-(6-chloro-1*H*-phenanthro[9,10-*d*]imidazol-2-yl)isophthalonitrile}, a selective microsomal prostaglandin E synthase 1 inhibitor, relieves pyresis and pain in preclinical models of inflammation. *J. Pharmacol. Exp. Ther.* **2008**, *326*, 754–763.
(10) Peters-Golden, M.; Henderson, W. R., Jr. Leukotrienes. *N. Engl. J. Med.* **2007**, *357*, 1841–1854.
(11) Fiorucci, S.; Meli, R.; Bucci, M.; Cirino, G. Dual inhibitors of cyclooxygenase and 5-lipoxygenase. A new avenue in anti-inflammatory therapy. *Biochem. Pharmacol.* **2001**, *62*, 1433–1438.
(12) Kulkarni, S. K.; Singh, V. P. Licofelone—A novel analgesic and anti-inflammatory agent. *Curr. Top. Med. Chem.* **2007**, *7*, 251–263.
(13) Koeberle, A.; Siemoneit, U.; Buehring, U.; Northoff, H.; Laufer, S.; Albrecht, W.; Werz, O. Licofelone suppresses prostaglandin E2 formation by interference with the inducible microsomal prostaglandin E2 synthase-1. *J. Pharmacol. Exp. Ther.* **2008**, *326*, 975–982.
(14) Wang, M.; Song, W. L.; Cheng, Y.; Fitzgerald, G. A. Microsomal prostaglandin E synthase-1 inhibition in cardiovascular inflammatory disease. *J. Intern. Med.* **2008**, *263*, 500–505.
(15) Rau, O.; Syha, Y.; Zettl, H.; Kock, M.; Bock, A.; Schubert-Zsilavecz, M. α-Alkyl substituted pirinixic acid derivatives as potent dual agonists of the peroxisome proliferator activated receptor α and γ. *Arch. Pharm. (Weinheim, Ger.)* **2008**, *341*, 191–195.
(16) Werz, O.; Greiner, C.; Koeberle, A.; Hoernig, C.; George, S.; Popescu, L.; Syha, I.; Schubert-Zsilavecz, M.; Steinhilber, D. Novel and potent inhibitors of 5-lipoxygenase product synthesis based on the structure of pirinixic acid. *J. Med. Chem.* **2008**, *51*, 5449–5453.
(17) D'Atri, G.; Gomarasca, P.; Resnati, G.; Tronconi, G.; Scolastico, C.; Sirtori, C. R. Novel pyrimidine and 1,3,5-triazine hypolipidemic agents. *J. Med. Chem.* **1984**, *27*, 1621–1629.
(18) Popescu, L.; Rau, O.; Bottcher, J.; Syha, Y.; Schubert-Zsilavecz, M. Quinoline-based derivatives of pirinixic acid as dual PPAR α/γ agonists. *Arch. Pharm. (Weinheim, Ger.)* **2007**, *340*, 367–371.
(19) Tateson, J. E.; Randall, R. W.; Reynolds, C. H.; Jackson, W. P.; Bhattacherjee, P.; Salmon, J. A.; Garland, L. G. Selective inhibition of arachidonate 5-lipoxygenase by novel acetohydroxamic acids: Biochemical assessment in vitro and ex vivo. *Br. J. Pharmacol.* **1988**, *94*, 528–539.
(20) Carter, G. W.; Young, P. R.; Albert, D. H.; Bouska, J.; Dyer, R.; Bell, R. L.; Summers, J. B.; Brooks, D. W. 5-Lipoxygenase inhibitory activity of zileuton. *J. Pharmacol. Exp. Ther.* **1991**, *256*, 929–937.
(21) Capdevila, J. H.; Morrow, J. D.; Belosludtsev, Y. Y.; Beauchamp, D. R.; DuBois, R. N.; Falck, J. R. The catalytic outcomes of the constitutive and the mitogen inducible isoforms of prostaglandin H2 synthase are markedly affected by glutathione and glutathione peroxidase(s). *Biochemistry* **1995**, *34*, 3325–3337.
(22) Jakobsson, P. J.; Thoren, S.; Morgenstern, R.; Samuelsson, B. Identification of human prostaglandin E synthase: A microsomal, glutathione-dependent, inducible enzyme, constituting a potential novel drug target. *Proc. Natl. Acad. Sci. U.S.A.* **1999**, *96*, 7220–7225.
(23) Asano, K.; Lilly, C. M.; Drazen, J. M. Prostaglandin G/H synthase-2 is the constitutive and dominant isoform in cultured human lung epithelial cells. *Am. J. Physiol.* **1996**, *271*, L126–L131.
(24) Celotti, F.; Laufer, S. Anti-inflammatory drugs: New multitarget compounds to face an old problem. The dual inhibition concept. *Pharmacol. Res.* **2001**, *43*, 429–436.
(25) Bias, P.; Buchner, A.; Klesser, B.; Laufer, S. The gastrointestinal tolerability of the LOX/COX inhibitor, licofelone, is similar to placebo and superior to naproxen therapy in healthy volunteers: Results from a randomized, controlled trial. *Am. J. Gastroenterol.* **2004**, *99*, 611–618.
(26) Vidal, C.; Gomez-Hernandez, A.; Sanchez-Galan, E.; Gonzalez, A.; Ortega, L.; Gomez-Gerique, J. A.; Tunon, J.; Egido, J. Licofelone, a balanced inhibitor of cyclooxygenase and 5-lipoxygenase, reduces inflammation in a rabbit model of atherosclerosis. *J. Pharmacol. Exp. Ther.* **2007**, *320*, 108–116.
(27) Dixon, R. A.; Diehl, R. E.; Opas, E.; Rands, E.; Vickers, P. J.; Evans, J. F.; Gillard, J. W.; Miller, D. K. Requirement of a 5-lipoxygenase-activating protein for leukotriene synthesis. *Nature* **1990**, *343*, 282–284.
(28) Fischer, L.; Hornig, M.; Pergola, C.; Meindl, N.; Franke, L.; Tanrikulu, Y.; Dodt, G.; Schneider, G.; Steinhilber, D.; Werz, O. The molecular mechanism of the inhibition by licofelone of the biosynthesis of 5-lipoxygenase products. *Br. J. Pharmacol.* **2007**, *152*, 471–480.
(29) Albert, D.; Zundorf, I.; Dingermann, T.; Muller, W. E.; Steinhilber, D.; Werz, O. Hyperforin is a dual inhibitor of cyclooxygenase-1 and 5-lipoxygenase. *Biochem. Pharmacol.* **2002**, *64*, 1767–1775.
(30) Werz, O.; Burkert, E.; Samuelsson, B.; Rådmark, O.; Steinhilber, D. Activation of 5-lipoxygenase by cell stress is calcium independent in human polymorphonuclear leukocytes. *Blood* **2002**, *99*, 1044–1052.
(31) Tretiakova, I.; Blaesius, D.; Maxia, L.; Wesselborg, S.; Schulze-Osthoff, K.; Cinatl, J., Jr.; Michaelis, M.; Werz, O. Myrtucommulone from *Myrtus communis* induces apoptosis in cancer cells via the mitochondrial pathway involving caspase-9. *Apoptosis* **2008**, *13*, 119–131.
(32) Fischer, L.; Szellas, D.; Rådmark, O.; Steinhilber, D.; Werz, O. Phosphorylation- and stimulus-dependent inhibition of cellular 5-lipoxygenase activity by nonredox-type inhibitors. *FASEB J.* **2003**, *17*, 949–951.
(33) Brungs, M.; Rådmark, O.; Samuelsson, B.; Steinhilber, D. Sequential induction of 5-lipoxygenase gene expression and activity in Mono Mac 6 cells by transforming growth factor β and 1,25-dihydroxyvitamin D3. *Proc. Natl. Acad. Sci. U.S.A.* **1995**, *92*, 107–111.
(34) Mitchell, J. A.; Akarasereenont, P.; Thiemermann, C.; Flower, R. J.; Vane, J. R. Selectivity of nonsteroidal antiinflammatory drugs as inhibitors of constitutive and inducible cyclooxygenase. *Proc. Natl. Acad. Sci. U.S.A.* **1993**, *90*, 11693–11697.

JM801085S

Supporting Information

Pirinixic acid derivatives as novel dual inhibitors of microsomal prostaglandin E_2 synthase and 5-lipoxygenase

Andreas Koeberle, Heiko Zettl, Christine Greiner, Mario Wurglics, Manfred Schubert-Zsilavecz and Oliver Werz

Contents

I Chemical synthesis
II Routine analytics by ^{1}H- and ^{13}C-NMR, mass spectrometry (ESI-) and elemental analysis
III References

I Chemical synthesis

The presented compounds were generally synthesized in a four step reaction as shown in the **Scheme**. First, the thiol group of thiobarbituric acid was substituted with the appropriate α-bromoethyl esters **(i)**. The introduction of alkyl chains longer than 4 carbons succeeds easier with triethylamine as conjugated base in DMF instead of NaOH in H_2O/EtOH. Aromatic nucleophilic substitution with $POCl_3$ **(ii)** gave the chlorinated pyrimidine derivatives. In the following step, treatment with the appropriate primary amine using triethylamine in refluxed EtOH **(iii)** resulted in mono-amination of the pyrimidine core. These compounds were hydrolyzed with LiOH in EtOH **(iv)** to give the desired carboxylic acids. A side path via a Williamson-like ether synthesis **(v)** led to 3,5-bis-ether pyrimidine derivatives which were hydrolyzed to the corresponding carboxylic acids as described (**iv**).

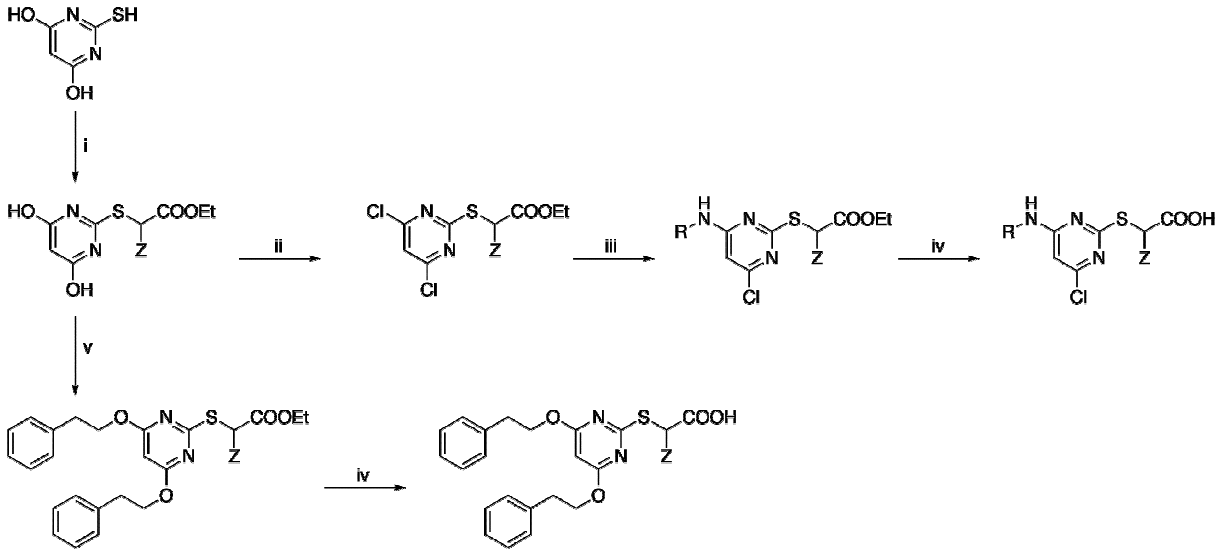

II Routine analytics by ^{1}H- and ^{13}C-NMR, mass spectrometry (ESI-) and elemental analysis

Structures of previously reported compounds **1**-**4** were confirmed by ^{1}H- and ^{13}C-NMR as well as by mass spectrometry (ESI-), and the purity (>98%) was checked by combustion analysis as described[1, 2].

Structures of novel compounds (**5a-7e**) were confirmed by ^{1}H- and ^{13}C-NMR as well as by mass spectrometry (ESI-), and the purity (>98%) was checked by combustion analysis as follows:

2-(4,6-Diphenethoxypyrimidin-2-ylthio)acetic acid (5a) mp = 114 °C. ^{1}H NMR (300.13 MHz, $(CD_3)_2SO$): δ 2.95 (t ,4H, Ph-CH_2, J=6.6Hz); 3.89 (s, 2H, S-CH_2); 4.46 (t, 4H, Pyr-O-CH_2, J=6.8Hz); 5.86 (s, 1H, Pyr-5*H*); 7.18-7.32 (m, 10H, Ph-*H).* ^{13}C NMR (75.45 MHz, $(CD_3)_2SO$): δ 33.21 (2C, Ph-*C*H_2); 34.44 (S-*C*H_2); 67.04 (2C; Pyr-O-*C*H_2); 85.74 (Pyr-C_5); 126.30 (2C, Ph-C_4); 128.31 (4C, Ph-C_2 + –C_6); 128.86 (4C, Ph-C_3 + –C_5); 137.92 (2C, Ph-C_1); 169.15 (Pyr-C_2); 170.06 (2C, Pyr-C_4 + -C_6); 170.20 (*C*OOH). MS (ESI+): *m/e* = 411.0 $[M+H]^+$.

2-(4,6-Diphenethoxypyrimidin-2-ylthio)hexanoic acid (5b) mp = 99 °C. ^{1}H NMR (300.13 MHz, $(CD_3)_2SO$): δ 0.81 (t, 3H, C*H*$_3$-Bu, J=7.1Hz); 1.23-1.38 (m, 4H, C*H*$_2$-Bu); 1.78-1.90 (m, 2H, C*H*$_2$-Bu); 2.98 (t ,4H, Ph-C*H*$_2$, J=6.9Hz); 4.29 (t, 1H, S-C*H*, J=7.2Hz); 4.46 (t, 4H, Pyr-O-C*H*$_2$, J=6.9Hz); 5.87 (s, 1H, Pyr-5*H*); 7.18-7.32 (m, 10H, Ph-*H).* ^{13}C NMR (75.45 MHz, $(CD_3)_2SO$): δ 13.70 (*C*H$_3$-Bu); 21.71 (*C*H$_2$-Bu); 28.92 (*C*H$_2$-Bu); 31.09 (*C*H$_2$-Bu); 34.44 (2C, Ph-*C*H$_2$); 47.61 (S-*C*H$_2$); 67.08 (2C; Pyr-O-*C*H$_2$); 85.87 (Pyr-C_5); 126.31 (2C, Ph-C_4); 128.30 (4C, Ph-C_2 + –C_6); 128.84 (4C, Ph-C_3 + –C_5); 137.88 (2C, Ph-C_1); 169.01 (Pyr-C_2); 170.03 (2C, Pyr-C_4 + -C_6); 172.70 (*C*OOH). MS (ESI+): *m/e* = 467.0 [M+H

Ethyl 2-(4,6-diphenethoxypyrimidin-2-ylthio)hexanoate (5c) clear oil. ^{1}H NMR (300.13 MHz, $(CD_3)_2SO$): δ 0.82 (t, 3H, C*H*$_3$-Bu, J=7.1Hz); 1.05 (t, 3H, -C*H*$_3$, J=7.1Hz); 1.26-1.34 (m, 4H, C*H*$_2$-Bu); 1.74-1.91 (m, 2H, C*H*$_2$-Bu); 2.98 (t ,4H, Ph-C*H*$_2$, J=7.1Hz); 4.11 (q, 2H, O-C*H*$_2$, J=7.1Hz); 4.32-4.48 (m, 5H, S-C*H*$_2$ + Pyr-O-C*H*$_2$); 5.89 (s, 1H, Pyr-5*H*); 7.19-7.32 (m, 10H, Ph-*H).* ^{13}C NMR (75.45 MHz, $(CD_3)_2SO$): δ 13.63 (*C*H$_3$-Bu); 13.83 (-*C*H$_3$); 21.60 (*C*H$_2$-Bu); 28.79 (*C*H$_2$-Bu); 30.72 (*C*H$_2$-Bu); 34.43 (2C, Ph-*C*H$_2$); 47.13 (S-*C*H$_2$); 60.90 (O-*C*H$_2$); 67.12 (2C; Pyr-O-*C*H$_2$); 86.01 (Pyr-C_5); 126.34 (2C, Ph-C_4); 128,12 (4C, Ph-C_2 + –C_6); 128.61 (4C, Ph-C_3 + –C_5); 137.80 (2C, Ph-C_1); 168.54 (Pyr-C_2); 170.07 (2C, Pyr-C_4 + -C_6); 171.35 (*C*OO). MS (ESI+): *m/e* = 495.2 $[M+H]^+$.

2-(4-Chloro-6-(phenethylamino)pyrimidin-2-ylthio)octanoic acid (6a) mp = 88 °C. ^{1}H NMR (300.13 MHz, $(CD_3)_2SO$): δ 0.82 (t, 3H, C*H*$_3$-Hex, J=6.5Hz); 1.21-1.28 (m, 6H, C*H*$_2$-Hex); 1.31-1.36 (m, 2H, C*H*$_2$-Hex); 1.74-1.89 (m, 2H, C*H*$_2$-Hex); 2.80 (t, 2H, Ph-C*H*$_2$, J=7.4Hz); 3.54 (q, 2H, C*H*$_2$-NH, J=5.9Hz); 4,31 (t, 1H, S-C*H*, J=7.2Hz); 6.21 (s, 1H, Pyr 5-*H*); 7.17-7.31 (m, 5H, Ph-*H)*; 7.91 (br s,1H, -N*H*). ^{13}C NMR (75.45 MHz, $(CD_3)_2SO$): δ 14.16 (*C*H$_3$-Hex); 21.89 (*C*H$_2$-Hex); 26.59 (*C*H$_2$-Hex); 28.11 (*C*H$_2$-Hex); 30.93 (*C*H$_2$-Hex); 31.46 (*C*H$_2$-Hex); 34.72 (Ph-*C*H$_2$); 41.63 (*C*H$_2$-NH); 47.13 (S-*C*H); 99.46 (Pyr-C_5); 126.13 (Ph-C_4); 128.27 (2C, Ph-C_2 + –C_6); 128.66 (2C, Ph-C_3 + –C_5); 139.12 (Ph-C_1); 156.33 (Pyr-C_4); 162.40 (Pyr-C_2); 169.66 (Pyr-C_6); 172.73 (*C*OOH). MS (ESI–): *m/e* = 406.1 (M–1).

2-(4-Chloro-6-(2-phenoxyethylamino)pyrimidin-2-ylthio)octanoic acid (6b) yellow oil. ^{1}H NMR (300.13 MHz, $(CD_3)_2SO$): δ 0.82 (t, 3H, C*H*$_3$-Hex, J=6.8Hz); 1.14-1.36 (m, 6H, C*H*$_2$-Hex); 1.77-1.90 (m, 2H, C*H*$_2$-Hex); 3.69 (t, 2H, C*H*$_2$-NH, J=4.2Hz); 4.06 (t, 2H, Ph-O-C*H*$_2$, J=5.4Hz); 4.25 (t, 1H, S-C*H*, J=7.2Hz); 6.29 (s, 1H, Pyr-5*H*); 6.92 (t, 3H, Ph-2*H* + -4*H* + -6*H*, J=7.0Hz*)*; 7.28 (t, 2H, Ph-3*H* + -5*H*, J=8.0Hz); 8.11 (br s,1H, -N*H*). ^{13}C NMR (75.45 MHz, $(CD_3)_2SO$): δ 13.84 (*C*H$_3$-Hex); 21.95 (*C*H$_2$-Hex); 26.62 (*C*H$_2$-Hex); 28.32 (*C*H$_2$-Hex); 31.04 (*C*H$_2$-Hex); 31.99 (*C*H$_2$-Hex); 39.75 (*C*H$_2$-NH); 47.29 (S-*C*H); 65.89 (Ph-O-*C*H$_2$); 99.39 (Pyr-C_5); 114.40 (2C, Ph-C_2 + –C_6); 120.68 (Ph-C_4); 129.45 (2C, Ph-C_3 + –C_5); 156.47 (Ph-C_1); 158.27(Pyr-C_4); 162.55 (Pyr-C_2); 170.34 (Pyr-C_6); 173.07 (*C*OOH). MS (ESI-): *m/e* = 422.0 [M-1].

Ethyl 2-(4-chloro-6-(2-phenoxyethylamino)pyrimidin-2-ylthio)octanoate (6c) yellow oil. ^{1}H NMR (300.13 MHz, $(CD_3)_2SO$): δ 0.82 (t, 3H, C*H*$_3$-Hex, J=6.9Hz); 1.12-1.19 (m, 5H, C*H*$_3$ + C*H*$_2$-Hex); 1.22-1.35 (m, 6H, C*H*$_2$-Hex); 1.73-1.87 (m, 2H, C*H*$_2$-Hex); 3.67 (t, 2H, C*H*$_2$-NH, J=5.7Hz); 4.03-4.15 (m, 4H, O-C*H*$_2$ + Ph-O-C*H*$_2$); 4.29 (t, 1H, S-C*H*, J=7.2Hz); 6.30 (s, 1H, Pyr-5*H*); 6.93 (t, 3H, Ph-2*H* + -4*H* + -6*H*, J=5.7Hz*)*; 7.28 (t, 2H, Ph-3*H* + -5*H*, J=8.0Hz); 8.11 (br s,1H, -N*H*). ^{13}C NMR (75.45 MHz, $(CD_3)_2SO$): δ 13.82 (*C*H$_3$); 13.93 (*C*H$_3$-Hex); 21.89 (*C*H$_2$-Hex); 26.48 (*C*H$_2$-Hex); 28.07 (*C*H$_2$-Hex); 30.90 (*C*H$_2$-Hex); 31.07 (*C*H$_2$-Hex); 39.68 (*C*H$_2$-NH); 47.04 (S-*C*H); 60.85 (O-*C*H$_2$); 65.76 (Ph-O-*C*H$_2$); 99.76 (Pyr-C_5); 114.41 (2C, Ph-C_2 + –C_6); 120.72 (Ph-C_4); 129.46 (2C, Ph-C_3 + –C_5); 156.45 (Ph-C_1); 158.22(Pyr-C_4); 162.60 (Pyr-C_2); 169.39 (Pyr-C_6); 171.37 (*C*OO). MS (ESI-): *m/e* = 452.0 $[M+H]^+$.

2-(4-(Biphenyl-4-ylamino)-6-chloropyrimidine-2-ylthio)octanoic acid (7a) mp = 127 °C. ^{1}H NMR (300.13 MHz, $(CD_3)_2SO$): δ 0.78 (t, 3H, C*H*$_3$-Hex, J=6.6Hz); 1.14-1.36 (m, 8H, C*H*$_2$-Hex); 1.79-1.92 (m, 2H, C*H*$_2$-Hex); 4.38 (t, 1H, S-C*H*, J=6.9Hz); 6.54 (s, 1H, Pyr-5*H*); 7.33 (t, 1H, Ph'-4*H*, J=7.4Hz); 7.45 (t, 2H, Ph-2*H* + 6*H*, J=7.5Hz); 7.63-7.66 (m, 6H, Ph-*H* + Ph'-*H*); 10.04 (s,1H, -N*H*). ^{13}C NMR (75.45 MHz, $(CD_3)_2SO$): δ 13.78 (*C*H$_3$-Hex); 21.88 (*C*H$_2$-Hex); 26.53 (*C*H$_2$-Hex); 28.09 (*C*H$_2$-Hex); 30.95 (*C*H$_2$-Hex); 31.71 (*C*H$_2$-Hex); 47.08 (S-*C*H); 101.16 (Pyr-*C*$_5$); 120.90 (2C, Ph-*C*$_2$ + –*C*$_6$); 126.20 (2C, Ph'-*C*$_2$ + –*C*$_6$); 126.97 (2C, Ph-*C*$_3$ + –*C*$_5$); 127.08 (Ph'-*C*$_4$); 128.88 (2C, Ph'-*C*$_3$ + –*C*$_5$); 135.18 (Ph-*C*$_4$); 137.95 (Ph'-*C*$_1$); 139.55 (Ph-*C*$_1$); 157.37 (Pyr-*C*$_6$); 160.50 (Pyr-*C*$_2$); 169.96 (Pyr-*C*$_4$); 172.41 (*C*OOH). MS (ESI -): *m/e* = 454.2 [M-1].

2-(4-(Biphenyl-4-ylmethylamino)-6-chloropyrimidin-2-ylthio)octanoic acid (7b) mp = 110 °C. ^{1}H NMR (300.13 MHz, $(CD_3)_2SO$): δ 0.77 (t, 3H, C*H*$_3$-Hex, J=6.3Hz); 1.14-1.28 (m, 8H, C*H*$_2$-Hex); 1.66-1.84 (m, 2H, C*H*$_2$-Hex); 4.23 (t, 1H, S-C*H*, J=7.1Hz); 4.49 (dd, 1H, C*H*$_{2A}$-NH, J_1=5.4Hz, J_2=15.5Hz); 4.65 (dd, 1H, C*H*$_{2B}$-NH, J_1=5.6Hz, J_2=15Hz); 6.31 (s, 1H, Pyr-5*H*); 7.31-7.47 (m, 5H, Ph-*H* + Ph'-*H)*; 7.61 (d, 2H, Ph-3*H* + Ph-5*H*, J=1.8Hz); 7.64 (d, 2H, Ph'-2*H* + Ph-6*H*, J=1.2Hz); 8.39 (t,1H, -N*H*, J=4.8Hz). ^{13}C NMR (75.45 MHz, $(CD_3)_2SO$): δ 13.80 (*C*H$_3$-Hex); 21.89 (*C*H$_2$-Hex); 26.50 (*C*H$_2$-Hex); 28.13 (*C*H$_2$-Hex); 30.95 (*C*H$_2$-Hex); 31.39 (*C*H$_2$-Hex); 43.29 (*C*H$_2$-NH); 47.26 (S-*C*H); 99.54 (Pyr-*C*$_5$); 126.50 (2C, Ph-*C*$_3$ + –*C*$_5$); 126.67 (2C, Ph'-*C*$_2$ + –*C*$_6$); 127.32 (Ph'-*C*$_4$); 127.89 (2C, Ph-*C*$_2$ + –*C*$_6$); 128.85 (2C, Ph'-*C*$_3$ + –*C*$_5$); 138.04 (Ph-*C*$_4$); 138.91 (Ph'-*C*$_1$); 139.82 (Ph-*C*$_1$); 156.57 (Pyr-*C*$_6$); 162.40 (Pyr-*C*$_4$); 169.76 (Pyr-*C*$_2$); 172.72 (*C*OOH). MS (ESI+): *m/e* = 470.1 $[M+H]^+$.

Ethyl 2-(4-(biphenyl-4-ylmethylamino)-6-chloropyrimidin-2-ylthio)octanoate (7c) yellow oil. ^{1}H NMR (300.13 MHz, $(CD_3)_2SO$): δ 0.82 (t, 3H, C*H*$_3$-Hex, J=7.9Hz); 1.10-1.23 (m, 11H, C*H*$_3$ + C*H*$_2$-Hex); 1.71-1.80 (m, 2H, C*H*$_2$-Hex); 4.07 (q, 2H, O-C*H*$_2$, J=7.2Hz); 4.26 (t, 1H, S-C*H*, J=7.2Hz); 4.56 (dd, 2H, C*H*$_2$-NH, J_1=5.6Hz, J_2=15Hz); 6.32 (s, 1H, Pyr-5*H*); 7.32-7.47 (m, 5H, Ph-*H* + Ph'-*H)*; 7.63 (m, 4H, Ph-*H* + Ph'-*H*); 8.42 (t,1H, -N*H*, J=6.0Hz). ^{13}C NMR (75.45 MHz, $(CD_3)_2SO$): δ 13.79 (*C*H$_3$-Hex); 13.93 (*C*H$_3$); 21.87 (*C*H$_2$-Hex); 26.44 (*C*H$_2$-Hex); 28.04 (*C*H$_2$-Hex); 30.89 (*C*H$_2$-Hex); 31.07 (*C*H$_2$-Hex); 43.22 (*C*H$_2$-NH); 47.00 (S-*C*H); 60.85 (O-*C*H$_2$); 99.65 (Pyr-*C*$_5$); 126.49 (2C, Ph-*C*$_3$ + –*C*$_5$); 126.67 (2C, Ph'-*C*$_2$ + –*C*$_6$); 127.33 (Ph'-*C*$_4$); 127.78 (2C, Ph-*C*$_2$ + –*C*$_6$); 128.86 (2C, Ph'-*C*$_3$ + –*C*$_5$); 137.98 (Ph-*C*$_4$); 138.92 (Ph'-*C*$_1$); 139.79 (Ph-*C*$_1$); 156.56 (Pyr-*C*$_6$); 162.43 (Pyr-*C*$_4$); 169.46 (Pyr-*C*$_2$); 171.36 (*C*OO). MS (ESI+): *m/e* = 498.3 $[M+H]^+$.

2-(4-Chloro-6-(4'-cyanobiphenyl-4-ylamino)pyrimidin-2-ylthio)octanoic acid (7d) mp = 111 °C. ^{1}H NMR (300.13 MHz, $(CD_3)_2SO$): δ 0.77 (t, 3H, C*H*$_3$-Hex, J=6.5Hz); 1.17-1.36 (m, 8H, C*H*$_2$-Hex); 1.77-1.94 (m, 2H, C*H*$_2$-Hex); 4.37 (t, 1H, S-C*H*, J=7.1Hz); 6.56 (s, 1H, Pyr-5*H*); 7.70-7.77 (m, 4H, Ph-*H*); 7.85-7.92 (m, 4H, Ph'-*H*); 10.13 (s,1H, -N*H*). ^{13}C NMR (75.45 MHz, $(CD_3)_2SO$): δ 13.77 (*C*H$_3$-Hex); 21.87 (*C*H$_2$-Hex); 26.49 (*C*H$_2$-Hex); 28.08 (*C*H$_2$-Hex); 30.93 (*C*H$_2$-Hex); 31.61 (*C*H$_2$-Hex); 47.13 (S-*C*H); 101.44 (Pyr-*C*$_5$); 109.50 (Ph'-*C*$_4$); 118.88 (-*C*N); 120.77 (2C, Ph-*C*$_2$ + –*C*$_6$); 126.92 (2C, Ph'-*C*$_2$ + –*C*$_6$); 127.50 (2C, Ph-*C*$_3$ + –*C*$_5$); 132.80 (2C, Ph'-*C*$_3$ + –*C*$_5$); 139.27 (Ph'-*C*$_1$); 143.97 (Ph-*C*$_1$); 157.48 (Pyr-*C*$_6$); 160.43 (Pyr-*C*$_2$); 170.02 (Pyr-*C*$_4$); 172.38 (*C*OOH). MS (ESI+): *m/e* = 481.0 $[M+H]^+$.

2-(4-Chloro-6-(5-methoxy-2-methylbiphenyl-4-ylamino)pyrimidin-2-ylthio)octanoic acid (7e) mp = 101 °C. ^{1}H NMR (300.13 MHz, $(CD_3)_2SO$): δ 0.78 (t, 3H, C*H*$_3$-Hex, J=6.9Hz); 1.16-1.30 (m, 8H, C*H*$_2$-Hex); 1.69-1.86 (m, 2H, C*H*$_2$-Hex); 2.17 (s, 3H, Ph-C*H*$_3$); 3.82 (s, 3H, Ph-O-C*H*$_3$); 4.39 (t, 1H, S-C*H*, J=7.1Hz); 6.61 (s, 1H, Pyr-5*H*); 6.88 (s, 1H, Ph-6*H*); 7.33-7.47 (m, 5H, Ph-*H* + Ph'-*H*); 7.69 (s, 1H, Ph-3*H*); 9.36 (s,1H, -N*H*). ^{13}C NMR (75.45 MHz,

$(CD_3)_2SO$): δ 13.79 (*C*H_3-Hex); 19.34 (Ph-*C*H_3); 21.85 (*C*H_2-Hex); 26.34 (*C*H_2-Hex); 28.05 (*C*H_2-Hex); 30.89 (*C*H_2-Hex); 31.76 (*C*H_2-Hex); 46.79 (S-*C*H); 55.78 (Ph-O-*C*H_3); 100.74 (Pyr-C_5); 112.86 (Ph-C_6); 125.27 (Ph-C_3); 125.82 (Ph'-C_4); 126.22 (Ph-C_1); 126.88 (Ph-C_2); 128.15 (2C, Ph'-C_2 + –C_6); 128.96 (2C, Ph'-C_3 + –C_5); 138.22 (Ph-C_4); 141.04 (Ph'-C_1); 149.32 (Ph-C_5); 157.41 (Pyr-C_4); 161.23 (Pyr-C_2); 169.46 (Pyr-C_6); 172.54 (*C*OOH). MS (ESI-): *m/e* = 498.2 [M-1].

Synthesis of key compounds **7b** and **7d**: Spectroscopic data of the synthetic intermediates described in the experimental section.

Ethyl 2-(4,6-dihydroxypyrimidin-2-ylthio)octanoate (Step (i))
^{1}H NMR (300.13 MHz, $(CD_3)_2SO$); δ 0.83 (t, 3H, C*H*$_3$-Hex, J=6.9Hz), 1.17 (t, 3H, C*H*$_3$, J=7.1Hz), 1.23-1.30 (m, 8H, C*H*$_2$-Hex), 1.76-1.88 (m, 2H, C*H*$_2$-Hex), 4.11 (q, 2H, OC*H*$_2$, J=7.1Hz), 4.50 (t, 1H, SC*H*, J=7.1Hz), 5.22 (s, 1H, Pyr-5*H*), 11.79 (br s, 2H, O*H*). MS (ESI+): *m/e* = 315.1 $[M+H]^+$.

Ethyl 2-(4,6-dichloropyrimidin-2-ylthio)octanoate (Step (ii))
^{1}H NMR (300.13 MHz, $CDCl_3$): δ 0.87 (t, 3H, C*H*$_3$-Hex, J=6.8Hz), 1.28 (t, 3H, C*H*$_3$, J=7.1Hz), 1.26-1.36 (m, 6H, C*H*$_2$-Hex), 1.43-1.49 (m, 2H, C*H*$_2$-Hex), 1.86-1.98 (m, 2H, C*H*$_2$-Hex), 4.20 (q, 2H, OC*H*$_2$, J=7.1Hz), 4.38 (t, 1H, SC*H*, J=7.2Hz), 7.03 (s, 1H, Pyr-5*H*). MS (ESI+): *m/e* = 350.9 $[M+H]^+$.

Ethyl 2-(4-(biphenyl-4-ylmethylamino)-6-chloropyrimidin-2-ylthio)octanoate (Step (iii), 7b-ester)
^{1}H-NMR (300.13 MHz, $(CD_3)_2SO$): δ 0.82 (t, 3H, C*H*$_3$-Hex, J=7.9Hz); 1.10-1.23 (m, 11H, C*H*$_3$ + C*H*$_2$-Hex); 1.71-1.80 (m, 2H, C*H*$_2$-Hex); 4.07 (q, 2H, O-C*H*$_2$, J=7.2Hz); 4.26 (t, 1H, S-C*H*, J=7.2Hz); 4.56 (dd, 2H, C*H*$_2$-NH, J_1=5.6Hz, J_2=15Hz); 6.32 (s, 1H, Pyr-5*H*); 7.32-7.47 (m, 5H, Ph-*H* + Ph'-*H)*; 7.63 (m, 4H, Ph-*H* + Ph'-*H*); 8.42 (t,1H, -N*H*, J=6.0Hz). MS (ESI+): *m/e* = 498.3 $[M+H]^+$.

Ethyl 2-(4-chloro-6-(4'-cyanobiphenyl-4-ylamino)pyrimidin-2-ylthio)octanoate (Step (iii), 7d-ester)
^{1}H-NMR (300.13 MHz, $(CD_3)_2SO$) δ 0.78 (t, 3H, C*H*$_3$-Hex, J=6.3Hz); 1.14 (t, 3H, -C*H*$_3$, J=6.9Hz); 1.17-1.37 (m, 8H, C*H*$_2$-Hex); 1.76-1.91 (m, 2H, C*H*$_2$-Hex); 4.10 (q, 2H, O-C*H*$_2$, J=7.2Hz); 4.43 (t, 1H, S-C*H*, J=7.2Hz); 6.56 (s, 1H, Pyr-5*H*); 7.67-7.77 (m, 4H, Ph-*H*); 7.84-7.91 (m, 4H, Ph'-*H*); 10.13 (s,1H, -N*H*). MS (ESI+): *m/e* = 509.2 $[M+H]^+$.

Elemental Analysis of Compounds

Compound	Molecular Formula	Expected			Found		
		C, %	H, %	N, %	C, %	H, %	N, %
2a	$C_{15}H_{16}ClN_3O_2S$	53.33	4.77	12.44	53.31	4.59	12.17
2b	$C_{16}H_{18}ClN_3O_2S$ x 0.4 H_2O	53.52	5.28	11.70	53.75	4.76	11.04

2c	$C_{18}H_{22}ClN_3O_2S$	56.91	5.84	11.06	57.09	5.86	10.87
2d	$C_{20}H_{26}ClN_3O_2S$	58.88	6.42	10.30	58.63	6.32	10.24
2e	$C_{22}H_{30}ClN_3O_2S$	60.60	6.94	9.64	60.72	7.12	9.81
2f	$C_{22}H_{30}ClN_3O_2S$ x 0.4 $C_4H_8O_2$ (ethyl acetate)	60.15	7.10	8.92	60.21	7.06	8.80
2g	$C_{20}H_{18}ClN_3O_2S$	60.07	4.54	10.51	59.86	4.70	10.35
2h	$C_{24}H_{20}ClN_3O_2S$ x 0.8 $C_4H_8O_2$ (ethyl acetate)	62.77	5.10	8.07	62.44	4.81	8.19
3a	$C_{21}H_{23}ClN_4O_2S$	58.53	5.38	13.00	58.26	5.39	12.79
3b	$C_{23}H_{27}ClN_4O_2S$	60.18	5.93	12.21	60.01	5.92	12.06
3c	$C_{21}H_{22}ClN_3O_3S$	58.39	5.13	9.73	58.52	5.07	9.45
3d	$C_{22}H_{25}ClN_4O_2S$	59.38	5.66	12.59	59.21	5.56	12.59
4	$C_{22}H_{24}ClF_6N_3O_4S$	45.88	4.20	7.30	46.05	4.39	7.27
5a	$C_{22}H_{22}N_2O_4S$	64.37	5.40	6.82	64.51	5.45	6.65
5b	$C_{26}H_{30}N_2O_4S$	66.93	6.48	6.00	67.13	6.69	5.78
5c	$C_{28}H_{34}N_2O_4S$	67.99	6.93	5.66	68.12	7.03	5.47
6a	$C_{20}H_{26}ClN_3O_2S$	58.88	6.42	10.30	58.68	6.42	10.18
6b	$C_{20}H_{26}ClN_3O_3S$	56.66	6.18	9.91	56.42	6.34	9.65
6c	$C_{22}H_{30}ClN_3O_3S$	58.46	6.69	9.30	58.18	6.78	9.08
7a	$C_{24}H_{26}ClN_3O_2S$	63.21	5.75	9.21	63.01	5.78	9.08
7b	$C_{25}H_{28}ClN_3O_2S$	63.88	6.00	8.94	63.65	6.01	8.76
7c	$C_{27}H_{32}ClN_3O_2S$	65.11	6.48	8.44	64.90	6.52	8.23
7d	$C_{25}H_{25}ClN_4O_2S$	62.42	5.24	11.65	62.26	5.33	11.49
7e	$C_{26}H_{30}ClN_3O_3S$	62.45	6.05	8.40	62.30	6.01	8.39

Compounds **7d (R)** and **7d (S)** were obtained by preparative HPLC of **7d** under following conditions:
chiral stationary phase: Chiralpak QD-AX (Column dimension, 150 x 4 mm ID)
eluent: methanol-glacial acetic acid-ammonium acetate (98:2:0.5; v/v/w)
flow rate: 1 mL/min; temperature, 25°; detection, UV 250 nm

Compound	**Molecular Formula**	**Enantiomeric Excess (ee)**	**Purity**	**Impurity Tracings**
7d (R)	$C_{25}H_{25}ClN_4O_2S$	98.8%	99.4%	0.6%
7d (S)	$C_{25}H_{25}ClN_4O_2S$	96.8%	98.4%	1.6%

Enantiomeric purity determination of **7d (R)**:

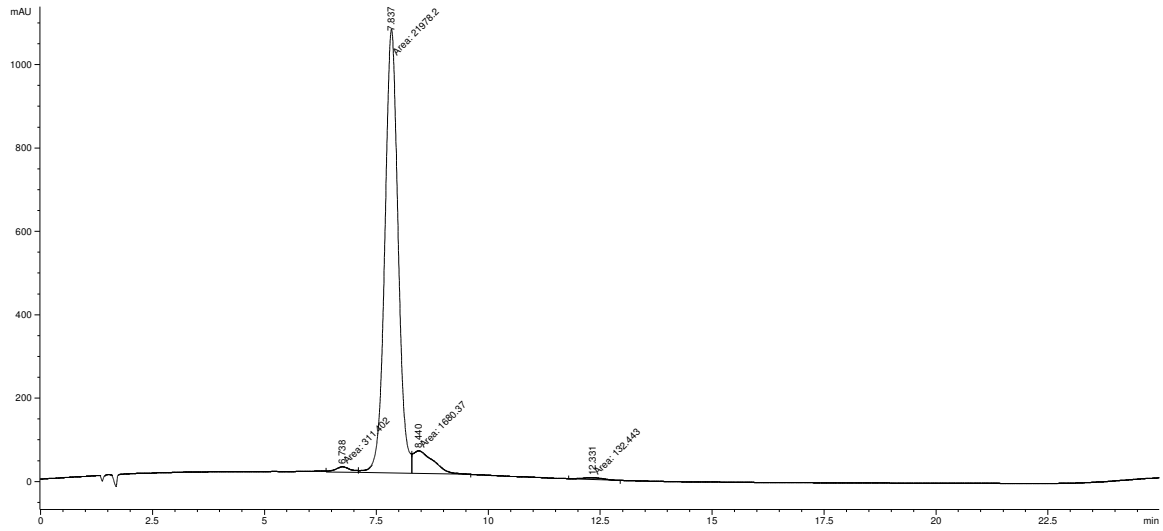

Enantiomeric purity determination of **7d (S)**:

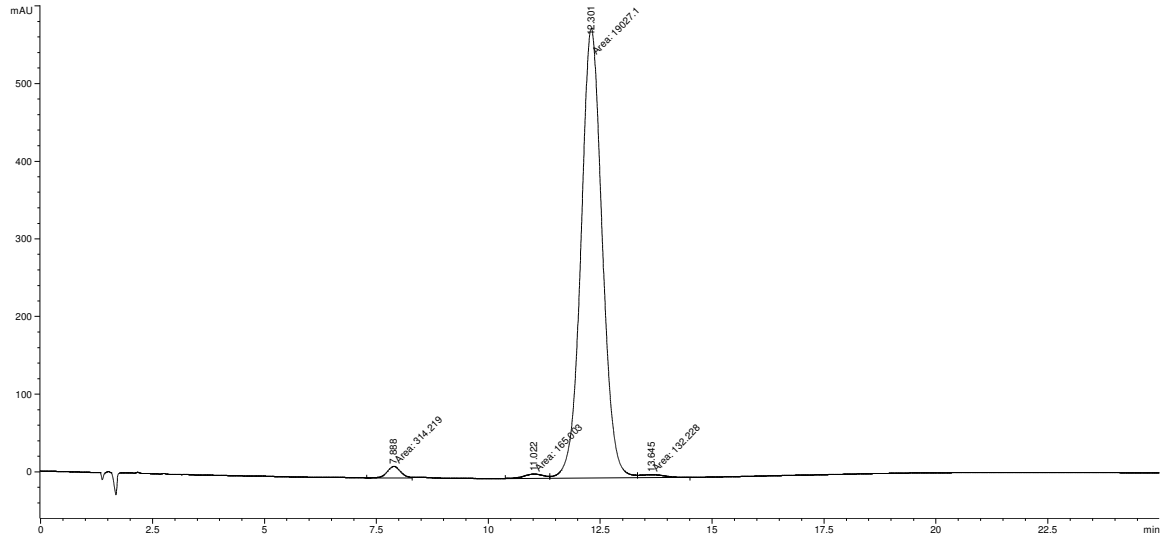

III References

1. Popescu, L.; Rau, O.; Bottcher, J.; Syha, Y.; Schubert-Zsilavecz, M., Quinoline-based derivatives of pirinixic acid as dual PPAR alpha/gamma agonists. *Arch Pharm (Weinheim)* **2007,** *340*, 367-371.
2. Rau, O.; Syha, Y.; Zettl, H.; Kock, M.; Bock, A.; Schubert-Zsilavecz, M., alpha-Alkyl Substituted Pirinixic Acid Derivatives as Potent Dual Agonists of the Peroxisome Proliferator Activated Receptor Alpha and Gamma. *Arch Pharm (Weinheim)* **2008,** *341*, 191-195.

GOETHE
UNIVERSITÄT
FRANKFURT AM MAIN

Johann Wolfgang Goethe-Universität Frankfurt am Main
Der Präsident • Recht und Organisation

Persönlich

FB Biochemie, Chemie und Pharmazie
Institut für Pharmazeutische Chemie
Herrn Dr. Heiko Zettl
Max-von-Laue-Str. 9
60438 Frankfurt/Main

- Hauspost -

Der Präsident

Recht und Organisation

Bearbeiter/in: von Scheven/AS
Az.: 1.45.10

Telefon +49 (0)69 798 28709
Telefax +49 (0)69 798 28214
E-Mail vonScheven@vdv.uni-frankfurt.de

www.uni-frankfurt.de

Datum: 02.03.2009

Diensterfindungen „Thiophenoletherderivate als duale Hemmstoffe der mikrosomalen Prostaglandin-E_2-Synthase und der 5-Lipoxygenase zur Verwendung als Arzneimittel“ Erfindungsmeldung vom 27.11.2008

Sehr geehrter Herr Dr. Zettl,

ich bedanke mich für Ihre Mitteilung.

Ich nehme im Umfang Ihrer Beteiligung die oben genannte Erfindung in Anspruch.

Mit freundlichen Grüßen
Im Auftrag

Christiane von Scheven